Fabrication of a Biomass-Polymeric Adsorbent for the Removal of Selected Metal Species, Nutrients and Pathogens in Aqueous Solutions

By

Mhlarhi Nsovo

Student no: 14014013

A dissertation submitted to the Department of Ecology and Resource Management, School of Environmental Sciences, University of Venda in full fulfillment of the requirements for Master of Environmental Sciences

Supervisor: Prof. Gitari, W. M
Co-Supervisors: Dr. Tavengwa, N.T, Dr. Ayinde W.B

June 2021

DECLARATION

I, Nsovo Mhlarhi, (student number: 14014013) hereby declare that this MSc proposal titled "**Fabrication of a Biomass-Polymeric Adsorbent for the Removal of Selected Metal Species, Nutrients and Pathogens in Aqueous Solutions"** is my work and has never been submitted to any higher learning institution and all sources have been acknowledged.

Mhlarhi Nsovo

Date: June 2021

ABSTRACT

Environmental pollution is a major problem that has increased rapidly many decades ago. This has affected the quality of water and has created serious environmental, social, economic, and political issues. Water pollution is mainly caused by chemical species such as chromium and cadmium; nutrients (nitrates and phosphates) and pathogens from natural and anthropogenic activities which cause health problems and in some cases death to both human and aquatic organisms. South Africa is a water-scarce country, and many of the water resources are threatened by human factors. In many cases, most of the water-treatment plants have been abandoned and are in a dire state which often leads to alternative sources of water for domestic activities. The consumption of this untreated water resulted in a lot of diseases and child mortality. In this sense, the biosorption process using a sustainable biomaterial for removing these pollutants has gained prominence due to several advantages it has over other technologies in solving these environmental menaces. The present study successfully developed and evaluated a systemic biomass polymeric adsorbent for the removal of toxic metals such as chromium and cadmium ions, nutrients (nitrate and phosphate ions), and pathogens from aqueous solutions. The bio-sorbent was fabricated by incorporating biomass (grapefruit peels) and algae (diatom) on a polymeric network for improved overall properties towards the selective toxic chemical and microbial pollutants. The structural and morphological properties of the various adsorbents were done by FTIR which show the various functional groups present in the adsorbents responsible for the sorption processes of Cr^{6+}, $Cd^{2+,}$ and PO_4^{3-}. The SEM-EDS showed different shapes and the elemental compositions that constitute each of the adsorbents. Furthermore, the XRD revealed an amorphous structure for grapefruit peel powder (GFP), diatom biomass, grapefruit peel/diatom (GFP/diatom), while the overall synthesized poly-phenylenediamine based biomass (pPD/GFP/diatom) was crystalline. The batch sorption studies on the uptakes of Cr^{6+}, $Cd^{2+,}$ and PO_4^{3-} from aqueous solutions by the various adsorbents were investigated as a function of pH, contact time, adsorbent dosage, and initial concentration. The respective adsorption kinetics processes by the GFP, diatom biomass, GFP/diatom, and pPD/GFP/diatom sorbent materials on Cr^{6+}, $Cd^{2+,}$ and PO_4^{3-} ions revealed that physisorption and chemisorption mechanisms were responsible for the adsorption processes as well governed by intra-particle diffusions. Freundlich and Langmuir adsorption isotherm models proved to be responsible for the sorption of Cr^{6+}, $Cd^{2+,}$ and PO_4^{3-} ions by the different adsorbents. The thermodynamic data revealed that the adsorption process was spontaneous and feasible in all the adsorbents across all temperatures. Furthermore, the antimicrobial activity of *Escherichia*

coli, *Staphylococcus aureus*, and *Klebsiella pneumoniae* by GFP, diatom biomass, GFP/diatom, and pPD/GFP/diatom showed that they had antimicrobial potency. Overall, these adsorbents present a promising ability to remediate inorganic pollutants in wastewater, allowing for the protection of the environment and living organisms.

Keywords: Water pollution, toxic chemical species, nutrients, grapefruit peel, diatom biomass, bio-sorption processes, antimicrobial property.

Acknowledgments

Firstly, I would like to thank God Almighty for the life He gave me, wisdom, good health, and for my family. I thank God for giving me the strength to complete this project.

My sincere gratitude to my supervisor Prof Gitari W.M for his patience, dedication, and assistance in the completion of this work.

I would like to thank my co-supervisors Dr. Tavengwa N.T and Dr. Ayinde W.B for their commitment and assistance, comments, suggestions and constructive criticism throughout the research project.

I would also like to express my gratitude to my parents (John and Suzan Nyiko Mhlarhi), my brothers (Ntsako and Tiyiselani Mhlarhi), and my sister (Rirhandzu) who have been supportive and encouraging throughout this work.

I would like to express my heartfelt gratitude to my grandmother (Catherine Bahlakile Nomvela, may her soul rest in peace) for raising me to be the person I am today.

To the Department of Ecology and Resource Management, I would like to give thanks for accepting me to be part of their master's group.

I would like also to thank the EnviRen 2020 class for the unity and assistance they provided.

List of figures

List of tables

Acronyms/ Abbreviations

ATSDR - Agency for Toxic Substances and Diseases Registry

BOD - Biological Oxygen Demand

CDC - Center for Disease Control

CP -*Citrus Paradisi*

DBPs - Disinfection byproducts

DNA - Deoxyribonucleic acid

DWAF - Department of Water Affairs and Forestry

DWS - Department of Water and Sanitation

EDS - Energy dispersive X-ray spectroscopy

FAAS - Flame atomic absorption spectrometry

FTIR - Fourier Transform Infrared Spectroscopy

HCl - Hydrochloric acid

IC - Ion chromatography

ICU - Intense care unit

KCl - Potassium chloride

MDR - Multidrug resistance

MEUF - Micellar enhance ultrafiltration

NaOH - Sodium hydroxide

PEUF - Poly Enhance ultrafiltration

P*m*PD -Poly-meta phenylenediamine

PPD - Poly (Para-phenylenediamine)

RCS - Reduced Chi-Square

RMSE - Root mean square errors

RO - Reverse osmosis

ROS - Reactive oxygen species

SANS - South African National Standards

SEM - Scanning electron microscopy

UF-Ultra - filtration

UV - Ultraviolet

WHO - World Health Organization

WWTPs - Wastewater treatment plants

XDR - Extremely drug resistance

XRD - X-Ray powder diffraction

Dissertation outline

The overall thesis is divided into 7 chapters, each with its specific details on how the dissertation was done. Their summaries are expanded below.

Chapter 1

This chapter gives a brief background of water pollution, its causes, and the impacts on humans as well as aquatic species. It also looks at how scientists have come up with new ways to combat the challenge of water pollution worldwide. Furthermore, the research objectives, hypothesis and significance were outlined.

Chapter 2

This chapter highlights in detail the causes and health effects of water pollutions coming from various sources (Cr^{6+}, Cd^{2+}, PO_4^{3-} and pathogens) and different techniques employed to eliminate the challenges associated with water pollution.

Chapter 3. Preparation, characterization and application of *Citrus paradisi* peel bio-sorbent uptakes of Cr and Cd ions in aqueous solutions

This chapter gives full details of how the experiment was carried out. It highlights the method of adsorbent preparation, solution preparation as well as the uptakes of Cr^{6+}, Cd^{2+} and PO_4^{3-} by *Citrus paradisi* bio-sorbent through batch experiments.

Chapter 4. Biosorption of toxic metal ions and nutrients from aqueous solution by diatom biomass

The biosorption of metal ions (Cr^{6+} and Cd^{2+}) and PO_4^{3-} ions by diatom biomass are fully described in this chapter. The details of adsorbent preparations, optimization procedures as well as the effect of the adsorbent on antimicrobial potency were tested.

Chapter 5. Biosorption, kinetic and thermodynamics studies of Cr and Cd metal ions and Phosphate ions by grapefruit peel/ diatom biomass adsorbent

This chapter gives details on the preparation of GFP/Diatom composite and its sorption uptakes on Cr^{6+}, Cd^{2+} and PO_4^{3-}, as well as determining the modeling parameters through kinetics, adsorption isotherms, and thermodynamics studies.

Chapter 6. Equilibrium, thermodynamic and kinetic investigations for biosorption of selected metal species, nutrients and pathogens in aqueous solutions by the fabricated biomass-polymeric adsorbent.

This chapter gives full details of the preparation of poly-phenylenediamine incorporated with GFP/diatom to make a biomass-polymeric adsorbent and test its efficiency in the removal of Cr^{6+}, Cd^{2+} and PO_4^{3-} ions from aqueous solutions as well as to test its antimicrobial potency. Furthermore, the kinetics, isotherms and thermodynamics were also determined to model the sorption process.

Chapter 7. Conclusions and recommendations

This is the last chapter that gives a detailed summary of the research findings as well as recommendations to improve the work done by opening new ways to explore for the better and effective ways to decontaminate water.

CHAPTER 1

1.1 Background Information

A variety of life forms depend on water to survive. Environmental pollution is a major problem that commenced many decades ago and has affected the cleanliness of water creating some serious environmental, political, social, and economic pressures globally (Kinzig *et al.*, 2013; Trevors, 2010). These concerns are mostly caused in the developing world due to industrial activities, poor sanitation, and inadequate waste management, which increases the world water stress resulting in human health risks and deterioration of environmental quality (Briggs, 2003). Thus, with environmental pollution, it is a challenge to maintain clean safe water for human consumption.

Surface and groundwater use has been of tremendous application across the globe for various purposes. However, the quality of such water has lost its value and is greatly affected by the discharging of heavy metals, sewage effluents, and other pollutants due to various natural and anthropogenic activities. Deterioration of these water resources quality has recently been observed in many equatorials (Odume et al., 2012; Singh et al., 2004; Tara et al., 2003) with the potential to cause contamination that poses a serious threat to human health and other living species.

According to several reports, water scarcity already affects every continent, with about 700 million people in over 43 countries suffering from water scarcity, and two-thirds of the world's population currently living in areas that experience water scarcity for at least one month a year (World Health Organization and UNICEF, 2017; Mekonnen and Hoekstra, 2016; Hameeteman, 2013). Water scarcity leads to declining water quality, thus, affecting the socio-economic conditions and aquatic environment. South Africa is one of the water-scarce countries due to an increase in temperatures and seasonal rainfall (Kock, 2017). It receives mean annual precipitation of 497 mm and mean annual evaporation of 1100 mm to 3000 mm, which exceeds water received from rain (Mantel et al., 2010; Dallas, 2000). South Africa has a limited and critical supply of water, and the quality of this water is being threatened by pollution arising from an increase in human population, urbanization, and rapid industrialization, which is the source of the economy.

Groundwater resources are particularly vulnerable to heavy-metal inputs, which are not degradable and may accumulate in living organisms as well as affecting the health and reproduction of many species, posing a serious threat to biological diversity in the ecosystems (Halpern et al., 2008). The pollution of water resources by heavy metals such as chromium, cadmium, and nutrients such as nitrates and phosphates as well as pathogens is a growing concern in all water resources. In some cases, these pollutants are found in trace amounts due to natural sources while in other cases are in high amounts due to anthropogenic activities.

Metal ions such as hexavalent chromium and cadmium are some of the most concerning toxic metals in water bodies that are carcinogenic and are persistent causing severe health problems such as organ damage, reduced growth and development, nervous system impairments, and oxidative stress on humans and animals (Lee et al., 2012). The sources resulting in contamination of this water come from a wide range of industries such as tanning, electroplating, smelting, paint pigments, batteries, mining, metal processing, electronics, and agriculture (Ibrahim and Mutawie, 2013; Gupta and Nayak, 2012; Mousavi and Seyedi, 2011).

Surface water, on the other hand, in addition to excessive discharge of toxic chemical species from industries, is mostly affected by nutrients, such as phosphates and nitrates, especially from agriculture and sewage water due to the dysfunction of sewage-treatment plants. This poses serious environmental problems, which affect human health and aquatic species when consumed in higher amounts. Excess nutrients result in oxygen deficiency due to algal bloom which consumes all the oxygen in water, thus affecting most aquatic species and often result in their death.

Water pollution also influences the breeding of pathogenic micro-organisms, which cause waterborne diseases (e.g., cholera, diarrhea, and gastrointestinal problems) especially in rural areas where lack of portable water is a burden. Globally, according to the World Health Organization, at least 2 billion people use drinking water sources contaminated with feces, and more than 3.4 million people die annually as a result of water-related diseases, thus, making it the highest source of disease and death around the world (W.H.O, 2011; Berman, 2009).

Studies have been carried out on how to remediate and mitigate these toxic chemical species and pathogens from water. Such methods for metal ion removal from aqueous solutions include chemical precipitation, chemical oxidation, and reduction, ion-exchange, filtration, electrochemical treatment, reverse osmosis, evaporative recovery, and solvent extraction (Mdlalose et al., 2017; Bilal et al., 2013; Saeed et al., 2010; Arief et al., 2008; Acar and Malkoc,

2004). However, these methods come with challenges of their own, for example, chemical precipitation is ineffective when metal ion concentrations are low or when they settle down (Bilal et al., 2013). These methods are also difficult to comply with strict demanding environmental regulations, time-consuming and the treatment costs are higher (Liu et al., 2013). Some of the techniques require high maintenance, for example, rejuvenating the resins in the ion-exchange methods to maintain the effective target pollutants' removal as well as the introduction of secondary pollutants (Bilal et al., 2013; Ferroudj et al., 2013).

The continued search for viable, improved properties and sustaining technologies propelled scientists to explore the development of composite materials for removing these pollutants through the use of eco-friendly and biological methods. Bio-sorption, phytoremediation, and biomonitoring using different materials as reported by several works of literature are the alternative safe methods for the clean-up and well-functioning pollutant-free water for improved human health and ecosystem (Saravanan et al., 2019; Kassaye et al., 2017). Bio-sorption is a method that is cost-effective, sustainable, and eco-friendly and does not require chemicals to aid in more pollution to the environment. Bio-sorption methods use naturally available bio-sorbent materials from algae, agricultural and forest, fungal, bacterial, activated carbon, and yeast (Bilal et al., 2013).

As already alluded to earlier, water pollution is a serious problem for the health of humans and the ecosystem as a whole. Therefore, an urgent need for developing robust, economically feasible, and environmentally friendly techniques to remove these pollutants from water and to safeguard the health of affected populations and ecosystems should be explored. This work involved the bioremediation of toxic metal ions, nutrients, and pathogens in water using a biomass polymeric adsorbent

1.2 Problem statement

Most surface and groundwater are vulnerable to waste discharge effluents from society. The source of effluents comes from industries (mining, tanning, electroplating, etc.), agricultural practices, sewage water, etc. (Kock, 2017). The pollution of water resources due to the indiscriminate disposal of toxic metals has been causing worldwide concern for the last few decades because they are hazardous to humans, terrestrial and aquatic ecosystems (Tchounwou et al., 2012; Matlala et al., 2011). This resulted in water regarded as "unfit" for drinking or other activities.

South Africa is a water-scarce country, and most of the water treatment plants are not functioning properly or have been abandoned. According to Sipho Kings of Mail and Guardian (2017), "South Africa's municipal sewage system has largely collapsed. Of the 824 treatment plants, maybe only 60 release clean water". Donnenfeld, (2018) indicated that South Africa only treats about 50% of its wastewater, while similarly arid Israel treats about 90%. The 'Green Drop' report of 2014, by the Department of Water and Sanitation (DWS), also concluded that about 25% of South Africa's wastewater treatment facilities are in a 'critical state' and need urgent intervention, while about another 25% are defined as 'high risk' in terms of disrepair (Makhafola, 2018). The dilapidating state of water and sanitation infrastructure in rural towns, especially in the provinces such as the Eastern Cape, Frees State, Mpumalanga, North West, and Limpopo have led to the growing incidences of raw sewage from municipal sanitary sewers contaminating local river systems.

Furthermore, the South African economic growth relies mostly on mining activities. Though these activities are important for economic growth, their effects on water quality and human health are of great concern (DWAF, 1996). Heavy metals are generally considered as inhibitors of life processes (Bonanno et al., 2017). Prolonged consumption of water containing toxic metals like cadmium in humans, affects almost all systems and functions of the human body, and also toxic to aquatic organisms at low concentrations. Additionally, a higher dosage of chromium (VI) causes respiratory, cardiovascular, gastrointestinal, and neurological problems in humans (Goyer, 2016; ATSDR, 2008). In aquatic species, acute exposure leads to reduced cell viability and stimulated Reactive Oxidation Species (ROS) production altering the glucose transport rate in the epithelial cells as well as hindering the ion-dependent ATPase in gills, kidneys, and intestines of coastal teleost at different concentrations (Goyer, 2016; Velma et al., 2009).

Additionally, high amounts of nutrients such as nitrates and phosphates in water cause the accumulation of algae, which depletes oxygen in the water and cause the death of aquatic organisms as well as terrestrial organisms that consume such water. Also, the contamination of water resources aid in pathogen accumulation in water which has become a problematic issue being the source of many water-related outbreaks of diseases if proper treatment and monitoring of water resources are not cared for (Haydar et al., 2016).

The exploration and development of biological and polymeric materials for effective removal and recovery of toxic metals, nutrients, and pathogens from the contaminated water have

emerged as a potential alternative method to conventional technique because of its excellent adsorption towards metal ions, nutrients, and pathogens, cost-effectiveness, eco-friendliness and sustainability (Mdlalose et al., 2017; Bhatnagar et al., 2015; Torab-Mostaedi et al., 2013; Saeed et al., 2010). Therefore, this study is aimed at developing a multifunctional (targets metal ions, nutrients and pathogens) biomaterial with a sustainable, cost-effective technique, which can reduce toxic substances from polluted water sources to environmentally acceptable levels.

1.3 Objectives

To develop and evaluate a biomass polymeric adsorbent for the removal of toxic metals (chromium and cadmium ions), nutrients (nitrate and phosphate ions), and pathogens from aqueous solutions.

1.3. 1 Specific objectives

1. To fabricate a biomass polymeric adsorbent using grapefruit, diatom biomass, and poly-phenylenediamine.
2. To evaluate the structural and morphological properties of the fabricated adsorbent materials.
3. To evaluate the sorption capacity of the adsorbent in removing metal species and nutrients.
4. To model the sorption processes using the fundamental adsorption isotherm and kinetic models.
5. To determine antibacterial activity of the biomass polymeric adsorbent.

1.4 Hypothesis

The developed biomass polymeric adsorbent can effectively remove toxic metal species, nutrients, and antimicrobial activity in water.

1.5 Significance of the study

Water pollution remains a global crisis affecting human health, terrestrial and aquatic organisms hence there is a need to solve this problem to have a clean environment. Safe wastewater treatment methods have always been a challenge to society; conventional wastewater treatment plants are not designed to remove toxic metal species like Cd, Pb, Cr but to reduce BOD, and nutrients. Most wastewater treatment plants in South Africa are in a dire state and some are receiving loads beyond their design capacity resulting in inadequate

treatment or discharge of raw sewage into the environment. An example is that of a case which was once shared on the news about the Vaal system due to the problems arising from the Emfuleni local municipality and Sedibeng district. This led to high coliform counts such as *E-coli*, which is the main source of water-borne diseases, which put the people of Sebokeng and other fellow South Africans at serious health risk, as well as causing an ecological disaster (Bega, 2018). The consequences thereof include eutrophication, blooming of harmful cyanobacteria, salinity, and toxic metal contamination of agricultural soils. Additionally, agricultural waste products such as grapefruit peels and algae biomass are known to create an ecological burden to the environment such as land and air pollution due to the decaying processes of the waste; damaging fish gills, producing toxins that affect molluscan shellfish, marine mammals, birds, and even humans (Trainer et al., 2008).

Consequently, this study will focus on using biomass materials due to their unique chemical composition, abundance, and renewability as an essential resource in the purification of polluted water towards environmental remediation. These materials will be incorporated onto a polymeric matrix to produce a sustainable, eco-friendly, and non-toxic multifunctional bio-based adsorbent material for simultaneous removal of chemical and microbial pollutants from water. This will also reduce the use of chemicals, which in the long run creates negative impacts on the environment and provide clean water to the people as well as improving the ecological status of water resources.

References

Acar, F.N. and Malkoc, E. 2004. The removal of chromium (VI) from aqueous solutions by Fagus orientalis L. *Bioresource Technology*, *94*(1), pp.13-15.

Agency for Toxic Substances and Disease Registry (ATSDR). (2008). Toxicological Profile for Chromium. Public Health Service, U.S. Department of Health and Human Services. Atlanta, GA

Arief, V.O., Trilestari, K., Sunarso, J., Indraswati, N. and Ismadji, S. 2008. Recent progress on biosorption of heavy metals from liquids using low cost biosorbents: characterization, biosorption parameters and mechanism studies. *CLEAN–Soil, Air, Water*, *36*(12), pp.937-962.

Bega, S. 2018. Sewage pollution from Emfuleni system sparks health and ecological 'crisis'. Accessed from https://www.iol.co.za/saturday-star/news/sewage-pollution-from-emfuleni-system-sparks-health-and-ecological-crisis-15503098

Berman, J., 2009. WHO: Waterborne disease is world's leading killer. *VOANews. US Government, Last updated on October*, *29*, p.12.

Bhatnagar, A., Sillanpää, M. and Witek-Krowiak, A., 2015. Agricultural waste peels as versatile biomass for water purification–a review. *Chemical Engineering Journal*, *270*, pp.244-271.

Bilal, M., Shah, J.A., Ashfaq, T., Gardazi, S.M.H., Tahir, A.A., Pervez, A., Haroon, H. and Mahmood, Q. 2013. Waste biomass adsorbents for copper removal from industrial wastewater-a review. *Journal of Hazardous Materials*, *263*, pp.322-333.

Bonanno, G., Borg, J.A. and Di Martino, V. 2017. Levels of heavy metals in wetland and marine vascular plants and their biomonitoring potential: a comparative assessment. *Science of the Total Environment*, 576, pp.796-806.

Briggs, D. 2003. Environmental pollution and the global burden of disease. *British Medical Bulletin*, *68*(1), pp.1-24.

Dallas, H.F. 2000. November. Ecological reference conditions for riverine macroinvertebrates and the River Health Programme, South Africa. In: Proceedings of the First WARFSA/WaterNet Symposium: Sustainable Use of Water Resources, pp. 1–10.

Donnenfeld, Z. 2018. S Africa wastewater facilities in disrepair. Accessed from http://www.engineeringnews.co.za/topic/zachary-donnenfeld

DWAF (Department of Water Affairs and Forestry). 1996. South African Water Quality Guidelines. Vol. 1: Domestic water use: 71.

Ferroudj, N., Nzimoto, J., Davidson, A., Talbot, D., Briot, E., Dupuis, V., Bée, A., Medjram, M.S. and Abramson, S. 2013. Maghemite nanoparticles and maghemite/silica nanocomposite microspheres as magnetic Fenton catalysts for the removal of water pollutants. *Applied Catalysis B: Environmental*, 136, pp.9-18.

Goyer, R.A. 2016. Metal Toxicology: Approaches and Methods. *Elsevier*.

Gupta, V.K. and Nayak, A. 2012. Cadmium removal and recovery from aqueous solutions by novel adsorbents prepared from orange peel and Fe_2O_3 nanoparticles. *Chemical Engineering Journal*, *180*, pp.81-90.

Halpern, B.S., Walbridge, S., Selkoe, K.A., Kappel, C.V., Micheli, F., D'agrosa, C., Bruno, J.F., Casey, K.S., Ebert, C., Fox, H.E. and Fujita, R. 2008. A global map of human impact on marine ecosystems. *Science*, *319*(5865), pp.948-952.

Hameeteman, E. 2013. Future water (In) security: facts, figures, and predictions. *Global Water Institute*, pp.1-16.

Haydar, S., Arshad, M. and Aziz, J.A. 2016. Evaluation of drinking water quality in urban areas of Pakistan: A case study of Southern Lahore. *Pakistan Journal of Engineering and Applied Sciences.*

Ibrahim, W.M. and Mutawie, H.H. 2013. Bioremoval of heavy metals from industrial effluent by fixed-bed column of red macroalgae. *Toxicology and Industrial Health*, 29(1), pp. 38-42.

Kassaye, G., Gabbiye, N. and Alemu, A., 2017. Phytoremediation of chromium from tannery wastewater using local plant species. *Water Practice & Technology*, *12*(4), pp.894-901.

Kinzig, A.P., Ehrlich, P.R., Alston, L.J., Arrow, K., Barrett, S., Buchman, T.G., Daily, G.C., Levin, B., Levin, S., Oppenheimer, M. and Ostrom, E. 2013. Social norms and global environmental challenges: the complex interaction of behaviors, values, and policy. *BioScience*, 63(3), pp.164-175.

Kock, A. 2017. Diatom diversity and response to water quality within the Makuleke Wetlands and Lake Sibaya (Doctoral dissertation, North-West University (South Africa), Potchefstroom Campus).

Lee, J.C., Son, Y.O., Pratheeshkumar, P. and Shi, X. 2012. Oxidative stress and metal carcinogenesis. *Free Radical Biology and Medicine*, 53(4), pp.742-757.

Liu, L., Wu, J., Li, X. and Ling, Y. 2013. Synthesis of poly (dimethyldiallylammonium chloride-co-acrylamide)-graft-triethylenetetramine-dithiocarbamate and its removal performance and mechanism of action towards heavy metal ions. *Separation and Purification Technology*, *103*, pp.92-100.

Makhafola, D. 2018. South African wastewater facilities in disrepair. Accessed from http://www.engineeringnews.co.za/article/s-africa-wastewater-facilities-in-disrepair-2018-07-06/rep_id:4136

Mantel, S.K., Hughes, D.A. and Muller, N.W.J. 2010. Ecological impacts of small dams on the South African rivers part 1: drivers of change - water quantity and quality. *SA Journal of Radiology*, 36(3), pp. 351-360.

Matlala, M.D., Taylor, J.C. and Harding, W.R. 2011. Development of a diatom index for wetland health. Pretoria: Water Research Commission.

Mdlalose, L., Balogun, M., Setshedi, K., Tukulula, M., Chimuka, L. and Chetty, A., 2017. Synthesis, characterization and optimization of poly (p-phenylenediamine)-based organoclay composite for Cr (VI) remediation. *Applied Clay Science*, *139*, pp.72-80.

Mekonnen, M.M. and Hoekstra, A.Y. 2016. Four billion people facing severe water scarcity. *Science Advances*, 2(2), p.e1500323.

Mousavi, H.Z. and Seyedi, S.R. 2011. Nettle ash as a low-cost adsorbent for the removal of nickel and cadmium from wastewater. *International Journal of Environmental Science and Technology*, 8(1), pp. 195-202.

Odume, O.N., Muller, W.J., Arimoro, F.O. and Palmer, C.G. 2012. The impact of water quality deterioration on macroinvertebrate communities in the Swartkops River, South Africa: a multimetric approach. *African Journal of Aquatic Science*, *37*(2), pp.191-200.

Saeed, A., Sharif, M. and Iqbal, M., 2010. Application potential of grapefruit peel as dye sorbent: kinetics, equilibrium and mechanism of crystal violet adsorption. *Journal of Hazardous Materials*, *179*(1-3), pp.564-572.

Saravanan, A., Jayasree, R., Hemavathy, R.V., Jeevanantham, S., Hamsini, S., Yaashikaa, P.R., Manivasagan, V. and Yuvaraj, D., 2019. Phytoremediation of Cr (VI) ion contaminated soil

using Black gram (Vigna mungo): Assessment of removal capacity. *Journal of Environmental Chemical Engineering*, *7*(3), p.103052.

Singh, K.P., Mohan, D., Sinha, S. and Dalwani, R. 2004. Impact assessment of treated/untreated wastewater toxicants discharged by sewage treatment plants on health, agricultural, and environmental quality in the wastewater disposal area. *Chemosphere*, 55(2), pp. 227-255.

Kings, S. 2017. 50000 litres of sewage flow into SA's rivers every second. *Mail and Gurdian.* Accessed from https://mg.co.za/article/2017 07 21

Tara, V., Yadav, A.V.S. and Bose, P. 2003. Analysis of photosynthetic activity in the most polluted stretch of river Ganga. *Water Research*, 37(1), pp. 67-77.

Tchounwou, P.B., Yedjou, C.G., Patlolla, A.K., and Sutton, D.J. 2012. Heavy metal toxicity and the environment. In Molecular, Clinical and Environmental Toxicology, 32(9-10), pp.133-164.

Torab-Mostaedi, M., Asadollahzadeh, M., Hemmati, A. and Khosravi, A. 2013. Equilibrium, kinetic, and thermodynamic studies for biosorption of cadmium and nickel on grapefruit peel. *Journal of the Taiwan Institute of Chemical Engineers*, *44*(2), pp.295-302.

Trainer, V.L., Hickey, B.M. and Bates, S.S. 2008. Toxic diatoms. *Oceans and Human Health: Risks and Remedies from the Sea*, pp.219-237.

Trevors, J.T., 2010. What is a Global Environmental Pollution Problem? *Water, Air, and Soil Pollution*, 210(1-4), pp 1–2

Velma, V., Vutukuru, S.S., and Tchounwou, P.B. 2009. Ecotoxicology of hexavalent chromium in freshwater fish: A Critical Review. *Reviews on Environmental Health*, 24(2), p. 129

WHO. (2011). Nitrate and nitrite in drinking water. Accessed from http://www.who.int/water_sanitation_health/dwq/chemicals/nitratenitrite2ndadd.pdf

World Health Organization and UNICEF, 2017. Progress on drinking water, sanitation and hygiene: 2017 update and SDG baselines.

CHAPTER 2

2.1 Introduction

Water pollution is a global concern affecting the world, especially African countries. Sources of water pollution (Fig. 1) can be from domestic and agricultural effluents, industrial waste, and oil spillage. These are caused mainly by population growth, development, and the lack of knowledge on good management practices, and this has accelerated the water pollution crisis throughout the world. Therefore, these sources of water are heavily polluted with toxic metals, nutrients, and pathogens resulting in poor water quality.

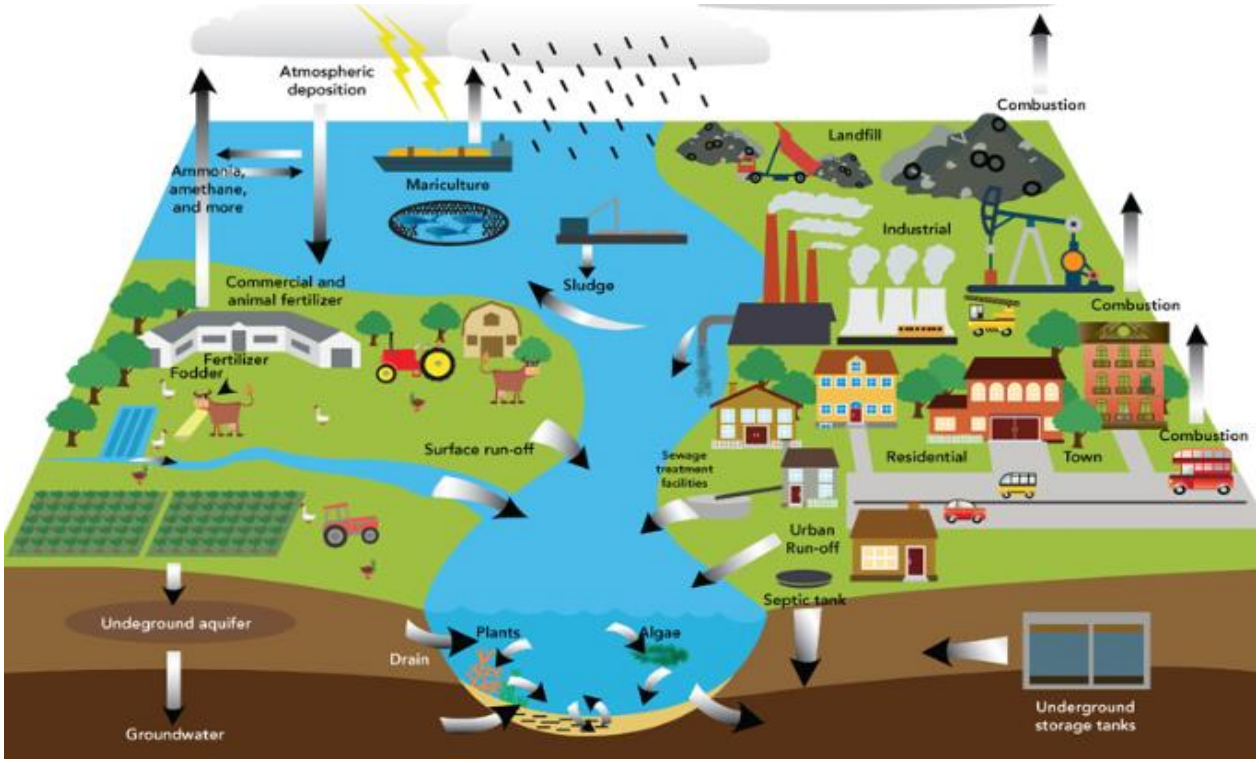

Fig. 1: Sources of water pollution (filterwater.com (2018)).

2.2 Heavy metals

Heavy metals are elements that occur naturally and are present in various concentrations in the environment. These are elements with a specific density higher than 5 gm/cm^3 or an atomic number of more than twenty and can be found in elemental form and other compounds (Khan et al., 2014; Ilyin et al., 2004). Their distributions in the environment are directed by the metal properties and the influences of environmental factors (Khlifi and Hamza-Chaffai, 2010). Heavy metal sources can be from natural or anthropogenic activities such as the burning of fossil fuels, mining, and smelting of metalliferous ores, municipal and industrial wastes,

pesticides as well as fertilizers (Al-Bahry et al., 2013; Al-Musharafi et al., 2012; Bourotte et al., 2009; Acar and Malkoc, 2004; Han et al., 2003). Heavy metals are directly and indirectly discharged into water bodies, and they are not easily removed since they are persistent (Uddin, 2017). In this study, the heavy metals of concern are Cr^{6+} and Cd^{2+}. These heavy metals are some of the concerning pollutants in the environment and cause a lot of health and environmental problems.

2.2.1 Chromium: Sources, uses, and impacts

Chromium is one of the metals which is necessary for animals and human beings. Bourotte et al. (2009) indicated that although natural sources of chromium are not common, mafic and ultramafic rocks show higher concentrations of chromium than other rock types. Chromium, as one of the pollutants, has positive and negative impacts. Although chromium is an abundant element in the earth's crust and occurs in oxidation states ranging from Cr^{2+} to Cr^{6+}, only the trivalent and hexavalent are of apparent significance, with the trivalent being more stable (Walker et al., 2019; Fishbein, 1981). Chromium (VI) is an oxi-anion, meaning it exists as chromate ($CrO4^{2-}$) and dichromate ($Cr_2O_7^{2-}$) (Shanker, 2019). The occurrence and distribution of chromium in the environment are illustrated in Fig. 2. In this figure, Cr occurs in two major oxidation states, which are Cr (III) and Cr (VI). Cr (III) may be oxidized to Cr (VI) by oxidizing compounds existing in the soil and at the same time Cr (VI) can be reduced to Cr (III) by chemicals such as MnO_2 in the presence of reduced MnO and organic acids from soil organic matter, soluble ferrous iron and reduced sulfur compounds (Cook et al., 2000).

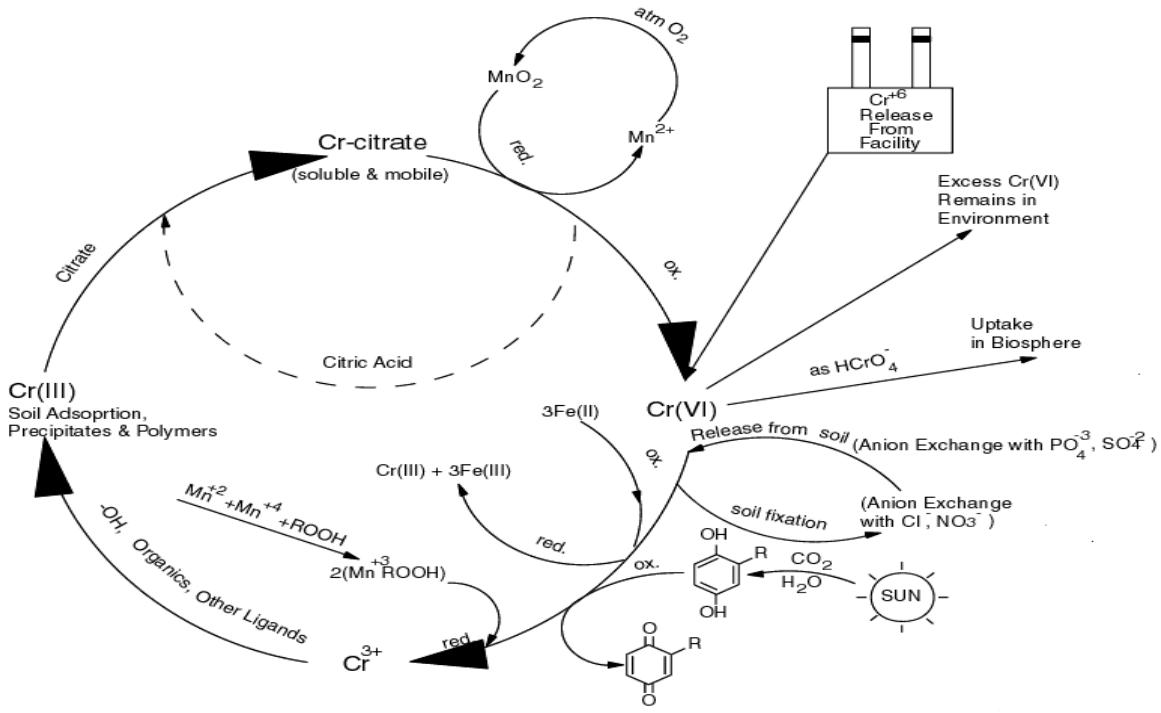

Fig. 2: The chromium cycle (USEPA, 2000).

Chromium species (Cr (III) and Cr (VI)) usually enter the environment from the discharge of various effluents from human anthropogenic activities such as chemical industries, steel works, electroplating, and tanning. The minimum tolerance limit for Cr is below 0.1 mg/L for discharge into surface water and 0.05 mg/L for potable drinking water (WHO, 1993). Moreover, chromium may contaminate drinking-water supply systems due to the corrosion inhibitors which are used in water pipes and containers or from underground water due to sanitary landfill leaching (Gupta and Nayak, 2012; Hosseini and Sarab, 2007).

Generally, chromium performs different functions within the body of living organisms, however, Cr (VI) is very toxic (Shraddha et al., 2015; Arief et al., 2008). Cr (VI) is associated with health problems such as skin rashes, weakened immune systems, kidney and liver damage, alteration of genetic material (DNA transcription processes), cancer, respiratory, cardiovascular, gastrointestinal, neurological problems in humans as well as damaging the sperm and reproductive systems in animals and sometimes death in humans (Goyer, 2016; Tchounwou, 2012; ATSDR, 2008; WHO/IPCS, 1998). Figure. 3 shows some of the health problems that are associated with Cr (VI).

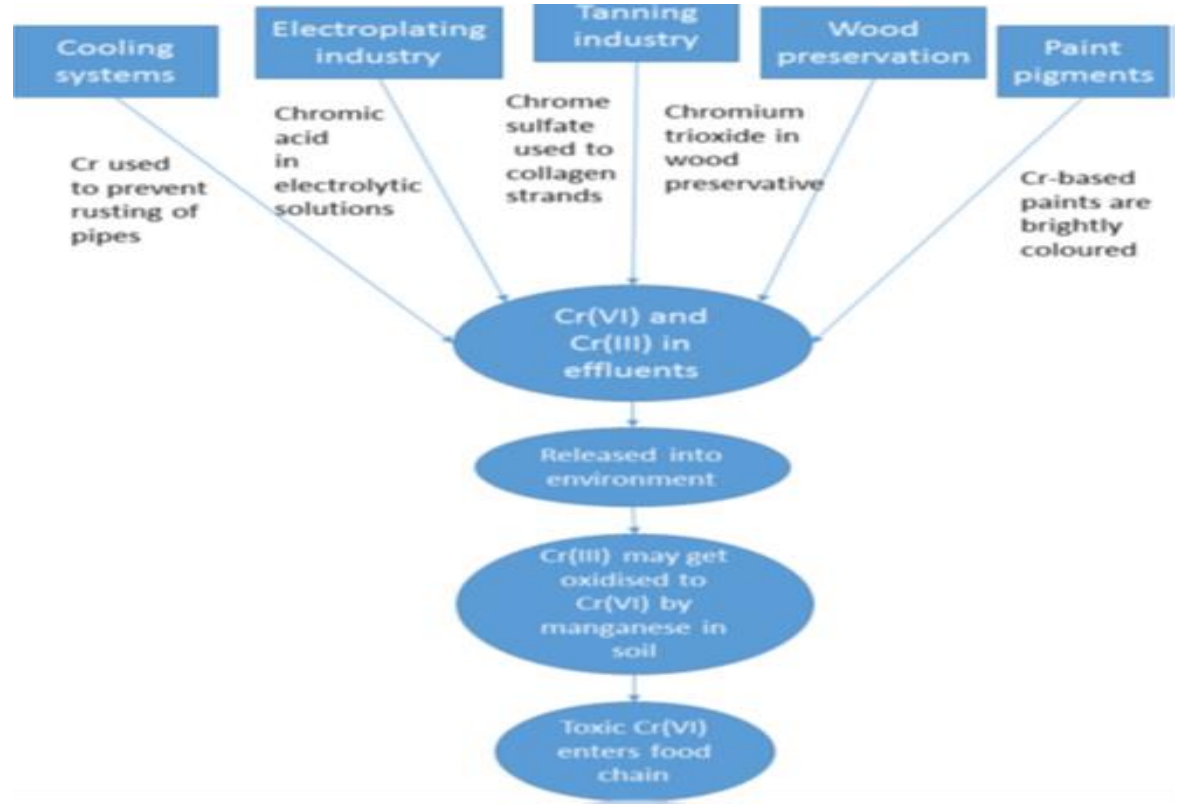

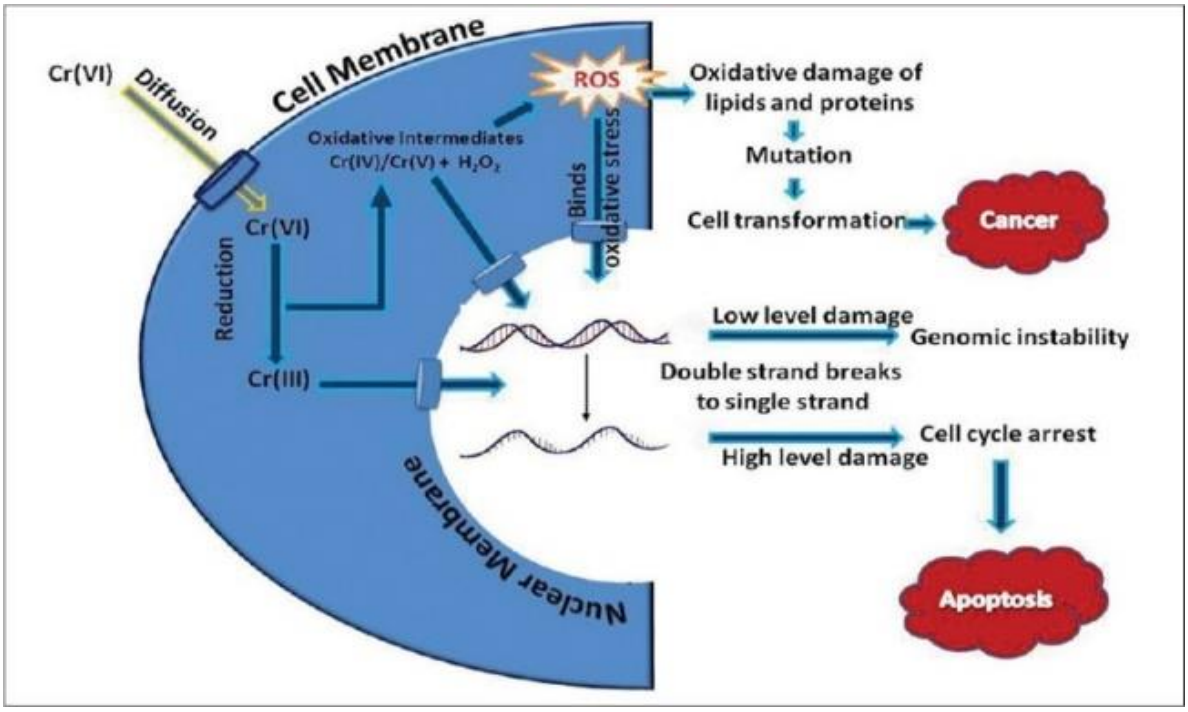

Fig. 3: Various releases and toxicity of hexavalent chromium (Mitra et al., 2017; Baduel et al., 2013)

In aquatic species, acute exposure of goldfish by chromium significantly leads to reduced cell viability and stimulated ROS production, and it alters the glucose transport rate in epithelial cells of the intestine of fish species, as well as affecting the osmoregulatory functions.

Furthermore, it hinders the ion-dependent ATPase in the gills, kidney, and intestine of coastal teleost at different concentrations (Goyer, 2016; Velma et al., 2009).

2.2.2 Cadmium: Sources, uses and impacts

Cadmium is one of the rarer elements in nature, frequently occurring with zinc in a Zn/Cd mixture, and can generally be from volcanic emissions, tobacco, industrial and agricultural activities, etc. (Adams et al., 2011; Fishbein, 1981). It can be found on the earth's crust, air soil, and water in small amounts from weathering of rocks. Cadmium has many uses for industrial applications such as high thermal and electrical conductivity, excellent corrosion resistance, low melting temperature, high ductility, cadmium-nickel batteries, photographic materials and is usually recovered as a by-product from the smelting and refining of zinc ores (Adams et al., 2011; Sahmoun et al., 2005). However, cadmium poses some serious health problems to humans and animals. Some of the health problems associated with cadmium include kidney damage, renal disorder, Itai Itai (excruciating pain in the bone) hepatic damage, lung damage, cancer, and hypertension. It also affects blood pressure, prostate function, and testosterone levels (Goyer, 2016; Martin and Griswold, 2009). In aquatic organisms, cadmium causes acute and chronic effects which ultimately cause death. For example, cadmium concentration of 0.03 mg/L kills small salmon fish (Barnes et al., 1997) and can cause hemolymph acidosis in crabs (Mebane, 2006; Rodríguez et al., 2001). Furthermore, cadmium causes high blood pressure, iron-poor blood, liver disease, and nerve/brain damage as well as affecting the birth weight and skeleton development in animals (Levit, 2010). Cadmium can be accumulated from the soil or irrigation water as shown in Fig. 4.

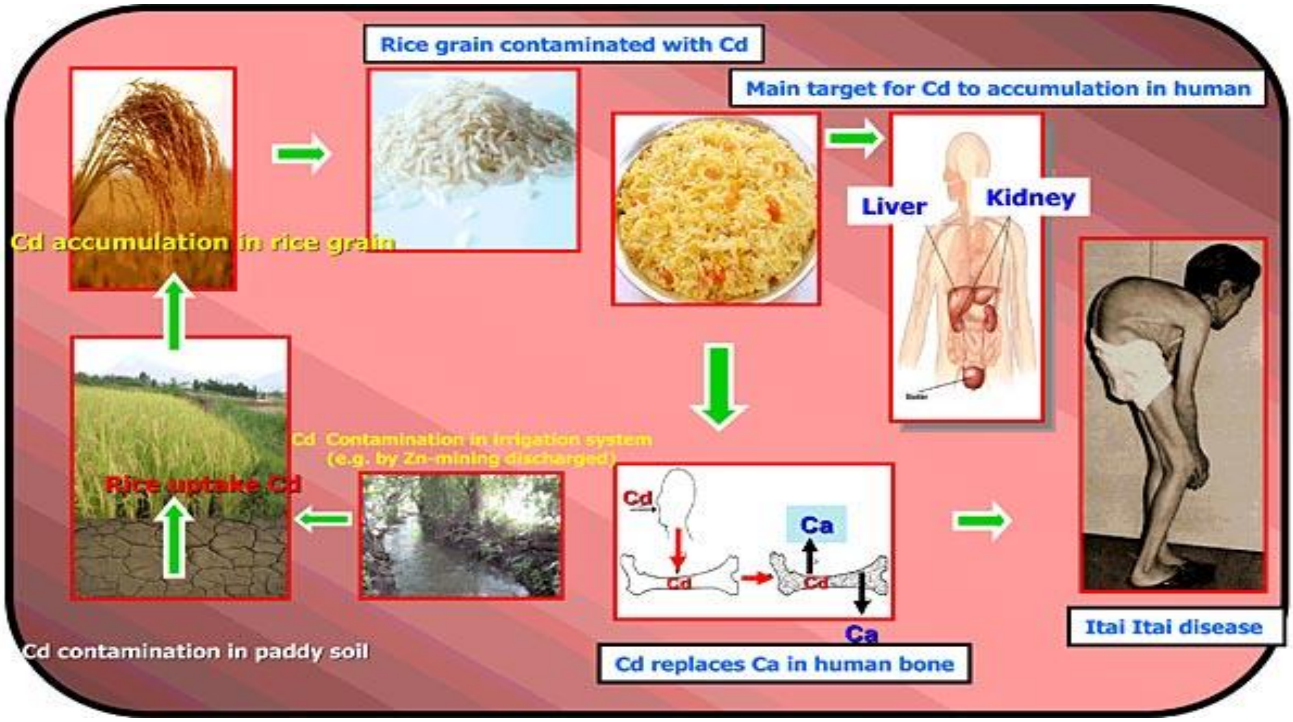

Fig. 4: Transportation and effects of cadmium on humans (Megan and Tehmeedah, 2013).

2.3 Nutrients

Water bodies require some nutrients to be healthy, but too much can be harmful. Phosphates and nitrates are nutrients that occur naturally in water, but they can be increased by anthropogenic activities. The waste generated through these activities leads to harmful effects, which can affect the quality and functioning of the ecosystem.

Phosphorus is an important nutrient, but when in excessive amounts, pollutes water resources. It is essential for cellular growth and reproduction especially in plants, and for converting sunlight into usable energy. The chemical compositions of phosphorus can be in oxo-acidic form, dihydrogen phosphate, hydrogen phosphates, phosphate, and phosphoric acid. It also occurs in dissolved organic and inorganic forms or attached to sediment particles (Hanrahan et al., 2005). According to Warwick et al. (2013), water resources are considered polluted with phosphates once the phosphorus concentration exceeds 0.025 mg/L. Moreover, the phosphate permissible limit set by SANS (2011) is 10 mg/L. Phosphate is naturally found in water at low concentrations but can be harmful when in excess. The distribution of phosphorus relating to the occurrence of phosphates in the environment is illustrated in Fig. 3.

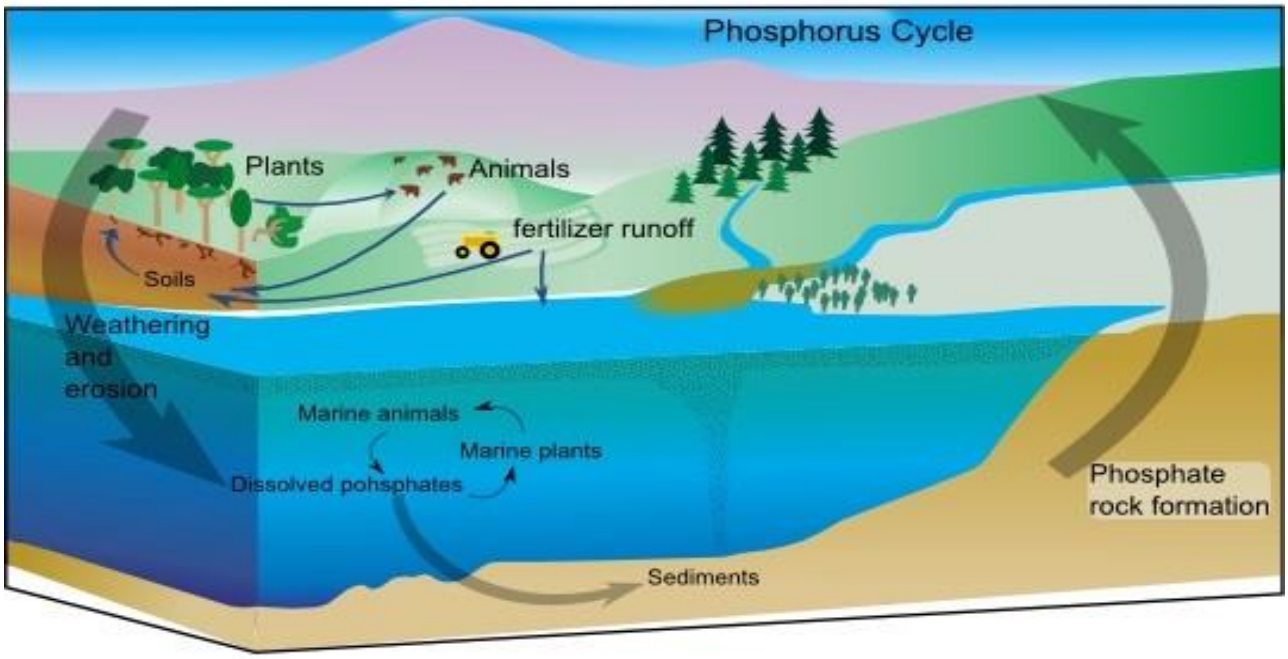

Figure 5: The phosphorus cycle (Biology dictionary, 2017).

Too much phosphates in water tend to be dire especially for aquatic organisms. The booming of phosphates causes eutrophication (Macintosh et al., 2018), and kills fish due to insufficient oxygen supply in water as well as an unpleasant smell which affects the quality of water and recreational activities. Generally, as highlighted earlier, phosphates are not toxic to people or animals, however, when present in very high amounts tend to cause some digestive problems (Kumar and Puri, 2012).

Nitrogen, on the other hand, is vital to the production of plant and animal tissues, it is used to synthesize proteins. However, it is among the major pollutants that contribute to environmental quality problems worldwide. Nitrification, and denitrification which is illustrated in Fig. 4. may occur in surface water, depending on the temperature and the pH (WHO, 2011). These are the processes that facilitate the nitrogen cycle. Nitrates have various uses for industrial purposes, especially in agriculture wherein they are used to make fertilizers. The agricultural sector is the major contributor to water pollution since these fertilizers and pesticides are discharged into the streams especially after irrigation or rainfall. This often affects the health of humans and animals over prolonged consumption, which often leads to death. A typical example resulting from higher levels of nitrate consumption in young children and pregnant women is a blue baby syndrome, methemoglobinemia, and nitrate poisoning in animals due to insufficient oxygen

supply in the blood (Kumar and Puri, 2012). Therefore, there is a need to reduce and maintain the natural nutrient level in water for the proper functioning of the ecosystem.

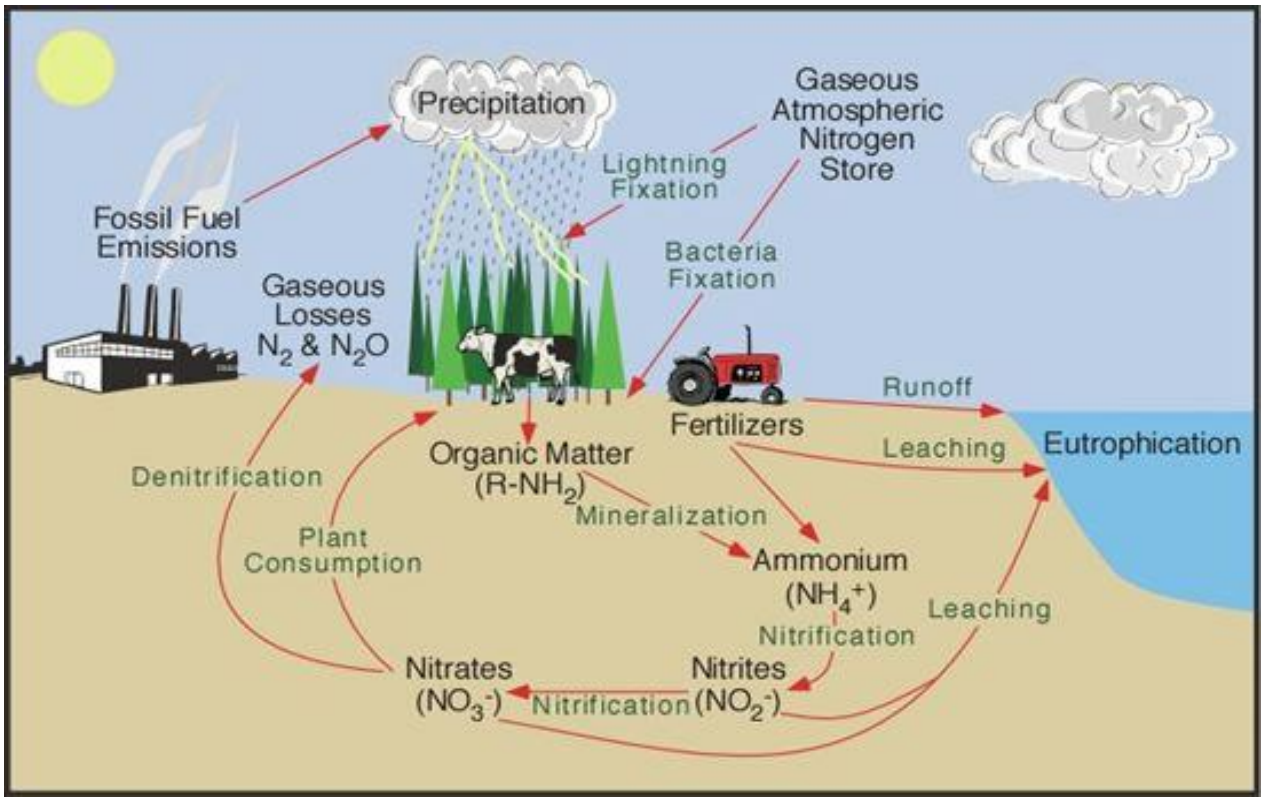

Figure 6: Sources and pathways of nitrate in the geosphere (www.physicalgeography.net), (Pidwirny, 2006)

2.4 Water borne pathogens

The majority of acute water-related diseases are often associated with microbiological contamination. In rural areas, the contamination of water sources is a result of contamination from routine activities such as manure applications, grazing operations, wastewater treatment plants (WWTPs), failing septic systems, washing of wildlife clothes, utensils, and livestock as well as drinking directly from the water source as a result of poor or lack of awareness and maintenance (Gumbo et al., 2016, Parajuli et al., 2009).

The major micro-organisms found in wastewater effluents are viruses, bacteria, fungi, protozoa, and helminths (Akpor and Muchie, 2011). These pollutants are of public health concern and have resulted in a high number of water-related diseases and death across the globe. Microbes are majorly distributed in nature, and their abundance and diversity may be used as an indicator for the suitability of water (Okpokwasili and Akujobi, 1996). Examples of water pathogens of high fecal origin associated with serious disease-causing pathogens include

Cryptosporidium species, *Escherichia coli*, Salmonella species, *Klebsiella pneumoniae*, *Entamoeba histolytica*, *Giardia* and *Cryptosporidium*, hepatitis A and Norwalk (Kumar and Puri, 2012; ODHS, 2002;). In this work, the bacterial pathogens of interest include *E-Coli*, *Klepsiella pneumoniae* and *Staphylococcus aureus*.

The coliform bacteria can have detrimental impacts on human beings such as vomiting, diarrhea, and nausea. These micro-organisms can cause various diseases such as cholera, gastroenteritis, giardiasis typhoid fever, dysentery, and hepatitis (Thilakarathne et al. 2018; Dankovich et al., 2016; Naidoo and Olaniran, 2013; Parker 1970). According to WHO/UNICEF (2015), waterborne diseases such as diarrhea and cholera are responsible for 2.2 million deaths each year, especially in developing countries, with the majority occurring in children under the age of five.

E-coli is a gram-negative bacterium that is found in healthy human and animal intestines. The presence of E-coli in water shows some indications of fecal contamination either from humans or animals. Moreover, eating uncooked meat, unpasteurized milk and person-to-person contact are some of the sources of getting *E-coli*. There are a variety of strains of *E-coli* and most of them are harmless, they can only cause mild diarrhea, however, the strain O157:H7 is known to be pathogenic and be associated with some of the above-mentioned sources and has led to deaths (ODHS, 2002). This strain belongs to a group of *E. coli* that produces a powerful toxin that damages the lining of the small intestines hence causing severe and bloody diarrhea. However, common methods of treating *E-coli* contaminated waters include the use of chlorine, ultraviolet light, or ozone. Moreover, common prevention methods for humans are to avoid eating undercooked meat, washing hands regularly, and drinking pasteurized milk or juice.

Additionally, *Klepsiella pneumoniae* is gram-negative bacteria that belong to the *Enterobacteriaceae* family. They are natural residents of the humans and animal microbiome, regularly colonizes human mucosal surfaces and gastrointestinal tract. Moreover, this kind of bacteria causes pneumonia, surgical wound infections, urinary tract infections (Effah et al., 2020). *K. pneumoniae* is very much common in the United States causing a variety of hospital-acquired pneumonia and this bacterium has been reported to colonize the Chinese ethnicity and people who experience chronic alcoholism. Furthermore, this organism has resulted in high extended hospitalization, mortality rates, and costs (Giske et al., 2008; Gupta, 2002). Moreover, this bacterium has some resistance towards antibiotics which makes it hard to treat patients infected by it (Lee et al., 2017; Giske et al., 2008).

Staphylococcus on the other hand, according to the Centers for Disease Control and Prevention (CDC) is a type of bacterial or a germ that is found in the nose of most people. It is a gram-positive bacterium that can cause infections, especially in health care units. Infections such as bacteraemia or sepsis (occurs when bacteria spread to the bloodstream of an individual); pneumonia (especially to people with underlying lung diseases); endocarditis (an infection of the heart valves can lead to heart failure or stroke). Moreover, when the staphylococcus bacteria travel in the bloodstream, it causes a bone infection which is known as osteomyelitis (Fortuin-de Smidt et al., 2015; CDC, 2011). Additionally, *S. Aureus* affects people with chronic conditions such as diabetes, cancer, vascular disease, eczema, lung disease, and people who inject drugs, including those in intensive care units (ICUs). However, it has also been reported that humans have antibacterial peptides such as human α- and β-defensins, cathelicidin LL-37, and others which are usually found in various parts of their bodies to protect against *S. aureus* (Nakatsuji et al., 2017; Chen et al., 2005). Other common methods of prevention are the practice of good hygiene and regular or frequent hand wash practices.

The lack of rational water management methods and improved sanitation has deteriorated both physicochemical and biological quality of ground and surface waters in South Africa. However, with improved water supply, proper wastewater treatment practices and sanitation with better management of water resources can reduce waterborne diseases, alleviate poverty, and even boost the economy.

2.5 Conventional wastewater treatments

Several technologies have been developed over the years to remove toxic metals from aqueous solutions. Conventional methods in the removal of heavy metal ions from wastewater include ion-exchange, solvent extraction, chemical precipitation, membrane filtration, electrochemical treatment, adsorption (Haimi et al., 2020; Nekouei et al., 2019; Sillanpää and Shestakova, 2017; Fu and Wang, 2011; Huang et al., 2006).

2.5.1 Ion-exchange

The ion exchange technique has been widely used for the removal of heavy metal ions from wastewater due to its several advantages (Kang et al., 2004). Ion-exchange resins, which could be synthetic or natural have specific abilities to exchange its cations with the metals` in the wastewater. In most cases, ion exchange enables replacing the undesirable ion with another one which is neutral within the environment, meaning an ion that is suitable for a particular environment. A good scenario is that of water purification where the mineral content has to be

removed from the water. For example, an H^+ resin will be added to the water to replace all the cations, through a secondary resin that contains OH^- will replace all the anions in the water, and this leaves the H^+ and OH^- reacting together to produce more water. Additionally, the most preferred resins are synthetic ones due to their effectiveness in removing heavy metals from water (Arroyo et al., 2019; Nekouei et al., 2019; Alyüz and Veli, 2009). According to Fu and Wang (2011), the most common cation exchangers are strongly acidic resins with sulfonic acid groups ($-SO_3H$) and weakly acid resins with carboxylic acid groups (-COOH). Moreover, the hydrogen ions on both groups serve as exchangeable ions with metal cations. For example, when the solution containing heavy metal passes through the cation column, metal ions are exchanged for hydrogen ions. However, there are certain parameters such as pH, temperature, initial metal concentration and contact time which tend to affect the uptake of heavy metal ions by ion-exchange resins (Gode and Pehlivan, 2006).

2.5.2 Chemical precipitation

Chemical precipitation is one of the effective and widely used chemical processes in industries because of its simplicity and inexpensive to operate (Ku and Jung, 2001). Additionally, Fu and Wang (2011) reported that chemicals tend to react with heavy metal ions and form insoluble precipitates which are separated from water by sedimentation or filtration. Moreover, the treated water is kept for reuse.

However, since precipitation is accompanied by flocculation or coagulation, one of the major problems is the formation of large amounts of sediments containing heavy metal ions. Furthermore, parameters such as pH, temperature and controlled stirring intensities seem to play important roles in determining the precipitation processes (Dąbrowski et al., 2004). Moreover, these drawbacks are time-consuming which sometimes make the chemical precipitation unsuitable for wastewater treatment. Chemical precipitation processes include hydroxide and sulfide precipitation whereby the hydroxide precipitation is the most common and widely used technique due to its simplicity and ease to use, low cost, and ease of pH control (Huisman et al., 2006). Moreover, a variety of hydroxide precipitations using lime, $Ca(OH)_2$ and NaOH to remove heavy metals have been reported (Chen et al., 2009; Mirbagheri and Hosseini, 2005; Baltpurvins et al., 1997). Apart from hydroxide precipitation, sulfide precipitation is effective for treating toxic heavy metal ions and has the advantage of producing solubilities of metal sulfide precipitates which are greatly lower than those of hydroxide precipitates (Fu and Wang, 2011).

2.5.3 Filtration

There are two primary types of filtration which involve particle and membrane filtration. Particle filtration is used to separate solids from liquids using either physical or mechanical means. The common types of filters in particle filtrations include self-cleaning filters, bag filters and cartridges. The characteristics which affect the choice of filters are the particle size, texture, density of particles, shape and quantity of adsorbent material.

Filtration generally uses pollutant capturing media such as zeolites, cotton, sand, charcoal, and polymeric membranes (Fauzi et al., 2020). One more type of filtration is membrane filtration which involves the use of reverse osmosis (RO), ultrafiltration, microfiltration, nanofiltration and electrodialysis (Fu and Wang, 2011). RO is one of the modern technologies invented to purify water using a semi-permeable membrane so that it can be suitable for a wide range of applications. Fig. 7. Illustrate a typical setup of the process. RO can remove up to 99% of the organics, dissolved salts and bacteria from water. However, some of the disadvantages of RO include removing essential minerals such as iron, calcium, manganese and fluoride together with the unwanted pollutants from the water. This becomes a problem especially for people who rarely eat foods that are rich in vitamins and minerals. When coupled with drinking demineralized water, such people become prone to vitamin and mineral deficiency.

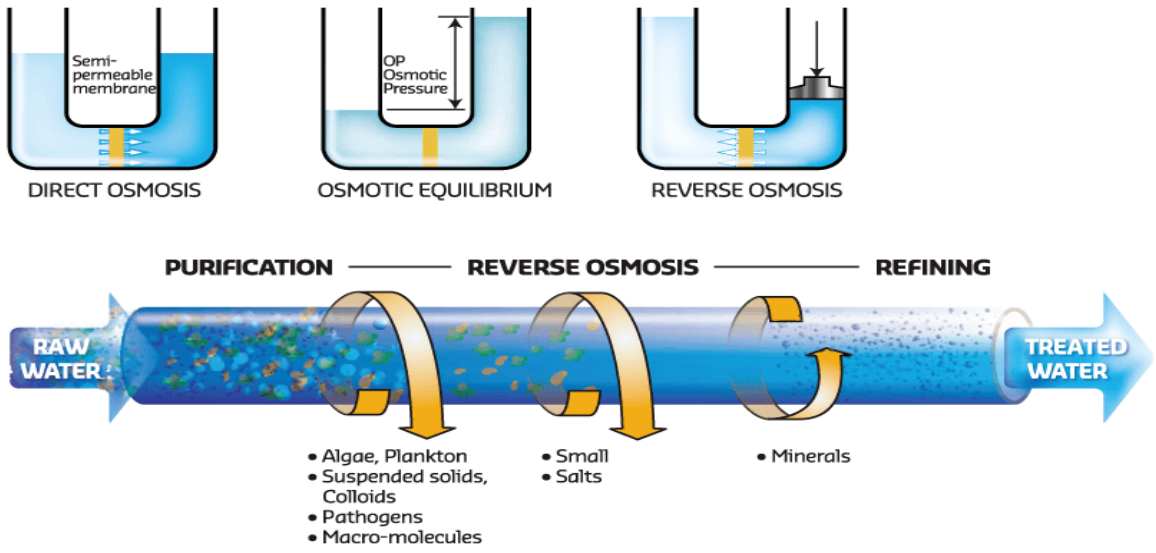

Fig. 7: Reverse osmosis model (Drink Filtered, 2020).

Additionally, ultrafiltration and microfiltration are usually used as precursors to reverse osmosis treatment. Furthermore, ultrafiltration (UF) removes particles larger than 10 nm and helps to remove organic material that has high molecular weight, silt and pathogens (Haimi et

al., 2020; Barredo-Damas et al., 2010). The advantages of this process include high flux and operation at low pressure. However, this technique cannot produce high quality of water to reuse, due to this, ultrafiltration is proposed to be used as a pretreatment for other membrane processes (Bourgeous et al., 2001). Other drawbacks have to do with the pore size of these membranes which is larger than the dissolved metal ions hence allow them to pass through the ultrafiltration membranes which affect the removal efficiency of metal ions. As a result, micellar enhanced ultrafiltration (MEUF) and polymer enhanced ultrafiltration (PEUF) have been proposed to obtain high removal efficiency of metal ions (Fu and Wang, 2011). Moreover, nanofiltration acts as an intermediate between RO and UF. The benefits of this technique include its reliability, easy to operate, high efficiency of pollutant removal and consumes low energy (Erikson,1988). A variety of studies reported good results on the removal and recovery of heavy metals from wastewater using nanofiltration on binary metals such as cadmium and nickel (Murthy and Chaudhari, 2009). Nanofiltration together with RO has also been reported to remove and recover metals such as copper and silver (Cséfalvay et al., 2009; Koseoglu and Kitis, 2009).

On the other hand, electrodialysis is used to separate cations and anions that are across charged by membranes that exchange from one solution to another using an electric field as the driving force (Gurreri et al., 2020; Fu and Wang, 2011). Electrodialysis can be used in various applications such as biochemistry, pharmaceuticals, and food processing (Gurreri et al., 2020). Moreover, it is also widely used in wastewater treatments to remove or recover metals and metal ions. Itoi et al. (1980) recovered 90% of Ni^{2+} from wastewater through a pilot study. Mohammadi et al. (2004) removed ~ 97% Cu^{2+}. Moreover, Cr removal and recovery by electrodialysis have also been studied and proved to work successfully (Dos Santos et al., 2019; Alvarado et al., 2013).

2.5.4 Electrochemical treatment

Electrochemical treatment is a process of treating wastewater by electrode reactions caused by the passing of electric current which helps to recover metals in their elemental metal (Sillanpää and Shestakova, 2017). The techniques involved in electrochemical treatment include electrocoagulation, electro-flotation, and electrodeposition which have gained prominence worldwide (Wang et al., 2007). Variety of studies reported successful results of heavy metal removal from electrocoagulation processes such as Zn^{2+}, Cu^{2+}, Ni^{2+}, Ag^{+} and $Cr_2O_7^{2-}$ (Heidmann and Calmano, 2008). Additionally, Parga et al. (2005) used this process for the

removal of arsenic with a removal efficiency of > 99 % while Ölmez, (2009), removed Cr (VI) with a removal efficiency of 100%.

Electro-flotation, on the other hand, involves floating pollutants on the surface of a water body generated from water electrolysis. Belkacem et al. (2008) studied the applications of electro-floatation of heavy metals using aluminum electrodes and yielded over 99% removal on cadmium, lead, copper, iron and others. One of the advantages of electro-flotation is being able to arrange electrodes to cover the whole surface of the flotation system, leaving nothing behind. Electrodeposition has usually been used for the recovery of metals from wastewater and is considered a clean technology due to the absence of permanent separation of heavy metals (Issabayeva et al., 2006). Apart from the successful results of heavy metal removal from electrochemical treatment, there are some drawbacks to this technique that have been generally reported which involves relatively large capital investment and the expensive electricity supply (Fu and Wang, 2011).

Although these techniques seem to work, with several disadvantages such as inefficient for treating high volumes of dilute discharge due to high reagent/energy cost, or incomplete metal removal. Researchers move to look for more convenient, less complicated, affordable, less cost and sustainable methods that involve using fewer chemical methods.

2.6 Microbial techniques

The overburdening of municipal sewage plants due to overpopulation, especially in urban areas, results in the discharge of partially treated sewage effluents which results in surface water contaminations (Hicks et al., 2017). As a result, a variety of techniques have been employed for the eradication or reduction of pathogens that are faced in water quality. However, the techniques towards pathogen removals are based on the sorption principle as well as disrupting the cell walls of the microbes, by attacking the cell membrane of the pathogen through what is known as chemically-cell death particularly towards or at the point of use (Dankovich et al., 2016).

The majority of acute water-related diseases are often associated with microbiological contamination. These pollutants are of public health concern and have resulted in a high number of water-related diseases, with over 3.4 million deaths, mostly children across the globe (WHO and UNICEF, 2017). As a result of this, new methods have been explored in using fewer toxic materials that are environmentally friendly and sustainable.

The common practices of pathogen treatment include chlorination, ceramic filtration, boiling water, UV water purification and ozone disinfection. However, the use of these conventional methods has their shortcomings such as high cost, toxic nature, and production of non-eco-friendly byproducts and nonbiodegradable stabilizing agents which tends to affect the environment and human beings (Singhal et al., 2011). Moreover, (UV) ultraviolet and chlorination become a challenge because they tend to form harmful carcinogenic disinfection byproducts (DBPs) (Dimapilis et al., 2018).

2.6.1 Chlorination

Chlorination is one of the water treatment methods used to purify water by using chlorine-rich compounds (liquids chlorine- sodium hypochlorite or dry chlorine- calcium hypochlorite) to kill pathogens. It does so by reacting with the cell components of the micro-organisms through diffusing and transporting into the cell, resulting in their death (Lee et al., 2011). Chlorination has been proven to be effective against bacteria and viruses, but sadly, it cannot inactivate all micro-organisms. The advantages of this method are that it is cheap and affordable, easy to use, quick to eliminate bacteria, controls odour, and prevents septicity. Moreover, it also helps to prevent the accumulation of toxic microorganisms in fish, shellfish, and other aquatic organisms (White, 1992; Haas and Hutzler, 1986). However, the other concern associated with chlorination is the formation of by-products (Chu et al., 2016; Richardson, 2011). Furthermore, the short-term health effects of chlorine in water (swimming pools) cause nausea, vomiting, a burning sensation in the throat, bloody nose, burning sensation and eye irritation, coughing or wheezing, chest pain, shortness of breath, irritated feeling on the skin and build-up of fluid in the lungs (Hattersley, 2003).

2.6.2 Ceramic filtration

Ceramic filtration systems involve the use of ceramic water filters that are easy to use, affordable because the filter is locally produced, and can easily be deployed at household levels for water purifications to provide safe drinking water for all. Moreover, ceramic water filters prove to reduce bacteria and protozoa in the laboratory, it also has a long life if the filter remains unbroken (Gumbo et al., 2016). The drawback associated with the ceramic filtration system is unknown effectiveness against viruses. The porosity is of microns which allows some contaminants to pass through. This occurs as a result of blockages of the pores due to continuous use of the ceramic water filter which results in poor trapping of pathogens. Therefore, necessitates cleaning of the ceramic water filters to remove the trapped contaminates (Kallman, et al., 2011). A typical ceramic filtration process is shown in Fig. 8.

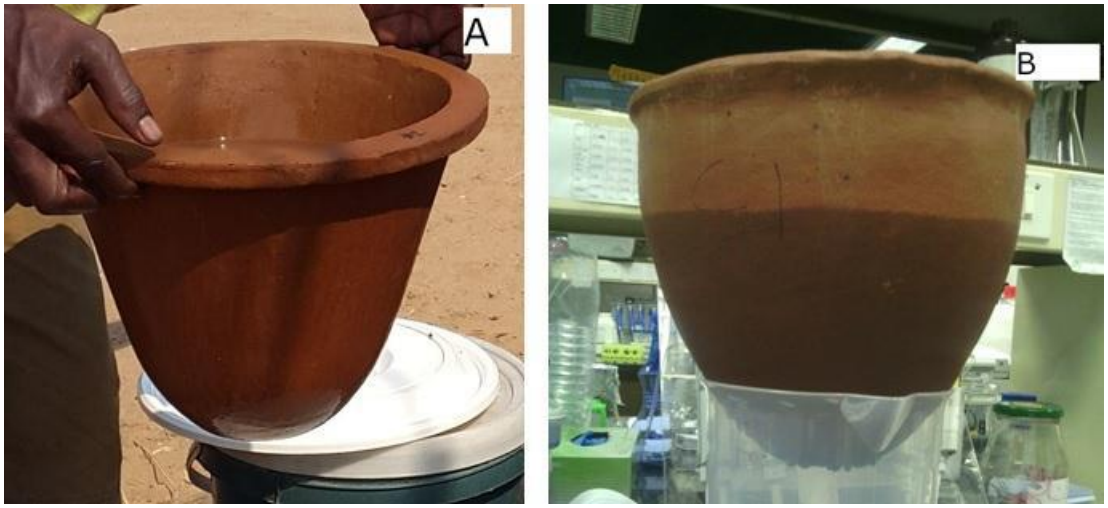

Fig. 8: Ceramic Water Filters (A) clay incorporated with silver nanoparticles from Mukondeni, Limpopo South Africa, (B) clay incorporated with sawdust from Sese, Zimbabwe. Adopted from Tshishonga and Gumbo (2017).

2.6.3 UV water purification

UV water purification is a water treatment technique that uses UV radiation to target and kill pathogenic microorganisms by altering the DNA in the cells and impeding reproduction (Gong et al., 2012; Hallmich and Gehr, 2010). This technique is known to be an effective disinfectant against viruses, bacteria, and even protozoans like *Giardia lamblia* cysts or *Cryptosporidium* oocysts, due to its strong germicidal (inactivating) ability. The benefits of using UV as a water purification technique are that it does not add chemicals to the water, it does not add taste or odors to the water, the disinfection has no residual disinfection, and it is very much effective against bacteria and viruses even protozoa as mentioned above. The drawback of this technique, however, is that it does not remove contaminants, does not work during a power outage, high operating costs, require lots of maintenance and regular lamp replacements.

2.6.4 Ozone disinfection

Ozone is a powerful natural oxidising agent and a disinfectant which destroys pathogens and compounds through oxidation. It is also regarded as a promising disinfectant mostly for drinking water treatment especially for the inactivation of microorganisms (Ding et al., 2019). Disinfecting by ozone has its economic and environmental benefits. It is low cost and safe to produce and apply, it is also excellent for breaking down microorganisms and endotoxins. It is environmentally friendly in that it eliminates the risk of residual chemicals by converting residual ozone back to oxygen within a short time. A study by Kowalski et al. (1998) revealed

that ozone disinfection on *E. coli* and *S. aureus* was a success with more than 99% death rate on microbial species.

2.7 Bio-sorption as a water purification method

Bio-sorption as an adsorption method has been explored over the years in the removal of contaminants in water due to its cost-effective approach, ease of operation, being selective and effective, simple to design, works well at low concentrations, and environmentally friendly as compared to the other conventional methods (Abbas et al. 2016; Bhatnagar et al., 2015; Hammaini et al., 2002).

2.7.1 Agricultural waste: Grapefruit peel

Agricultural waste and by-products often create a serious environmental issue. However, these waste products have recently been utilized towards environmental remediation of toxic chemical species in polluted water. Bhatnagar et al. (2015) reviewed the importance of various agricultural waste peels as adsorbents for the removal of a variety of aquatic pollutants. The usefulness of these waste products in solving the environmental challenges is based on phytochemical properties (essential oils, fibers, phenols, vitamin c, antioxidants) cellulose, and polar functional groups of lignin. These inherent phytochemical species can bind aquatic pollutants through different binding mechanisms (Bhatnagar et al., 2015).

Agricultural bio-wastes such as banana skins, grapefruit peels, macadamia nutshells, hazelnut husk, and rice husks are effective in removing chromium (Cr) and Cd from wastewater (Qu et al., 2018; Deshmukh et al., 2017; Pakade et al., 2017; Pakade et al., 2016; Imamoglu et al., 2015; Park et al., 2008). The peel of grapefruits generally contains several water-soluble and insoluble monomers and polymers, containing carboxyl and hydroxyl functional groups, which bind cationic metal ions in an aqueous solution (Bhatnagar et al., 2015; Blackbum 2004). The peel of grapefruit has successfully been used to remove Cd (II), Ni (II), and crystal violet dye with high removal capacity via ion-exchange mechanisms from wastewater (Schiewer and Iqbal, 2014; Torab-Mostaedi et al., 2013; Saeed et al., 2010). Furthermore, Luo et al. (2014) utilized activated carbon from the grapefruit peel to remove malachite green from wastewater. On the other hand, Han et al. (2017) used the activated carbon from grapefruit peel to remove heavy metal Cu^{2+} ions. According to Rosales et al. (2016), grapefruit peels were used for the removal of chromium (VI) and leather dyes from tanning industries with a maximum uptake of 37.4 mg/g for the dyes, and 39.1 mg/g for the Cr (VI) sorption.

Citrus fruits and its peels are also known to possess antiviral, anticancer, anti-inflammatory, antiallergenic, analgesic activity (Benavente-García et al., 1997). They have also been reported to be biologically active, allopathic and antioxidants in nature as well as having bio-regulatory properties (Caccioni et al., 1994). Negi and Jayaprakasha (2001) reported the antibacterial potency of grapefruit peel extracted with hexane, acetone, chloroform and methanol against pathogens. The extracts, according to their report, were more effective against Gram-positive than Gram-negative bacteria. Vasek et al. (2015) also established that the essential oil of grapefruit peel has very strong potential applicability as a natural antibacterial agent. Hence grapefruit peels due to its phytochemical properties have antibacterial capabilities to help disinfect pathogens in water.

2.7.2 Algae

Marine biology researchers have recently used marine species for environmental remediation. Important marine alga is diatoms (Figure 7), which are unicellular photosynthetic micro-organisms found in aquatic and sub-aerial environments with high species diversity (Smucker and Vis, 2011). Diatoms are characterized by a unicellular silica-based cell wall and are a source of oxygen and the main food producers for animals (Borowitzka, 2013; Field et al., 1998). These types of algae are responsible for 40% to 45% of the total production of organic carbon compounds in the oceans, and they are important for the biogeochemical cycling of elements (Sarthou et al., 2005; Mann, 1999). Diatoms require nutrients such as nitrogen, phosphorus, silicon, and trace metals to survive and when they die, they form diatomaceous earth (Trainer et al., 2008). Diatoms are used for biomonitoring and assessment of the ecological status of rivers as indicators of water quality such as nutrient enrichment, acidification, and metal contamination (Dalu and Froneman, 2016). Diatoms can be used as a biological approach to removing toxic pollutants in the environment. Examples of diatoms include *Aulacoseira granulata, Gomphonema parvulum, Navicula sp*. and *Nitzschia sp*. (Kock, 2017).

Despite all the importance of diatoms, excessive growth of diatoms in the aquatic systems, however, can pose a serious problem. When they reach a bloom stage, they grow spines that can damage fish gills, produce toxins that affect the molluscan shellfish, marine mammals, birds, and even humans (Trainer et al., 2008). They can also cause paralytic, diarrheic and neurotoxic shellfish poisoning as well as ciguatera fish poisoning (Landsberg et al., 2005). In humans, they can cause gastrointestinal problems as well as unusual nervous system

abnormalities, which can be seen through vomiting, abdominal cramps, diarrhea, headache and loss of short-term memory (Trainer et al., 2008; Perl et al., 1990).

The use of algae in removing toxic pollutants from aqueous solutions has been well reported (Kock, 2017; Yu et al., 2012). According to Yan et al. (2010), a biological approach using adsorption and biomass growth such as bacteria, algae and plants can be used for the removal of phosphates in water. Sbihi et al. (2014) used *planothidium lanceolatum* diatom as an adsorbent for the efficient removal of heavy metals (Cu, Cd and Zn) from wastewater. Diatoms were also used as filters for the removal of heavy metal cations from synthetic solutions containing As^{3+}, Ag^{+}, Ni^{2+}, Cr^{6+} and Pb^{2+}, and it was found that the removal rate was up to 95% for the rest of the metals (Hernández-Ávila et al., 2017; Kunugi et al., 2014). Yu et al. (2012) used chemically modified diatoms silica to remove mercury ions in water. Diatom use for the removal of metallic ions from aqueous solutions has been due to their negatively charged surface (Kunugi et al., 2014).

Fig. 9: Diatom (https://microscopesandmonsters.wordpress.com/tag/palaeontology/).

2.7.3 Phenylenediamines (PpD)

Adsorption of toxic metals and organic pollutants using polymers as carrier matrices have been proven to be effective because they are easily and effectively produced in a wide variety of compositions. These polymers can be modified into specific sorbents by introducing a variety of ligands in order to increase the adsorption capacity (Zhao et al., 2010; Zhang and Chen., 2002). The aniline polymers and its derivatives are known to be effective adsorbents for heavy metals and aromatic pollutants due to selective binding capacity and inherent multi-functional

groups (Stejskal 2015; Olad and Nabavi 2007). Among the derivative of polyaniline are the polyaromatic amines (diphenylamines and phenylenediamines). These amines have been extensively used in metal ion remediation over the conventional adsorbents due to the functional groups, the binding interaction of pollutants through electrostatic attraction, coordination or complex formation, hydrogen bonding and π-π stacking interaction (Mdlalose et al., 2017; Wang et al. 2008). Phenylenediamines ($C_6H_4(NH_2)_2$) (pPD) is a low toxicity diamine used as a component of engineering polymers and composites due to its unique properties, which include high-temperature stability, high strength, chemical and electrical resistance (Stejskal, 2015; Yu et al, 2013). It can be found in textile and hair dyes, in photographic developing agents as well as an antioxidant in rubber compounds when it is in para-phenylenediamine (Al-Suwaidi and Ahmed, 2010).

Various polymerization techniques have been reported by studies especially on the synthesis of polyaromatic diamine used for environmental pollution monitoring and remediation, which include chemical polymerization, electrochemical polymerization, and enzyme-catalysed oxidative polymerization.

2.7.3.1 Chemical polymerization

This is a widely used polymerization technique due to its simplicity to produce polyaromatic diamines and polydiphenylamines. The polymerization technique mechanism assumes that the polymerization occurs according to cation-radical interaction followed by poly recombination of cation-radical intermediates during oxidation (Orlov et al. 2006). The chemical oxidation methods occur by adding an oxidant into the reaction mixture of a monomer solution. For instance, in a normal polymerization reaction, a measured amount of p-phenylenediamine is dissolved in a minimal amount of diluted hydrochloric acid solution. The solution is further mixed with an oxidant such as ammonium peroxydisulphate which changes the solution colour related to the polyaromatic diamine formation. It is therefore is left for 24 h and the residue is collected by filtration or centrifuging and washed by deionized water (Mdlalose et al., 2017).

Huang et al. (2006) discovered that the polymerization of phenylenediamine isomers strongly depends on the monomer structure as well as the solution polymerization medium in the adsorption behavior of metal ions on micro-particles. According to Stejskal (2015), the polymerization of aromatic diamines such as phenylenediamines is usually prepared in an acidic medium (HCl and glacial acetic acid) using effective oxidants which includes persulphate, iodine, hydrogen peroxide, iron (III) chloride, ceric ammonium nitrate and copper

nitrate. Usually, the resultant product is dried at 60 or less to avoid crosslinking of polymers (Li et al., 2002).

2.7.3.2 Electrochemical polymerization

The principle of electrochemical polymerization is based on the deposition of the polymer onto the surface of solid electrode material and the polymerization process is attained by the existence of electrical current through a solution of the monomer, solvent and electrolyte mixture (Fomo et al., 2019). Generally, electrochemical polymerization is used for the synthesis of electroactive conducting polymer films due to its simplicity and reproducibility (Zhao et al., 2011). Moreover, the polymerization techniques involved in electrochemical polymerization for aromatic amines include constant current (galvanostatic), cyclic voltammetry (potentiodynamic) and constant potential (potentiostatic) (Fomo et al., 2019; Li et al., 2002).

The electrochemical polymerization technique produces thin films which are deposited at the surface of the electrode. Moreover, the suitable power supply for this technique is cyclic voltammetry due to its potential of revealing the reversibility of electron transfer during the polymerization process as well as scanning the electroactivity of the polymer film. Moreover, the cyclic voltammetry is dependent on the species and concentration of the monomer, electrolyte and electrode used. Furthermore, electrochemical polymerization has been found convenient and used on various immobile conducting polymers (Heinze et al., 2010).

2.7.3.3 Enzyme-catalysed oxidative polymerization

Polyaromatic amines can also be produced by enzyme-catalysed oxidative polymerization. A typical example of this polymerization process involved using horseradish peroxidative as a catalyst in a mixture of 1,4-dioxane and phosphate buffer to give out polymeric materials by Li et al. (2002), where it was noted that a high concentration of 1,4-dioxane decreased the yield of the polymerization process, which could have been due to the catalyst (horseradish peroxidative) denaturation by 1,4-dioxane. Moreover, the enzyme-catalysed polymerization method is dependent on the reaction time, solvent composition, monomer properties and the amount of oxidant (Mdlalose et al., 2017).

Furthermore, **s**tudies have shown the applicability of these amines and their isomers in the removal of toxic chemical species in wastewater. Yu et al. (2013) reported that different oxidation states of P*m*PD (poly-meta-phenylenediamine) as an adsorbent can bind Cr (VI) ion through electrostatic interactions with the reduction of Cr (VI) to Cr (III). This was supported

by (Yu et al., 2013) who discovered that P*m*PD exhibits excellent redox properties and are favorable for Cr (VI) adsorption. Furthermore, Jouad et al. (2005) used polydiphenylamine resin for the removal of Ni, Cu, Zn, Pb and Cd with the total sorption capacity of 57.3 mg g^{-1} for Ni (II), 23 mg g^{-1} for Cu (II), 36.9 mg g^{-1} for Zn (II), 19 mg g^{-1} for Pb (II) and 24.5 mg g^{-l} for Cd (II). Several works have also been conducted on pPd derivatives and its composites; and were proven to be effective in the remediation of metal pollutants in water (Tian et al., 2015; Nabid et al., 2014; Li et al., 2011; Jouad et al., 2005). According to Huang et al. (2006), the search for an effective and economical method of eliminating toxic heavy-metal ions requires the consideration of unconventional materials and processes. Bio-sorption is a method of using green-based materials considered to solve environmental issues, it has been reported that various low-cost adsorbents developed from different origins show little or poor adsorption potential for the removal of aquatic pollutants. Therefore, this work revolves around developing a robust, sustainable and multifunctional bio-based/biopolymer materials adsorbents for the removal of these pollutants in water.

References

Abbas, A., Al-Amer, A.M., Laoui,T., Al-Marri, M.J., Nasser,M.S., Khraisheh, ,. And Atieh, M.A., 2016. Heavy metal removal from aqueous solution by advanced carbon nanotubes: Critical review of adsorption applications. *Separation and Purification Technology, 157*, pp.141-161.

Acar, F.N. and Malkoc, E. 2004. The removal of chromium (VI) from aqueous solutions by Fagus orientalis L. *Bioresource Technology, 94*(1), pp.13-15.

Adams, S.V., Newcomb, P.A., Shafer, M.M., Atkinson, C., Bowles, E.J.A., Newton, K.M. and Lampe, J.W. 2011. Sources of cadmium exposure among healthy premenopausal women. *Science of the Total Environment, 409*(9), pp.1632-1637.

Agency for Toxic Substances and Disease Registry (ATSDR). (2008). Toxicological Profile for Chromium. Public Health Service, U.S. Department of Health and Human Services. Atlanta, GA

Akpor, O. B. and Muchie, B., 2011. Environmental and public health implications of wastewater quality. *African Journal of Biotechnology, 10*(13), pp. 2379-2387.

Al-Bahry, S., Mahmoud, I., Al-Rawahy, S. and Paulson, J.R., 2013. Egg contamination as an indicator of environmental health. In *Eggs: Nutrition, Consumption and Health*, pp. 1-24.

Al-Musharafi S. K., Mahmoud I. Y. and Al-Bahry S. N., 2012. Heavy metal contamination from treated sewage effluents. *WIT Transactions on Ecology and the Environment*, 164, pp. 381-9

Alvarado, L., Torres, I.R., and Chen, A., 2013. Integration of ion exchange and electrodeionization as a new approach for the continuous treatment of hexavalent chromium wastewater. *Separation and purification Technology*, 105, pp. 55–62.

Alyüz, B. and Veli, S., 2009. Kinetics and equilibrium studies for the removal of nickel and zinc from aqueous solutions by ion exchange resins. *Journal of Hazardous Materials, 167*(1-3), pp.482-488.

Al-Suwaidi, A. and Ahmed, H., 2010. Determination of para-phenylenediamine (PPD) in henna in the United Arab Emirates. *International Journal of Environmental Research and Public Health, 7*(4), pp.1681-1693.

Arief, V.O., Trilestari, K., Sunarso, J., Indraswati, N. and Ismadji, S., 2008. Recent progress on biosorption of heavy metals from liquids using low cost biosorbents: characterization, biosorption parameters and mechanism studies. *CLEAN-Soil, Air, Water*, *36*(12), pp.937-962.

Baltpurvins, K.A., Burns, R.C., Lawrance, G.A. and Stuart, A.D., 1997. Effect of electrolyte composition on zinc hydroxide precipitation by lime. *Water Research*, *31*(5), pp.973-980.

Barnes, K.H., Meyer, J.L. and Freeman, B.J., 1997. Sedimentation and Georgia's fishes: An analysis of existing information and future research. Georgia Institute of Technology.

Barredo-Damas, S., Alcaina-Miranda, M.I., Bes-Piá, A., Iborra-Clar, M.I., Iborra-Clar, A. and Mendoza-Roca, J.A., 2010. Ceramic membrane behavior in textile wastewater ultrafiltration. *Desalination*, *250*(2), pp.623-628.

Belkacem, M., Khodir, M. and Abdelkrim, S., 2008. Treatment characteristics of textile wastewater and removal of heavy metals using the electroflotation technique. *Desalination*, *228*(1-3), pp.245-254.

Benavente-García, O., Castillo, J., Marin, F.R., Ortuño, A. and Del Río, J.A., 1997. Uses and properties of citrus flavonoids. *Journal of Agricultural and Food Chemistry*, *45*(12), pp.4505-4515.

Bhatnagar, A., Sillanpää, M. and Witek-Krowiak, A., 2015. Agricultural waste peels as versatile biomass for water purification–a review. *Chemical Engineering Journal*, *270*, pp.244-271.

Biology dictionary, 2017. Phosphorus Cycle. Accessed from https://biologydictionary.net/phosphorus-cycle/

Blackbum, R.S., 2004. Natural polysaccharides, their interactions with dye molecules: applications in effluent treatment. *Environmental Science & Technology*, *38*(18), pp. 4905-4909.

Borowitzka, M.A., 2013. High-value products from microalgae-their development and commercialisation. *Journal of Applied Phycology*, *25*(3), pp.743-756.

Bourgeous, K.N., Darby, J.L. and Tchobanoglous, G., 2001. Ultrafiltration of wastewater: effects of particles, mode of operation, and backwash effectiveness. *Water Research*, *35*(1), pp.77-90.

Bourotte, C., Bertolo, R., Almodovar, M. and Hirata, R., 2009. Natural occurrence of hexavalent chromium in a sedimentary aquifer in Urânia, State of São Paulo, Brazil. *Anais da Academia Brasileira de Ciências*, *81*(2), pp.227-242.

Caccioni, D.R.L., Ruberto, G., Wang, C. and Rapisarda, P., 1994. Role of essential oil components on the resistance of citrus fruits to Penicillium spp. *Environmental biotic factors in integrated plant disease control. Poznan, Polland*, pp 185-188.

Centers for disease control and prevention (CDC), 2011. *Staphylococcus aureus* in Healthcare Settings. Accessed from https://www.cdc.gov/hai/organisms/staph.html

Chen, X., Niyonsaba, F., Ushio, H., Okuda, D., Nagaoka, I., Ikeda, S., Okumura, K. and Ogawa, H., 2005. Synergistic effect of antibacterial agents human β-defensins, cathelicidin LL-37 and lysozyme against Staphylococcus aureus and Escherichia coli. *Journal of Dermatological Science*, *40*(2), pp.123-132.

Chen, Q.Y., Luo, Z., Hills, C., Xue, G. and Tyrer, M., 2009. Precipitation of heavy metals from wastewater using simulated flue gas: sequent additions of fly ash, lime and carbon dioxide. *Water Research*, 43(10), pp. 2605-2614.

Chu, W., Hu, J., Bond, T., Gao, N., Xu, B. and Yin, D., 2016. Water temperature significantly impacts the formation of iodinated haloacetamides during persulfate oxidation. *Water Research*, *98*, pp.47-55.

Cook, K.R., Sims, R., Harten, A. and Pacetti, J., 2000. In situ treatment of soil and groundwater contaminated with chromium: technical resource guide. *Washington, DC, US: Environmental Protection Agency*, pp.31-33.

Cséfalvay, E., Pauer, V. and Mizsey, P., 2009. Recovery of copper from process waters by nanofiltration and reverse osmosis. *Desalination*, 240 (1-3), pp. 132-142

Dąbrowski, A., Hubicki, Z., Podkościelny, P. and Robens, E., 2004. Selective removal of the heavy metal ions from waters and industrial wastewaters by ion-exchange method. *Chemosphere*, *56*(2), pp.91-106.

Dalu, T. and Froneman, P.W. 2016. Diatom-based water quality monitoring in southern Africa: challenges and future prospects. *Water SA*. 42(4), pp. 551-559.

Dankovich, T.A., Levine, J.S., Potgieter, N., Dillingham, R. and Smith, J.A., 2016. Inactivation of bacteria from contaminated streams in Limpopo, South Africa by silver-or copper-

nanoparticle paper filters. *Environmental Science: Water Research & Technology*, *2*(1), pp.85-96.

Deshmukh, P.D., Khadse, G.K., Shinde, V.M. and Labhasetwar, P., 2017. Cadmium removal from aqueous solutions using dried banana peels as an adsorbent: kinetics and equilibrium modeling. *Journal of Bioremediation & Biodegradation*, *8*(03), pp.1-7

Dimapilis, E.A.S., Hsu, C.S., Mendoza, R.M.O. and Lu, M.C., 2018. Zinc oxide nanoparticles for water disinfection. *Sustainable Environment Research*, *28*(2), pp.47-56.

Ding, W., Jin, W., Cao, S., Zhou, X., Wang, C., Jiang, Q., Huang, H., Tu, R., Han, S.F. and Wang, Q., 2019. Ozone disinfection of chlorine-resistant bacteria in drinking water. *Water Research*, *160*, pp.339-349.

dos Santos, C.S.L., Reis, M.M.H., Cardoso, V.L. and de Resende, M.M., 2019. Electrodialysis for removal of chromium (VI) from effluent: Analysis of concentrated solution saturation. *Journal of Environmental Chemical Engineering*, *7*(5), p. 103380.

Drink Filtered. 2020. The pros and cons of a reverse osmosis water filter. Accessed from https://www.drinkfiltered.com/posts/pros-cons-reverse-osmosis-water-filters

Erikson, P., 1988. Nanofiltration extends the range of membrane filtration. *Environmental Progress*, *7* (1), pp. 58-62.

Eugenio Sportoletti Baduel. 2013. Toxicity of Hexavalent Chromium. Accessed from flipper.diff.org/app/items/info/5530.

Fauzi, A., Hapidin, D.A., Munir, M.M., Iskandar, F. and Khairurrijal, K., 2020. A superhydrophilic bilayer structure of a nylon 6 nanofiber/cellulose membrane and its characterization as potential water filtration media. *RSC Advances*, *10*(29), pp.17205-17216.

Field, C.B., Behrenfeld, M.J., Randerson, J.T. and Falkowski, P., 1998. Primary production of the biosphere: integrating terrestrial and oceanic components. *Science*, *281*(5374), pp.237-240.

Filterwater.com. 2018. Water pollution. Accessed from https://www.filterwater.com/t-articles.water-pollution.aspx

Fishbein, L., 1981. Sources, transport and alterations of metal compounds: an overview. I. Arsenic, beryllium, cadmium, chromium, and nickel. *Environmental Health Perspectives*, *40*, pp.43-64.

Fomo, G., Waryo, T., Feleni, U., Baker, P. and Iwuoha, E., 2019. Electrochemical Polymerization. *Functional Polymers; Jafar Mazumder, MA, Sheardown, H., Al-Ahmed, A., Eds*, pp.105-131.

Fortuin-de Smidt, M.C., Singh-Moodley, A., Badat, R., Quan, V., Kularatne, R., Nana, T., Lekalakala, R., Govender, N.P. and Perovic, O., 2015. Staphylococcus aureus bacteraemia in Gauteng academic hospitals, South Africa. *International Journal of Infectious Diseases*, *30*, pp.41-48.

Fu, F. and Wang, Q., 2011. Removal of heavy metal ions from wastewaters: a review. *Journal of Environmental Management*, *92*(3), pp.407-418.

Giske, C.G., Monnet, D.L., Cars, O. and Carmeli, Y., 2008. Clinical and economic impact of common multidrug-resistant gram-negative bacilli. *Antimicrobial Agents and Chemotherapy*, *52*(3), pp.813-821.

Gode, F. and Pehlivan, E., 2006. Removal of chromium (III) from aqueous solutions using Lewatit S 100: the effect of pH, time, metal concentration and temperature. *Journal of Hazardous Materials*, *136*(2), pp.330-337.

Gong, A.S., Lanzl, C.A., Cwiertny, D.M. and Walker, S.L., 2012. Lack of influence of extracellular polymeric substances (EPS) level on hydroxyl radical mediated disinfection of Escherichia coli. *Environmental Science & Technology*, *46*(1), pp.241-249.

Goyer, R.A., 2016. *Metal Toxicology: Approaches and Methods*. Elsevier.

Gumbo, J.R., Dzaga, R.A. and Nethengwe, N.S., 2016. Impact on water quality of Nandoni water reservoir downstream of municipal sewage plants in Vhembe District, South Africa. *Sustainability*, *8*(7), p.597.

Gupta, A., 2002. Hospital-acquired infections in the neonatal intensive care unit-Klebsiella pneumoniae. In *Seminars in Perinatology*, 26 (5), pp. 340-345

Gupta, V.K., Nayak, A., 2012. Cadmium removal and recovery from aqueous solutions by novel adsorbents prepared from orange peel and Fe_2O_3 nanoparticles. *Chemical Engineering Journal*, 180, pp. 81-90.

Gurreri, L., Tamburini, A., Cipollina, A. and Micale, G., 2020. Electrodialysis applications in wastewater treatment for environmental protection and resources recovery: A systematic review on progress and perspectives. *Membranes*, *10*(7), p.146.

Haas, C.N. and Hutzler, N.J., 1986. Wastewater disinfection and infectious disease risks. *Critical Reviews in Environmental Science and Technology*, *17*(1): pp.1-20.

Haimi, H., Risteelä, S., Di Pofi, M. and Lahtinen, J., 2020. Upgrade of the Taskila WWTP with a MBR line: The first treatment results, performance assessment and lessons learnt. *Water Practice and Technology*, 15 (4), 1111–1125.

Hallmich, C. and Gehr, R., 2010. Effect of pre-and post-UV disinfection conditions on photoreactivation of fecal coliforms in wastewater effluents. *Water Research*, *44*(9), pp.2885-2893.

Hammaini, A., Ballester, A., Blázquez, M.L., González, F. and Muñoz, J., 2002. Effect of the presence of lead on the biosorption of copper, cadmium and zinc by activated sludge. *Hydrometallurgy*, *67*(1-3), pp.109-116.

Han F. X, Banin A, Kingery W. L, Triplett G. B, Zhou L. X, Zheng S. J, Ding W. X. (2003). New approach to studies of heavy metal redistribution in soil. *Advances in Environmental Research*. 8: pp.113-120.

Han, C.H., Zhang, R.M., Cheng, T. and Zhang, X., 2017. Effect of Activated Carbon Prepared from Grapefruit Peel on the Treatment of Heavy Metal Copper. *DEStech Transactions on Engineering and Technology Research*, (apetc).

Hanrahan, G., Salmassi, T.M., Khachikian, C.S. and Foster, K.L., 2005. Reduced inorganic phosphorus in the natural environment: significance, speciation and determination. *Talanta*, *66*(2), pp.435-444.

Hattersley, J.G. (2003). The negative health effects of chlorine. *Journal of the Australasian College of Nutritional and Environmental Medicine. 22*(2): p. 15.

Heidmann, I. and Calmano, W., 2008. Removal of Zn (II), Cu (II), Ni (II), Ag(I) and Cr (VI) present in aqueous solutions by aluminium electrocoagulation. *Journal of Hazardous Materials*, *152* (3), pp. 934-941.

Heinze, J., Frontana-Uribe, B.A. and Ludwigs, S., 2010. Electrochemistry of conducting polymers, Persistent Models and new concepts. *Chemical reviews*, *110*(8), pp.4724-4771.

Hernández-Ávila, J., Salinas-Rodríguez, E., Cerecedo-Sáenz, E., Reyes-Valderrama, M., Arenas-Flores, A., Román-Gutiérrez, A.D. and Rodríguez-Lugo, V., 2017. Diatoms and Their Capability for Heavy Metal Removal by Cationic Exchange. *Metals*, *7*(5), p.169.

Hicks, K.A., Loomer, H.A., Fuzzen, M.L., Kleywegt, S., Tetreault, G.R., McMaster, M.E. and Servos, M.R., 2017. δ15N tracks changes in the assimilation of sewage-derived nutrients into a riverine food web before and after major process alterations at two municipal wastewater treatment plants. *Ecological Indicators*, *72*, pp.747-758.

Hosseini, M.S. and Sarab, A.R.R., 2007. Cr (III)/Cr (VI) speciation in water samples by extractive separation using Amberlite CG-50 and final determination by FAAS. *International Journal of Environmental and Analytical Chemistry*, *87*(5), pp.375-385.

Huang, M.R., Peng, Q.Y. and Li, X.G., 2006. Rapid and effective adsorption of lead ions on fine poly (phenylenediamine) microparticles. *Chemistry-A European Journal*, *12*(16), pp.4341-4350.

Huisman, J.L., Schouten, G. and Schultz, C., 2006. Biologically produced sulphide for purification of process streams, effluent treatment and recovery of metals in the metal and mining industry. *Hydrometallurgy*, *83*(1-4), pp.106-113.

IIyin, I., Berg, T., Dutchak, S. and Pacyna, J., 2004. Heavy metals. *EMEP Assessment Part I European Perspective. Norwegian Meteorological Institute, Oslo, Norway*, pp.107-128.

Imamoglu, M., Yıldız, H., Altundag, H. and Turhan, Y., 2015. Efficient removal of Cd (II) from aqueous solution by dehydrated hazelnut husk carbon. *Journal of Dispersion Science and Technology*, *36*(2), pp.284-290.

Issabayeva, G., Aroua, M.K. and Sulaiman, N.M., 2006. Electrodeposition of copper and lead on palm shell activated carbon in a flow-through electrolytic cell. *Desalination*, *194*(1-3), pp.192-201.

Itoi, S., Nakamura, I. and Kawahara, T., 1980. Electrodialytic recovery process of metal finishing wastewater. *Desalination*, 32, pp. 383-389.

Jouad, E.M., Jourjon, F., Le Guillanton, G. and Elothmani, D., 2005. Removal of metal ions in aqueous solutions by organic polymers: Use of a polydiphenylamine resin. *Desalination*, 180(1-3), pp.271-276.

Kallman, E.N., Oyanedel-Craver, V.A. and Smith, J.A., 2011. Ceramic filters impregnated with silver nanoparticles for point-of-use water treatment in rural Guatemala. *Journal of Environmental Engineering*, *137*(6), pp.407-415.

Kang, S.Y., Lee, J.U., Moon, S.H. and Kim, K.W., 2004. Competitive adsorption characteristics of Co^{2+}, Ni^{2+}, and Cr^{3+} by IRN-77 cation exchange resin in synthesized wastewater. *Chemosphere*, 56 (2), pp.141-147.

Khan, F.A., Ahmad, R., Khan, H. and Ullah, N., 2014. Geographical impact of heavy metals on Euphorbia heliscopia. *Life Science Journal*, *11*(3s).

Khlifi, R. and Hamza-Chaffai, A., 2010. Head and neck cancer due to heavy metal exposure via tobacco smoking and professional exposure: a review. *Toxicology and applied pharmacology*, *248*(2), pp.71-88.

Kock, A., 2017. Diatom diversity and response to water quality within the Makuleke Wetlands and Lake Sibaya (Doctoral dissertation, North-West University (South Africa), Potchefstroom Campus).

Koseoglu, H. and Kitis, M., 2009. The recovery of silver from mining wastewaters using hybrid cyanidation and high-pressure membrane process. *Minerals Engineering, 22*(5), pp. 440-444.

Kowalski, W.J., Bahnfleth, W.P. and Whittam, T.S., 1998. Ozone. *Science and Engineering*, 20, pp. 205-221.

Ku, Y. and Jung, I.L., 2001. Photocatalytic reduction of Cr (VI) in aqueous solutions by UV irradiation with the presence of titanium dioxide. *Water Research, 35*(1), pp. 135-142.

Kumar, M. and Puri, A., 2012. A review of permissible limits of drinking water. *Indian Journal of Occupational and Environmental Medicine*, *16*(1), p.40.

Kunugi, M., Sekiguchi, T., Onizawa, H. and Jimbo, I., 2014. Utilization of Diatoms to Collect Metallic Ions. *Proceedings of the School of Engineering of Tokai University*, *39*, pp.13-17.

Landsberg, J., Van Dolah, F. and Doucette, G., 2005. Marine and estuarine harmful algal blooms: impacts on human and animal health. In *Oceans and Health: Pathogens in the Marine Environment* (pp. 165-215). Springer, Boston, MA.

Lee, C.R., Lee, J.H., Park, K.S., Jeon, J.H., Kim, Y.B., Cha, C.J., Jeong, B.C. and Lee, S.H., 2017. Antimicrobial resistance of hypervirulent Klebsiella pneumoniae: epidemiology, hypervirulence-associated determinants, and resistance mechanisms. *Frontiers in Cellular and Infection Microbiology*, *7*, p.483.

Lee, W.H., Wahman, D.G., Bishop, P.L. and Pressman, J.G., 2011. Free chlorine and monochloramine application to nitrifying biofilm: comparison of biofilm penetration, activity, and viability. *Environmental Science & Technology*, *45*(4), pp.1412-1419.

Levit, S.M., 2010. A literature review of effects of cadmium on fish. *The Nature Conservancy*, p.15.

Li, X.G., Huang, M.R., Duan, W. and Yang, Y.L., 2002. Novel multifunctional polymers from aromatic diamines by oxidative polymerizations. *Chemical Reviews*, *102*(9), pp.2925-3030.

Li, Q., Qian, Y., Cui, H., Zhang, Q., Tang, R. and Zhai, J., 2011. Preparation of poly (aniline-1, 8-diaminonaphthalene) and its application as adsorbent for selective removal of Cr (VI) ions. *Chemical Engineering Journal*, *173*(3), pp.715-721

Luo, L.D., Huang, H.Y., Bi, J.H., Tan, L.L., Zhang, H. and Zhang, D., 2014. Optimization of malachite green by KOH-Modified grapefruit peel activated carbon: Application of Response Surface Methodology. In *Applied Mechanics and Materials*, 529, pp. 611-615.

Macintosh, K.A., Mayer, B.K., McDowell, R.W., Powers, S.M., Baker, L.A., Boyer, T.H. and Rittmann, B.E., 2018. Managing diffuse phosphorus at the source versus at the sink. *Environmental Science and Technology. 52*, pp 11995-12009.

Mann, D.G., 1999. The species concept in diatoms. *Phycologia*, *38*(6), pp.437-495.

Martin, S. and Griswold, W., 2009. Human health effects of heavy metals. *Environmental Science and Technology briefs for citizens*, 15, pp.1-6.

Mdlalose, L., Balogun, M., Setshedi, K., Tukulula, M., Chimuka, L. and Chetty, A., 2017. Synthesis, characterization and optimization of poly (p-phenylenediamine)-based organoclay composite for Cr (VI) remediation. *Applied Clay Science*, *139*, pp.72-80.

Mebane, C.A., 2006. Cadmium risks to freshwater life: Derivation and validation of low-effect criteria values using laboratory and field studies. US Department of the Interior, US Geological Survey.

Mirbagheri, S.A. and Hosseini, S.N., 2005. Pilot plant investigation on petrochemical wastewater treatmentfor the removal of copper and chromium with the objective of reuse. *Desalination*, *171*(1), pp.85-93.

Mitra, S., Sarkar, A. and Sen, S., 2017. Removal of chromium from industrial effluents using nanotechnology: a review. *Nanotechnology for Environmental Engineering*, *2*(1), p.11.

Mohammadi, T., Moheb, A., Sadrzadeh, M. and Razmi, A., 2004. Separation of copper ions by electrodialysis using Taguchi experimental design. *Desalination*, 169 (1), pp. 21–31

Murthy, Z.V.P. and Chaudhari, L.B., 2009. Separation of binary heavy metals from aqueous solutions by nanofiltration and characterization of the membrane using Spiegler- Kedem model. *Chemical Engineering Journal, 150* (1), pp 181-187.

Nabid, M.R., Sedghi, R., Behbahani, M., Arvan, B., Heravi, M.M. and Oskooie, H.A., 2014. Application of Poly 1, 8-diaminonaphthalene/multiwalled carbon nanotubes-COOH hybrid material as an efficient sorbent for trace determination of cadmium and lead ions in water samples. *Journal of Molecular Recognition*, *27*(7), pp.421-428.

Naidoo, S. and Olaniran, A., 2013. Treated wastewater effluent as a source of microbial pollution of surface water resources. *International Journal of Environmental Research and Public Health*, *11*(1), pp.249-270.

Nakatsuji, T., Chen, T.H., Narala, S., Chun, K.A., Two, A.M., Yun, T., Shafiq, F., Kotol, P.F., Bouslimani, A., Melnik, A.V. and Latif, H., 2017. Antimicrobials from human skin commensal bacteria protect against Staphylococcus aureus and are deficient in atopic dermatitis. *Science Translational Medicine*, *9*(378).

Negi, P. and Jayaprakasha, G., 2001. Antibacterial activity of grapefruit (Citrus paradisi) peel extracts. *European Food Research and Technology*, *213*(6), pp.484-487.

Nekouei, R.K., Pahlevani, F., Assefi, M., Maroufi, S. and Sahajwalla, V., 2019. Selective isolation of heavy metals from spent electronic waste solution by macroporous ion-exchange resins. *Journal of Hazardous Materials*, *371*, pp.389-396.

ODHS (2002). Coliform Bacteria. Technical Bulletin - Health Effects Information. Oregon Department of Health Services. *Environmental Toxicology Section*, pp. 1-6.

Okpokwasili, G.C. and Akujobi, T.C., 1996. Bacteriological indicators of tropical water quality. *Environmental Toxicology and Water Quality: An International Journal, 11*(2), pp. 77-81.

Olad, A. and Nabavi, R., 2007. Application of polyaniline for the reduction of toxic Cr (VI) in water. *Journal of Hazardous Materials, 147*(3), pp.845-851.

Ölmez, T., 2009. The optimization of Cr (VI) reduction and removal by electrocoagulation using response surface methodology. *Journal of Hazardous Materials, 162* (2-3), pp.1371-1378.

Orlov, A. V., Ozkan, S.Z., Bondarenko,G.N. and Karpacheva, G.P., 2006. Oxidative polymerization of diphenylamine: Synthesis and structure of polymers. *Polymer Science Series B, 48*(1), pp.5–10.

Pakade, V.E., Maremeni, L.C., Ntuli, T.D. and Tavengwa, N.T., 2016. Application of quaternized activated carbon derived from Macadamia nutshells for the removal of hexavalent chromium from aqueous solutions. *South African Journal of Chemistry*, *69*, pp.180-188.

Pakade, V.E., Ntuli, T.D. and Ofomaja, A.E., 2017. Biosorption of hexavalent chromium from aqueous solutions by Macadamia nutshell powder. *Applied Water Science, 7*(6), pp.3015-3030.

Parajuli, P.B., Mankin, K.R. and Barnes, P.L., 2009. Source specific fecal bacteria modeling using soil and water assessment tool model. *Bioresource Technology*, *100*(2), pp.953-963.

Parga, J.R., Cocke, D.L., Valenzuela, J.L., Gomes, J.A., Kesmez, M., Irwin, G., Moreno, H. and Weir, M., 2005. Arsenic removal via electrocoagulation from heavy metal contaminated groundwater in La Comarca Lagunera México. *Journal of Hazardous Materials, 124* (1-3), pp. 247-254.

Park D., Lim, S.R., Yun, Y.S. and Park, J.M., 2008. Development of a new Cr (VI)-bio sorbent from agricultural biowaste. *Bioresource Technology, 99* (18), pp. 8810-8818.

Parker, C.D. 1970. Experiences with anaerobic lagoons in Australia.

Perl, T.M., Bédard, L., Kosatsky, T., Hockin, J.C., Todd, E.C. and Remis, R.S., 1990. An outbreak of toxic encephalopathy caused by eating mussels contaminated with domoic acid. *New England Journal of Medicine*, *322*(25), pp.1775-1780.

Pidwirny, M. 2006. "The nitrogen cycle". Fundamentals of Physical Geography, 2nd Edition. Accessed from http://www.physicalgeography.net/fundamentals/9s.html.

Qu, J., Meng, X., Jiang, X., You, H., Wang, P. and Ye, X., 2018. Enhanced removal of Cd (II) from water using sulfur-functionalized rice husk: characterization, adsorptive performance and mechanism exploration. *Journal of Cleaner Production*, *183*, pp.880-886.

Richardson, S.D., 2011. Disinfection by-products: formation and occurrence in drinking water.

Rodríguez E.M., Bigi R., Medesani, D.A., Stella, V.S., Greco, L.S.L., Moreno, P.A.R., Monserrat, J.M., Pellerano, G.N. and Ansaldo, M., 2001. Acute and chronic effects of cadmium on blood homeostasis of an estuarine crab, Chasmagnathus granulata, and the modifying effect of salinity. *Brazilian Journal of Medical and Biological Research*, 34(4), pp.509-518.

Rosales, E., Meijide, J., Tavares, T., Pazos, M. and Sanromán, M.A., 2016. Grapefruit peelings as a promising biosorbent for the removal of leather dyes and hexavalent chromium. *Process Safety and Environmental Protection*, *101*, pp.61-71.

Saeed, A., Sharif, M. and Iqbal, M., 2010. Application potential of grapefruit peel as dye sorbent: kinetics, equilibrium and mechanism of crystal violet adsorption. *Journal of hazardous materials*, *179*(1-3), pp.564-572

Sahmoun, A.E., Case, L.D., Jackson, S.A. and Schwartz, G.G., 2005. Cadmium and prostate cancer: a critical epidemiologic analysis. *Cancer Investigation*, *23*(3), pp.256-263.

SANS (South African National Standard), 2011. South African National Standard No 241 for Wastewater Treatment. South African Bureau of Standards, Pretoria, Republic of South Africa.

Sarthou, G., Timmermans, K.R., Blain, S. and Tréguer, P., 2005. Growth physiology and fate of diatoms in the ocean: a review. *Journal of Sea Research*, *53*(1-2), pp.25-42.

Sbihi, K., Cherifi, O., Bertrand, M. and El Gharmali, A., 2014. Biosorption of metals (Cd, Cu and Zn) by the freshwater diatom Planothidium lanceolatum: a laboratory study. *Diatom Research*, *29*(1), pp.55-63.

Schiewer, S. and Iqbal, M., 2014. Physicochemical characterization and mechanism analysis of native and protonated grapefruit peels adsorbing cadmium. *Desalination and Water Treatment, 52* (31-33), pp. 5900-5911.

Shanker, A.K., 2019. Chromium: environmental pollution, health effects and mode of action.

Shraddha, C., Manimita, D., Harshita, N., Poornima, P., Swati, P., Archana., and Mahavir, Y., 2015. Implementation of phytoremediation to remediate heavy metals from tannery waste: A review. *Advances in Applied Science Research, 6*(3):119-128

Sillanpää, M. and Shestakova, M., 2017. Electrochemical water treatment methods: *Fundamentals, Methods and Full-scale Applications*. Butterworth-Heinemann.

Singhal, G., Bhavesh, R., Kasariya, K., Sharma, A.R. and Singh, R.P., 2011. Biosynthesis of silver nanoparticles using Ocimum sanctum (Tulsi) leaf extract and screening its antimicrobial activity. *Journal of Nanoparticle Research*, *13*(7), pp.2981-2988.

Smucker, N.J. and Vis, M.L., 2011. Spatial factors contribute to benthic diatom structure in streams across spatial scales: considerations for biomonitoring. *Ecological Indicators, 11*(5), pp.1191-1203.

Stejskal, J., 2015. Polymers of phenylenediamines. *Progress in Polymer Science*, *41*, pp.1-31.

Tchounwou, P.B., Yedjou, C.G., Patlolla, A.K., and Sutton, D.J. 2012. Heavy metal toxicity and the environment. In Molecular, Clinical and Environmental Toxicology, 32(9-10), pp.133-164.

Thilakarathne, M., Sridhar, V. and Karthikeyan, R., 2018. Spatially explicit pollutant load-integrated in-stream E. coli concentration modeling in a mixed land-use catchment. *Water Research, 144*, pp.87-103.

Tian, Z., Yang, B., Cui, G., Zhang, L., Guo, Y. and Yan, S., 2015. Synthesis of poly (m-phenylenediamine)/iron oxide/acid oxidized multi-wall carbon nanotubes for removal of hexavalent chromium. *Rsc Advances*, *5*(3), pp.2266-2275.

Torab-Mostaedi, M., Asadollahzadeh, M., Hemmati, A. and Khosravi, A., 2013. Equilibrium, kinetic, and thermodynamic studies for biosorption of cadmium and nickel on grapefruit peel. *Journal of the Taiwan Institute of Chemical Engineers*, *44*(2), pp.295-302.

Trainer, V.L., Hickey, B.M. and Bates, S.S., 2008. Toxic diatoms. *Oceans and Human Health: Risks and Remedies from the Sea*, pp.219-237.

Uddin, M.K., 2017. A review on the adsorption of heavy metals by clay minerals, with special focus on the past decade. *Chemical Engineering Journal*, 308, pp.438–462.

USEPA, 2000. In situ treatment of soil and groundwater contaminated with chromium. *Technical Resource Guide No*

Vasek, O.M., Cáceres, L.M., Chamorro, E.R. and Velasco, G.A., 2015. Antibacterial activity of Citrus paradisi essential oil. *Journal of Natural Products*, *8*, pp.16-26.

Velma, V., Vutukuru, S.S. and Tchounwou, P.B., 2009. Ecotoxicology of hexavalent chromium in freshwater fish: a critical review. *Reviews on Environmental Health*, *24*(2), p.129.

Walker, D.B., Baumgartner, D.J., Gerba, C.P. and Fitzsimmons, K., 2019. Surface water pollution. In *Environmental and Pollution Science* (pp. 261-292). Academic Press.

Wang, L.K., Hung, Y.T. and Shammas, N.K. eds., 2007. *Advanced Physicochemical Treatment*

Wang, J.J., Jiang, J., Hu, B. and Yu, S.H., 2008. Uniformly shaped poly (p-phenylenediamine) microparticles: shape-controlled synthesis and their potential application for the removal of lead ions from water. *Advanced Functional Materials*, *18*(7), pp.1105-1111.

Warwick, C., Guerreiro, A. and Soares, A., 2013. Sensing and analysis of soluble phosphates in environmental samples: A review. *Biosensors and Bioelectronics*, *41*, pp.1-11.

White, G.C., 1992. Handbook of Chlorination and Alternative Disinfectants. Vol. 3.

WHO, 1993. Guidelines for drinking water quality. World Health Organization

WHO, 2011. Guidelines for drinking water quality.4th Edn., World Health Organization, Geneva.

WHO/IPCS. World Health Organization. (1988). Environmental Health Criteria 61. Geneva, Switzerland.

World Health Organization, WHO/UNICEF Joint Water Supply and Sanitation Monitoring Programme, 2015. Progress on sanitation and drinking water: 2015 update and MDG assessment. World Health Organization.

World Health Organization and UNICEF, 2017. Progress on drinking water, sanitation and hygiene: 2017 update and SDG baselines.

WPCF Task Force on Wastewater Disinfection. (1986). Wastewater Disinfection Manual of Practice No. FD-I 0. Water Pollution Control Federation. Alexandria, VA.

Yan, L.G., Xu, Y.Y., Yu, H.Q., Xin, X.D., Wei, Q. and Du, B., 2010. Adsorption of phosphate from aqueous solution by hydroxy-aluminum, hydroxy-iron and hydroxy-iron-aluminum pillared bentonites. *Journal of Hazardous Materials, 179* (1-3), pp.244-250.

Yu, Y., Addai-Mensah, J. and Losic, D., 2012. Functionalized diatom silica microparticles for removal of mercury ions. *Science and Technology of Advanced Materials*.

Yu, W., Zhang, L., Wang, H. and Chai, L., 2013. Adsorption of Cr (VI) using synthetic poly(m-phenylenediamine). *Journal of Hazardous Materials, 260*, pp.789-795.

Zhang, L.M. and Chen, D.Q., 2002. An investigation of adsorption of lead (II) and copper (II) ions by water-insoluble starch graft copolymers. *Colloids and surfaces A: physicochemical and Engineering Aspects*, *205*(3), pp.231-236.

Zhao, Y.G., Shen, H.Y., Pan, S.D. and Hu, M.Q., 2010. Synthesis, characterization and properties of ethylenediamine-functionalized Fe3O4 magnetic polymers for removal of Cr (VI) in wastewater. *Journal of Hazardous Materials*, *182*(1-3), pp.295-302.

Zhao, Y., Nakanishi, S., Watanabe, K. and Hashimoto, K., 2011. Hydroxylated and aminated polyaniline nanowire networks for improving anode performance in microbial fuel cells. *Journal of Bioscience and Bioengineering*, *112*(1), pp. 63-66.

CHAPTER 3

Preparation, characterization, and application of *Citrus paradisi* peel bio-sorbent uptakes of Cr and Cd ions in aqueous solutions

3.1 Abstract

The present study focuses on evaluating the biosorption of cadmium and chromium ions in an aqueous solution by *Citrus paradisi* (CP) (Grapefruit Red peel) on a laboratory scale. Surface morphology and mineralogical properties of the bio-sorbent were examined by SEM-EDS, XRD, and FTIR analysis. The results obtained from SEM images display a flaky-cavity shape-like structure while the XRD displays an amorphous phase without a clearly defined shape. Moreover, results from the FTIR show the carboxyl, hydroxyl, and amino groups being the most dominant functional groups responsible for the metal ions biosorption processes. Batch sorption studies with equilibrium isotherms, kinetics, and thermodynamic parameters were performed on the adsorbent to validate the experimental data. The overall biosorption kinetic results indicated that the mechanisms not only depend on the pseudo-second-order process but were also governed by intraparticle diffusion mechanisms. The Freundlich model best described the equilibrium data better than the Langmuir model. The maximum sorption capacities of Cr and Cd ions at room temperature were found to be 90.09 and 47.17 mg/g respectively. Thermodynamic parameters depict that the surface interactions were endothermic, spontaneous, and favorable across the different sorption temperatures. These results indicated that CP could serve as a potentially low-cost bio-sorbent in the remediation of Cr and Cd ions from polluted water.

Keywords: Water pollution; biosorption; metal ions; Grapefruit peel bio-sorbent

3.2 Introduction

The pollution of water resources from natural and anthropogenic activities has been a major environmental problem worldwide, which degrades the quality and quantity of water. The major causes of water pollution are effluents mainly from sewage and mining sectors, agricultural activities, tanning, electroplating, and metal processing industries, as well as volcanic activities, weathering, geology, etc. (Gupta and Nayak, 2012; Henze, 1992). The discharging of these effluents associated with heavy metal ions due to their high aqueous

solubility from time to time into streams and rivers adversely affects ecosystems and human health upon prolonged exposure (Dyer et al., 2003).

Some trace elements such as Cu, Mn, Fe, Ni, Cr, and Zn are essential for living organism metabolisms but toxic in high amounts. Moreover, other metals such as Cd, Pb, As, Cr, and Hg are toxic even at low concentrations due to their carcinogenic and persistent nature (Bilal et al., 2013; Ben-Ali et al., 2017). Metal ions such as hexavalent chromium (Cr (VI)), and cadmium (Cd^{2+}) are some of the most concerning toxic ions in water that causes severe health problems like organ damage, reduced growth and development, nervous system impairments and oxidative stress on humans and animals (Wu et al., 2018; Lee et al., 2012). The tolerance limit for Cr (VI) for discharge into inland surface waters is 0.1 mg/L and in potable water is 0.05 mg/L (Regmi et al., 2015). Equally, the World Health Organization prescribed a maximum limit of cadmium to be 10µg/L in drinking water (WHO, 2011).

Studies have been conducted in trying to come up with better ways to remediate the levels of heavy metal ions before discharge into the environment. As such, different methods, and materials for metal ion removal from aqueous solutions have been thoroughly investigated, studied, and reviewed (Ibrahim et al., 2016). This includes chemical precipitation, chemical oxidation, and reduction, ion-exchange, filtration, electrochemical treatment, reverse osmosis, evaporative recovery, solvent extraction (Mdlalose et al., 2017; Arief et al., 2008.). However, such treatment processes are often associated with drawbacks, which include difficulty in operation, high operational costs, and the release of secondary pollutants (Regmi et al., 2015). Recently, remediation of chemical species using biological materials has emerged as a potential alternative to existing conventional techniques. This is because of its cost-effectiveness, eco-friendliness, economic reusability, regeneration ability, and the potential of metal recovery, etc. (Monteiro et al., 2011). Bio-sorbent materials from algae, waste agricultural materials, fungal, bacterial, activated carbon, and yeast have shown high removal efficiency of such pollutants from wastewater (Romero-Cano et al., 2016).

Among the agricultural waste materials that could be useful as bio-sorbents for the removal of metal ions removal is grapefruit peel (*Citrus paradisi*). Grapefruit production is considered important globally because of its great economic value for the human diet. Grapefruit peels which are mainly wastes of ecological problems, whose disposal by incineration and the consequent global warming effect, constitute a global challenge. Furthermore, the peels contain water-soluble and insoluble monomers and polymers containing carboxyl and hydroxyl

functional groups, which bind metal ions in an aqueous solution (Bhatnagar et al, 2015). *Citrus paradisi* has the potential to remove crystal violet dye, malachite green, nickel (II), copper (II) and other toxic metal ions in aqueous solutions (Han et al., 2017; Rosales et al., 2016; Schiewer and Iqbal, 2013; Saeed et al., 2010).

This study seeks to utilize the waste grapefruit peel due to its abundance in nature, unique phytochemicals, and functional groups to design an adsorbent that is eco-friendly, sustainable and to evaluate the biosorption capacity of using the waste of the peels for the removal of Cr and Cd ions from aqueous solutions. The physicochemical characteristics of the adsorbent were carried out; batch sorption analysis on the effect of different experimental parameters such as contact time, dosage, initial metal concentration, pH and temperature were performed to examine its removal efficiency. Lastly, the biosorption thermodynamics, adsorption kinetics and isotherms were determined using the experimental data.

3.3 Materials and methods

3.3.1 Chemicals and reagents

The chemicals used for the experiments were of analytical reagent grade. $CdN_2O_6{\cdot}4H_2O$, $K_2Cr_2O_7$, HCl, NaOH, and KCl chemicals used were purchased from Rochelle chemicals (Johannesburg, South Africa) and were used directly without further purification. Ultrapure Milli-Q water (18.2 MΩ/cm) was used in the preparation and dilution of standards throughout the experiment.

3.3.2 Preparation of the bio-sorbent

Grapefruit was bought from a local supermarket (Thohoyandou, South Africa). The peels were removed from the fruit and washed thoroughly with tap water. Later washed with Ultrapure milliQwater (18.2 MΩ/cm). The peels were dried in an oven (Eco-Therm, model 920) at 60˚C for 24 h. The dried material was ground in a blender (Philips domestic, 400 W 1.5 L; HR 2103) and sieved to the desired particle size and used for experiments without any further treatment.

3.3.3 Preparation of stock solutions

Stock solutions of 1000 mg/L Cd and Cr ions were prepared by dissolving 2.744 g of $CdN_2O_6{\cdot}4H_2O$ and 2.82 g of $K_2Cr_2O_7$ in a 1L volumetric flask with Ultrapure milliQwater (18.2 MΩ/cm). The solutions used in conducting the experiments were obtained by diluting the metal ion stock solutions to known initial concentration which was used for the experiments.

3.3.4 Instruments

An ALPHA Bruker FT-IR Spectrophotometer (Berlin, Germany) was used to identify functional groups on solid samples of grapefruit peel in the range of (400-4000 cm^{-1}). XRD type PANalytical X'Pert Pro powder diffractometer was utilized for qualitative and quantitative mineralogical analysis. The samples were prepared according to the standardized Panalytical backloading system, which provides a nearly random distribution of the particles, a Pro powder diffractometer in θ–θ configuration with an X'Celerator detector and variable divergence- and fixed receiving slits with Fe filtered Co-Kα radiation (λ=1.789Å) was utilized. The mineralogy was determined by selecting the best–fitting pattern from the ICSD database to the measured diffraction pattern, using X'Pert Highscore plus software. The surface morphology of the adsorbent was determined with SEM and SEM-EDS to provide the elemental composition of the adsorbent with an (FEI Nova NanoSEM 230 with the field emission gun equipped with an Oxford Xmax SDD detector operating at an accelerating voltage of 20Kv) for the EDS detector (Oxford X-Max with INCA software) were used to characterize the sorbent materials. Flame Atomic Absorption Spectrometry (FAAS) type (PINAACLE 900T) was used to analyze the metal ions in aqueous samples.

3.3.5 Point of zero charge (pHpzc)

The pH at point-of-zero charge was determined by mixing 0.2 g of grapefruit peel in 0.1 M KCl solutions. The pH of solutions was then adjusted to desired values between 3 and 11 by adding 0.1 M HCl or 0.1 M NaOH using pH meter type (ACCSEN PC 8). A volume of 50 mL of KCl solution was pipetted into plastic bottles. The bottles were shaken on a thermostat water bath shaker at 150 rpm for 24 h at room temperature. After equilibration, the equilibrium pH (pH_f) of each mixture was measured. The intersection pH-initial versus ΔpH curve gives the pHpzc value.

3.3.6 Adsorption procedure

The adsorption experiments were carried out to determine the effect of different experimental parameters such as contact time, dosage, initial metal ion concentration, pH, and temperature between 298-313 K. Contact time was varied from 1 to 120 min. The effect of adsorbent dosage was evaluated by varying dosage from 0.05 to 0.4 g. The adsorption isotherms experiments were examined by varying the metal ion concentration between 10-200 mg/L. All experiments were evaluated by using 50 mL of Cr and Cd solutions. After the shaking time elapsed, samples

were filtered with filter papers (Munktell Ahlsrom 3HW 125 mm), and the residual concentration was analyzed by FAAS spectrometer.

The adsorption capacities of grapefruit peel for Cr and Cd ions were calculated using (Eq. 1 and 2).

$$q = (C_o - C_e) \times \frac{V}{w} \quad (1)$$

$$\% \text{ Removal } = \frac{(C_o - C_e)}{C_o} \times 100 \quad (2)$$

where Co is the initial metal ions concentration (mg/L); Ce is the metal ions concentration at equilibrium (mg/L); V is the volume of solution (L) and w mass of the adsorbent (g).

3.4 Results and discussion

3.4.1 FTIR analysis

The bands of the FT-IR spectrum revealed a wide diversity of the main functional groups inherent in the raw grapefruit peel (Fig. 10). These peaks were found at 3298.58, 2925.27, 1731.90, 1619.71, 1234.16, and 1024.05 cm^{-1}. The broad band stretching at 3298.58 cm^{-1} is typical characteristics of O–H groups which may correspond to the vibrations of cellulose, hemicellulose, lignin within the peel as well as that of absorbed water, (Köseoğlu and Akmil-Başar, 2015; Farinella et al., 2007). The stretching vibrations occurring at 2925.27 cm^{-1} corresponded to the -C-H group displaying aliphatic vibrations of lignin polysaccharides including cellulose and hemicellulose (Nguyen et al., 2013). Stretching of esters or fatty acids at 1731.90 cm^{-1} was displayed by the -C=O which are due to carboxyl groups of pectin, lignin, and hemicellulose typical of any agricultural waste products (Hameed and Daud, 2008). The -N-H bands at 1619.71 cm^{-1} display amino groups which are bending, while the band at 1234.16 cm^{-1} displayed the stretching vibration band of -C-O attached to an ester due to non-ionic carboxyl groups (–COOH, $–COOCH_3$) (Saeed et al., 2010). The strong C-O band at 1024.05 cm^{-1} as a result of C–OH indicated the stretching vibrations of alcoholic groups and carboxylic acids which confirmed the lignin structure of the grapefruit peel (Torab-Mostaedi et al.,-2013; Iqbal et al., 2009). Studies have shown that the most important materials in agricultural waste products contain lots of phytochemical properties, polar functional groups of biopolymers that possess an affinity for complexation with metal ions (Bayuo et al., 2019; Bhatnagar et al., 2015; Ofomaja and Ho, 2007). Consequently, indicating that these functional groups may play a role in the biosorption process.

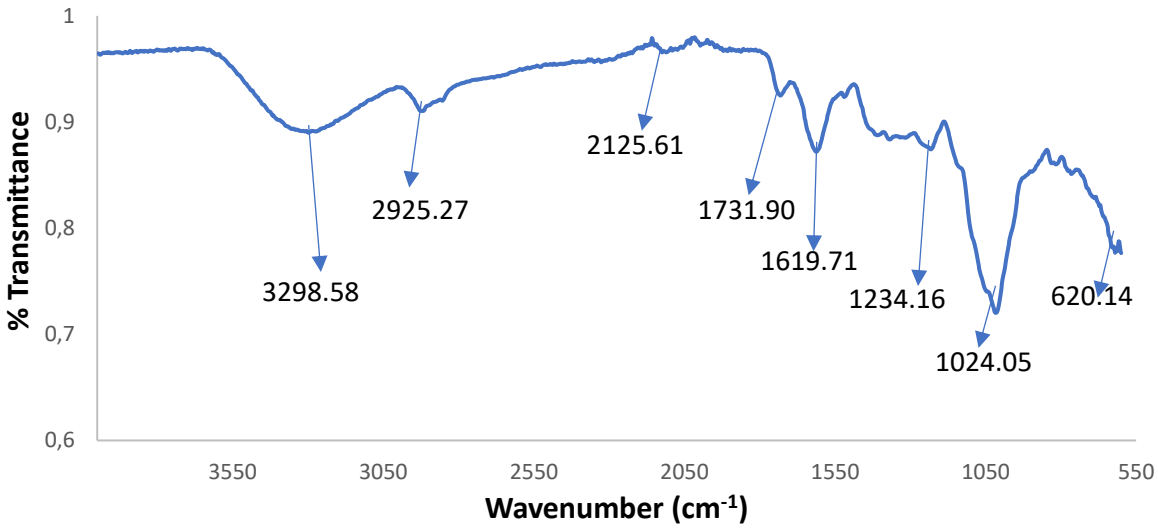

Fig. 10. FTIR spectrum of *Citrus paradisi* peel bio-sorbent

3.4.2 XRD results

The XRD spectra are mainly used to describe the mineral phase of an adsorbent. The XRD spectra of the *Citrus paradisi* peel bio-sorbent is shown in Fig. 11. The diffractogram shows that the bio-sorbent phase is not crystalline but amorphous, which is expected from biomass materials. The distinctive peak appearing between 23.98 and 25.78˚could be attributed to the presence of cellulose and hemicellulose base components embedded in the bio-sorbent (Ciolacu et al., 2011).

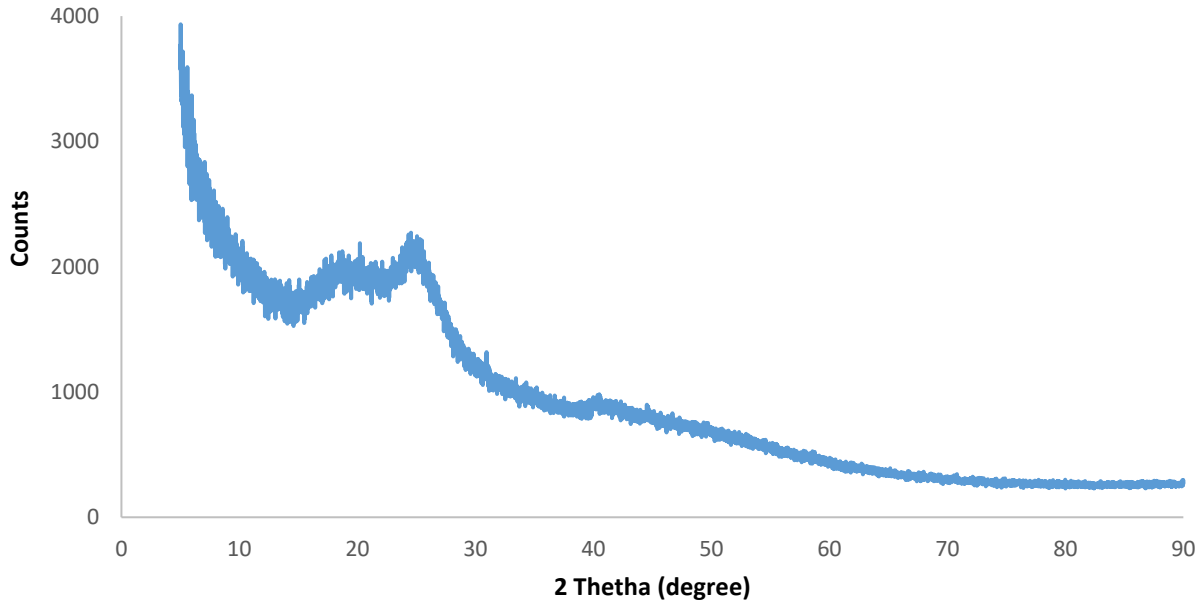

Fig. 11. X-ray diffractogram of *Citrus paradisi* peel bio-sorbent

3.4.3 Surface morphology

Fig. 12 shows the SEM images at different magnifications of the *Citrus paradisi* peel bio-sorbent powder, together with the corresponding EDS spectra. The SEM images (Fig. 12(a) and (b)) display a flakey, cavity shape like structure which is capable of up-taking metal ions. A similar observation was reported by Torab-Mostaedi et al. (2013). Moreover, the material changes to a smoother surface after the biosorption process with time (Fig. 12 (d;f)). Furthermore, the EDS spectrum (Fig. 12 (c)) shows the major elements present in the bio-sorbent, with carbon and oxygen having a higher percentage weight abundance. This is typical of agricultural biomass composition. However, in Figs. 12 (e) and (g), traces of Cr and Cd were observed in the EDS spectra, which confirmed the binding of Cr and Cd to the structural active sites in the *Citrus paradisi* peel bio-sorbent.

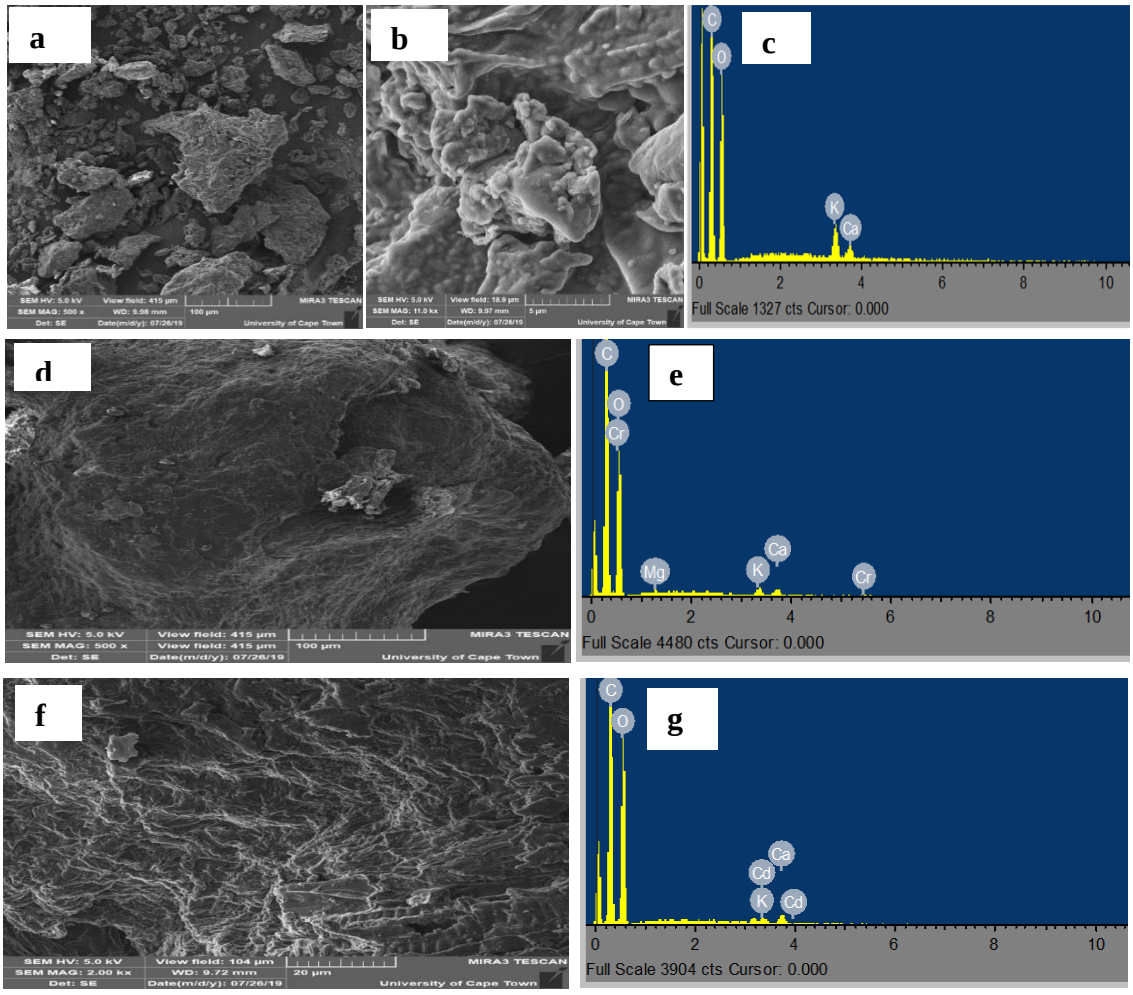

Fig. 12. SEM-EDS (a-c) before biosorption at different magnifications; (d-g) after the biosorption of Cr and Cd ions by *Citrus paradisi* peel bio-sorbent.

3.5 Batch biosorption experiments

3.5.1. Effect of contact time and adsorption kinetics

The uptake efficiency of Cr and Cd ions by *Citrus paradisi* peel bio-sorbent experimental data was evaluated at different contact times. As shown in Fig. 13, the rate of percentage removal and adsorption capacity of Cr and Cd ions increased gradually with time. Comparatively, both Cr and Cd ion uptakes were rapid at the early time of biosorption and gradually reaches an equilibrium where the plateau remained constant. The rise in the percentage removal of both Cr and Cd ion by the *Citrus paradisi* peel bio-sorbent was an indication of an increase in the accessibility of the metal ions to the bio-sorbent active binding sites, which became occupied towards the equilibrium.

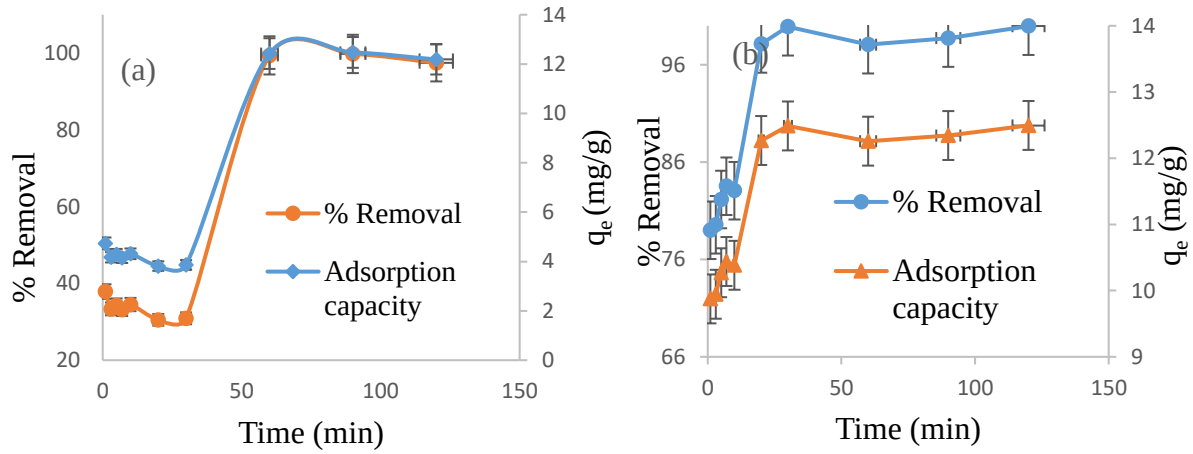

Fig. 13. (a-b) The effect of contact time for Cr and Cd uptakes respectively by *Citrus paradisi* peel bio-sorbent (Experimental conditions: dosage: 0.2 g; shaking speed of 250 rpm; a volume of 50 mL and initial concentration of 50 mg/L of Cr and Cd ions.)

Thereafter, reaching its maximum adsorption capacity leading to a reduction in the driving force for the biosorption process. The biosorption rate phenomenon may be associated with the inherent *Citrus paradisi* peel bio-sorbent phytochemical functional groups as shown in the FT-IR spectrum (section 3.1). The highest percentage removal for both Cr and Cd ions by the bio-sorbent was observed to be > 95% with an adsorption capacity of 12.43 and 12.48 mg/g at 60 and 30 min of optimum time, respectively. These respective metal ions optimum contact times reached were then used for subsequent experiments. The maximum biosorption attainment by Cd ion at a lesser time compared to Cr ion revealed that *Citrus paradisi* peel bio-sorbent has a higher affinity for Cd to Cr ion in solution.

The kinetic adsorption data were simulated using the reaction-based and diffusion-based models to explain the metal ions biosorption phenomenon and mechanisms. Figs. 14; 15 and 16 show the linear biosorption kinetics curve fittings using the pseudo-first-order (Lagergren, 1898) (Eq. 3), pseudo-second-order (Ho, 2006) (Eq. 4), and intra-particle diffusion (Weber and Morris, 1963) (Eq. 5) respectively.

$$\log(q_e - q_t) = \log q_e - \frac{k_1}{2.303} t \quad (3)$$

where q_e and q_t (mg/g) are the amounts of sorbed per unit mass of the biosorbent at time t while k_1 is the pseudo-first-order adsorption rate constant in min^{-1} at equilibrium.

$$\frac{t}{q_t} = \frac{1}{k_2 q_e^2} + \frac{1}{q_e} t \quad (4)$$

where k_2 (g/mg/min) is the equilibrium rate constant of pseudo-second-order adsorption.

The different plots and parameters obtained from the fittings of the metal ions experimental data to both pseudo-first-order and pseudo-second-order kinetic rate are shown in Figs. 14-15 and Table 1. The Cr and Cd ions fittings on the plots (Figs. 14-15) show a better correlation of determination (R^2) for pseudo-second-order compared to the pseudo-first-order kinetic model. Consequently, the biosorption kinetics favors the pseudo-second-order kinetics model rather than pseudo-first-order kinetics for Cr and Cd ions. Hence, the reaction occurred via chemisorption and it is associated with ion exchange between the adsorbent and the adsorbate rather than the weak Van der Waal's force of attraction (Wang and Wang 2008; Ho and McKay, 2009).

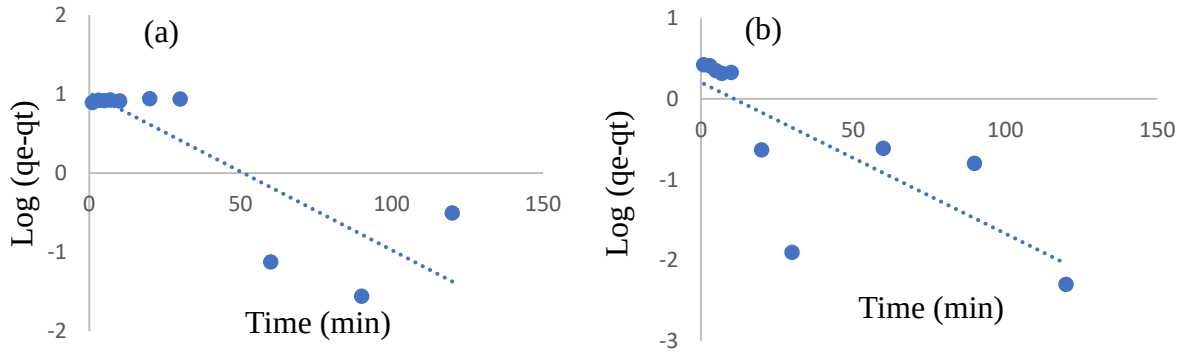

Fig. 14. Pseudo-first-order plots for Cr (a); and Cd (b) ions.

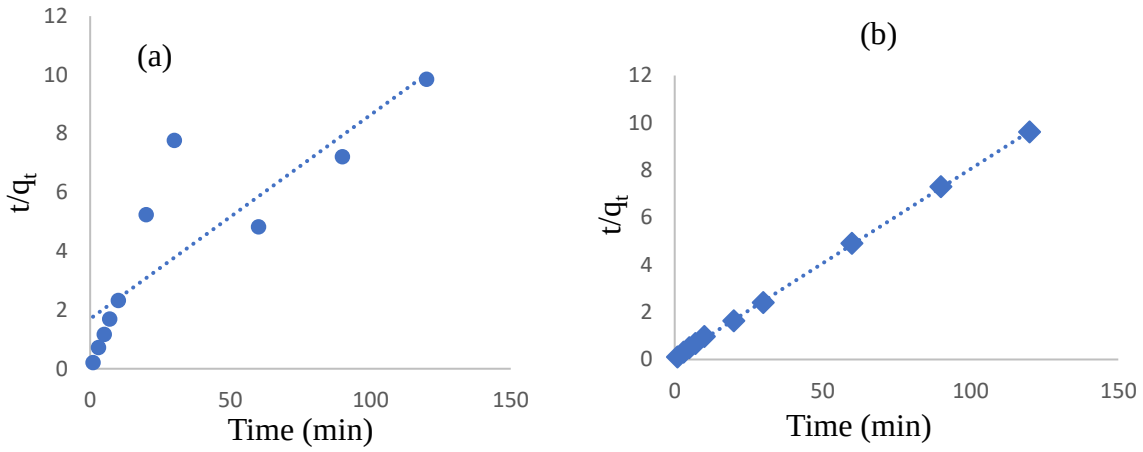

Fig. 15. Pseudo-second-order plots for Cr (a) and Cd (b) ions.

Furthermore, the intra-particle diffusion (Eq. 5). describes the mass transfer of sorbates from the external surface into the pores of the bio-sorbent and is used to determine the diffusion mechanism and rate-limiting step controlling biosorption processes (Ho et al., 2000).

$$q_t = k_i t^{0.5} + C \quad (5)$$

where q_t is the amount adsorbed (mg/g) concerning time (t) (min); K_{id} is the intra-particle diffusion rate constant in (mg/g/min) and C is a constant related to the thickness of the boundary layer (mg g^{-1}).

Fig. 16 and Table 1 illustrate the diffusion processes and the calculated parameters occurring at the surface of the bio-sorbent by the mass transfer of both Cr and Cd ions. As shown from the results (Fig. 16 (a-b)), the plots display multi-linearity phases in both metal ions uptake by the *Citrus paradisi* peel bio-sorbent. The Cr curve (Fig. 16a) shows two phases of diffusions while that of Cd ion (Fig. 16b) reveals three diffusion phases. The first phase usually shows the interaction of adsorbate particles with increasing rapidness at the surface of the adsorbent. The second phase indicates the particle diffusion through the interior of the adsorbent and supports electrostatic attraction between the adsorbent and adsorbate, while the third phase shows particles getting diffused into the pores of the adsorbent as the process continues. Equally, the thickness boundary of the *Citrus paradisi* peel bio-sorbent layer is higher in the biosorption process for Cd to Cr ions as the diffusion phases increase.

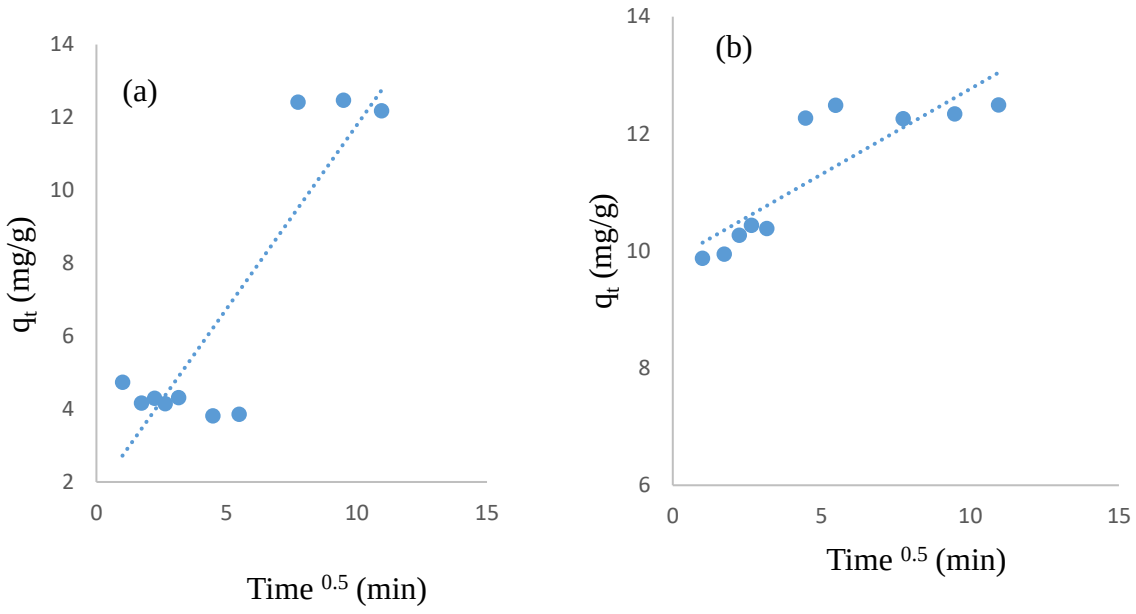

Fig. 16. A plot of intra-particle diffusion for chromium (a) and cadmium (b) ions by *Citrus paradisi* peel bio-sorbent.

Table 1: Kinetic fittings for Cr and Cd metal ions by *Citrus paradisi* peel bio-sorbent.

Linear kinetic models	Parameter	Cr values	Cd values
Pseudo-first order	k_1 (min^{-1})	0.046	0.043
	q_{calc}	10.275	1.600
	R^2	0.699	0.607
Pseudo-second order	k_2 (g/ mg min)	0.003	0.081
	q_{calc}	14.409	12.547
	R^2	0.735	0.999
Intra-particle diffusion	K_{id}	1.008	0.292
	C	1.713	9.849
	R^2	0.769	0.739

3.5.2 Effect of adsorbent dosage

Fig. 17 shows the effect of *Citrus paradisi* peel bio-sorbent amount (between 0.05 to 0.4 g) on the biosorption efficiency of Cr and Cd ions. The graph (Fig. 17a) showed that Cr ion adsorption capacity decreased with increasing sorbent dosage. The same trend was observed in the uptake of Cd by the bio-sorbent. Comparatively, Cr ion was observed with the highest removal rate of over 90% at 0.35 g while Cd ions uptake was ~ 85% at 0.2 g of the bio-sorbent. This might be due to the availability of more active binding biosorption sites with a high affinity for the metal ion species with the gradual increase of the adsorbent amount.

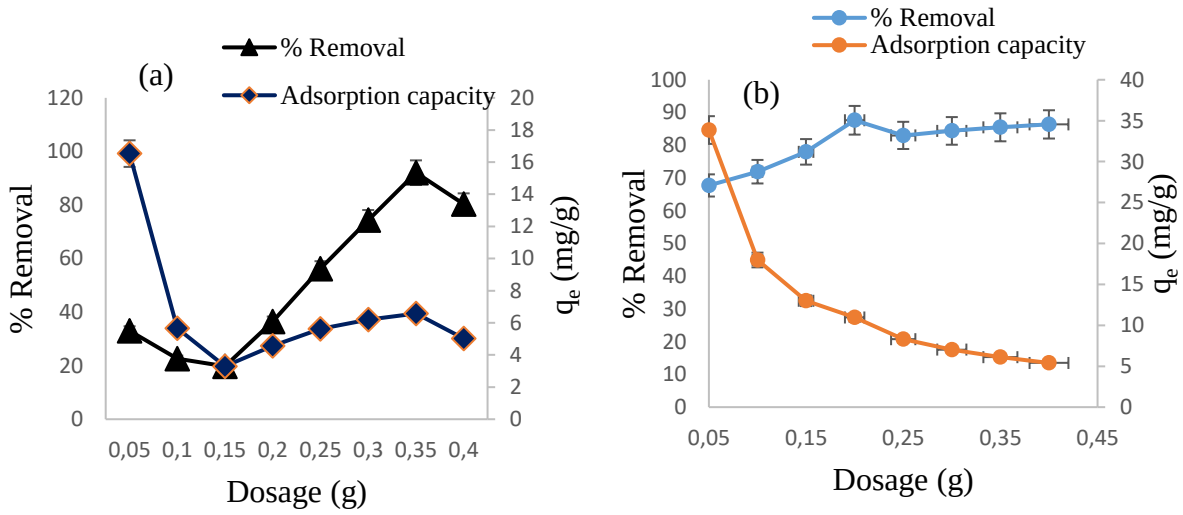

Fig. 17. The effect of adsorbent dosage for chromium (a) and cadmium (b) against percentage removal and adsorption capacity (contact time of 60 and 30 min for Cr and Cd ions respectively, initial concentration of 50 mg/L, neutral pH, the temperature of 298K, solution volume of 50 mL, shaking speed of 250 rpm)

3.5.3 Effect of initial concentration and adsorption isotherms

The biosorption efficiency of the Citrus *paradisi* peel bio-sorbent at different initial concentrations of both Cr and Cd ions is shown in Fig. 18(a-b). From the graphs, it was observed that the adsorption capacity of the bio-sorbent increased, while the percentage removal decreased with an increase in the metal ion concentration. This could be related to the reduction in the mass gradient between the sorbent-sorbate interphase from saturation and occupation of the available sites on the bio-sorbent.

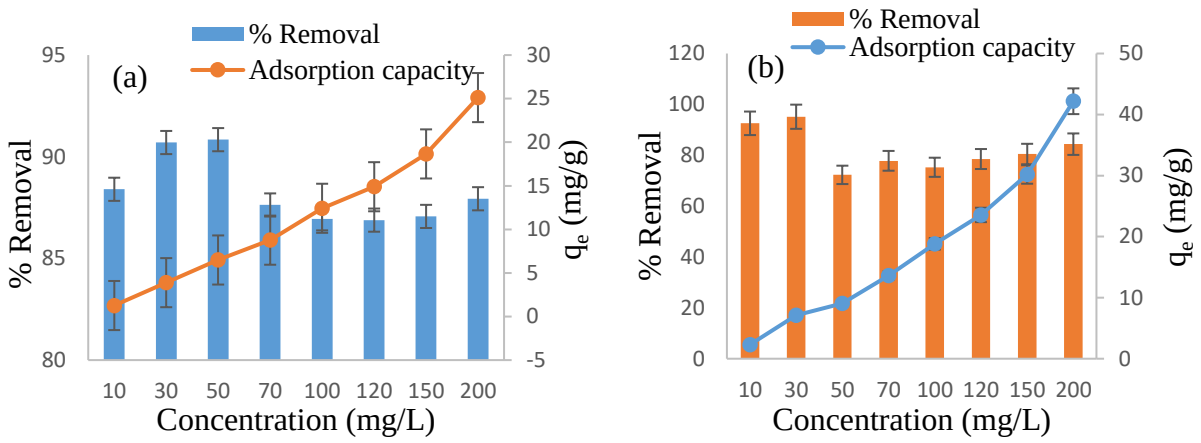

Fig. 18. Variation of adsorption capacities and the percentage removal against an initial concentration of Cr (a) and Cd (b) ions, respectively. (Experimental conditions: Optimum time 60 and 30 min, a dosage of 0.35 g and 0.2 g for Cr and Cd ions respectively at solution volume of 50 mL and shaking speed of 250 rpm)

The biosorption of Cr and Cd ions by *Citrus paradisi* peel bio-sorbent were modelled using the linearize Langmuir (1916) (Eq. 6), Freundlich (1907) (Eq. 8) and Dubinin-Radushkevich (DR) (1960) (Eq. 9) isotherms with the experimental data. The favourability of the model fittings was assessed using the correlation of determination (R^2)

$$\frac{C_e}{q_e} = \frac{1}{K_L q_m} + \frac{1}{q_m} C_e \qquad (6)$$

where C_e (mg/L) is the equilibrium metal ion concentration; q_e is the amount of bio-sorbent (mg/g); q_m (mg/g) is for a complete monolayer sorption capacity of the bio-sorbent; K_L is Langmuir biosorption equilibrium constant (L/mg). These parameters can be obtained by the plot of C_e/q_e against C_e.

Moreover, the favourability for the Langmuir sorption process can be further tested by the values of 'R_L', the dimensionless separation factor (Eq. 7).

$$R_L = \frac{1}{1 + k_L C_i} \qquad (7)$$

where ka is the Langmuir isotherm constant and Ci is the initial concentration of Cr or Cd (mg/L). R_L, indicates the type of Langmuir isotherm to be irreversible if ($R_L = 0$), favourable ($0 < R_L < 1$), linear ($R_L = 1$) or unfavourable ($R_L > 1$).

Furthermore, the linear form of the Freundlich equation isotherm (Eq. 8) was also used to predict the biosorption processes. This model can be applied to multilayer biosorption with heterogeneous surfaces due to its energetic distribution of active sites (Toor and Jin, 2012).

$$\log q_e = \log K_F + \frac{1}{n}\log C_e \quad (8)$$

where K_F and 1/n are empirical constants that show the biosorption capacity and adsorption intensity, respectively. These can be obtained by plotting log qe against log Ce. The condition for adsorption material is favourable if the n value lies within the range of 1 and 10.

Equally, the D-R isotherm (Eq. 9) is concerned with the mean free energy of the biosorption processes as well as the effects of the porous nature of the bio-sorbent. With D-R isotherm, if E is between 8 and 16 kJ/mol, adsorption occurred vial chemisorption and if E is less than 8kJ/mol this adsorption occurred via physisorption.

$$\ln q_e = \ln q_{max} - \beta_D \varepsilon^2 \quad (9)$$

where $q_{max\ (mg/g)}$ is the adsorption capacity of adsorbent; β_D is the coefficient constant that is related to the mean sorption energy. ε is the Polanyi potential which is the mean adsorption energy.

Table 2 displays the summary of both Cr and Cd ions biosorption isotherms parameters by *Citrus paradisi* peel bio-sorbent. From the data obtained, it is evident that the uptakes of Cr and Cd ions by the bio-sorbent fitted well towards Freundlich than Langmuir isotherms based on the higher values of correlation of determination (R^2). The favourability of the biosorption processes was also shown by both separation factor R_L and the intensity (n). The biosorption capacity of 90.09 and 47.17 (mg/g) for Cr and Cd ion by the *Citrus paradisi* peel bio-sorbent at room temperature were recorded. Equally, in Table 2, the DR mean adsorption energy was less than 8kJ/mol for both Cr and Cd which means the reaction involved the physisorption phenomenon. It is also evident that the R^2 value for DR isotherm was better than Langmuir but less as compared to Freundlich. Therefore, in this study, Freundlich stands to be better than DR and Langmuir isotherms, thus making it a suitable model for this study indicating that the conditions were favourable for multilayer adsorption processes.

Table 2: An illustration of isotherms for Cr and Cd ions at room temperature

Isotherms	Cr ion	Cd ion
Langmuir		
Q_m (mg/g)	90.09	47.17
K_L (L/mg)	0.014	0.026
R^2	0.415	0.297
R_L	0.590	0.435
Freundlich		
K_F [(mg/g)/(mg/L)^n]	1.316	3.48
n	1.13	1.72
R^2	0.981	0.834
Dubinin-Radushkevvich		
β_D (mol^2/kJ^2)	1.00E-06	5.00E-07
qmax(mg/g)	13.08	20.04
E (kJ/mol)	0.707	1
R^2	0.802	0.743

3.5.4 The effect of temperature and thermodynamics

The effect of temperature and the thermodynamics for the biosorption of Cr and Cd ions onto *Citrus paradisi* peel bio-sorbent was studied at different temperatures ranges of 298-313 K. It was observed that as the temperature increased, so were the values for the free Gibbs energy change (ΔG°) which confirmed the feasibility and spontaneous nature of the adsorption process. The thermodynamic parameters, free energy change, entropy, and enthalpy were all calculated from the equations given below:

$$\mathrm{In}K_D = \frac{\Delta S^{\circ}}{R} - \frac{\Delta H^{\circ}}{RT} \quad (10)$$

where, ΔS° (J/mol K) and ΔH° (KJ/mol) are the entropy and enthalpy change respectively during biosorption process, which was calculated from the intercept and slope of the linear plot.

$$\Delta G^{\circ} = \Delta H^{\circ} - T\Delta S^{\circ} \quad (11)$$

where ΔG represents the free Gibbs energy change, R and T represent the ideal gas constant (8.314 J mol^{-1} K^{-1}) and absolute temperature (K)

$$K_D = \frac{C_S}{C_e} \quad (12)$$

where K_D is the equilibrium constant at a constant temperature, C_e (mg/L) and C_s (mg/L) are equilibrium concentrations of sorbate and the amount of sorbate adsorbed, respectively.

From Table 3, the ΔH° values (34.28 and 29.24 KJ/mol) for Cr and Cd ion respectively indicate an endothermic reaction process. The ΔS° values are positive for both Cr ion (206.07 J/mol K) and Cd ion (196.34 J/mol K), an indication that increased randomness occurred at the solid-solution interface during the adsorption process (Bağda et al., 2017). While the free Gibbs energy change (ΔG°) values were calculated for Cr ion to be -27.13, -28.16, -30.22 kJ/mol and for Cd ion to be -29.27, -30.25, and -32.22 kJ/mol for 298 K, 303 K, and 313 K, respectively. The ΔG° values suggested that the adsorption process was favourable and spontaneous.

Table 3: Thermodynamic parameters for Cr and Cd ions by *Citrus paradisi* peel bio-sorbent

	Cr ion			Cd ion		
Temperature (K)	ΔH◦ (KJ/mol)	ΔS◦ (J/mol K)	ΔG◦ (kJ/mol)	ΔH◦ (KJ/mol)	ΔS◦ (J/mol K)	ΔG◦ (kJ/mol)
	34.28	206.07		29.24	196.34	
298			-27.13			-29.27
303			-28.16			-30.25
313			-30.22			-32.22

3.5.5 Effects of pH and point of zero charge

In adsorption studies, the removal efficiency of any chemical species in aqueous solutions depends on changing the chemistry of adsorbent–adsorbate interphase. Fig. 19(a-b) shows the effect of pH on biosorption of the metal ions by *Citrus paradisi* peel bio-sorbent. The maximum percentage of removal was obtained at pH 7 (99.53 %) and pH 9 (87.9 %) for Cr and Cd ions, respectively. The bio-sorbent uptake efficiencies on both ions decrease sharply at pH 11. This could be because of the precipitation of both metal ions, at this alkaline region associated with the hydroxyl groups competing through ion exchange. Furthermore, the point of zero charge (pHpzc) (Fig. 19(c)) was determined to assess the surface charge of the adsorbent. The pHpzc is defined as the pH point where the sorbent surface charge takes a zero value. As shown in Fig. 19 (b), the pHpzc was obtained at pH 3.6 which is lower than the pH solutions of Cr (pH

7) and Cd (pH 9) ions removal by the bio-sorbent. Consequently, the surface charge of the bio-sorbent possesses an overall positive charge unit. Therefore, the reaction mechanism was strongly favoured below the pH at point of zero charge.

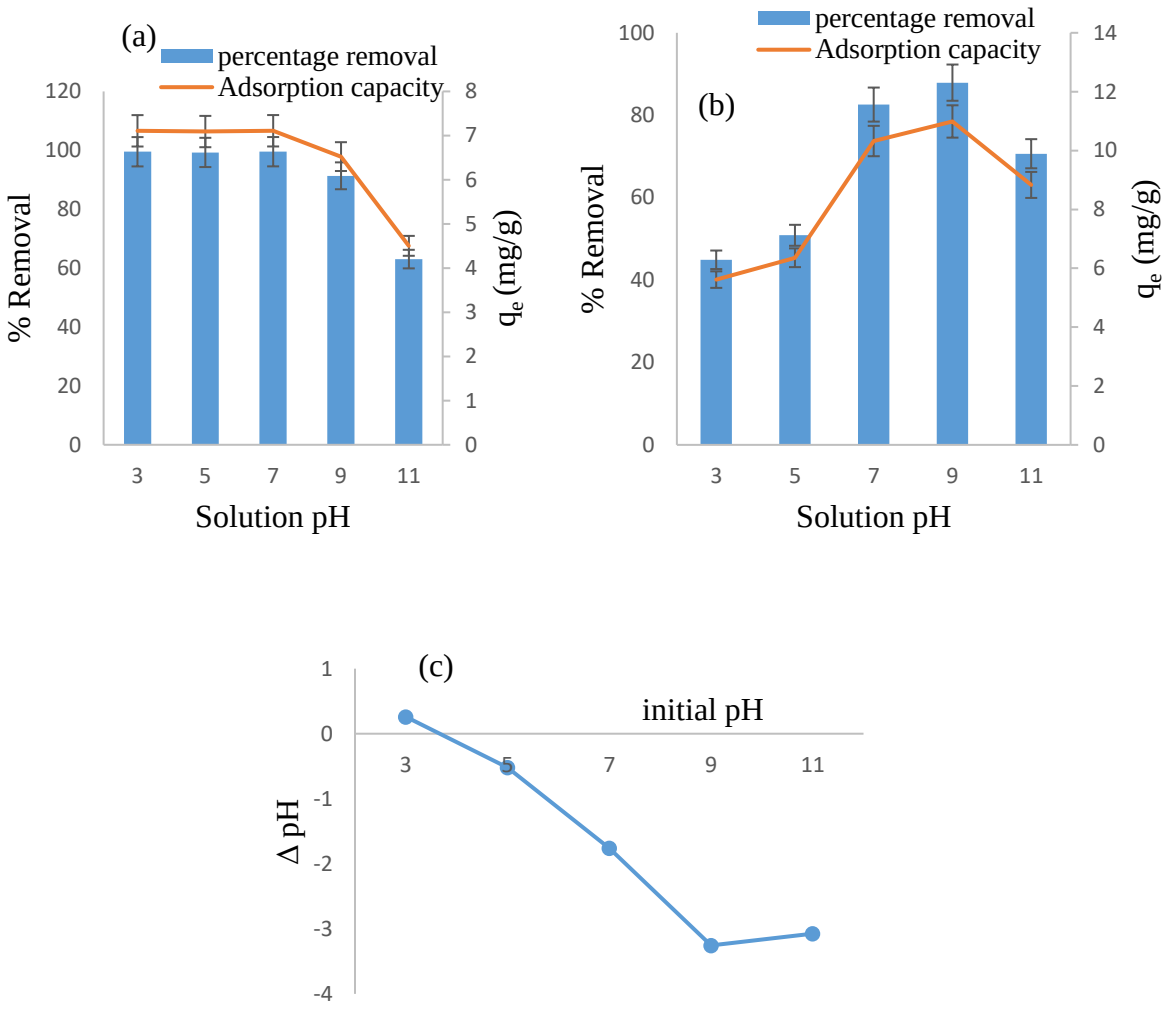

Fig. 19 Effect of pH for chromium (a) and cadmium (b) ions against percentage removal and adsorption capacity; The pHpzc (c) at various pH values. (optimum time of 60 and 30 min; optimum dosage of 0.35g and 0.2g for Cr and Cd ions respectively; temperature of 298K, initial concentration of 50mg/L and volume of 50mL at shaking speed of 250rpm.)

3.6 Mechanistic information

The main functional groups of *Citrus paradisi* peel bio-sorbent which were observed from the FTIR spectroscopy having much influence in the process included the carboxyl, hydroxyl, and amino groups that had the potential of binding metal ions in water. These were reported in the literature to have much influence on metal ion reduction and complexation (Li et al., 2017; Liu

et al., 2015; Kantar et al., 2008). The ionic charges of these functional groups (-COO^-, -OH^-, -N-H_2^+) played a role in the sorption process of Cr (VI) and Cd (II) ions in an aqueous solution. Moreover, Cr exists as an oxyanion, with two different species which are chromate (CrO_4^{2-}) and dichromate ($Cr_2O_7^{2-}$) carrying a negatively charged ion while Cd^{2+} carries a positively charged ion. The pH of the solution also plays a role in adsorption processes. Unceta et al. (2010) revealed that chemical species of Cr (VI) range from chromate (CrO_4^{2-}) at pH (6.5-14) through hydrogen chromate ($HCrO_4^-$) and dichromate ($Cr_2O_7^{2-}$) at pH (0.7-6.5) to chromic acid (H_2CrO_4) at pH < 0.7. This work also revealed those trends, from the effect of pH and pHpzc, Cr percentage removal was high at low pH (acidic) where the surface is positively charged, while Cd percentage removal was high at a high pH (alkaline) where the surface of the adsorbent was negatively charged. This proves the electrostatic attractions between the adsorbent and the adsorbate.

The proposed ion exchange from the adsorbent to the adsorbate is as follows: The O-H and the COOH groups can bind to Cd^{2+} via ionic bonding through electrostatic attractions since they are negatively charged which becomes easier to be attracted to Cd reducing its quantity in water. While on the other hand, Cr^{6+} got attached to the amino groups which are positively charged (-N-H_2^+), hence reducing Cr quantity in water. Furthermore, the other supporting data is the sorption kinetics, which indicated that both metal ions fitted better on pseudo-second-order reactions, which meant the reaction process occurred via chemisorption.

3.7 Phosphates and Nitrates adsorption efficiency by the grapefruit peel

The performance of grapefruit peel on the sorption of PO_4^{3-} and NO_3^- ions was very poor. With the initial concentration of 50 mg/L of NO_3^-, the final concentration was exceeding the initial concentration even when the peels were used on deionized water, which leads to believe that grapefruit peel might be releasing some nitrates into the water. However, on PO_4^{3-}, the results were slightly different. After the sorption process, the results showed some capacity of PO_4^{3-} removal though the % was very low. Hence grapefruit peels can be recommended to be used as a fertilizer since it contains high amounts of NO_3^-.

3.8 Conclusion

The present study aimed to evaluate the biosorption of Cr^{6+} and Cd^{2+}ions in an aqueous solution by *Citrus paradisi* (Grapefruit Red peel). Based on the results that were obtained, it can be concluded that *Citrus paradisi* was a good adsorbent for the removal of the metal ions of interest (Cr and Cd) as the percentage removals were both > 95% and the adsorption capacities were 12.43 and 12.48 mg/g respectively and obtained at the optimum contact time of 60 and 30 min respectively. The adsorbent dosage was 0.35 g and 0.2 g for Cr and Cd respectively with an initial metal concentration of 50 mg/L. The adsorbent pH was optimum at 7 (99.53% removal) and 9 (87.9% removal) for Cr and Cd ions, respectively. The adsorption data fitted well to the Freundlich isotherm model, which indicated that adsorption occurred on a multi-layered surface. Moreover, the sorption kinetics fitted better to pseudo-second-order reaction kinetics, which indicated that the reaction process occurred through chemisorption for both Cr and Cd. The availability of -COOH, -OH, and $-N-H^{+}$ functional groups in the grapefruit peel played a significant role in metal ion complexation and reduction as well as binding Cr and Cd metal ions. The thermodynamics data revealed that the reaction was endothermic, and the adsorption process was favorable and spontaneous as well as indicating an increase in randomness of Cr and Cd ions at the bio-sorbent solution interface.

References

Arief, V.O., Trilestari, K., Sunarso, J., Indraswati, N. and Ismadji, S., 2008. Recent progress on biosorption of heavy metals from liquids using low cost biosorbents: characterization, biosorption parameters and mechanism studies. *CLEAN–Soil, Air, Water*, *36*(12), pp.937-962.

Bağda, E., Tuzen, M. and Sarı, A., 2017. Equilibrium, thermodynamic and kinetic investigations for biosorption of uranium with green algae (Cladophora hutchinsiae). *Journal of Environmental Radioactivity*, 175, pp.7-14.

Bayuo, J., Abukari, M.A. and Pelig-Ba, K.B., 2019. Equilibrium isotherm studies for the sorption of hexavalent chromium (VI) onto groundnut shell. *IOSR Journal of Applied Chemistry (IOSR-JAC)*, 11(12), pp.40-46

Ben-Ali, S., Jaouali, I., Souissi-Najar, S. and Ouederni, A., 2017. Characterization and adsorption capacity of raw pomegranate peel biosorbent for copper removal. *Journal of Cleaner Production*, *142*, pp.3809-3821.

Bhatnagar, A., Sillanpää, M. and Witek-Krowiak, A., 2015. Agricultural waste peels as versatile biomass for water purification–A review. *Chemical Engineering Journal*, 270, pp. 244-271.

Bilal, M., Shah, J.A., Ashfaq, T., Gardazi, S.M.H., Tahir, A.A., Pervez, A., Haroon, H. and Mahmood, Q., 2013. Waste biomass adsorbents for copper removal from industrial wastewater—a review. *Journal of Hazardous Materials*, 263, pp. 322-333.

Ciolacu, D., Ciolacu, F. and Popa, V.I., 2011. Amorphous cellulose-structure and characterization. *Cellulose Chemistry and Technology*, 45(1), p.13.

Dada, A.O., Olalekan, A.P., Olatunya, A.M. and Dada, O.J.I.J.C., 2012. Langmuir, Freundlich, Temkin and Dubinin–Radushkevich isotherms studies of equilibrium sorption of Zn^{2+} unto phosphoric acid modified rice husk. *IOSR Journal of Applied Chemistry*, 3(1), pp.38-45.

Dubinin, M., 1960. The potential theory of adsorption of gases and vapors for adsorbents with energetically nonuniform surfaces. *Chemical Reviews*, *60*(2), pp.235-241.

Dyer, S.D., Peng, C., McAvoy, D.C., Fendinger, N.J., Masscheleyn, P., Castillo, L.V. and Lim, J.M.U., 2003. The influence of untreated wastewater to aquatic communities in the Balatuin River, The Philippines. *Chemosphere*, 52 (1), pp. 43-53.

Farinella, N.V., Matos, G.D. and Arruda, M.A.Z., 2007. Grape bagasse as a potential bio-sorbent of metals in effluent treatments. *Bioresource Technology*, 98(10), pp. 1940-1946.

Freundlich, H., 1907. Über die adsorption in lösungen. *Zeitschrift für physikalische Chemie*, *57*(1), pp.385-470.

Gupta, V.K. and Nayak, A., 2012. Cadmium removal and recovery from aqueous solutions by novel adsorbents prepared from orange peel and Fe_2O_3 nanoparticles. *Chemical Engineering Journal*, *180*, pp. 81-90.

Hameed, B.H. and Daud, F.B.M., 2008. Adsorption studies of basic dye on activated carbon derived from agricultural waste: Hevea brasiliensis seed coat. *Chemical Engineering Journal*, *139*(1), pp. 48-55.

Han, C.H., Zhang, R.M., Cheng, T. and Zhang, X., 2017. Effect of Activated Carbon Prepared from Grapefruit Peel on the Treatment of Heavy Metal Copper. *DEStech Transactions on Engineering and Technology Research*, (apetc).

Henze, M., 1992. Characterization of wastewater for modelling of activated sludge processes. *Water Science and Technology*, 25(6), pp. 1-15.

Ho, Y.S., 2006. Review of second-order models for adsorption systems. *Journal of Hazardous Materials*, 136(3), pp. 681-689.

Ho, Y.S. and McKay, G., 1999. Pseudo-second order model for sorption processes. Process *Biochemistry*, 34(5), pp. 451-465.

Ho, Y.S., Ng, J.C.Y. and McKay, G., 2000. Kinetics of pollutant sorption by bio-sorbents. *Separation and Purification Methods*, 29(2), pp. 189-232.

Ibrahim, W.M., Hassan, A.F. and Azab, Y.A., 2016. Biosorption of toxic heavy metals from aqueous solution by Ulva lactuca activated carbon. *Egyptian Journal of Basic and Applied Sciences*, 3(3), pp. 241-249.

Iqbal, M., Schiewer, S. and Cameron, R., 2009. Mechanistic elucidation and evaluation of biosorption of metal ions by grapefruit peel using FTIR spectroscopy, kinetics and isotherms modeling, cations displacement and EDX analysis. *Journal of Chemical Technology and Biotechnology*, 84(10), pp. 1516-1526.

Kantar, C., Cetin, Z. and Demiray, H., 2008. In situ stabilization of chromium (VI) in polluted soils using organic ligands: The role of galacturonic, glucuronic and alginic acids. *Journal of Hazardous Materials*, 159 (2-3), pp. 287-293.

Köseoğlu, E. and Akmil-Başar, C., 2015. Preparation, structural evaluation and adsorptive properties of activated carbon from agricultural waste biomass. *Advanced Powder Technology*, 26(3), pp. 811-818.

Lagergren, S., 1898. Zur theorie der sogenannten adsorption geloster stoffe. Kungliga svenska vetenskapsakademiens. Handlingar, 24, pp. 1-39.

Langmuir, I., 1916. The constitution and fundamental properties of solids and liquids. *Journal of the American Chemical Society*, *38*, pp. 2221–2295.

Lee, J.C., Son, Y.O., Pratheeshkumar, P. and Shi, X., 2012. Oxidative stress and metal carcinogenesis. *Free Radical Biology and Medicine*, 53(4), pp. 742-757.

Li, Y., Bian, Y., Qin, H., Zhang, Y. and Bian, Z., 2017. Photocatalytic reduction behavior of hexavalent chromium on hydroxyl modified titanium dioxide. Applied Catalysis B: *Environmental*, 206, pp. 293-299.

Liu, W., Zhang, J., Jin, Y., Zhao, X. and Cai, Z., 2015. Adsorption of Pb (II), Cd (II) and Zn (II) by extracellular polymeric substances extracted from aerobic granular sludge: Efficiency of protein. *Journal of Environmental Chemical Engineering*, 3(2), pp. 1223-1232.

Mdlalose, L., Balogun, M., Setshedi, K., Tukulula, M., Chimuka, L. and Chetty, A., 2017. Synthesis, characterization and optimization of poly (p-phenylenediamine)-based organoclay composite for Cr (VI) remediation. *Applied Clay Science*, *139*, pp.72-80.

Monteiro C.M., Castro P.M.L. and Malcata F.X., 2011. Microalga-mediated bioremediation of heavy metal contaminated surface waters. *Environmental Pollution*, 20, pp. 365–385.

Nguyen, H.D., Mai, T.T.T., Nguyen, N.B., Dang, T.D., Le, M.L.P. and Dang, T.T., 2013. A novel method for preparing microfibrillated cellulose from bamboo fibers. Advances in Natural Sciences: *Nanoscience and Nanotechnology*, 4(1), p. 015016.

Ofomaja, A.E. and Ho, Y.S., 2007. Effect of pH on cadmium biosorption by coconut copra meal. *Journal of Hazardous Materials*, 139(2), pp. 356-362.

Regmi, S., Ghimire, K.N., Pokhrel, M.R. and Khadka, D.B., 2015. Adsorptive Removal and Recovery of Aluminium (III), Iron (II), and Chromium (VI) onto a Low Cost Functionalized Phragmities Karka Waste. *Journal of Institute of Science and Technology*, 20(2), pp. 145-152.

Romero-Cano, L.A., Gonzalez-Gutierrez, L.V. and Baldenegro-Perez, L.A., 2016. Bio-sorbents prepared from orange peels using Instant Controlled Pressure Drop for Cu (II) and phenol removal. *Industrial Crops and Products*, 84, pp. 344-349.

Rosales, E., Meijide, J., Tavares, T., Pazos, M. and Sanromán, M.A., 2016. Grapefruit peelings as a promising bio-sorbent for the removal of leather dyes and hexavalent chromium. *Process Safety and Environmental Protection*, *101*, pp. 61-71.

Saeed, A., Sharif, M. and Iqbal, M., 2010. Application potential of grapefruit peel as dye sorbent: kinetics, equilibrium and mechanism of crystal violet adsorption. *Journal of Hazardous Materials, 179* (1-3), pp. 564-572.

Schiewer, S. and Iqbal, M., 2013. Physicochemical characterization and mechanism analysis of native and protonated grapefruit peels adsorbing cadmium. *Desalination. Water Treatment*, 52, pp. 5900–5911.

Toor, M. and Jin, B., 2012. Adsorption characteristics, isotherm, kinetics, and diffusion of modified natural bentonite for removing diazo dye. *Chemical Engineering Journal*. 187, pp. 79-88.

Torab-Mostaedi, M., Asadollahzadeh, M., Hemmati, A. and Khosravi, A., 2013. Equilibrium, kinetic, and thermodynamic studies for biosorption of cadmium and nickel on grapefruit peel. *Journal of the Taiwan Institute of Chemical Engineers*, *44*(2), pp. 295-302.

Unceta, N., Séby, F., Malherbe, J. and Donard, O.F.X., 2010. Chromium speciation in solid matrices and regulation: a review. *Analytical and Bioanalytical Chemistry*, *397*(3), pp.1097-1111.

Wang, L. and Wang, A., 2008. Adsorption properties of Congo Red from aqueous solution onto surfactant-modified montmorillonite. *Journal of Hazardous Materials*, *160*(1), pp. 173-180.

Weber, W.J. and Morris, J.C., 1963. Kinetics of adsorption on carbon from solution. *Journal of the Sanitary Engineering Division*, *89*(2), pp. 31-60.

WHO, 2011. Guidelines for drinking water quality.4th Edn., World Health Organization, Geneva.

Wu, S., Dai, X., Cheng, T. and Li, S., 2018. Highly sensitive and selective ion-imprinted polymers based on one-step electrodeposition of chitosan-graphene nanocomposites for the determination of Cr (VI). *Carbohydrate polymers*, *195*, pp.199-206.

.

CHAPTER 4

Biosorption of toxic metal ions and nutrients from aqueous solution by diatom biomass

4.1 Abstract

This paper presents the biosorption of Cr^{6+}, Cd^{2+} and PO_4^{3-} ions by diatom biomass and its sorption processes. The adsorbent was characterized by XRD, FTIR and SEM-EDS analysis. The morphological data revealed that diatom biomass is an aluminosilicate material. The FTIR spectra revealed Si-O, O-H, N-H, and C-O as the main functional groups present on the surface of the adsorbent. The SEM-EDS revealed that the surface of the adsorbent was rough, irregular and without a clearly defined shape and was composed of aluminosilicate material. The batch sorption studies indicated that diatom biomass worked as a good adsorbent for Cr^{6+}, $Cd^{2+,}$ and PO_4^{3-} at the optimum contact times of 20 min; 30 min and 60 min respectively. The optimum dosage for Cr^{6+}, Cd^{2+} and PO_4^{3-} were obtained at 0.25 g, 0.15 g and 0.35 g. The pH for both Cr^{6+} and PO_4^{3-} was optimum at around pH 3 while for Cd^{2+} it was obtained at an optimum pH of 7. The overall kinetic results indicated that pseudo-second-order sorption was the rate-limiting step, which meant that chemisorption was the responsible mechanism for the adsorption process between the surface of the diatom biomass and the pollutants. The adsorption model that best described the equilibrium data was Freundlich isotherm. Additionally, the maximum adsorption capacities obtained for Cr^{6+} was 5.66 (mg/g) at 313 K; for Cd^{2+} was 5.27 (mg/g) at 313 K while PO_4^{3-} was 19.13 (mg/g) at 298 K. Furthermore, the thermodynamic data revealed that the biosorption process was favorable and spontaneous across all temperatures. This proved that the adsorbent material is suitable for wastewater treatment.

Keywords: Biosorption, chromium and cadmium ions, phosphates, diatom biomass

4.2 Introduction

Water pollution remains a major problem affecting the world up-to-date. This is usually caused by releasing untreated wastewater from mining, sewage, agriculture, and domestic activities. The problems related to polluted water escalate every day. This affects both humans and other living organisms all over the world. Hence, scientists and researchers are always working towards finding the best solutions to solve these menaces by coming up with new methods and technologies.

Heavy metals are known to be persistent and non-biodegradable in the environment which makes it hard to treat them, and most of them are toxic and carcinogenic (Abbasi et al., 2013; Gebrekidan et al., 2013). Examples of heavy metals include silver, copper, mercury, nickel, cadmium, arsenic, chromium and lead. Some small amounts of heavy metals such as Mn, Se, Cr, Fe, Zn, and Ni provide vital nutrients for the living organism as well as biochemical and physiological functions in plants and animals (Tchounwou et al., 2012). However, in large amounts, they tend to be toxic and cause harmful health effects due to their ability to bioaccumulate in the tissues of living organisms. The toxicity of heavy metals depends on many factors which include the dose, route of exposure, chemical species with age, gender, genetics, and nutritional status of exposed individuals (Tchounwou et al., 2004).

Nutrients such as phosphates also have their role to play in the environment. Their sources can be from natural phenomena, which involve the leaching of phosphate from rock deposits or from anthropogenic activities which include agricultural runoff, industrial effluents, use of detergents and the decomposition of organic waste materials (Kumar et al., 2012). In plants, they serve as one of the primary nutrients they need to survive. Apart from their natural role, phosphates are also useful for a wide range of industrial purposes. Phosphates can be used in beverages and sugar industries, to prevent the formation of scaling and to inhibit corrosion, to produce detergents, and to produce fertilizers in the agricultural sector (Badamasi et al., 2019; Mas-Torres et al., 2004; Mathur 1995). However, these uses come at a cost for the environment because of the way they leach out or discharged into surface waters. When they are in excess, they create environmental problems such as eutrophication which depletes the oxygen supply needed by aquatic organisms. This causes foul-smelling of phytoplankton which reduces water clarity and quality. It further limits light penetration, reducing growth and causing the death of plants and aquatic organisms thereby depopulating them and disrupt the ecosystem balance (Lin et al., 2019; Chislock et al., 2013). The phosphates maximum permissible limit by World Health Organization (WHO) is set to be 5 mg/L.

Various technologies have been implemented to tackle these challenges, which include ion exchange, chemical precipitation, coagulation, filtration for metal ions and phosphorus treatment uses processes such as sedimentation, uptake by algal biomass and precipitation (Fauzi et al., 2020; Ukhurebor et al., 2020; Nekouei et al., 2019; Chen et al., 2009; Kayombo et al., 2004).

However, these technologies have their drawbacks which involve high maintenance cost, the production of secondary pollutants, expensive and being complicated (Cao et al., 2018; El-Zayat, 2009). Biosorption has recently gained prominence due to its availability, cost-effectiveness, easy to use, and high efficiency (Al-Homaidan et al., 2018; Javanbakht et al., 2014). Biosorption involves using living organisms to purify or remediate polluted water. Generally, algae have gained prominence over the years due to their high production efficiency and wide range of applications as animal feed, human food (due to the high protein, amino acids, fiber, and micronutrients), can be used in cosmetic industries due to their skin properties which include anti-aging and body benefits; can also be used as fertilizers and biofuels (Matos, 2017; Matos et al., 2016; Enzing et al., 2014).

In this research, diatom biomass was used as an adsorbent to remove Cr^{6+} and Cd^{2+} metal ions as well as PO_4^{3-} from wastewater. Diatoms are naturally living available micro-organisms which are photosynthetic. Additionally, diatoms are characterized by a unicellular silica-based wall and are found in aquatic and subaerial environments with high species diversity (Smucker and Vis, 2011). They are generally used for biomonitoring and assessment of the ecological status of rivers as indicators of water quality (Dalu and Froneman, 2016; Kelly et al., 2008). Moreover, they can be used as a biological approach for removing toxic pollutants in water.

Various studies have been conducted on diatoms for the removal of heavy metals especially cations due to their negatively charged surface (Hernández-Ávila et al., 2017; Kunugi et al., 2014; Sbihi et al., 2014). Similarly, they were also used to remove phosphates from water (Yan et al., 2010).

With the information gathered so far, the knowledge on the application of diatom biomass for heavy metal removal in water seems to be scanty when compared to other algae such as the green-blue algae. Some people, especially those who have fish farms, fish tanks, or aquariums see diatom as a problem that ruins the beauty or cleanliness of their water containers, while others see them as an ecological burden that needs to be eradicated. However, this study reveals

the usefulness of this abundance, naturally available, cheap, and accessible resource which can be used directly as a powerful tool to eliminate heavy metals and phosphates in water.

4.3 Materials and methods

4.3.1 Chemicals and reagents

The chemicals that were used to conduct experiments in this research were of analytical reagent grade. KCl, HCl, NaOH, $CdN_2O_6 \cdot 4H_2O$, $K_2Cr_2O_7$ and KH_2PO_4 used were purchased from Rochelle Chemicals (Johannesburg, South Africa). The chemicals were used directly without further purification. In preparation of stock solutions and the dilutions of standards, Ultrapure Milli-Q water (18.2 MΩ/cm) was used.

4.3.2 Preparation of adsorbents

The diatom biomass was collected from the Mvudi River Thohoyandou, South Africa with geographic coordinates of 22°59,012' S 030°26,585' E. The biomass was washed thoroughly with Millipore water (18.2 MΩ/cm) and filtered. It was then dried in an oven (Eco-Therm, model 920) at 60˚C for 24 h. The dried material was ground (mortar and pistil) and used for experiments without any further treatment.

4.3.3 Preparation of stock solutions

The stock solutions with concentrations of 1000 mg/L Cr^{6+}, Cd^{2+}, and PO_4^{3-} solutions were prepared by dissolving 2.744 g of $CdN_2O_6 \cdot 4H_2O$, 2.82 g of $K_2Cr_2O_7$ and 1.44 g KH_2PO_4 in a 1L volumetric flask with Ultrapure milliQwater respectively. The working solutions were prepared by diluting the stock solutions to 50 mg/L to conduct the experiments.

4.3.4 Instruments

Various functional groups on the solid surface of the diatom biomass were identified by an ALPHA Bruker FTIR Spectrophotometer (Berlin, Germany) within the range of 400-4000 cm^{-1}. The mineralogical and phase identification was determined by XRD, type PANalytical X'Pert Pro powder diffractometer for qualitative sample analysis. The surface morphology was determined by SEM and the EDS to provide the elemental composition of the adsorbent with an FEI Nova NanoSEM 230 with the field emission gun equipped with an Oxford Xmax SDD detector operating at an accelerating voltage of 20Kv. For the EDS detector, Oxford X-Max with INCA software was used to characterize the sorbent material. The filtrates of Cr^{6+} and Cd^{2+} were analyzed by FAAS type (PINAACLE 900T) and phosphate was analyzed by Metrohm 850 professional Ion chromatography (IC).

4.3.5 Point of zero charge (pHpzc)

The pH at point-of-zero charge was determined by mixing 0.2 g of diatom biomass in 0.1 M KCl solutions. The pH of solutions was adjusted to desired values between 3 and 11 by adding 0.1 M HCl or 0.1 M NaOH. A volume of 50 mL solutions was pipetted into plastic bottles which were agitated on a thermostat water bath shaker at 150 rpm for 24 h at room temperature. The equilibrium pH (pH_f) of each mixture was measured and the intersection pH-initial against ΔpH curve gave the pHpzc value.

4.3.6 Adsorption procedure

The adsorption experiments were carried out to determine the effect of different experimental parameters such as contact time, dosage, initial concentration, pH and temperature. Contact time was varied from 1 to 120 min. The effect of adsorbent dosage was evaluated by varying dosage from 0.05 to 0.4 g. The effect of initial metal concentration and adsorption isotherms were evaluated by varying concentrations from 10 to 200 mg/L. Moreover, the solution pH was evaluated by adjusting from 3 to 11 using 0.1 M NaOH and 0.1 M HCl. All experiments were carried out using 50 mL of Cr^{6+}, Cd^{2+} and PO_4^{3-}. After shaking time elapsed, metal ion samples were filtered and analyzed by FAAS spectrometer and the PO_4^{3-} ions by IC. The adsorption capacity and removal efficiency of diatom biomass for Cr^{6+}, $Cd^{2+,}$ and PO_4^{3-} ions were calculated by equations (1) and (2).

$$q = (C_0 - C_e) \times \frac{V}{w} \quad (1)$$

$$\%\ \text{Removal} = \frac{(C_0 - C_e)}{C_0} \times 100 \quad (2)$$

where Co is the initial metal ions concentration (mg/L); Ce is the metal ions concentration at equilibrium (mg/L); V is the volume of solution (L) and w is the mass of the adsorbent (g).

4.4 Results and discussion

4.4.1 XRD

The mineral phase of the diatom biomass was revealed by the X-ray diffraction spectrum. It indicated the pattern of the biomass to be between the range of 5-80 theta which can be observed from Fig 20. Furthermore, the X-ray diffraction spectrum indicated that there are no clear mineral phases that can be observed on the surface of the diatom biomass except that the biomass does not display any crystallinity but an amorphous pattern which is typical of biomass materials.

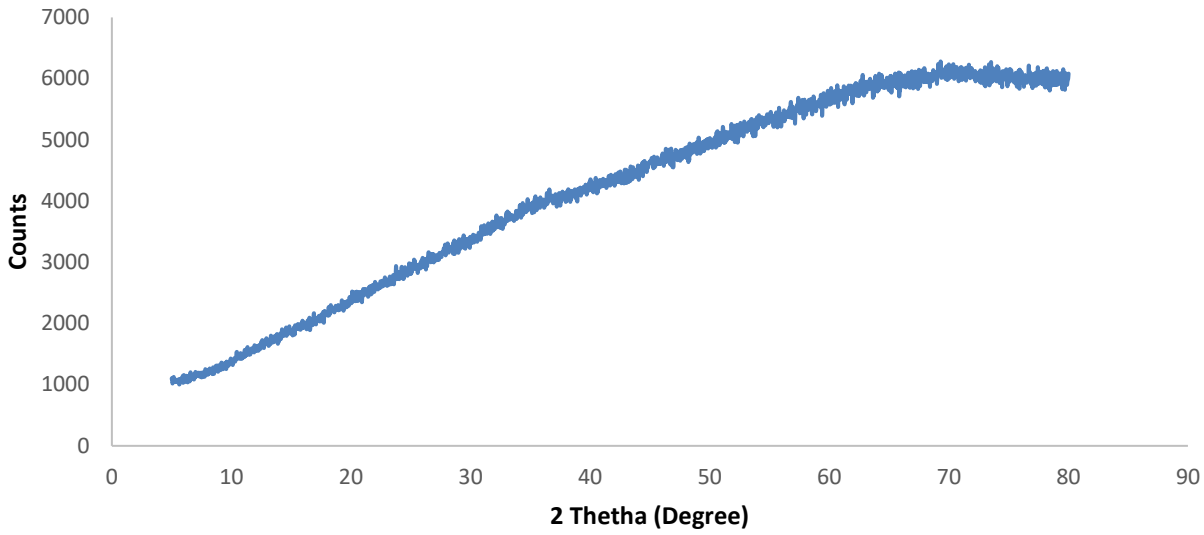

Fig. 20. XRD spectrum for diatom biomass

4.4.2 FTIR

Fig. 21 illustrates the FT-IR spectra for the raw diatom biomass and after sorption of Cr^{6+}, Cd^{2+} and PO_4^{3-}, revealing different functional groups that are present on the surface. The peaks were obtained at 3423.13, 1634.04, and 1032.24 cm^{-1}. From the data, the stretching and vibration of the structural O-H group and the broad band at 3423.13 cm^{-1} could be as a result of the hydroxyl groups of the phenolic group and water (Ibrahim et al., 2016; Mudzielwana et al., 2016). Moreover, the peak at 1640.16 cm^{-1} revealed the bending N-H groups which displayed the amino groups which are also present on the surface of the diatom biomass. Furthermore, a strong band at 1032.24 cm^{-1} was observed which could be as a result of stretching and vibration of Si-O groups as well as the C-O groups indicating the carboxylic acids with vibrations of alcoholic groups in the diatom biomass. However, after the sorption of Cr^{6+}, Cd^{2+} metals ions as well as phosphates ions, there was a reduction in the broad stretching band of the OH groups and N-H groups suggesting that they had a major role in the removal rate of the above-mentioned ions. Furthermore, it is known from the literature that the hydroxyl and amino groups play a major role in the removal of metal ions (Wang et al., 2020).

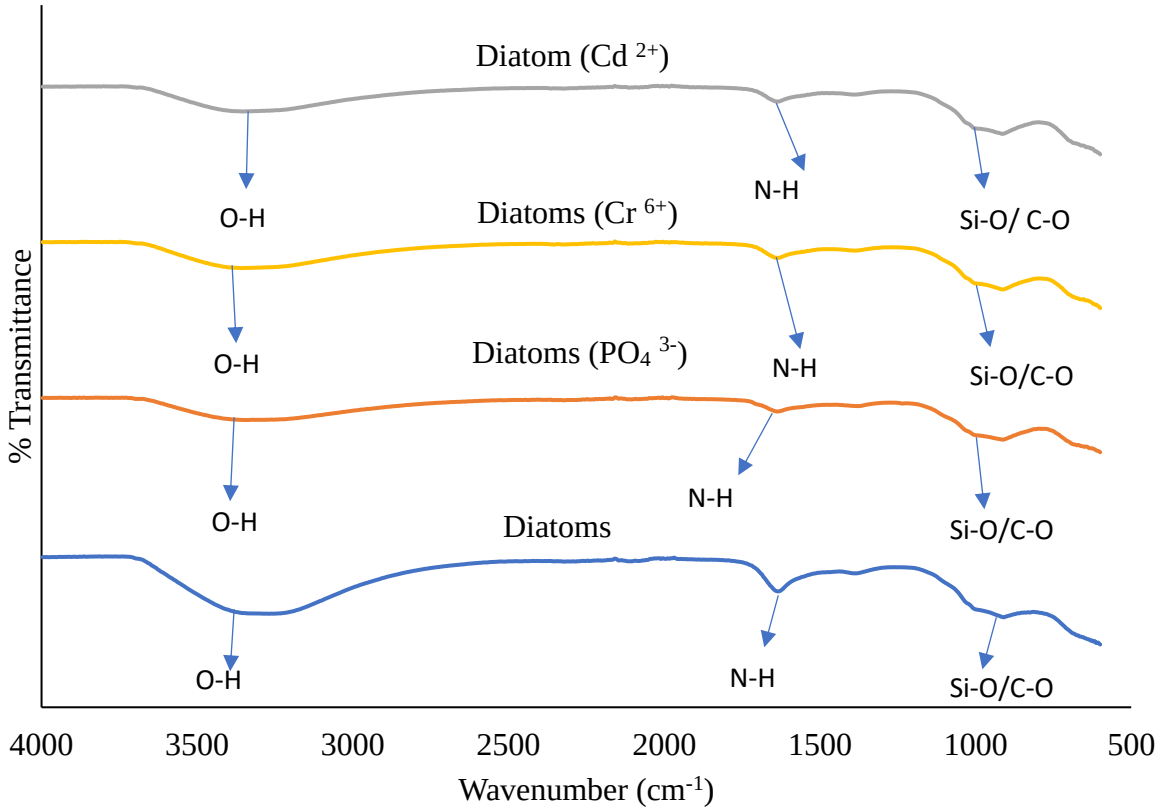

Fig. 21. FTIR spectra for diatom biomass before and after the treatment of Cd^{2+}, $Cr^{6+,}$ and PO_4^{3-} ions.

4.4.3 Surface morphology

Fig. 22 shows the surface morphologies of the raw diatom biomass and after the treatment of Cr^{6+} and Cd^{2+} metal ions as well as PO_4^{3-} ions. From the raw diatom biomass (a), the surface is rough, irregular and without a clearly defined shape which is typical of biomass materials. The EDS for the raw diatom biomass (Fig. 22(a)), revealed some of the elements that were present on the surface of the adsorbent which includes Mg, Fe, Al, Si with C and O. This indicated that the material was composed of aluminosilicate as validated by the EDS spectra. Furthermore, after the treatment of Cr^{6+}, Cd^{2+} and PO_4^{3-} ions (Fig. 22(b-d)), the morphology was slightly changed into rectangular, spike-like shapes, having pores on the surface, after interacting with the above-mentioned ions. Furthermore, a successful adsorption process on the metal ions as well as phosphate ions is further revealed by their presence on the respective EDS spectra.

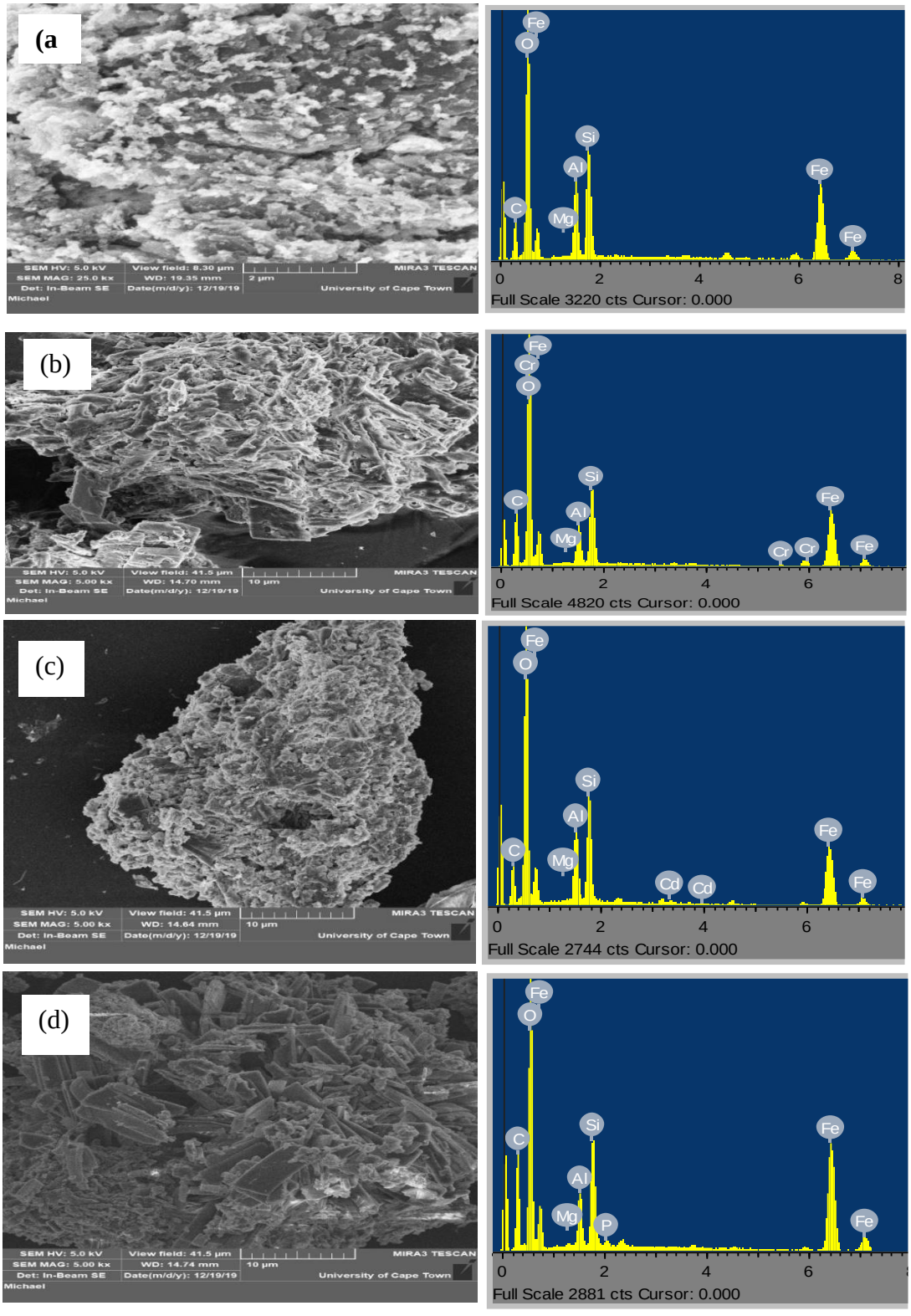

Fig. 22. Morphological data for diatom biomass alone (a); diatom biomass after treatment of Cr^{6+} (b); Cd^{2+} (c) and PO_4^{3-} (d).

4.5 Batch experimental results

4.5.1 Effect of contact time and kinetic modeling

The effect of contact time for Cd^{2+}, Cr^{6+} and PO_4^{3-} ions were evaluated between the ranges of 1-120 min to evaluate the uptake efficiency of these ions by diatom biomass. Fig. 23 shows the percentage removal and the adsorption capacity to be increasing with time. Moreover, the rise in percentage removal is an indication of an increase in the accessibility and vacant active binding sites at the surface of the diatom biomass and the presence of various functional groups of the biomass material. From the results obtained, the highest Cr^{6+}, the highest percentage removal was 28.36% and the adsorption capacity was 3.55 mg/g at an optimum contact time of 30 min. for Cd^{2+}, the percentage removal was 74.36% and the adsorption capacity was 9.29 mg/g which were obtained at 20 min. While for PO_4^{3-}, the percentage removal which was selected at the optimum contact time of 60 min was over 58% with the adsorption capacity of 7.29 mg/g.

Generally, diatoms are known to have a negatively charged surface, which enables them to adsorb positively charged metal ions (Hernández-Ávila et al., 2017; Kunugi et al., 2014), hence higher Cd^{2+} percentage removal and adsorption capacity at a lesser time than Cr^{6+} (which exist s as an oxy-anion) and PO_4^{3-}. The overall results showed that at the beginning of time, the reaction was rapid since there were a lot of active sites available for the adsorption process to occur until the adsorbent becomes saturated, and all sites occupied leading to a low driving force for the adsorption process.

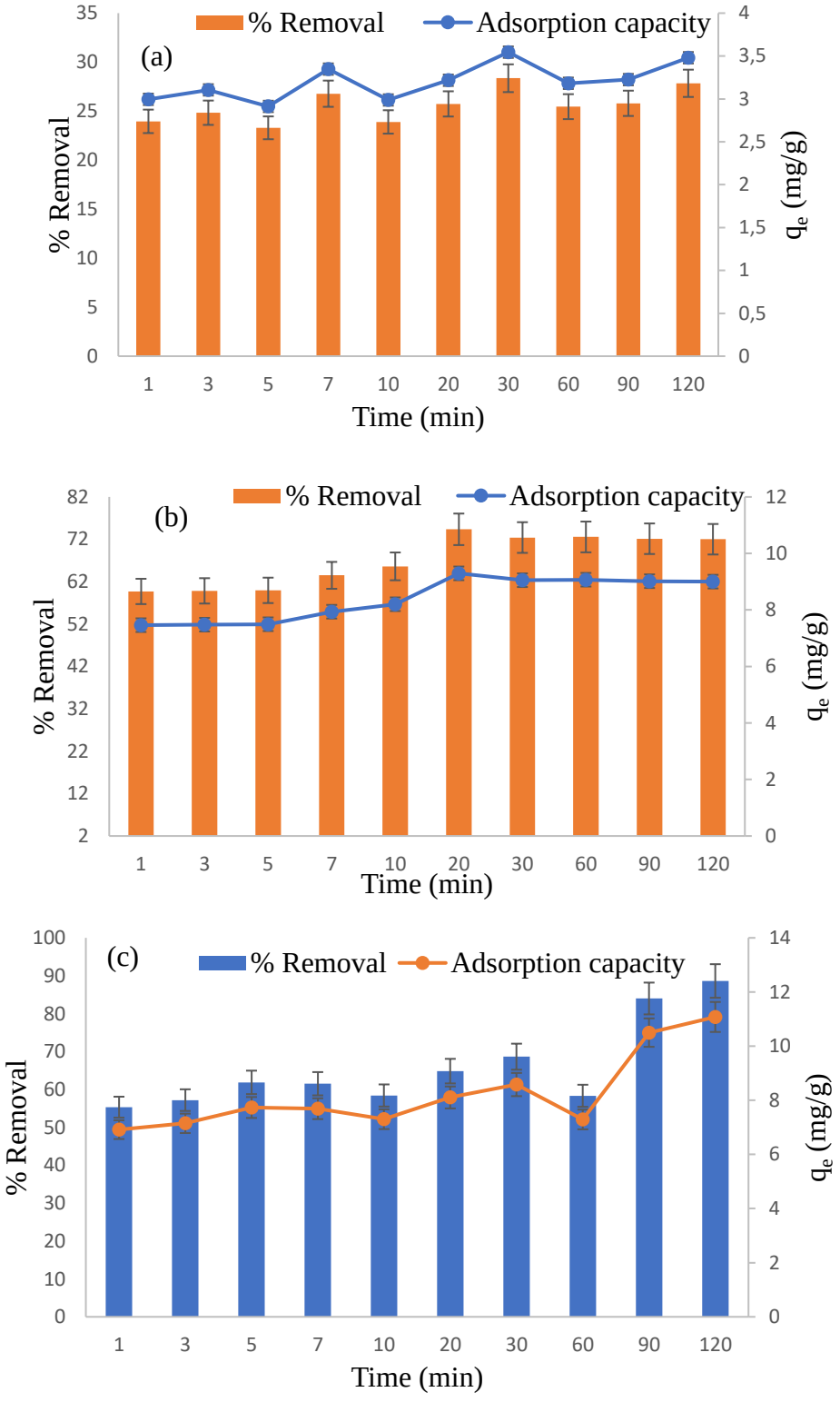

Fig. 23. Effect of contact time for Cr^{6+} (a); Cd^{2+} (b) and PO_4^{3-} (C) against percentage removal and adsorption capacity. (Experimental conditions: dosage, 0.2 g; volume, 50 mL; initial concentration, 50 mg/L; pH, neutral; temperature, 298 K and shaking speed, 250 rpm).

The kinetic model studies were used to assess the mechanisms that occur during the adsorption process to time. Fig. 24 shows the adsorption kinetics graphs to predict the rate of uptake and processes of an adsorbate to adsorbent with pseudo-first-order (Lagergren, 1898), pseudo-second-order (Ho et al., 1999) through non-linear as well as the linear intra-particle diffusion expressions in Table 5. The models are expressed in equations (3) – (5) respectively.

$$q_t = q_e(1 - e^{-kit}) \quad (3)$$

where qe and qt (mg/g) are the amounts of adsorption at pseudo-first-order at time t (min) while k_1 (min $^{-1}$) is the pseudo-first-order adsorption rate constant at equilibrium.

$$q_t = \frac{qe^2\, k_2 t}{1 + k_2\, q_e t} \quad (4)$$

where k_2 (g/mg/min) is the equilibrium rate constant of pseudo-second-order adsorption.

$$q_t = k_t t^{0.5} + ci \quad (5)$$

where qt is the amount adsorbed (mg/g) concerning time (t) (min); K_t is the intra-particle diffusion rate constant in (mg/g/min) and C_i is a constant related to the thickness of the boundary layer (mg/g).

Fig. 24 (a-c) shows the results of pseudo-first order and pseudo-second-order kinetic models for Cr^{6+}, Cd^{2+}, and PO_4^{3-} ions respectively. The results for pseudo-first-order coefficient of determination (R^2) of Cr^{6+}, Cd^{2+} and PO_4^{3-} were 0.99; 0.97; 0.81 respectively. The root mean square errors (RMSE) were 0.20; 0.68 and 1.36 while the RCS values were 0.01; 0.05 and 0.20 respectively. However, pseudo-second-order present different results for Cr^{6+}, $Cd^{2+,}$ and PO_4^{3-}, where the R^2 values were 0.61; 0.74 and 0.83. The RMSE were 0.18; 0.52 and 1.22 while the RCS values were 0.01; 0.03 and 0.16 respectively. Based on the R^2 values obtained, pseudo-first-order was the rate-limiting step for Cr^{6+}, Cd^{2+} and PO_4^{3-} ions which indicated that physisorption was the mechanism responsible for the adsorption process. However, when including other evaluation parameters, the results proved that pseudo-second-order is the rate-limiting step due to lower values of RSME and RCS. This suggested that both physisorption and chemisorption mechanisms were responsible for the reaction process. This can further be elaborated. At the initial stage during physisorption, the adsorption process occurs between the surface of the diatom adsorbent and the adsorbate ions which involves a reversible reaction governed by the weak Van der Waal's force of attraction. As the reaction goes further, chemisorption occurs, where there is an interaction between the adsorbent functional groups as

already alluded by the FTIR and the adsorbent ions which result in ion exchange as well as the force of attractions or repulsions.

The last kinetic model investigated, the intra-particle diffusion, basically describes the transfer of analytes from the external surface into the pores of the adsorbent (Ho et al., 2000).

Usually, the process of diffusion is divided into three steps in which the adsorption process takes place, firstly, diffusion through the liquid film to the surface of the adsorbent involves a rapidness reaction at the surface of the adsorbent. Secondly, diffusion through the pore liquid which is the intra-particle diffusion-indicating ion exchange mechanisms and electrostatic attractions between the adsorbate and the adsorbent facilitating a chemical process. Thirdly, the adsorption and desorption between the active sites of the adsorbent and the adsorbate. At this stage, the adsorbate ions attach themselves to the internal surface of the adsorbent (Xu et al., 2018; Ho et al., 2000).

Table 5 represents the intra-particle diffusion parameters which include the coefficient of determination, the intra-particle diffusion constant rate (mg/g/min) and the constant related to the thickness of the boundary layer (mg/g). The overall results for the adsorbates showed that the coefficient of determination (R^2) values were 0.35; 0. 63 and 0.96 while the diffusion rate constants were 0.04; 0.18 and 0.08 (mg/g/min) and the thickness of the boundary layer was 3.02; 7.54 and 2.09 for Cr^{6+}, Cd^{2+} and PO_4^{3-} respectively.

Based on these results, Cd^{2+} and PO_4^{3-} showed a better coefficient of determination results than Cr^{6+}, which indicated a better adsorption process for them. This could be due to the electric charges of Cd^{2+} and the adsorbent resulting in electrostatic attractions and ion exchange mechanisms while for PO_4^{3-}, it could be due to the interaction between the functional groups of the diatoms with the adsorbate since diatoms use nutrients such as phosphates amongst others for their growth and survival (Kamyaba et al., 2019). Moreover, Cr^{6+} poor results could be due to electrostatic repulsions between the surface of the diatom biomass and Cr^{6+} (CrO_4^{2-}, $Cr_2O_7^{2-}$) ions. Hernández-Ávila et al. (2017) also reported that diatoms showed low efficiency towards Cr^{6+}. This is because Cr^{6+} is an oxyanion as already alluded to above.

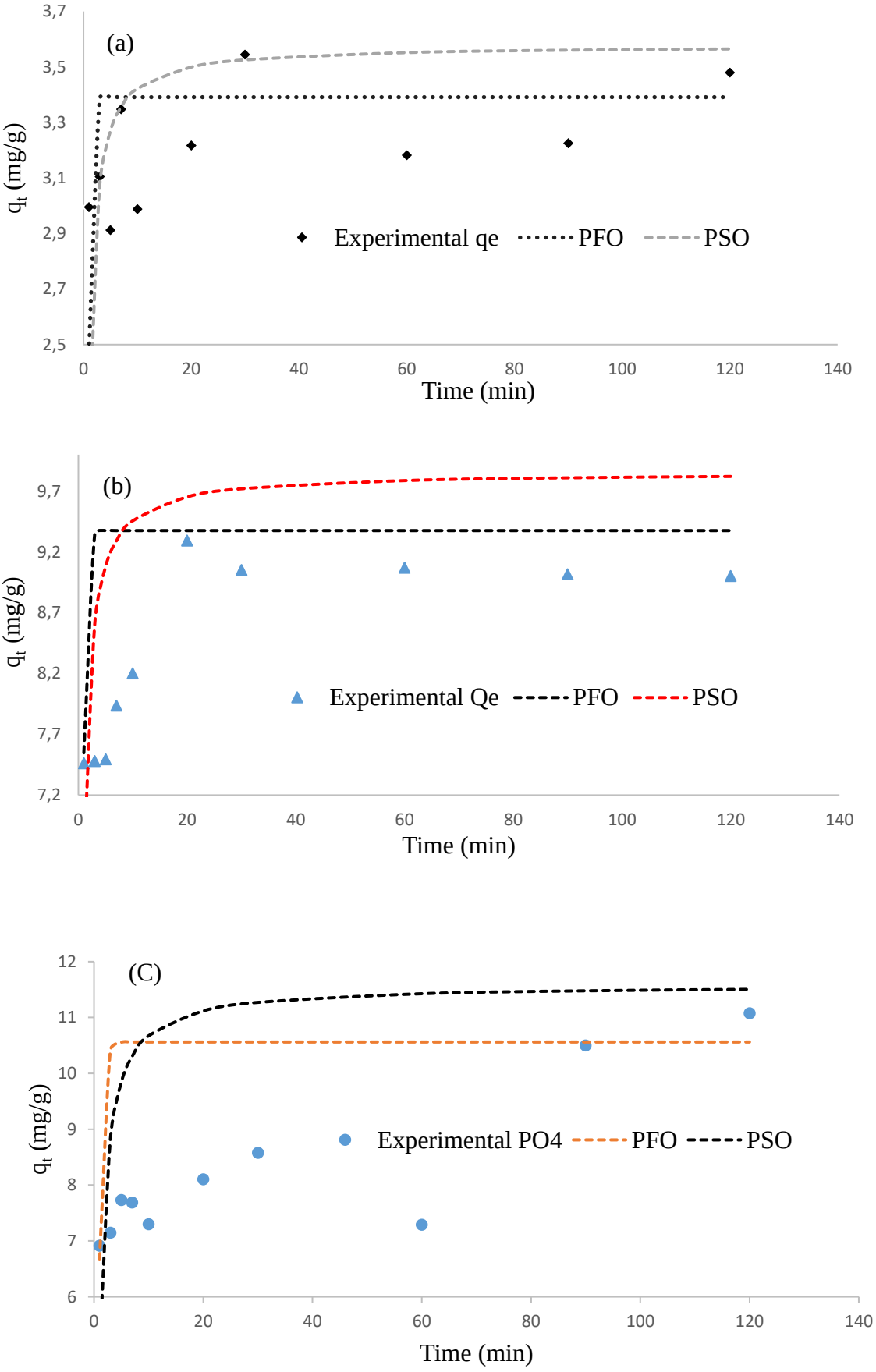

Fig. 24. Non-linear adsorption kinetic plots for Cr^{6+} (a), Cd^{2+} (b) and PO_4^{3-} (c).

Table 4: Non-linear kinetic models for Cr^{6+}, Cd^{2+} and PO_4^{3-} in aqueous solutions.

Kinetic model	Parameter	Cr^{6+}	Cd^{2+}	PO_4^{3-}
PFO	k_1	2.64	2.04	1.64
	q_t	3.22	8.51	8.40
	R^2	0.99	0.97	0.81
	RCS	0.01	0.05	0.20
	RSME	0.20	0.68	1.36
PSO	k_2	2.53	0.40	0.25
	q_t	3.27	8.80	8.83
	R^2	0.61	0.74	0.83
	RCS	0.01	0.03	0.16
	RSME	0.18	0.52	1.22

Table 5: Linear kinetics parameters for Cr^{6+}, Cd^{2+} and PO_4^{3-} ions in aqueous solutions.

Intra-particle diffusion	Parameter	Cr^{6+}	Cd^{2+}	PO_4^{3-}
	K_{id}	0.04	0.18	0.08
	C	3.02	7.54	2.09
	R^2	0.35	0.63	0.96

4.5.2 Effect of adsorbent dosage for Cr^{6+}, Cd^{2+} and PO_4^{3-} ions

The effect of adsorbent dosage was determined by varying various adsorbent mass ranging from 0.05 to 0.4 g. The percentage removal for Cr^{6+}, $Cd^{2+,}$ and PO_4^{3-} increased with an increase in adsorbent dose. This was due to the available active binding sites for the metal ions and nutrient ions which were introduced as the mass of the adsorbent was increased. Moreover, the adsorbent dose played a significant role in the Cr^{6+}, Cd^{2+} and PO_4^{3-} uptake from water. The optimum adsorbent dose for Cr^{6+}, Cd^{2+} and PO_4^{3-} was obtained at 0.15 g with 16.06% removal, 0.25 g with 80.19% and 0.35 g with 72.07% respectively. The optimum adsorbent doses were further used for successive experiments.

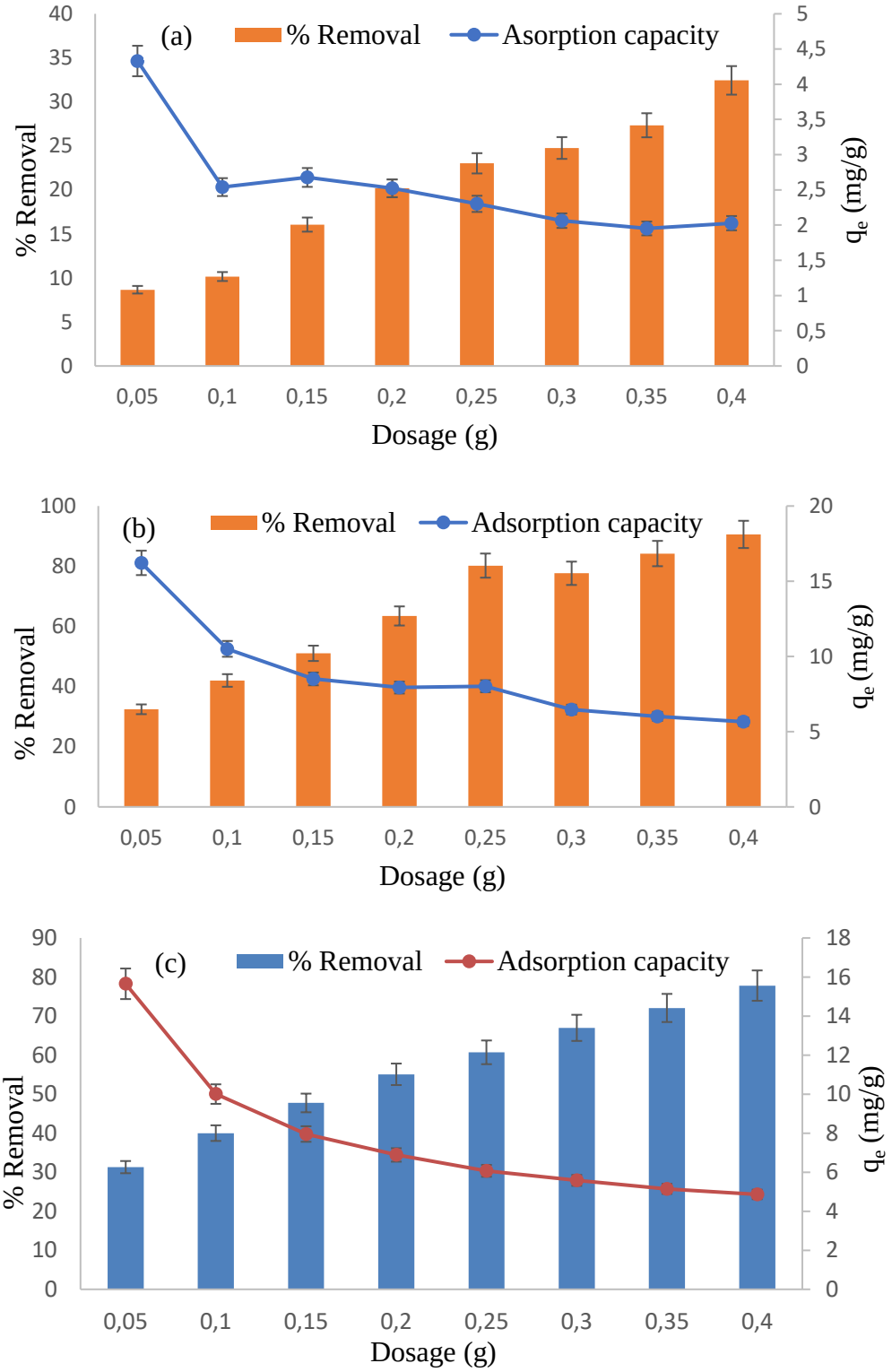

Fig. 25. Effect of adsorbent dosage for Cr^{6+} (a); Cd^{2+} (b) and PO_4^{3-} (c) by diatom biomass. (Experimental conditions: Time, 30 min; 20 min and 60 min for Cr^{6+}, Cd^{2+} and PO_4^{3-} respectively; pH, neutral; temperature, 298 K; volume of 50 mL; initial concentration, 50 mg/L and shaking speed, 250 rpm).

4.5.3 Effect of pH and pHpzc for Cr^{6+}, Cd^{2+} and PO_4^{3-} ions in aqueous solutions.

pHpzc is defined as the point where the net surface of the material has a zero charge. In this study, it was used to determine the surface charge of the diatom biomass to determine the chemical processes that are responsible for the removal of Cr^{6+}, Cd^{2+} and PO_4^{3-} ions. Additionally, the surface is positively charged when the pH is below pHpzc and negatively charged when the pH is above pHpzc. The pHpzc was found to be around 6.

Furthermore, the change in the chemistry of the adsorbent-adsorbate interphase determines the removal efficiency of any chemical species in aqueous solutions. Fig. 26 (b;d), shows sorption capacity for Cr^{6+} and PO_4^{3-} to be decreasing with an increase in pH with the highest percentage removal obtained at pH 3 to be 42.72% and 99.88% respectively. This could be as a result of electrostatic attractions between the Cr^{6+} and PO_4^{3-} ions with the surface of the adsorbent at pH below 6 being positively charged, hence a major decrease can be observed on both sides. Fig. 26(c) shows sorption capacity for Cd^{2+} to be increasing with an increase in pH with optimum pH of 7 at 98.69% removal rate. This could be as a result of electrostatic repulsion between Cd^{2+} ions and the surface charge of the adsorbent before pH 6 since the surface is positively charged. But beyond pH 6, there was a major increase in the sorption capacity and removal efficiency of Cd^{2+} ions since the surface of the material was negatively charged.

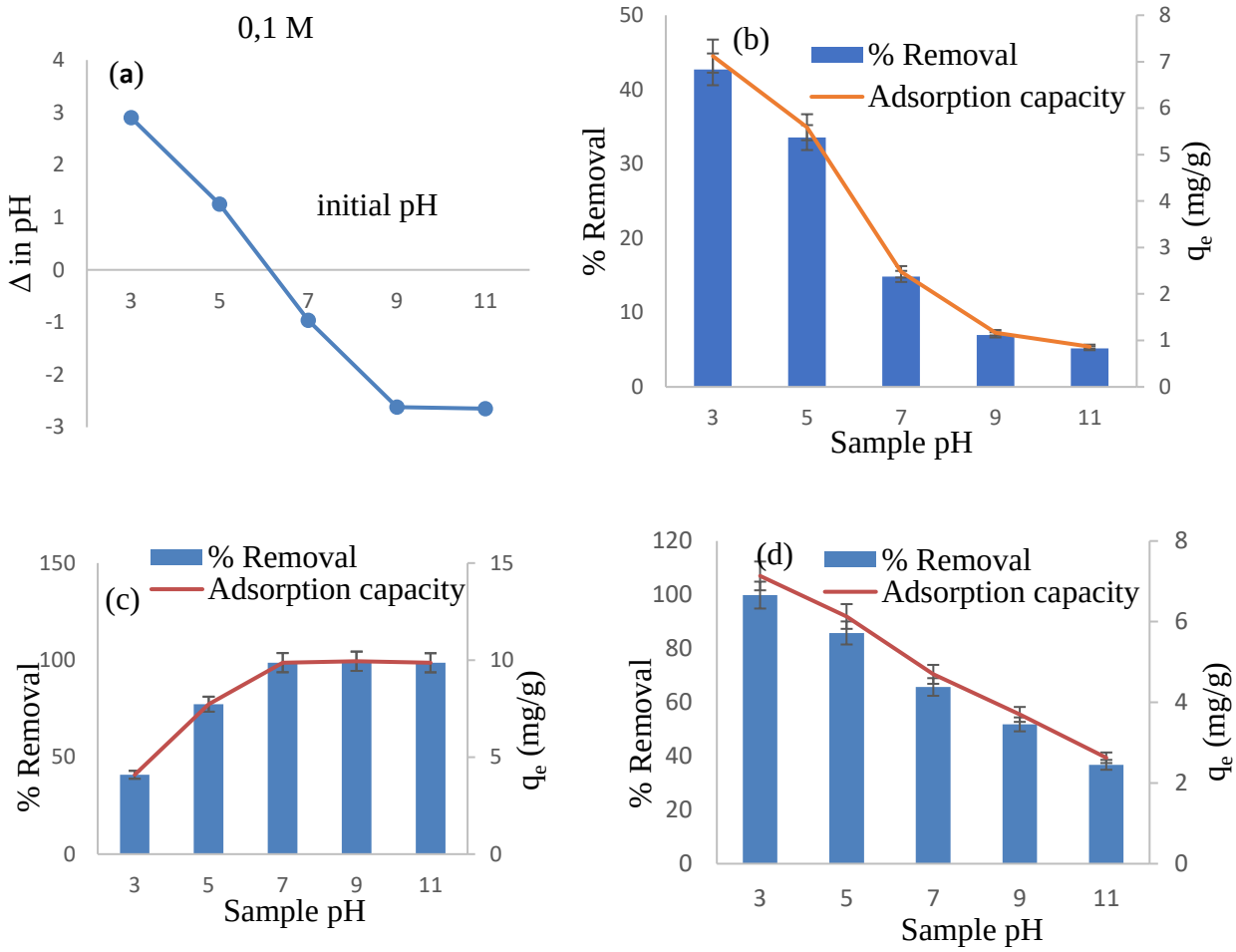

Fig. 26. pHpzc for the diatom biomass (a) and the effect of pH for Cr^{6+} (b), Cd^{2+} (c)and PO_4^{3-} (d). (Experimental conditions: Time, 30 min; 20 min and 60 min; initial concentration, 50 mg/L; dosage, 0.15 g; 0.25 g and 0.35 g for Cr^{6+}, Cd^{2+} and PO_4^{3-}; temperature, 298K; volume, 50 mL; shaking speed, 250 rpm).

4.5.4 Effect of initial concentration and adsorption isotherms.

Figure 27 illustrates the effect of initial concentration at various temperatures for Cr^{6+}, Cd^{2+} and PO_4^{3}. It was observed from the graphs that the percentage removal of the discussed pollutants decreased with an increase in initial concentrations as temperatures increased. This could be due to a reduced mass gradient between the adsorbent and the adsorbate interaction as a result of active sites being all occupied. This is similar to what was obtained by Parlayici et al. (2015). However, the adsorption capacity was increasing with an increase in initial concentrations as temperature increased. This could be due to saturation and the occupation of all the active binding sites of the diatom biomass. Furthermore, the temperature seemed to be playing a role in enhancing the adsorption capacity of the adsorbent in adsorption processes.

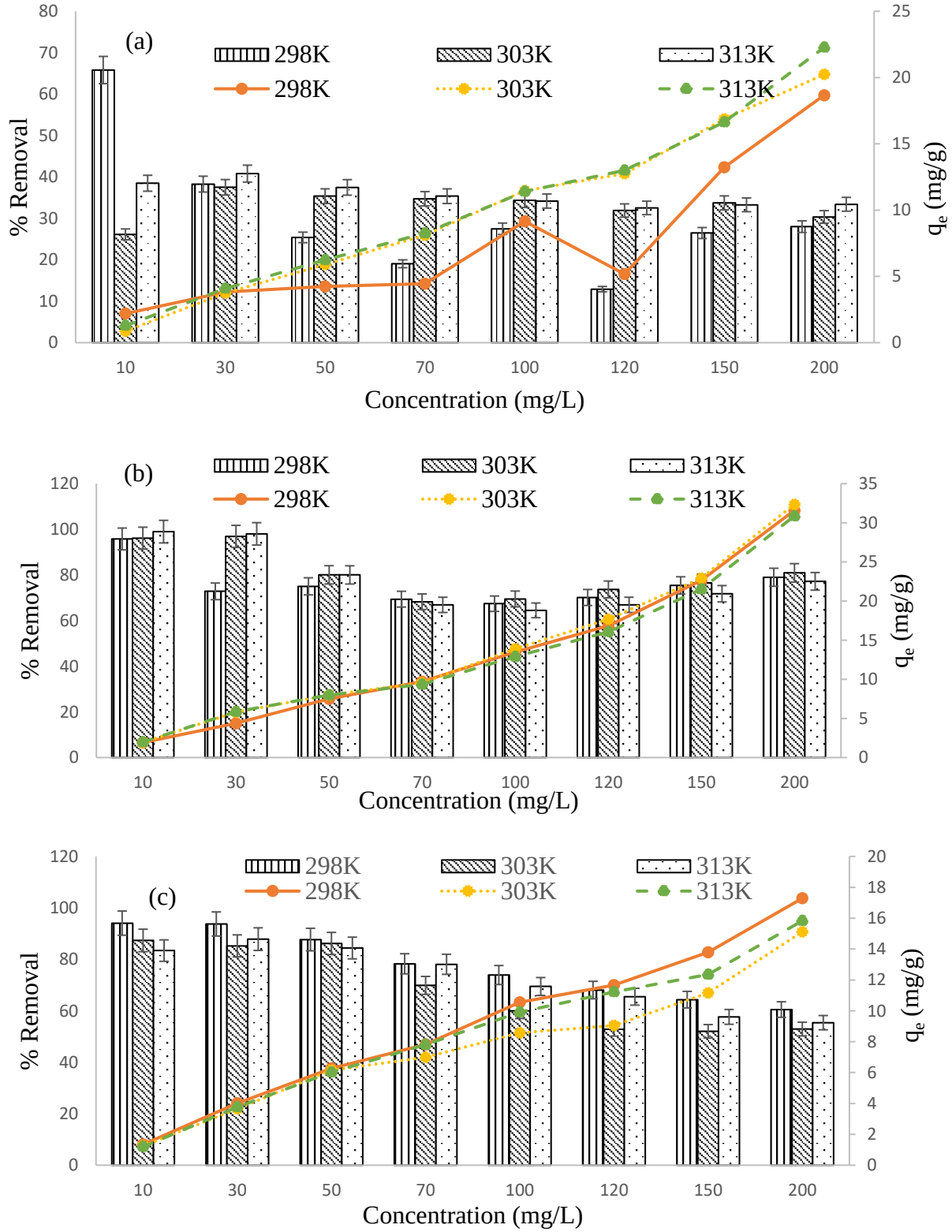

Fig. 27. Effect of initial concentration for Cr^{6+} (a), Cd^{2+} (b) and PO_4^{3-} (c) ions. (Experimental conditions: Time, 24 h; volume, 50 mL; dosage, 0.15 g; 0.25 g and 0.35 g for Cr^{6+}, Cd^{2+} and PO_4^{3-}; pH, neutral; shaking speed, 250 rpm).

The adsorption isotherms for Cr^{6+}, Cd^{2+} and PO_4^{3-} were modeled using the empirical and theoretical Freundlich and Langmuir isotherms. Langmuir isotherm indicates that adsorption occurs uniformly on all active sites of the adsorbent and ions form a monolayer (Aigbe et al., 2018). Generally, Langmuir isotherm explains that once all active sites have been occupied by the adsorbate, there will be no adsorption taking place. Yang et al. (2019) supported this by indicating that all active sites have equal binding energy that attracts a single adsorbate. Furthermore, a good fit of this isotherm indicates monolayer adsorption (Teng and Hsieh 1998) The non-linear equation is given by equation (6).

$$q_e = \frac{q_m K_L C_e}{1+K_L C_e} \quad (6)$$

where q_e (mg/g) is the adsorption capacity; q_m (mg/g) is the theoretical maximum adsorption capacity; C_e (mg/L) is the equilibrium concentration; k_L (L/mg) is the Langmuir biosorption equilibrium constant. These parameters can be obtained by the plot of C_e/q_e against C_e.

Moreover, Langmuir isotherm can be further determined through a dimensionless parameter called the separation factor R_L which is given by equation (7).

$$R_L = \frac{1}{1 + k_L C_i} \quad (7)$$

where K_L is Langmuir isotherm constant, and C_i (mg/L) is the initial ion concentration. R_L provides an indication of whether the adsorption is favorable ($0 < R_L < 1$), irreversible ($R_L = 0$), unfavorable ($R_L > 1$) or linear ($R_L = 1$).

Freundlich isotherm model was also used to determine the interaction between adsorbate molecules adsorbed onto the heterogeneous surface of the adsorbent to create a multi-layered surface. The non-linear equation of the Freundlich isotherm is expressed in equation (8).

$$q_e K_f C e^{\frac{1}{n}} \quad (8)$$

where K_f and 1/n are empirical constants that show the biosorption capacity and the adsorption intensity respectively. When $0 < 1/n < 1$, the adsorption is favorable; when $1/n > 1$, the adsorption is unfavorable and when $1/n = 1$, the adsorption is irreversible.

The data obtained from Table 6 shows the non-linearized parameters of Freundlich and Langmuir models for Cr^{6+}, Cd^{2+} and PO_4^{3-} sorption by diatom biomass adsorbent at various temperatures. From the table, based on various parameters such as the coefficient of

determination (R^2), adjusted coefficient of determination (adjusted R^2), reduced chi-square, it is evident that the adsorption process favors both Freundlich and Langmuir isotherms. However, the isotherm that favored the adsorption process of the adsorbates was found to be Freundlich. This was also supported by the R^2 values for Freundlich which were higher than those of Langmuir as well as the n values which were $0 < 1/n < 1$ across all temperatures which showed favorability for Freundlich. Thus, indicating adsorption occurred on a multilayer surface at the sorbate-sorbent interphase with a higher affinity for PO_4^{3-} and Cd^{2+}.

The maximum adsorption capacities obtained for Cr^{6+} and Cd^{2+} metal ions were increasing with an increase in temperature while for PO_4^{3-} ions, the adsorption capacities were decreasing with an increase in temperature. An increase in temperature plays a role in the adsorption capacities of the metal ions but not on PO_4^{3-} ions. The adsorption capacities for PO_4^{3-} were higher than those of the metal ions. This could be due to higher utilization of phosphates by diatoms for their survival as mentioned earlier.

The other isotherm model that is used in adsorption is Dubinin Radushkevich (D-R). This model is concerned about the bio-sorbent porosity and the adsorption energy. The values obtained through the adsorption energy depending on whether if E is between 8 and 16 kJ/mol, adsorption is said to have occurred via chemisorption and if E is less than 8 kJ/mol, adsorption occurred via physisorption. The D-R model can be expressed as:

$$lnq_e = lnq_o - \beta e^2 \qquad (9)$$

where qe (mg/g) is the amount of ions adsorbed per unit weight of adsorbent, q_o being the maximum adsorption capacity, β is the coefficient constant, E (KJ/mol) is the mean sorption energy, Ɛ is the Polanyi potential. The mean sorption energy is illustrated as equation (10).

$$E = \sqrt{\frac{1}{2\beta}} \qquad (10)$$

where R is the gas constant (J/mol K) and T is the temperature (K).

In Table 6, DR- isotherm is presented to determine the mean free energy of the sorption process and to determine the porous nature of the adsorbent. The parameters for Cr^{6+}, Cd^{2+} and PO_4^{3-} were also presented. Generally, the data indicated that the Q_{max} value of the adsorbates increases with an increase in temperature though fluctuations can be observed, which indicated a high affinity for the adsorbates. It also indicated the significance of temperature towards

adsorption capacity. Furthermore, the DR mean adsorption energy was less than 8kJ/mol for all the adsorbates which means the reaction involved the physisorption phenomenon.

The overall sorption process performed poorly for Cr^{6+} metal ion as opposed to Cd^{2+} and PO_4^{3-} which could be due to the surface of diatoms being known to be negatively charged causing electrostatic repulsions between the Cr^{6+} ions since it exists as dichromate ($Cr_2O_7^{2-}$) and chromate (CrO_4^{2-}) as already discussed on earlier. However, for PO_4^{3-} is not the same even though the ions are negatively charged, as already alluded, this is because diatoms use nutrients such as phosphates amongst others to survive hence there a huge reduction or favourability for phosphates than the metal ions. As for Cd^{2+}, the mechanisms responsible are the electrostatic attractions and ion exchange between the adsorbent and Cd^{2+} ions.

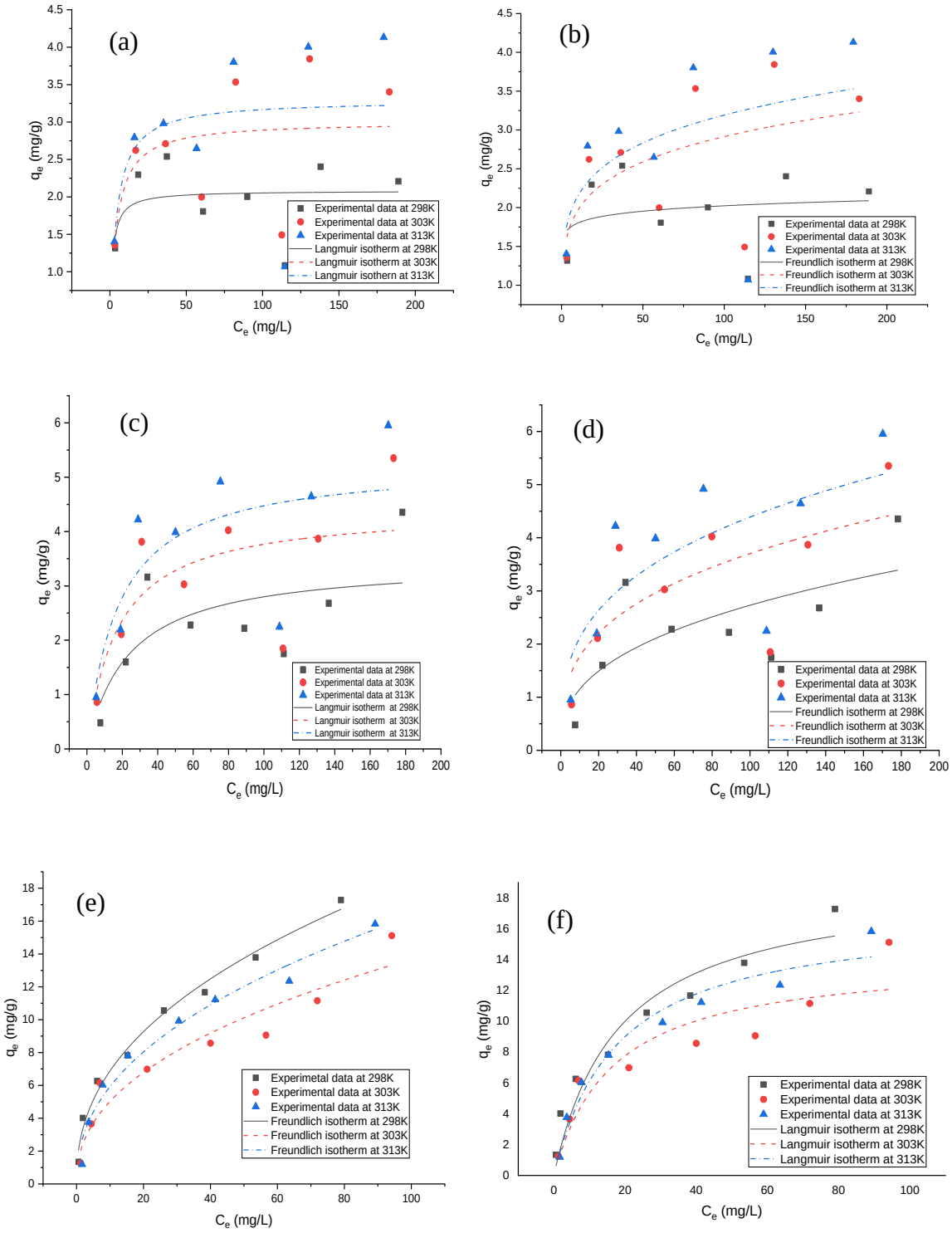

Fig. 28. Graphs showing Langmuir and Freundlich isotherms for Cr^{6+} (a;b), Cd^{2+} (c;d) and PO_4^{3-} (e;f) ions.

Table 6: The non-linear isotherm parameters for Langmuir, Freundlich and DR models

	Cr^{6+}			Cd^{2+}			PO_4^{3-}		
Temperature (K)	298	303	313	298	303	313	298	303	313
Langmuir									
Qm (mg/g)	3.84	5.32	5.66	3.46	4.42	5.27	19.13	14.18	17.01
K_L (L/mg)	0.49	0.21	0.22	0.04	0.06	0.06	0.06	0.06	0.06
R^2	0.64	0.41	0.40	0.50	0.52	0.58	0.93	0.84	0.96
Adj R^2	0.57	0.31	0.30	0.41	0.44	0.51	0.92	0.82	0.95
R_L	0.04	0.09	0.08	0.32	0.26	0.26	0.26	0.25	0.26
RCS	0.17	1.66	2.05	0.78	1.17	1.38	2.30	3.44	1.05
Freundlich									
K_F ((mg/g)/(mg/L)n)	2.59	2.19	2.25	0.49	0.84	1.02	2.56	1.84	2.16
n	0.08	0.18	0.19	0.38	0.32	0.32	0.43	0.44	0.44
R^2	0.34	0.42	0.43	0.51	0.51	0.54	0.99	0.92	0.97
Adj R^2	0.23	0.32	0.33	0.43	0.43	0.46	0.99	0.90	0.97
RCS	0.30	1.65	1.95	0.75	1.19	1.51	0.40	1.81	0.73
Dubinin-Radushkevvich									
βD (mol^2/kJ^2)	3.00E-06	3.00E-05	1.00E-05	2.00E-07	2.00E-07	5.00E-08	4.00E-07	9.00E-07	1.00E-06
q_{max}(mg/g)	7.13	11.20	11.15	13.08	15.14	13.77	10.03	8.52	9.97
E (kJ/mol)	0.29	0.09	0.16	1.12	1.12	2.24	1.12	0.75	0.71
R^2	0.36	0.82	0.74	0.54	0.74	0.69	0.80	0.80	0.88

4.5.5 Thermodynamics

The thermodynamics parameters by diatom biomass adsorbent for the biosorption of Cr^{6+}, Cd^{2+} and PO_4^{3-} ions was determined at various temperatures ranging between 298 and 313 K. The thermodynamic parameters such as the Gibbs free energy change, entropy and enthalpy change were all used to determine the degree of randomness, type of reaction, rate of spontaneity during sorption of the above-mentioned ions by the diatom biomass material. The following equations were used to determine the thermodynamics parameters:

$$\mathrm{In}K_D = \frac{\Delta H^\circ}{R} + \frac{\Delta S^\circ}{R} \quad (11)$$

where, ΔH° (KJ/mol) and ΔS° (J/mol K) are the enthalpy and entropy change respectively during biosorption process, which was calculated from the intercept and slope of the linear plot.

$$\Delta G^\circ = \Delta H^\circ - T\Delta S^\circ \quad (12)$$

where ΔG is the free Gibbs energy change, R and T represent the ideal gas constant (8.314 J mol^{-1} K^{-1}) and absolute temperature (K)

$$K_D = \frac{C_s}{C_e} \quad (13)$$

where K_D is the equilibrium constant at a constant temperature, C_e (mg/L) and C_s (mg/L) are equilibrium concentrations of sorbate and the amount of sorbate adsorbed, respectively.

Results were obtained for the thermodynamic parameters for Cr^{6+}, Cd^{2+} and PO_4^{3-} as illustrated in Table 7. It was observed that as the temperature increased, so were the values for the free Gibbs energy change (ΔG°) which confirmed the feasibility and spontaneous nature of the adsorption process. Furthermore, the reaction was endothermic for Cr^{6+} and Cd^{2+} and their values were higher than 40 KJ/mol, which indicated that the adsorption by diatom adsorbent is chemisorption which was also validated by the adsorption kinetics. However, for PO_4^{3-}, it was an exothermic reaction. This was validated by a positive ΔH° for Cr^{6+} and Cd^{2+} and a negative ΔH° for PO_4^{3-}. Furthermore, the positive ΔS° indicated an increase in randomness for the adsorbates during the reaction process which supports ion exchange mechanisms at their respective pH values.

Table 7: Illustrates the thermodynamic parameters for Cr^{6+}, Cd^{2+} and PO_4^{3-}

	Cr^{6+}	Cd^{2+}	PO_4^{3-}
ΔH◦ (KJ/mol)	550.07	211.99	-15.51
ΔS◦ (J/mol K)	1928.35	803.76	53.89
ΔG◦ (kJ/mol)			
298	-574.1	-239.31	-16.075
303	-583.74	-243.33	-16.344
313	-603.02	-251.36	-16.883

4.6 Conclusion

The morphological data confirmed an interaction of the diatom biomass adsorbent towards metal ions and nutrients confirmed by different characterizations including FTIR, XRD, and the SEM-EDS. It was observed that the adsorbent has the potential to remove Cr^{6+}, $Cd^{2+,}$ and PO_4^{3-} in aqueous solutions. The sorption capacity of the diatom biomass depended on the optimization parameters such as contact time, adsorbent dosage, pH, and initial concentration of the adsorbates. The sorption kinetics fitted better on pseudo-second-order for both metal ions and nutrients, indicating chemisorption as the responsible mechanism in the reaction. The adsorption data fitted well in the Freundlich isotherm model, which indicated that adsorption occurred on a multi-layered surface heterogeneity which was attained by non-linear isotherms models for Freundlich and Langmuir. The thermodynamics data revealed that the reaction was endothermic for Cr^{6+} and Cd^{2+} and was exothermic for PO_4^{3-}, and the adsorption process was favorable and spontaneous across all temperatures as well as indicating an increase in randomness of adsorbate by the adsorbent solution interface.

References

Abbasi, A.M., Iqbal, J., Khan, M.A. and Shah, M.H., 2013. Health risk assessment and multivariate apportionment of trace metals in wild leafy vegetables from Lesser Himalayas, Pakistan. *Ecotoxicology and Environmental Safety*, *92*, pp.237-244.

Aigbe, U.O., Ho, W.H., Maity, A., Khenfouch, M. and Srinivasu, V., 2018, March. Removal of hexavalent chromium from wastewater using PPy/Fe_3O_4 magnetic nanocomposite influenced by rotating magnetic field from two pole three-phase induction motor. In *Journal of Physics: Conference Series*, 984 (1), pp. 012008.

Al-Homaidan, A.A., Al-Qahtani, H.S., Al-Ghanayem, A.A., Ameen, F. and Ibraheem, I.B., 2018. Potential use of green algae as a biosorbent for hexavalent chromium removal from aqueous solutions. *Saudi Journal of Biological Sciences*, *25*(8), pp.1733-1738.

Badamasi, H., Yaro, M.N., Ibrahim, A. and Bashir, I.A., 2019. Impacts of Phosphates on Water Quality and Aquatic Life.

Cao, D.Q., Song, X., Fang, X.M., Yang, W.Y., Hao, X.D., Iritani, E. and Katagiri, N., 2018. Membrane filtration-based recovery of extracellular polymer substances from excess sludge and analysis of their heavy metal ion adsorption properties. *Chemical Engineering Journal*, *354*, pp.866-874.

Chen, Q.Y., Luo, Z., Hills, C., Xue, G. and Tyrer, M., 2009. Precipitation of heavy metals from wastewater using simulated flue gas: sequent additions of fly ash, lime and carbon dioxide. *Water Research*, 43(10), pp. 2605-2614.

Chislock, M. F., Doster, E., Zitomer, R. A. and Wilson, A. E., 2013. Eutrophication: Causes, Consequences, and Controls in Aquatic Ecosystems. *Nature Education Knowledge*, *4*(4), pp. 10.

Dalu, T. and Froneman, P.W. 2016. Diatom-based water quality monitoring in southern Africa: challenges and future prospects. *Water SA. 42*(4), PP.551-559.

El-Zayat, M., 2009. Removal of heavy metals by using activated carbon produced from cotton stalks.

Enzing, C., Ploeg, M., Barbosa, M. and Sijtsma, L., 2014. Microalgae-based products for the food and feed sector: an outlook for Europe. *JRC Scientific and Policy Reports*, pp. 19-37.

Fauzi, A., Hapidin, D.A., Munir, M.M., Iskandar, F. and Khairurrijal, K., 2020. A superhydrophilic bilayer structure of a nylon 6 nanofiber/cellulose membrane and its characterization as potential water filtration media. *RSC Advances*, *10*(29), pp.17205-17216.

Gebrekidan, A., Weldegebriel, Y., Hadera, A. and Van der Bruggen, B., 2013. Toxicological assessment of heavy metals accumulated in vegetables and fruits grown in Ginfel river near Sheba Tannery, Tigray, Northern Ethiopia. *Ecotoxicology and Environmental Safety*, *95*, pp.171-178.

Hernández-Ávila, J., Salinas-Rodríguez, E., Cerecedo-Sáenz, E., Reyes-Valderrama, M., Arenas-Flores, A., Román-Gutiérrez, A.D. and Rodríguez-Lugo, V., 2017. Diatoms and Their Capability for Heavy Metal Removal by Cationic Exchange. *Metals*, *7*(5), p.169.

Ho, Y.S., Ng, J.C.Y., McKay, G., 2000. Kinetics of pollutant sorption by bio-sorbents. Separation and purification methods. 29(2), 189-232.

Ho, Y.S., Wase, D.A.J. and Forester, C.F., 1999. Kinetic studies of competitive heavy metal adsorption by sphagnum peat. *Environmental Technology*, 17, pp. 441-443.

Ibrahim, W.M., Hassan, A.F., Azab, Y.A., 2016. Biosorption of toxic heavy metals from aqueous solution by Ulva lactuca activated carbon. *Egyptian Journal of Basic and Applied Sciences. 3*(3), 241-249.

Javanbakht, V., Alavi, S.A. and Zilouei, H., 2014. Mechanisms of heavy metal removal using microorganisms as biosorbent. *Water Science and Technology*, *69*(9), pp.1775-1787.

Kamyaba, H., Leeb, C.T., Chelliapana, S., Khademic, T., Talaiekhozanid, A. and Rezaniae, S., 2019. Role of microalgal biotechnology in environmental sustainability-a mini review. *Chemical Engineering*.

Kayombo, S.T.S.A., Mbwette, T.S.A., Katima, J.H.Y., Ladegaard, N. and Jrgensen, S.E., 2004. Waste stabilization ponds and constructed wetlands: design manual.

Kelly, M., Juggins, S., Guthrie, R., Pritchard, S., Jamieson, J., Rippey, B., Hirst, H. and Yallop, M., 2008. Assessment of ecological status in UK rivers using diatoms. *Freshwater Biology*, *53*(2), pp.403-422.

Kumar, B., Sharma, V. and Gaur, K.S., 2012. Studies on Phosphate in Reference to Zooplankton: A Short review. E*cosystems*, *22*(19), pp.23-24.

Kunugi, M., Sekiguchi, T., Onizawa, H. and Jimbo, I., 2014. Utilization of Diatoms to Collect Metallic Ions. *Proceedings of the School of Engineering of Tokai University*, *39*, pp.13-17.

Lagergren, S., 1898. Zur theorie der sogenannten adsorption geloster stoffe. Kungliga svenska vetenskapsakademiens. Handlingar. 24, 1-39.

Lin, J.W., Wang, X. and Zhan, Y., 2019. Effect of precipitation pH and coexisting magnesium ion on phosphate adsorption onto hydrous zirconium oxide. *Journal of Environmental Sciences*, *76*(2), pp.170–190.

Mas-Torres, F., Estela, J.M., Miró, M., Cladera, A. and Cerdà, V., 2004. Sequential injection spectrophotometric determination of orthophosphate in beverages, wastewaters and urine samples by electrogeneration of molybdenum blue using tubular flow-through electrodes. *Analytica Chimica Acta*, *510*(1), pp.61-68.

Mathur R. Handbook of Cane Sugar Technology, 1995, 2nd Ed. Oxford and IBH Publishing Co, Pvt, Ltd, New Del. Pp. 621.

Matos, Â.P., 2017. The impact of microalgae in food science and technology. *Journal of the American Oil Chemists' Society*, *94*(11), pp. 1333-1350.

Matos, Â.P., Feller, R., Moecke, E.H.S., de Oliveira, J.V., Junior, A.F., Derner, R.B. and Sant'Anna, E.S., 2016. Chemical characterization of six microalgae with potential utility for food application. *Journal of the American Oil Chemists' Society*, *93*(7), pp. 963-972.

Mudzielwana, R., Gitari, M.W. and Msagati, T.A., 2016. Characterization of smectite-rich clay soil: Implication for groundwater defluoridation. *South African Journal of Science*, *112*(11-12), pp.1-8.

Naidoo, S. and Olaniran, A., 2013. Treated wastewater effluent as a source of microbial pollution of surface water resources. *International Journal of Environmental Research and Public Health*, *11*(1), pp.249-270.

Nekouei, R.K., Pahlevani, F., Assefi, M., Maroufi, S. and Sahajwalla, V., 2019. Selective isolation of heavy metals from spent electronic waste solution by macroporous ion-exchange resins. *Journal of Hazardous Materials*, *371*, pp.389-396.

Parlayici, S., Eskizeybek, V., Avcı, A. and Pehlivan, E., 2015. Removal of chromium (VI) using activated carbon-supported-functionalized carbon nanotubes. *Journal of Nanostructure in Chemistry*, *5*(3), pp.255-263.

Sbihi, K., Cherifi, O., Bertrand, M. and El Gharmali, A., 2014. Biosorption of metals (Cd, Cu and Zn) by the freshwater diatom Planothidium lanceolatum: a laboratory study. *Diatom Research*, *29*(1), pp.55-63.

Smucker, N.J. and Vis, M.L., 2011. Spatial factors contribute to benthic diatom structure in streams across spatial scales: considerations for biomonitoring. *Ecological Indicators*, *11*(5), pp.1191-1203.

Tchounwou, P.B., Centeno, J.A. and Patlolla, A.K., 2004. Arsenic toxicity, mutagenesis, and carcinogenesis–a health risk assessment and management approach. *Molecular and Cellular Biochemistry*, *255*(1), pp.47-55.

Tchounwou, P.B., Yedjou, C.G., Patlolla, A.K., and Sutton, D.J. 2012. Heavy metal toxicity and the environment. In Molecular, Clinical and Environmental Toxicology, 32(9-10), pp.133-164.

Teng, H., and Hsieh, C., 1998. Influence of surface characteristics on liquid-phase adsorption of phenol by activated carbons prepared from bituminous coal. *Industrial and Engineering Chemistry Research*, **37**(9), pp 3618-3624.

Ukhurebor, K.E., Aigbe, U.O., Onyancha, R.B., Nwankwo, W., Osibote, O.A., Paumo, H.K., Ama, O.M., Adetunji, C.O. and Siloko, I.U., 2020. Effect of hexavalent chromium on the environment and removal techniques: A review. *Journal of environmental management*, 280, pp. 111809

Wang, L., Wang, A., 2008. Adsorption properties of Congo Red from aqueous solution onto surfactant-modified montmorillonite. *Journal of Hazardous Materials*, *160*(1), pp.173-180.

Wang, P., Sun, D., Deng, M., Zhang, S., Bi, Q., Zhao, W. and Huang, F., 2020. Amorphous phosphated titanium oxide with amino and hydroxyl bifunctional groups for highly efficient heavy metal removal. *Environmental Science: Nano*, *7*(4), pp.1266-1274.

WHO. 2003. Guidelines for drinking water quality. 2nd edition. Recommendation. World Health organization Geneva. pp. 30-113.

World Health Organization, WHO/UNICEF Joint Water Supply and Sanitation Monitoring Programme, 2015. Progress on sanitation and drinking water: 2015 update and MDG assessment. World Health Organization.

Xu, J., Cao, Z., Zhang, Y., Yuan, Z., Lou, Z., Xu, X. and Wang, X., 2018. A review of functionalized carbon nanotubes and graphene for heavy metal adsorption from water: Preparation, application, and mechanism. *Chemosphere*, *195*, pp.351-364.

Yan, L.G., Xu, Y.Y., Yu, H.Q., Xin, X.D., Wei, Q. and Du, B., 2010. Adsorption of phosphate from aqueous solution by hydroxy-aluminum, hydroxy-iron and hydroxy-iron-aluminum pillared bentonites. Journal of hazardous materials, 179 (1-3), pp.244-250.

Yang, J., Hou, B., Wang, J., Tian, B., Bi, J., Wang, N., Li, X. and Huang, X., 2019. Nanomaterials for the removal of heavy metals from wastewater. *Nanomaterials*, *9*(3), pp.424.

CHAPTER 5

Biosorption, kinetics and thermodynamics studies of Cr^{6+} and Cd^{2+} metal ions and PO_4^{3-} ions by grapefruit peel/ diatom adsorbent

5.1 Abstract

Water pollution remains a global concern that affects human health and the environment. Various techniques have been developed to reduce or eliminate this problem. Most of these techniques, however, are expensive and require a lot of energy and capital to work. This study focused on the use of biosorption as a cost-effective and environmentally friendly technique to remediate water polluted by Cr^{6+} and Cd^{2+} metal ions as well as PO_4^{3-} by grapefruit peel/ diatom (GFP/ diatom) adsorbent. The FTIR spectrum showed O-H, N-H, C-O, and Si-O as the main functional groups present on the surface of the adsorbent. The XRD shows the composite to be slightly amorphous which is typical of biomass materials. Moreover, the SEM images showed some irregular, cavity shapes. The batch sorption studies indicated that GFP/ diatom adsorbent worked as a good adsorbent for Cr^{6+} and Cd^{2+} and PO_4^{3-} at the optimum contact time of 60 min, the optimum dosage of 0.35 g, pH of 3 for Cr^{6+} and PO_4^{3-} and 7 for Cd^{2+}. The overall kinetic results indicated that the sorption processes followed pseudo-first-order and governed also by the intraparticle diffusion mechanism. The adsorption model that best described the equilibrium data for the metal ions was Langmuir. However, for PO_4^{3-}, Freundlich adsorption isotherm was the best model that described the equilibrium data. Additionally, the maximum adsorption capacities obtained for Cr^{6+} was 1.409 (mg/g) at 303 K; Cd^{2+} was 1.340 (mg/g) at 313 K, while PO_4^{3-} was 33.454 (mg/g) at 313 K. Furthermore, the thermodynamic data revealed that the biosorption process was spontaneous and feasible for the adsorbates across all temperatures. This showed that the adsorbent could decontaminate pollutants in wastewater.

Keywords: Biosorption, kinetics, thermodynamics, Cr^{6+}, Cd^{2+}, PO_4^{3-}, grapefruit peel/diatom adsorbent.

5.2 Introduction

Water is the most essential resource that is required by all living organisms to survive in their daily activities. The need for clean water is of uttermost importance, hence we need to keep this precious resource clean at all cost. However, water pollution seems to be the world's concern as it affects the livelihood of people and their surrounding environment. The pollution of water resources is influenced by either natural or human activities. Heavy metals such as Cr^{6+} and Cd^{2+} are part of pollutants influenced by human activities as well as nutrients such as PO_4^{3-} and have been on the rise since.

Some of the sources of these heavy metals and nutrients by anthropogenic activities include tanning and textile industries, plating, alloying, fertilizers and pesticides uses (Li et al., 2015; Rowbotham et al., 2000). On the other hand, PO_4^{3-} sources can be from natural sources which include rock deposits containing phosphates and anthropogenic sources which include agricultural practices such as pesticide use and industries that produce detergents, sugar and beverages (Badamasi et al., 2019; Kabata-Pendias, 2010). The wastewater that is produced contains complex materials which sometimes makes the treatment of the effluents, especially from textile industries, more challenging and difficult (Paździor et al., 2019).

Furthermore, chromium is regarded as a micro-nutrient that becomes toxic at higher amounts (Bolan et al., 2013). Metals like Cd^{2+} are regarded as non-essential heavy metals and a priority hazardous substance in the water policy field (Decision, 2001). However, through leaching into the environment, heavy metals become bioavailable to living organisms, and since they are not degradable, they bioaccumulate throughout the trophic levels of the food chain, through soil-plant-human or soil-plant-animal-human ingestion, thereby causing poisoning and health problems to human beings (WHO, 2017; Vareda et al., 2016).

Some of the health effects due to Cr^{6+} and Cd^{2+} infested water that affect humans include lung cancer, dermatitis, kidney failure, gastrointestinal impairment and respiratory tract irritation (Mitra et al., 2017; Oliveira, 2012). For aquatic or marine species, Cr^{6+} have been reported to be cytotoxic to green sea turtle cell and lungs (Speer et al., 2019). Cd^{2+} on the other hand is known as a bio-toxic element that is widely distributed in aquatic ecosystems and toxic to aquatic organisms. Some of the catastrophic effects of Cd^{2+} include damage to the DNA and disruption of cellular homeostasis (Macías-Mayorga et al., 2015; Chang et al., 2009).

Excess nutrients such as phosphates in water tend to cause eutrophication which results in algal blooms that block sunlight from reaching underlying plants and further deplete the oxygen

levels resulting in hypoxic dead zones that fails to support aquatic organism (Jebakumar et al., 2018).

Therefore, wastewater treatment is a necessity these days to re-use water for various purposes. Various methods can be applied for the treatment of wastewater which includes physical, chemical, biochemical and other methods such as oxidation, membrane filtration and coagulation (Soltani et al., 2020; Albadarin et al., 2017). However, some of these methods have many disadvantages. For example, difficulty in operation and high maintenance cost (Kumar et al., 2015). Recently, alternative methods have been developed which involve the use of biological materials for the remediation of chemical species in water as well as nutrients. One of those methods involves biosorption due to its eco-friendliness, cost-effectiveness, the potential to recover metals and economic reusability (Mustafa et al, 2016; Akpor and Muchie, 2010).

Bio-sorbent materials from agricultural waste such as algae, fungi and activated carbon have resulted in great removal efficiency for metal ions (Ali Redha, 2020; Guo et al., 2019; Rangabhashiyam and Balasubramanian, 2019; Gururajan and Belur, 2018; Renu et al., 2017). For phosphates, polymeric materials have been used also for their remediation (Mdlalose et al., 2017). Hence in this study, biosorption using grapefruit peel (GFP) powder incorporated with diatom biomass has been selected as a natural unmodified bio-sorbent due to its wide availability in nature, accessibility, easy to use, and cost-effectiveness. Moreover, it is a sustainable method since it uses waste materials that are considered a nuisance and problematic in the environment as alluded to in previous chapters. Furthermore, to the best of our knowledge, this is the first study that has been conducted on the biosorption of Cr^{6+} and Cd^{2+} metal ions and PO_4^{3-} by GFP/ diatom adsorbent.

5.3 Material and methods

5.3.1 Chemicals and reagents

Experiments were conducted using analytical reagent-grade chemicals. $K_2Cr_2O_7$, $CdN_2O_6{\cdot}4H_2O$, KCl, HCl and NaOH were all purchased from Rochelle Chemicals (Johannesburg, South Africa). The chemicals were used directly without further purification. Deionized water was used to prepare stock solutions and to dilute standards during the entire experiment.

5.3.2 Preparation of adsorbent

The GFP/diatom adsorbent was prepared by mixing dried grapefruit peel powder and diatom biomass powder in a ratio of 2:1 (w/w). The dried adsorbent was then mixed in a beaker with deionized water (1% w/v). The solution was then filtered and dried in an oven at 60˚C for 24 h. The dried adsorbent was crushed into a fine powder and used for further experiments.

5.3.3 Preparation of stock solutions

Different concentrations of 1000 mg/L cadmium, chromium and phosphate solutions were prepared by dissolving 2.744 g of $CdN_2O_6 \cdot 4H_2O$, 2.82 g of $K_2Cr_2O_7$ and 1.44 g of KH_2PO_4 in 1 L volumetric flasks with Millipore water respectively. A 50 mg/L of the respective ions was prepared from the stock solutions and used for subsequent experiments.

5.3.4 Instruments

The surface morphology was determined by SEM and the EDS to provide the elemental composition of the adsorbent with an FEI Nova NanoSEM 230 with the field emission gun equipped with an Oxford Xmax SDD detector operating at an accelerating voltage of 20Kv. For the EDS detector, Oxford X-Max with INCA software was used to characterize the sorbent materials. An ALPHA Bruker FTIR spectrophotometer (Berlin, Germany) was used for solid samples of GFP/diatom adsorbent for identification of various functional groups present within the range of 400-4000 cm^{-1}. The mineralogical and phase identification was determined by XRD, type PANalytical X'Pert Pro powder diffractometer for qualitative sample analysis. The filtrates of Cr^{6+} and Cd^{2+} were analysed by a Thermo iCAP 6200 ICP AES and PO_4^{3-} was analyzed using ion chromatography.

5.3.5 Point of zero charge (pHpzc)

The pH at point-of-zero charge was determined by mixing 0.2 g of GFP/diatom adsorbent in 0.01 M KCl solutions. The pH of solutions was adjusted to desired values between 3 and 11 by adding 0.1 M HCl or 0.1 M NaOH. A volume of 50 mL solutions was added into plastic bottles which were agitated on a thermostat water bath shaker at 150 rpm for 24 h at room temperature. The equilibrium pH (pH_f) of each mixture was measured and the intersection pH-initial against ΔpH curve gave the pHpzc value.

5.3.6 Adsorption procedure

Adsorption experiments were carried out to determine the effect of various parameters such as initial metal concentration, pH, dosage, contact time and the effect of temperature and thermodynamics at various temperatures (298 K, 303 K and 313 K). The effect of initial metal

concentration and adsorption isotherms were evaluated by varying the concentration from 10 to 200 mg/L. The various solution pH ranging from 3 to11 was carried out and adjusted using 0.1 M NaOH and 0.1 M HCl. The adsorbent dosage was evaluated by varying different dosages from 0.1 to 0.5 g. Moreover, the effect of contact time was varied from 1 to 120 min. All experiments were carried out using 50 mL of Cr^{6+}, Cd^{2+} and PO_4^{3-}. After the shaking time had elapsed, samples were filtered and analyzed by ICP AES for the metal ions and IC for the phosphate ions. The adsorption capacity and the removal efficiency of GFP/diatom adsorbent regarding Cr^{6+}, Cd^{2+} and PO_4^{3-} were calculated by equations (1) and (2).

$$q = (C_0 - C_e) \times \frac{V}{w} \quad (1)$$

$$\% \text{ Removal } = \frac{(C_0 - C_e)}{C_0} \times 100 \quad (2)$$

where Co is the initial concentration (mg/L), Ce is the concentration at equilibrium (mg/L), V is the volume of solution (L) and w is the mass of the adsorbent (g).

5.4 Results and discussions

5.4.1 FTIR analysis

Various functional groups of the GFP/diatom adsorbent are displayed in Fig. 29. The peaks were obtained at around 3325 cm^{-1}, between 1623-1615 cm^{-1}, 1009-962 cm^{-1} and 913 cm^{-1}. The data reveal that OH groups of lignin, hemicellulose and cellulose due to the grapefruit peel or could be OH groups of the phenolic groups from the diatom biomass (Ibrahim et al., 2016; Köseoğlu and Akmil-Başar, 2015). The region between 1623-1615 could be attributed to the N-H band which displays amino groups. Additionally, the region between 1009-962 cm^{-1} could be the vibration of C-OH- which is attributed to stretching vibrations of alcoholic groups and carboxylic acids as well as Si-O from the diatom biomass. Furthermore, 913 cm^{-1} could be attributed to the Si-O-Si band (Sbihi et al., 2014). Moreover, it was observed that after sorption of Cr^{6+}, Cd^{2+} and PO_4^{3-} ions, there was a reduction in the intensities of some of the functional groups, which suggested that they played a major role in the biosorption processes of Cr^{6+}, Cd^{2+} and PO_4^{3-} ions.

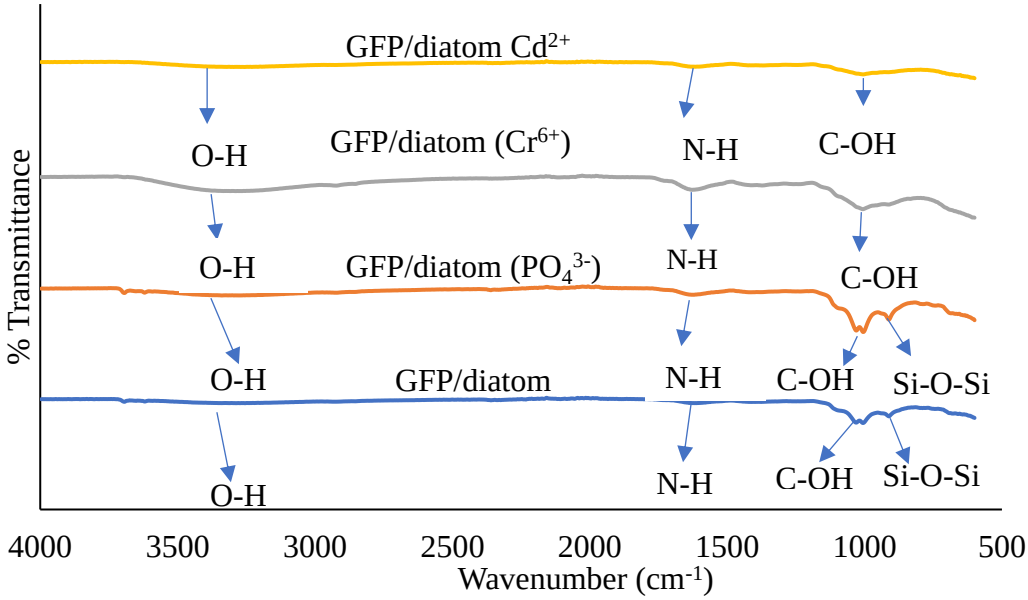

Fig. 29. FTIR spectra showing different functional groups present on the surface of the adsorbent.

5.4.2 XRD results

The mineral phase of the GFP/diatom adsorbent was revealed by the X-ray diffraction spectrum. It showed the pattern of the composite to be between the range of 5-80 theta which can be observed from Fig. 30. The X-ray diffraction spectrum indicated that there are no clear mineral phases that can be observed on the surface of the composite and that the composite does not display any crystallinity but an amorphous pattern which is typical of grapefruit peels and diatom biomass as discussed in previous chapters. Furthermore, amorphous adsorbents are said to have high adsorption capacity due to their highly hydrated and porous structures (Su et al., 2013)

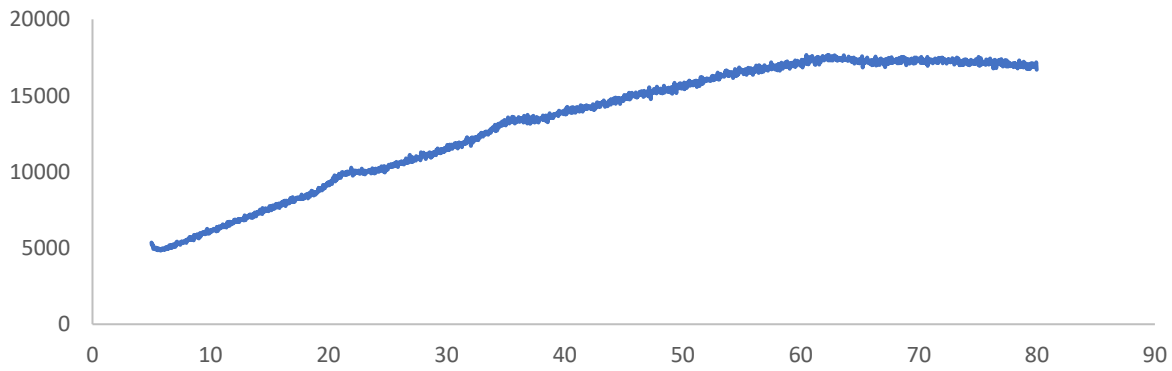

Fig. 30. X-ray diffractogram of GFP/ diatom adsorbent after treatment of Cr^{6+} and Cd^{2+} and PO_4^{3-}.

5.4.3 SEM-EDS

The surface morphology of the GPF/diatom adsorbent is displayed in Fig. 31. In this figure, it was observed that the morphology of the bare composite shows some spherical shapes which look agglomerated. Its respective EDS showing all the elemental compositions present on the surface of the GFP/diatom adsorbent is given. Elements like Fe, Mg, Al and Si as well as C, Ca, K and O were present which are typical of biomass materials as already alluded to in previous chapters. Moreover, Fig. 31 (b-d) shows Cr^{6+}, $Cd^{2+,}$ and PO_4^{3-} (as P) after treatment, and it was observed that the morphology has been modified into finer grains which is due to agitation with time and causing the adsorbate molecules to be attached on the surface of the adsorbent resulting in a slight change in morphology of the adsorbent. Furthermore, the EDS spectrum on Fig. 31 (b-d) shows the presence of removed pollutants (Cr^{6+}, Cd^{2+} and PO_4^{3-}) on the surface of the adsorbent which further confirmed that the adsorption process was successful.

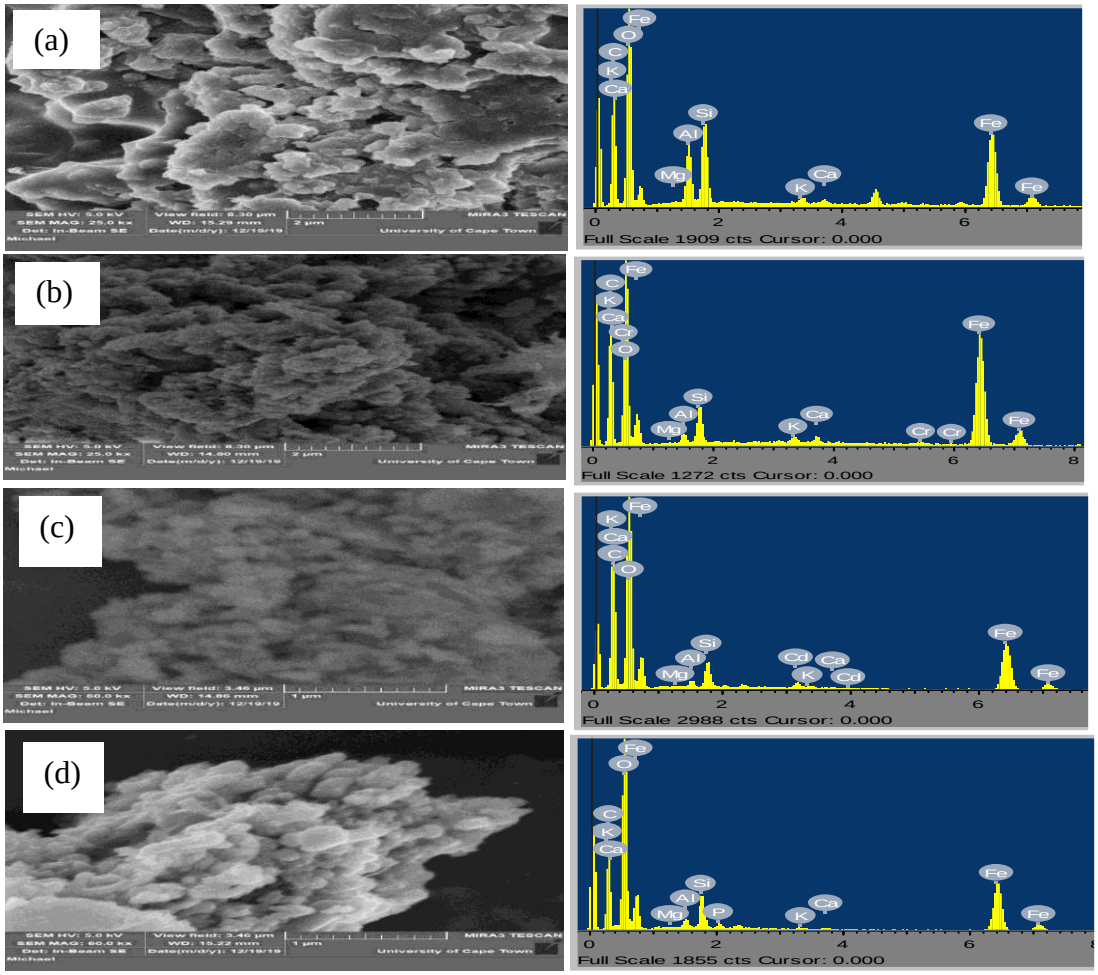

Fig. 31. SEM images of GFP/ diatom adsorbent (a), after treatment with Cr^{6+} (b), Cd^{2+} (c) and PO_4^{3-} (d) with their respective EDS spectra.

5.5 Batch experimental results

5.5.1 Effect of pH and pHpzc

The pHpzc was used to determine the surface charge of the GFP/diatom adsorbent to determine the chemical processes that are responsible for the removal of Cr^{6+}, Cd^{2+} and PO_4^{3-} ions in this study. The pHpzc was obtained around pH 4.8 (Fig. 32 (a)). The pH values obtained below 4.8 in solutions indicated that the surface is positively charged and after pH 4.8, the surface was negatively charged.

Additionally, pH is one of the important parameters in adsorption processes because it tells us about the change in chemistry that occurs between the adsorbent and adsorbate in solutions. Fig. 32 ((b)-(d)) shows a decrease in the sorption capacity for Cr^{6+} and PO_4^{3-} as the pH increased with the highest percentage removal of 36.9% and 47% obtained at pH 3, respectively. This could be due to the high protonated adsorbent surface at low pH which makes a strong electrostatic attraction between the surface charges of the adsorbent and the ions of the adsorbates (Cr (VI), oxy-anion (CrO_4^{2-}, $Cr_2O_7^{2-}$) and PO_4^{3-}). Similar trends were also obtained by Verma and Balomajumder (2020). However, the decrease after pH 4.8 could be due to an increase in OH^- ions which caused a repulsive force or electrostatic repulsion since the surface of the adsorbent is negatively charged (Tatarchuk et al., 2021).

Furthermore, in alkaline solutions, the OH^- groups are in higher concentrations and compete with the negatively charged adsorbates (CrO_4^{2-}, $Cr_2O_7^{2-}$ and PO_4^{3-}) by occupying most of the sites on the surface of the adsorbent which result in the low adsorption capacity and removal efficiency. Moreover, Fig. 32 (c) shows an increase in the sorption capacity as the pH increases, this is due to electrostatic attractions between the Cd^{2+} ions and the surface of the adsorbent material. Hence the highest percentage removal was almost > 99% at pH 5, and further remained at equilibrium as the pH increased.

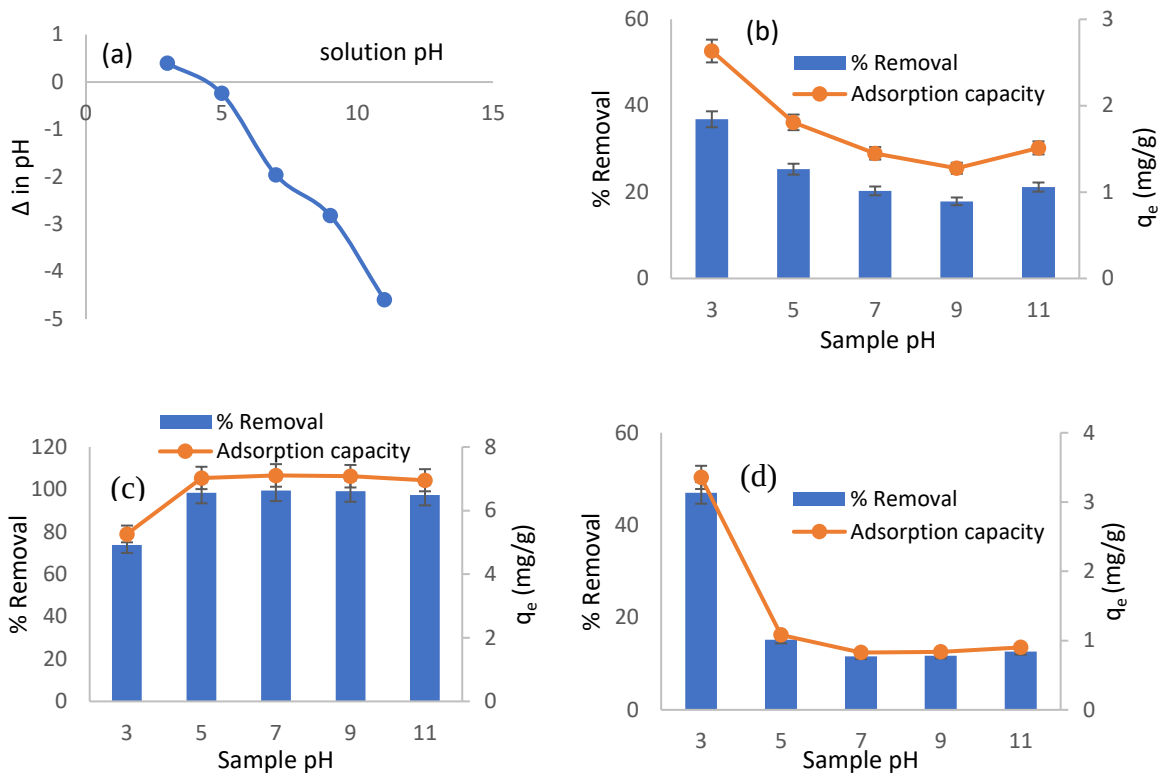

Fig. 32. The pHpzc (a) at various pH values and the effect of pH for Cr^{6+}, Cd^{2+} and PO_4^{3-} (b-d) against percentage removal and adsorption capacity. (Experimental conditions: Time, 60 min; dosage, 0.35 g; initial concentration, 50 mg/L; volume, 50 mL; shaking speed, 250 rpm).

5.5.2 Effect of contact time and kinetic modeling

The effect of contact time was varied from 1 to 120 min to determine the optimum time that yielded high percentage removal and adsorption capacity during the adsorption process. Fig. 33 shows the results obtained for Cr^{6+}, Cd^{2+} and PO_4^{3-} during the sorption process concerning time. It was observed that both adsorption capacity and percentage removal increased gradually at the beginning which indicated that the active sites of the adsorbent were vacant which was an indication of an increase in the accessibility of the adsorbates to the bio-sorbent active binding sites, which became occupied towards the equilibrium, although fluctuations also occurred (Dehghani et al., 2015; Tutu et al., 2013). The highest percentage removal was obtained at 10 min (17.9 %), 90 min (12.58 %), 60 min (32.40 %) for Cr^{6+}, Cd^{2+} and PO_4^{3-} respectively. From the data, it was observed that PO_4^{3-} removal yielded better results in terms of the sorption efficiency and adsorption capacity than the metal ions. This is as a result of the presence of diatoms that could be utilizing them, which further reveal that the adsorbent has a high affinity for PO_4^{3-} ion than the metal ions.

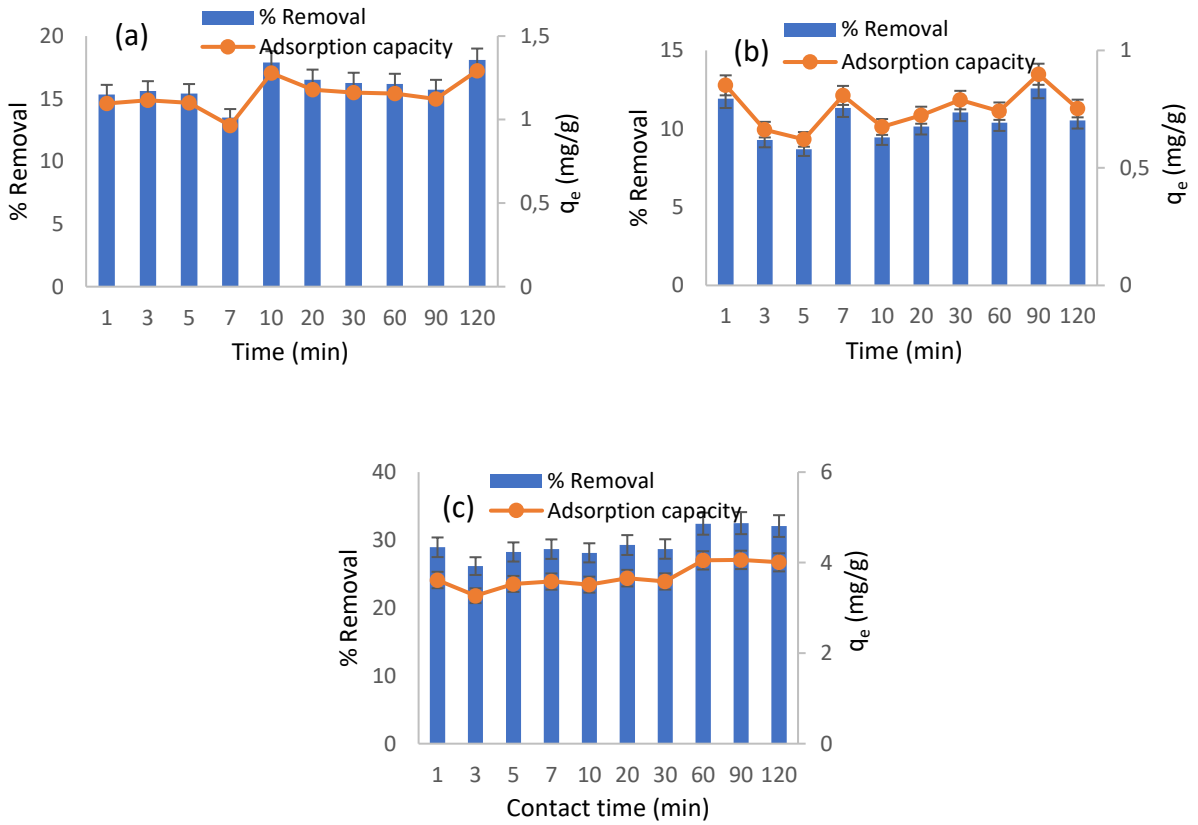

Fig. 33. Effect of contact time for Cr^{6+}, Cd^{2+} and PO_4^{3-} (a-c) at various times against percentage removal and adsorption capacity. (Experimental conditions: dosage, 0.2 g; volume, 50 mL; neutral pH; initial concentration, 50 mg/L and shaking speed, 250 rpm).

The kinetic studies were done to assess the mechanisms that occur during the adsorption process with respect to time. Fig. 34 shows the adsorption kinetics graphs which predict the rate of uptake processes of Cr^{6+}, Cd^{2+} and PO_4^{3-} by the GFP/diatom adsorbent. The adsorption kinetics used in this study included the pseudo-first-order (Singh and Tiwari, 1997; Lagergren, 1898) and pseudo-second-order (Ho and McKay, 1999) which were determined through the non-linear expressions. The last form of adsorption kinetic was the intra-particle diffusion which was determined through linear expressions. The models are expressed in equations (3) and (5) respectively.

$$q_t = q_e(1 - e^{-kit}) \quad (3)$$

$$q_t = \frac{qe^2\, k_2 t}{1 + k_2\, q_e t} \quad (4)$$

$$q_t = k_t t^{0.5} + ci \quad (5)$$

where q_e and q_t (mg/g) are the amount of adsorption at pseudo-first-order at time t (min), k_1 is the pseudo-first-order adsorption rate constant min^{-1} at equilibrium, while k_2 (g/mg/min) is the equilibrium rate constant of pseudo-second-order adsorption. For the intra-diffusion kinetics, q_t is the amount adsorbed (mg/g) concerning time (t) (min), k_t is the intra-particle diffusion rate constant in (mg/g/min) and C_i is a constant related to the thickness of the boundary layer (mg/g).

The pseudo-first-order and pseudo-second order kinetic model parameters for Cr^{6+}, Cd^{2+}, and PO_4^{3-} ions are displayed in Table 8, where the coefficient of determination (R^2) for Cr^{6+}, Cd^{2+} and PO_4^{3-} were all > 0.99 respectively. The root mean square errors (RMSE) were 0.068; 0.087 and 0.263, while the reduced chi-square (RCS) values were 0.0032; 0.009 and 0.017 for pseudo-first-order kinetics. However, pseudo-second order results showed that the R^2 values were 0.0035; 0.219 and 0.7415. The RMSE were 0.068; 0.087 and 0.2439 while the RCS values were 0.0032; 0.009 and 0.0145 for Cr^{6+}, Cd^{2+}, and PO_4^{3-} respectively.

The R^2 values of pseudo-first-order and pseudo-second-order kinetic models were obtained and the rate-limiting step for adsorption kinetics for Cr^{6+}, Cd^{2+} and PO_4^3 was pseudo-first-order kinetics which indicated that adsorption mechanisms occurred via physisorption. However, with the evaluation parameters such as RSME and RCS, the data also indicated that both physisorption and chemisorption played a role in the mechanisms involved in the adsorption of the metal ions as well as the nutrient ions by the GPF/diatom adsorbent with physisorption being more favorable. This means the reaction mechanisms that occurred on the surface of the GPF/diatom adsorbent were associated with weak Van der Waal's force of attraction and it is generally found to be reversible.

The last kinetic model is intra-particle diffusion, which describes the transfer of analytes from the external surface into the pores of the adsorbent (Ho et al., 2000). It is characterized by a linear relationship between the amount adsorbed at a time (q_t) and the square root of the time (Allen et al., 1989).

Usually, the process of diffusion takes place in three parts in which adsorption process takes place, (i) diffusion through the liquid film to the surface of the adsorbent (ii) diffusion through the pore liquid (iii) the adsorption and desorption between the active sites of the adsorbent and the adsorbate (Xu et al., 2018)

The overall results in Table 9 showed that the coefficient of determination values were 0.0267; 0.1196 and 0.7691, while the diffusion rate constant was 0.0032; 0.0087 and 0.0674 (mg/g/min) and the thickness of the boundary layer was 1.3133; 0.7098 and 3.3577 for Cr^{6+}, Cd^{2+} and PO_4^{3-} respectively. Based on the intra-particle diffusion rate, the results showed better results for PO_4^{3-} than Cr^{6+} and Cd^{2+}, this could be due to the interaction between the functional groups of the diatoms within the adsorbate since diatoms use nutrients such as phosphates amongst others for their growth and survival (Kamyaba et al., 2019; Abdel-Raouf et al., 2012). However, the poor results obtained from the metal ions could be due to low intensities of the carboxyl group which are known to play a significant role in the remediation of metal cations in wastewater (Abdel-Raouf et al., 2012).

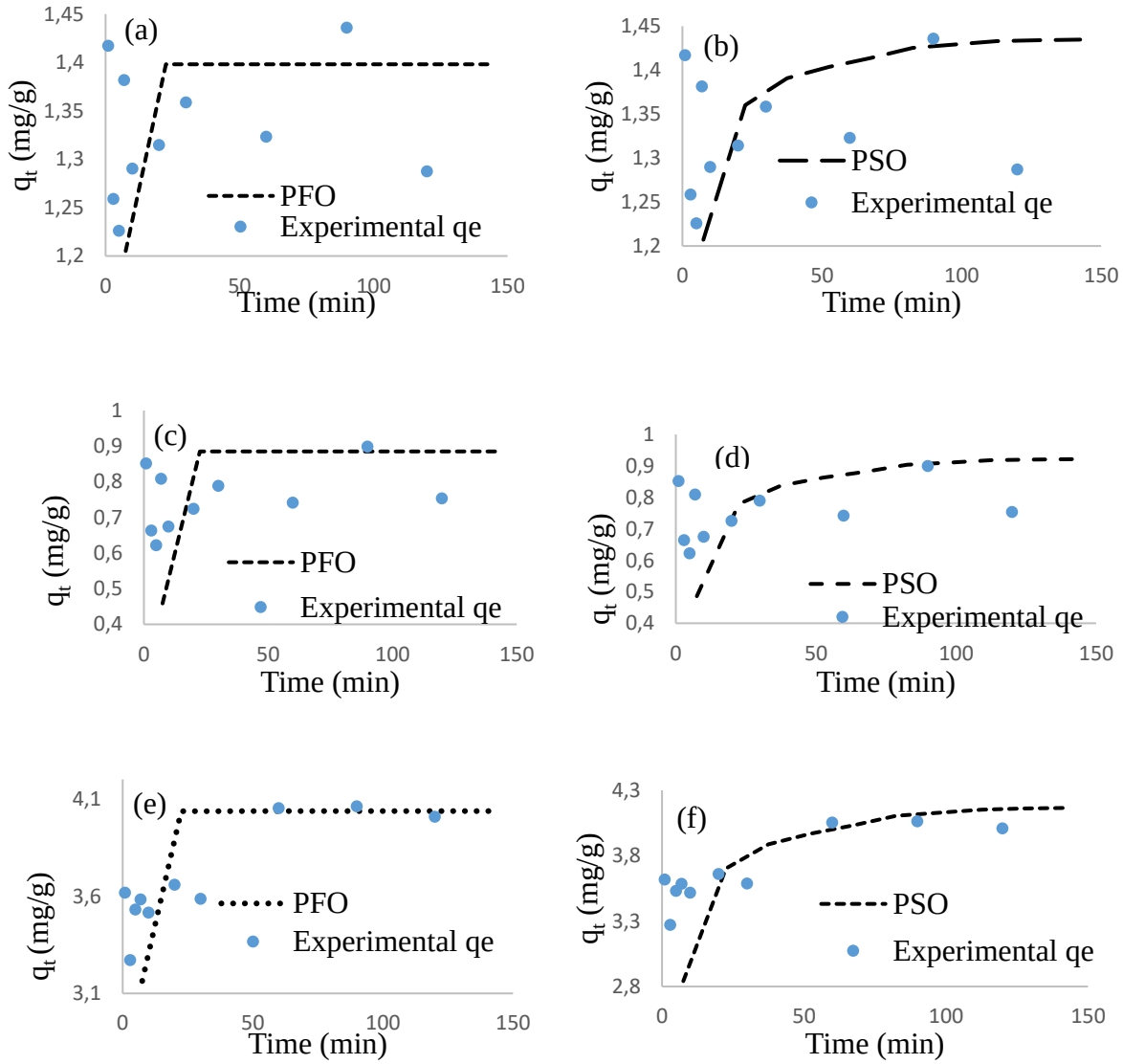

Fig. 34. Non-linear adsorption kinetic plots for Cr^{6+} (a;b), Cd^{2+} (c;d) and PO_4^{3-} (e;f) in aqueous solutions.

Table 8: Non-linear adsorption kinetic models for Cr^{6+}, Cd^{2+} and PO_4^{3-} in aqueous solutions.

Non- linear	Parameter	Cr^{6+}	Cd^{2+}	PO_4^{3-}
PFO	k_1	11.140	15.482	3.840
	q_t	1.329	0.752	3.695
	R^2	0.999	0.999	0.998
	RCS	0.003	0.009	0.017
	RSME	0.068	0.087	0.263
PSO	k_2	4.187	4.555	2.541
	q_t	1.329	0.752	3.757
	R^2	0.004	0.219	0.745
	RCS	0.003	0.009	0.015
	RSME	0.068	0.087	0.244

Table 9: Linear kinetics parameters for Cr^{6+}, Cd^{2+} and PO_4^{3-} ions in aqueous solutions

Intra-particle diffusion	Parameter	Cr^{6+}	Cd^{2+}	PO_4^{3-}
	K_{id}	0.003	0.009	0.067
	C	1.313	0.710	3.358
	R^2	0.027	0.120	0.769

5.5.3 Effect of adsorbent dosage on Cr^{6+}, Cd^{2+} metal ions and PO_4^{3-} ions

The effect of adsorbent dosage against percentage removal and adsorption capacity has been illustrated in Fig. 35 for Cr^{6+}, Cd^{2+} and PO_4^{3-} ions in aqueous solutions. The graphs indicated that the percentage removal increased with an increase in the dosage of the adsorbent. This could because of the introduction of new vacant sites as the GFP/diatom adsorbent was increased and the concentration of the adsorbates remained constant, which resulted in a rapid sorption efficiency (Mahmoodi and Najafi, 2012). However, the adsorption capacity decreased with an increase in the mass of the GFP/diatom adsorbent. This is due to adsorption competition between GFP/diatom adsorbent molecules and the concentration gradient of Cr^{6+}, Cd^{2+} and PO_4^{3-} ions. Furthermore, it could also be due to agglomerations of the GFP/diatom adsorbent by the adsorbate solutions passing through. The optimum dosage was obtained at 0.5 g, 0.3 g and 0.35 g for Cr^{6+}, Cd^{2+} and PO_4^{3-}.

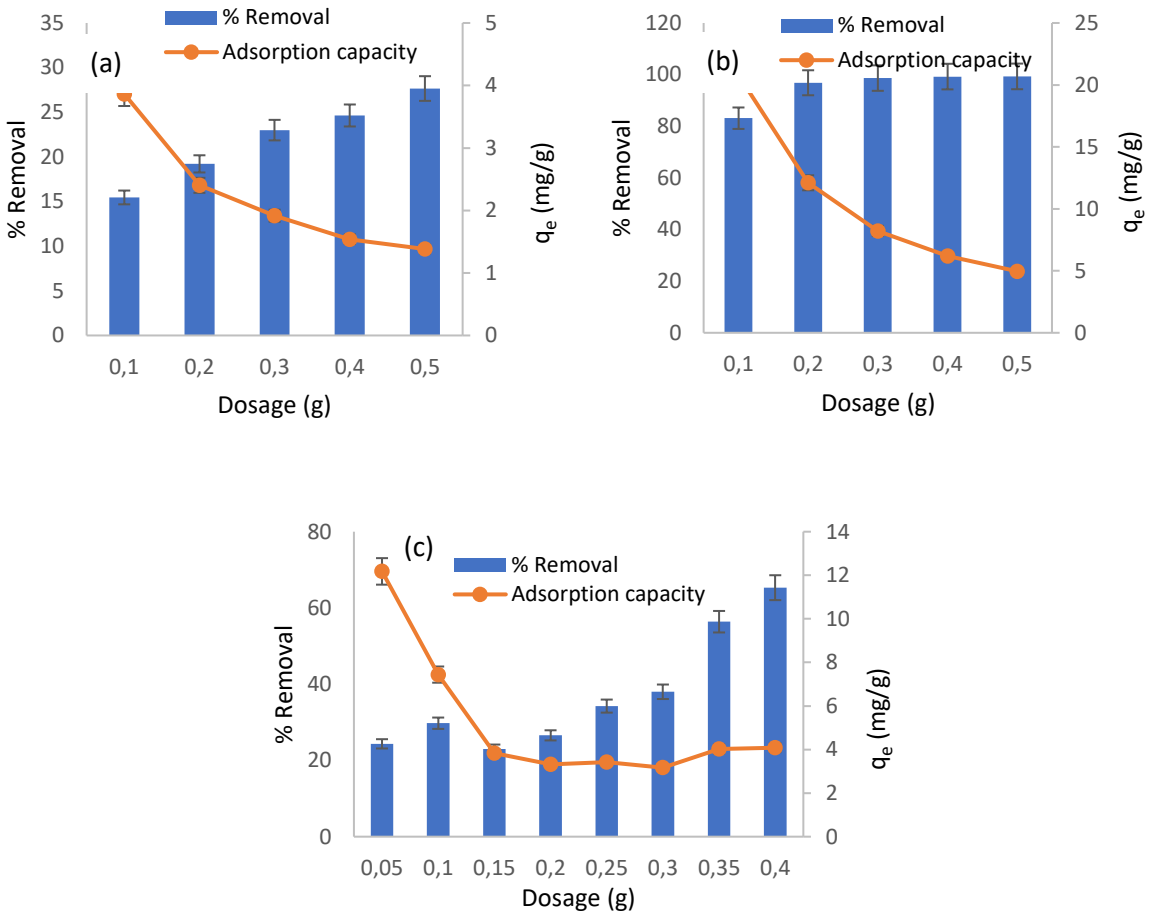

Fig. 35. Effect of adsorbent dosage for Cr^{6+}, Cd^{2+} and PO_4^{3-} ions (a-c). (Experimental conditions: Time, 60 min; temperature, 298 K; neutral pH, volume, 50 mL; initial concentration, 50 mg/L and shaking speed of 250 rpm).

5.5.4 Effect of initial concentration and adsorption isotherms

Fig. 36 shows the effect of initial concentration for Cr^{6+}, Cd^{2+} metals (a-b) and PO_4^{3-} (c) ions in solutions at various temperatures. The results revealed that the higher the concentration, the higher the adsorption capacity and the percentage removal for the metal ions by the adsorbent as temperature increases. The increase in adsorption capacity could be due to the active sites of the adsorbent surrounded with more adsorbate ions in the solution which enhanced the adsorption process due to the higher driving force of the concentration gradient. Similar results were obtained by Abdi et al. (2017).

Contrary to Cr^{6+} and Cd^{2+}, it was observed that the adsorption capacity for PO_4^{3-} increased with an increase in concentration while the percentage removal decreased as temperature increases. The decrease in the percentage removal could be due to the reduction in the mass gradient between the adsorbent and adsorbate interphase because of saturation of adsorbent active sites.

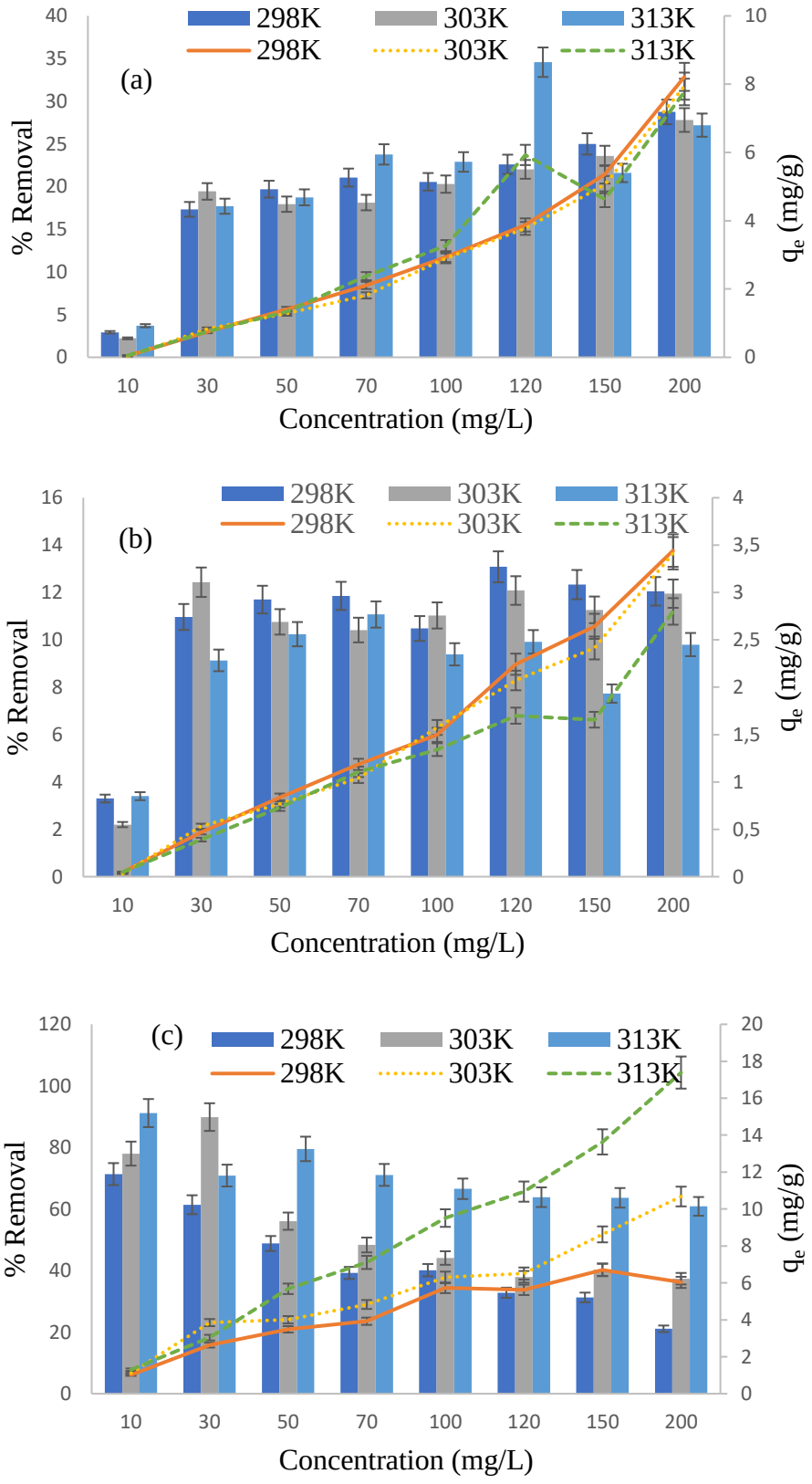

Fig. 36. Effect of initial concentration for Cr^{6+}, Cd^{2+} and PO_4^{3-} against percentage removal and adsorption capacity at various temperatures. (Experimental conditions: Time, 24 h; dosage, 0.35 g; neutral pH; volume, 50 mL; shaking speed, 250 rpm).

Furthermore, the adsorption isotherms for Cr^{6+}, Cd^{2+} and PO_4^{3-} were modeled using Freundlich and Langmuir. Langmuir was used to describing the biosorption process which occurs on a monolayer surface or before a relative pressure of unity is reached (Liu et al., 2019). The non-linear Langmuir equation is given below:

$$q_e = \frac{q_m K_L C_e}{1+K_L C_e} \quad (6)$$

where q_e is the adsorption capacity (mg/g), q_m (mg/g) is the maximum adsorption capacity, C_e (mg/L) is the equilibrium concentration, k_L is the Langmuir biosorption equilibrium constant (L/mg). A plot of C_e/q_e against C_e gives the Langmuir parameters.

Langmuir isotherm can further be determined through a dimensionless separation factor, which is R_L and it is given in equation (7).

$$R_L = \frac{1}{1 + k_L C_i} \quad (7)$$

where C_i (mg/L) is the initial ion concentration, K_L is Langmuir isotherm constant and R_L provides an indication of whether the adsorption is unfavorable ($R_L > 1$), favorable ($0 < R_L < 1$), irreversible ($R_L = 0$) or linear ($R_L = 1$).

Furthermore, the Freundlich isotherm model was also used to determine whether adsorption occurred on a heterogeneous surface to create a multi-layered surface (Freundlich, 1907). The non-linear equation of the Freundlich isotherm is expressed in equation (8).

$$q_e K_f Ce^{\frac{1}{n}} \quad (8)$$

where K_f and 1/n are empirical constants that show the biosorption capacity and the adsorption intensity respectively. When $0 < 1/n < 1$, the adsorption is favorable; when $1/n > 1$, the adsorption is unfavorable and when $1/n = 1$, the adsorption is irreversible.

Fig. 37 and Table 10 show the non-linearized plots of Langmuir and Freundlich isotherm models and their respective parameters for Cr^{6+}, Cd^{2+} and PO_4^{3-} sorption by GFP/diatom adsorbent that occurred at different temperatures. The results obtained from the table are based on the values of coefficient of determination (R^2), adjusted coefficient of determinations (adjusted R^2), reduced chi-square (RCS) as well as the Langmuir dimensionless separation factor (R_L) and the Freundlich adsorption intensity (n). It can be concluded that the adsorption process underwent both Langmuir and Freundlich isotherms.

The R^2 values for Cr^{6+} and Cd^{2+} were higher on Langmuir than Freundlich, which based on this alone, the adsorption process for the metal ions occurred on a monolayered surface. This was further supported by R_L values which were greater than 0 and lower than 1 which indicated that adsorption was favorable for Langmuir adsorption isotherm. However, for PO_4^{3-}, the R^2 values were higher on Freundlich than Langmuir, which indicated that adsorption for the phosphate ions occurred on a heterogeneous multilayer surface. Furthermore, the Freundlich n values were less than 1 across all temperatures for all adsorbates indicating favorability for adsorption by Freundlich.

Furthermore, the maximum adsorption capacities obtained for Cr^{6+} were 1.288, 1.409 and 1.045 (mg/g); Cd^{2+} were 1.281, 1.243 and 1.340 (mg/g) while PO_4^{3-} were 7.525, 15.891 and 33.454 (mg/g) which were increasing with temperature (298K-313K). This indicated that temperature played a role in increasing the adsorption capacity of the GFP/diatom adsorbent. Additionally, the adsorption capacities for PO_4^{3-} were higher than those obtained from Cr^{6+} and Cd^{2+} metal ions and could be due to that the adsorbents used in this study were in their natural form without further modification and such adsorbents are reported to have low adsorption capacities (Vareda et al., 2019). As for the high adsorption capacities for PO_4^{3-}, this could be because of the high utilization by diatoms as alluded to earlier which has a high affinity for phosphates than the metal ions.

The third isotherm model that was used for adsorption in this study was the Dubinin Radushkevich (D-R). D-R is concerned about the adsorption energy during the reaction process and the porosity of the bio-sorbent. Usually, the adsorption process will be said to have occurred via physisorption if E is less than 8 kJ/mol and via chemisorption, if E is between 8 and 16 kJ/mol. The linear D-R model can be expressed as

$$lnq_e = lnq_o - \beta e^2 \quad (9)$$

where q_e (mg/g) is the amount of ions adsorbed per unit weight of adsorbent, q_o being the maximum adsorption capacity, β is the coefficient constant, E (KJ/mol) is the mean sorption energy, Ɛ is the Polanyi potential. The mean sorption energy can be illustrated as equation (10) below:

$$E = \sqrt{\frac{1}{2\beta}} \quad (10)$$

where R is the gas constant (J/mol K) and T is the temperature (K).

In Table 10, the data indicated that the Q_{max} values for Cr^{6+} and PO_4^{3-} adsorbates increased with an increase in temperature through the highest values were obtained in PO_4^{3-} followed by Cr^{6+}. This indicated that temperature played a significant role in enhancing the adsorption capacity of the adsorbent towards Cr^{6+} and PO_4^{3-} ions. The Q_{max} values for Cd^{2+} however, were decreasing with an increase in temperature. This means temperature shows no influence on the adsorption capacity of the adsorbent material towards the adsorbate, which could be due to difficulty in ion-exchange mechanisms (El-Rahman et al., 2006).

The R^2 values were higher for Cr^{6+} and Cd^{2+} metal ions than for PO_4^{3-} and they were increasing with an increase in temperature for the metal ions while decreasing with an increase in temperature for PO_4^{3-}. This shows attractions towards the metal ions as better R^2 values indicate a better coefficient of determination in the adsorption process. Furthermore, the D-R mean adsorption energy was less than 8 kJ/mol for all the adsorbates which means the reaction involved the physisorption phenomenon. This showed that the adsorption mechanism responsible for the reaction by GFP/diatom adsorbent was governed by both physisorption and chemisorption processes and the reaction was favorable. In expatiations, at the beginning of the adsorption process, the ions of Cr^{6+}, Cd^{2+} and PO_4^{3-} were attached on the surface of the GFP/diatom adsorbent and further diffused as the reaction proceeded, where the ions reacted with the functional properties of the GFP/diatom adsorbent.

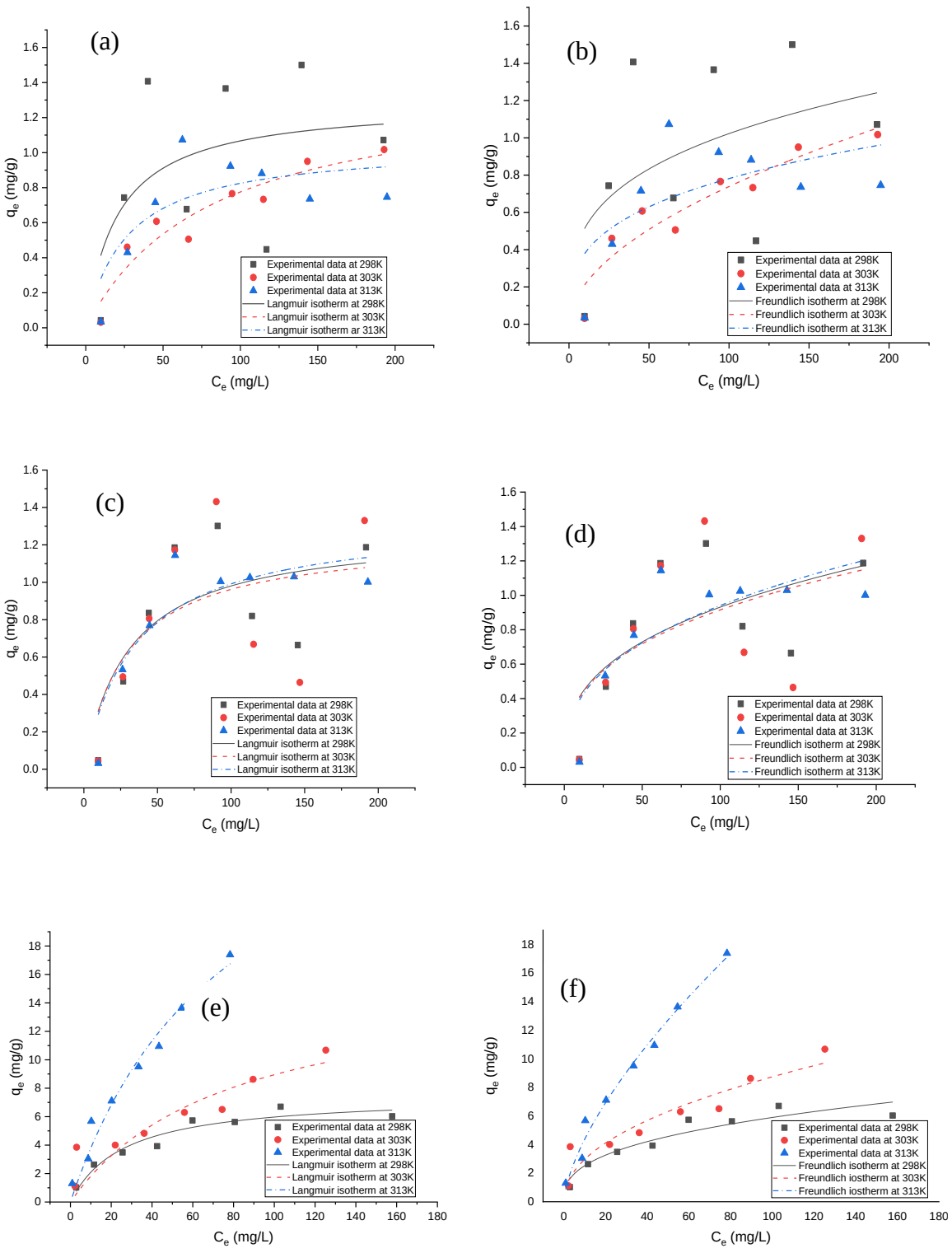

Fig. 37. Graphs showing Langmuir and Freundlich adsorption isotherms for Cr^{6+} (a;b), Cd^{2+} (c;d) and PO_4^{3-} (e;f) ions.

Table 10: The non-linear isotherm parameters for Langmuir, Freundlich and DR models

	Cr^{6+}			Cd^{2+}			PO_4^{3-}		
Temperature (K)	298	303	313	298	303	313	298	303	313
Langmuir									
Q_m (mg/g)	1.29	1.41	1.05	1.28	1.24	1.34	7.53	15.89	33.45
K_L (L/mg)	0.05	0.01	0.04	0.03	0.03	0.03	0.04	0.01	0. 01
R^2	0.36	0.91	0.66	0.59	0.42	0.82	0.94	0.78	0.97
Adj R^2	0.25	0.89	0.60	0.52	0.33	0.79	0.93	0.74	0.97
R_L	0.29	0.63	0.35	0.38	0.37	0.42	0.34	0.61	0.61
RCS	0.20	0.01	0.04	0.09	0.16	0.03	0.28	2.31	1.00
Freundlich									
K_F [(mg/g)/(mg/L)n]	0.26	0.06	0.19	0.18	0.18	0.17	1.08	1.01	0.95
n	0.30	0.54	0.31	0.35	0.35	0.38	0.37	0.47	0.66
R^2	0.27	0.89	0.47	0.46	0.34	0.67	0.90	0.88	0.98
Adj R^2	0.15	0.87	0.38	0.38	0.23	0.62	0.88	0.86	0.98
RCS	0.23	0.01	0.07	0.11	0.18	0.05	0.45	1.26	0.54
Dubinin-Radushkevvich									
βD (mol^2/kJ^2)	8.00E-05	8.00E-05	7.00E-05	6.00E-05	7.00E-05	5.00E-05	3.00E-06	2.00E-06	5.00E-07
q_{max}(mg/g)	3.39	3.30	3.58	1.70	1.67	1.36	4.79	6.69	8.56
E (kJ/mol)	0.08	0.08	0.09	0.09	0.09	0.10	0.41	0.50	1.00
R^2	0.89	0.90	0.87	0.87	0.90	0.87	0.79	0.76	0.62

5.5.5 Thermodynamics

The thermodynamics parameters by GFP/ diatom adsorbent for the biosorption of Cr^{6+}, Cd^{2+} and PO_4^{3-} ions was determined at different temperatures which ranged between 298 and 313 K. From the data obtained, it was observed that the free Gibbs energy change (ΔG°) increased with an increase in temperature, which indicated how feasible and spontaneous was the nature of the adsorption process. Moreover, the degree of randomness, type of reaction, rate of spontaneity during the adsorption process by the GFP/diatom adsorbent were determined by various thermodynamic parameters such as the Gibbs free energy change as already mentioned, the entropy, and enthalpy change. The following equations were used to determine the thermodynamics parameters:

$$\mathrm{In}K_D = \frac{\Delta H^{\circ}}{R} + \frac{\Delta S^{\circ}}{R} \quad (11)$$

where, ΔH° (KJ/mol) and ΔS° (J/mol K) are the enthalpy and entropy change respectively during biosorption process, which was calculated from the intercept and slope of the linear plot.

$$\Delta G^{\circ} = \Delta H^{\circ} - T\Delta S^{\circ} \quad (12)$$

where ΔG is the free Gibbs energy change, R and T represent the ideal gas constant (8.314 J mol^{-1} K^{-1}) and absolute temperature (K)

$$K_D = \frac{C_s}{C_e} \quad (13)$$

where K_D is the equilibrium constant at a constant temperature, C_e (mg/L) and C_s (mg/L) are equilibrium concentrations of sorbate and the amount of sorbate adsorbed, respectively.

The results obtained for the thermodynamic parameters for Cr^{6+}, Cd^{2+} and PO_4^{3-} are illustrated in Table 11. From the data, the reaction which occurred during sorption of the adsorbates by the composite was endothermic for Cr^{6+} and PO_4^{3-}. However, for Cd^{2+}, it was an exothermic reaction. The results were validated by a positive ΔH° for Cr^{6+} and PO_4^{3-} and a negative ΔH° for Cd^{2+}. Furthermore, the results showed that Gibbs free energy change (ΔG°) values for all the adsorbates were increasingly negative values, which indicated that the reactions which occurred were spontaneous and feasible (Debnath and Ghosh, 2008).

Moreover, the positive ΔS° indicated that there was an increase in randomness for Cr^{6+} and Cd^{2+} adsorbates during the reaction process which supports the ion-exchange adsorption mechanisms at their respective adsorption pH values. However, PO_4^{3-} ΔS° was negative, which indicated a decrease in the randomness for the adsorbate by the GFP/diatom adsorbent.

Furthermore, $\Delta H°$ values for Cr^{6+} and Cd^{2+} were less than 40 KJ/mol, which indicates that the adsorption by GFP/diatom adsorbent is physisorption which was also validated by the adsorption kinetics.

Table 11: Thermodynamic parameters for Cr^{6+}, Cd^{2+} and PO_4^{3-}

	Cr^{6+}	Cd^{2+}	PO_4^{3-}
ΔH◦ (KJ/mol)	1.496	-9.392	50.086
ΔS◦ (J/mol K)	98.854	70.508	-68.909
		ΔG◦ (kJ/mol)	
298 K	-29.457	-21.021	-0.317
303 K	-29.951	-21.373	-0.322
313 K	-30.940	-22.078	-0.332

5.6 Conclusion

The morphological data by FTIR, XRD and the SEM-EDS characterizations confirmed the interaction of metal ions and nutrients by various functional groups in the GPF/diatom adsorbent. Furthermore, the adsorbent has the potential to remove Cr^{6+}, Cd^{2+} and PO_4^{3-} in aqueous solutions in its original states without any modifications or alterations. The optimization parameters such as contact time, adsorbent dosage, pH, and initial concentration of the adsorbates played a role in the sorption capacity of the adsorbent. The sorption kinetics revealed that the pseudo-first-order was the rate-limiting step for the adsorbates, indicating that physisorption was the responsible adsorption mechanism. The adsorption equilibrium data for the metal ions was best described by Langmuir isotherm, indicating that adsorption occurred on a monolayer surface. For phosphates, Freundlich isotherm best described the equilibrium adsorption data, which indicated that adsorption occurred on a multi-layered heterogeneous surface. The thermodynamics data revealed that the reaction was endothermic for Cr^{6+} and Cd^{2+} and was exothermic for PO_4^{3-}, and the reaction processes were feasible and spontaneous across all temperatures for the adsorbates. Furthermore, there was an increase in randomness of adsorbate by the adsorbent solution interface for Cr^{6+} and Cd^{2+} metal ions while for phosphates there was a decrease in the randomness of the adsorbate by the GPF/diatom adsorbent solutions.

References

Abdel-Raouf, N., Al-Homaidan, A.A. and Ibraheem, I.B.M., 2012. Agricultural importance of algae. *African Journal of Biotechnology*, *11*(54), pp.11648-11658.

Abdi, J., Vossoughi, M., Mahmoodi, N.M. and Alemzadeh, I., 2017. Synthesis of metal-organic framework hybrid nanocomposites based on GO and CNT with high adsorption capacity for dye removal. *Chemical Engineering Journal*, *326*, pp.1145-1158.

Akpor, O.B. and Muchie, M., 2010. Remediation of heavy metals in drinking water and wastewater treatment systems: processes and applications. *International Journal of Physical Sciences*, *5*(12), pp.1807-1817.

Albadarin, A.B., Collins, M.N., Naushad, M., Shirazian, S., Walker, G. and Mangwandi, C., 2017. Activated lignin-chitosan extruded blends for efficient adsorption of methylene blue. *Chemical Engineering Journal*, *307*, pp.264-272.

Ali Redha, A., 2020. Removal of heavy metals from aqueous media by biosorption. *Arab Journal of Basic and Applied Sciences*, *27*(1), pp.183-193.

Badamasi, H., Yaro, M.N., Ibrahim, A. and Bashir, I.A., Impacts of Phosphates on Water Quality and Aquatic Life.

Bolan, N.S., Choppala, G., Kunhikrishnan, A., Park, J. and Naidu, R., 2013. Microbial transformation of trace elements in soils in relation to bioavailability and remediation. *Reviews of Environmental Contamination and Toxicology*, pp.1-56.

Chang, M., Wang, W.N., Wang, A.L., Tian, T.T., Wang, P., Zheng, Y. and Liu, Y., 2009. Effects of cadmium on respiratory burst, intracellular Ca^{2+} and DNA damage in the white shrimp Litopenaeus vannamei. *Comparative Biochemistry and Physiology Part C: Toxicology & Pharmacology*, *149*(4), pp.581-586.

Debnath, S. and Ghosh, U.C., 2008. Kinetics, isotherm and thermodynamics for Cr (III) and Cr (VI) adsorption from aqueous solutions by crystalline hydrous titanium oxide. *The Journal of Chemical Thermodynamics*, *40*(1), pp.67-77.

Decision, E.C., 2001. 2455/2001/EC of the European Parliament and of the Council of November 20, 2001 establishing the list of priority substances in the field of water policy and amending Directive 2000/60. *EC (L 331 of 15-12-2001)*.

Dehghani, M.H., Taher, M.M., Bajpai, A.K., Heibati, B., Tyagi, I., Asif, M., Agarwal, S. and Gupta, V.K., 2015. Removal of noxious Cr (VI) ions using single-walled carbon nanotubes and multi-walled carbon nanotubes. *Chemical Engineering Journal*, 279, pp. 344-352.

El-Rahman, K.A., El-Kamash, A.M., El-Sourougy, M.R. and Abdel-Moniem, N.M., 2006. Thermodynamic modeling for the removal of Cs+, Sr2+, Ca2+ and Mg2+ ions from aqueous waste solutions using zeolite A. *Journal of Radioanalytical and Nuclear Chemistry*, *268*(2), pp.221-230.

Freundlich, H., 1907. Über die adsorption in lösungen. *Zeitschrift für physikalische Chemie*, *57*(1), pp.385-470.

Guo, J., Song, Y., Ji, X., Ji, L., Cai, L., Wang, Y., Zhang, H. and Song, W., 2019. Preparation and characterization of nanoporous activated carbon derived from prawn shell and its application for removal of heavy metal ions. *Materials*, *12*(2), p.241.

Gururajan, K. and Belur, P.D., 2018. Screening and selection of indigenous metal tolerant fungal isolates for heavy metal removal, *Environmental Technology & Innovation*, *9*, pp.91-99.

Ho, Y.S., Ng, J.C.Y., McKay, G., 2000. Kinetics of pollutant sorption by bio-sorbents. *Separation and Purification Methods*. 29(2), 189-232.

Ho, Y.S. and McKay, G., 1999. Pseudo-second order model for sorption processes. *Process Biochemistry*, *34*(5), pp.451-465.

Ibrahim, W.M., Hassan, A.F., Azab, Y.A., 2016. Biosorption of toxic heavy metals from aqueous solution by Ulva lactuca activated carbon. *Egyptian Journal of Basic and Applied Sciences. 3*(3), pp.241-249.

Jebakumar, J.P.P., Nandhagopal, G., Babu, B.R., Ragumaran, S. and Ravichandran, V., 2018. Impact of coastal power plant cooling system on planktonic diversity of a polluted creek system. *Marine Pollution Bulletin*, *133*, pp. 378-391.

Kabata-Pendias, A., 2010. *Trace elements in soils and plants*. CRC press.

Köseoğlu, E., Akmil-Başar, C., 2015. Preparation, structural evaluation and adsorptive properties of activated carbon from agricultural waste biomass. *Advanced Powder Technology*, *26*(3), pp.811-818.

Kumar, K.S., Dahms, H.U., Won, E.J., Lee, J.S. and Shin, K.H., 2015. Microalgae-A promising tool for heavy metal remediation. *Ecotoxicology and Environmental Safety*, *113*, pp.329-352.

Li, P., Lin, C., Cheng, H., Duan, X. and Lei, K., 2015. Contamination and health risks of soil heavy metals around a lead/zinc smelter in southwestern China. *Ecotoxicology and Environmental Safety*, *113*, pp.391-399.

Liu, L., Luo, X.B., Ding, L. and Luo, S.L., 2019. Application of nanotechnology in the removal of heavy metal from water. In *Nanomaterials for the removal of pollutants and resource reutilization* (pp. 83-147). Elsevier.

Macías-Mayorga, D., Laiz, I., Moreno-Garrido, I. and Blasco, J., 2015. Is oxidative stress related to cadmium accumulation in the Mollusc Crassostrea angulata? *Aquatic Toxicology*, *161*, pp.231-241.

Mahmoodi, N.M. and Najafi, F., 2012. Synthesis, amine functionalization and dye removal ability of titania/silica nano-hybrid. *Microporous and Mesoporous Materials*, *156*, pp.153-160.

Mdlalose, L., Balogun, M., Setshedi, K., Tukulula, M., Chimuka, L. and Chetty, A., 2017. Synthesis, characterization and optimization of poly (p-phenylenediamine)-based organoclay composite for Cr (VI) remediation. *Applied Clay Science*, *139*, pp.72-80.

Mitra, S., Sarkar, A. and Sen, S., 2017. Removal of chromium from industrial effluents using nanotechnology: a review. *Nanotechnology Environment Engineering*, *2*, pp.1-14

Mustafa, G., Wyns, K., Buekenhoudt, A. and Meynen, V., 2016. Antifouling grafting of ceramic membranes validated in a variety of challenging wastewaters. *Water Research*, *104*, pp.242-253.

Oliveira, H., 2012. Chromium as an environmental pollutant: insights on induced plant toxicity. *Journal of Botany*.

Paździor, K., Bilińska, L. and Ledakowicz, S., 2019. A review of the existing and emerging technologies in the combination of AOPs and biological processes in industrial textile wastewater treatment. *Chemical Engineering Journal*, *376*, pp.120597.

Rangabhashiyam, S. and Balasubramanian, P., 2019. Characteristics, performances, equilibrium and kinetic modeling aspects of heavy metal removal using algae. *Bioresource Technology Reports*, *5*, pp.261-279.

Renu, M.A., Singh, K., Upadhyaya, S. and Dohare, R.K., 2017. Removal of heavy metals from wastewater using modified agricultural adsorbents. *Materials Today: Proceedings*, *4*(9), pp.10534-10538.

Rowbotham, A.L., Levy, L.S. and Shuker, L.K., 2000. Chromium in the environment: an evaluation of exposure of the UK general population and possible adverse health effects. *Journal of Toxicology and Environmental Health Part B: Critical Reviews*, *3*(3), pp.145-178.

Sbihi, K., Cherifi, O., Bertrand, M. and El Gharmali, A., 2014. Biosorption of metals (Cd, Cu and Zn) by the freshwater diatom Planothidium lanceolatum: a laboratory study. *Diatom research*, *29*(1), pp.55-63.

Singh, V.K. and Tiwari, P.N., 1997. Removal and recovery of chromium (VI) from industrial wastewater. *Journal of Chemical Technology & Biotechnology: International Research in Process, Environmental AND Clean Technology*, *69*(3), pp.376-382.

Soltani, R., Marjani, A., Hosseini, M. and Shirazian, S., 2020. Synthesis and characterization of novel N-methylimidazolium-functionalized KCC-1: A highly efficient anion exchanger of hexavalent chromium. *Chemosphere*, *239*, pp.124735.

Speer, R.M., Wise, S.S., Croom-Perez, T.J., Aboueissa, A.M., Martin-Bras, M., Barandiaran, M., Bermúdez, E. and Wise Sr, J.P., 2019. A comparison of particulate hexavalent chromium cytotoxicity and genotoxicity in human and leatherback sea turtle lung cells from a one environmental health perspective. *Toxicology and Applied Pharmacology*, *376*, pp. 70-81.

Tatarchuk, T., Myslin, M., Lapchuk, I., Shyichuk, A., Murthy, A.P., Gargula, R., Kurzydło, P., Bogacz, B.F. and Pędziwiatr, A.T., 2021. Magnesium-zinc ferrites as magnetic adsorbents for Cr (VI) and Ni (II) ions removal: cation distribution and antistructure modeling. *Chemosphere*, *270*, p.129414.

Tutu, H., Bakatula, E., Dlamini, S., Rosenberg, E., Kailasam, V. and Cukrowska, E.M., 2013. Kinetic, equilibrium and thermodynamic modelling of the sorption of metals from aqueous solution by a silica polyamine composite. *Water SA*, *39*(4), pp.437-444.

Vareda, J.P., Valente, A.J. and Durães, L., 2016. Heavy metals in Iberian soils: Removal by current adsorbents/amendments and prospective for aerogels. *Advances in Colloid and Interface Science*, *237*, pp.28-42.

Vareda, J.P., Valente, A.J. and Durães, L., 2019. Assessment of heavy metal pollution from anthropogenic activities and remediation strategies: A review. *Journal of Environmental Management*, *246*, pp.101-118.

Verma, B. and Balomajumder, C., 2020. Magnetic magnesium ferrite–doped multi-walled carbon nanotubes: an advanced treatment of chromium-containing wastewater. *Environmental Science and Pollution Research*, pp.1-11.

World Health Organization, 2017. *Guidelines for drinking-water quality*. World Health Organization. *Fourth edition.*

Xu, J., Cao, Z., Zhang, Y., Yuan, Z., Lou, Z., Xu, X. and Wang, X., 2018. A review of functionalized carbon nanotubes and graphene for heavy metal adsorption from water: Preparation, application, and mechanism. *Chemosphere*, *195*, pp.351-364.

CHAPTER 6

Equilibrium thermodynamic and kinetic investigations for biosorption of selected metal species, nutrients, and pathogens in aqueous solutions by a fabricated biomass-polymeric adsorbent.

6.1 Abstract

Water pollution by heavy metals, nutrients, and pathogens continues to threaten human life and the overall environment. Researchers and scientists all over the world put in efforts to look for better techniques that will help eliminate this threat to the existence of life on earth. Various methods exist so far to solve these problems, however, most of them require large capital, high maintenance costs, and even produce secondary pollutants. Hence in this study, biosorption using poly-phenylenediamine/grapefruit peel/diatom (pPD/GFP/diatom) adsorbent was used as the best sustainable technique to remediate water polluted by Cr^{6+} and Cd^{2+} metal ions as well as PO_4^{3-} ions due to its cost-effectiveness and environmentally friendliness. The XRD revealed that pPD/GFP/diatom adsorbent was composed of crystalline mineral phases. The FTIR revealed that the pPD/GFP/diatom adsorbent contained a variety of functional groups which played a role in the sorption efficiency of the adsorbates. The SEM images revealed a spherical or pebble-like shape with the appearance of pores and the EDS revealed Mg, Fe, Al, Si with N, Ca, K, C, and O. The uptakes of Cr^{6+}, $Cd^{2+,}$ and PO_4^{3-} from aqueous solutions by pPD/GFP/diatom adsorbent were investigated as a function of sample pH, contact time, and initial concentration through batch studies. The overall kinetic results indicated that sorption processes followed both pseudo-first-order and pseudo-second-order and were governed also by the intraparticle diffusion mechanism. The adsorption equilibrium data were best described by Freundlich isotherm for Cr^{6+}, Cd^{2+} and PO_4^{3-} ions. The maximum adsorption capacities obtained for Cr^{6+}, Cd^{2+} and PO_4^{3-} were 12.68 (mg/g) at 303 K; 21.90 (mg/g) at 313 K and 33.45 (mg/g) at 313 K respectively. Furthermore, the thermodynamic data revealed that the biosorption process was spontaneous and favorable across all temperatures. The data also revealed that most of the adsorbents had antimicrobial potency towards *Escherichia coli and Klebsiella pneumoniae* due to their inherent functional properties. This indicated that the material is suitable for wastewater treatment.

Keywords: Biosorption, pathogens, Cr^{6+}, Cd^{2+}, PO_4^{3-}, biomass-polymeric adsorbent.

6.2 Introduction

Water is life and a most precious resource for human beings. The human body contains about 60% of water. it is a scarce resource that is arid in some parts of the world. Water serves a lot of functions. It is home to some species, while to others it is a means of survival. Water can be used for a variety of activities such as irrigation of crops and animals to drink in agriculture, to generate electricity and washing minerals in industries, as well as for household uses which include drinking, washing clothes, producing food, and most importantly to maintain a clean and healthy environment (Zare et., 2016).

Water bodies have been polluted extensively from various human activities such as mining, agriculture and sewage wastewater from municipalities. Water used from these sectors is directly discharged or washed off into rivers and other water sources, leaving them polluted and dirty. This affects aquatic organisms as well as human health. There are four categories of pollutants which include physical (e.g., sediments or material suspended from soil erosion), chemical (e.g., metals, pesticides and insecticides), biological (bacterial, viruses and parasites) and radiological- elements that can emit ionizing radiation (e.g., plutonium and uranium) (Zare et al., 2018; Nebel and Wright,1993).

Heavy metal pollution is the most important and common environmental problem threatening human life throughout the world due to its toxicity and mobility in natural water ecosystems. Heavy metals end up in aquatic environments in various ways via natural or anthropogenic sources which include metal plating, tanneries, batteries, fertilizers, pesticides, paper industries domestic sewage, leaching from landfills, storm runoff, shipping, and harbor activities as well as the atmosphere (Sonone et al., 2020; Sud et al., 2008). Some heavy metals such as copper, zinc, iron, and manganese are essential to maintain body metabolism but are toxic when in high amounts. However, heavy metals, such as arsenic, copper, zinc, nickel, cadmium, chromium, mercury and lead are toxic cause serious human health problems. Some of the health problems associated with cadmium metal ion include high blood pressure, kidney damage, and destruction of testicular tissue, osteoporosis and destruction of red blood cells while chromium can cause severe health problems such as skin irritation and lung cancer (Zare et al., 2018; Schoeters et al., 2006; Järup et al., 1998).

Furthermore, microbial contamination is a growing concern that has been in existence for ages. The most common waterborne pathogens that are found in wastewater are viruses, bacteria, fungi, protozoa, and helminths (Akpor and Muchie, 2011). Pathogens of high fecal origin are

usually the ones affecting the water quality of surface water include *Escherichia coli*, *Salmonella* species, *Staphylococcus* species and *Klebsiella pneumoniae*. The common sources of these pathogens come from municipal sewage effluents, animal dropping which ends up in agriculture through irrigation as well as in surface water. This affects human health and aquatic organisms by causing pneumonia, diarrhea, cholera, nausea and sometimes even death in children under 5 years (WHO/UNICEF, 2015; Naidoo and Olaniran, 2013).

Due to the inefficiency of conventional treatment methods to remove toxic chemical species and to disinfect pathogens from water, various techniques have been conducted by researchers to reduce water contamination challenges. These techniques of wastewater treatment include oxidation, membrane filtration, coagulation and activated sludge (Asadollahzadeh et al., 2018; Albadarin et al., 2017). Furthermore, convention methods for microbial contamination include chlorination, ceramic filtration and UV water purification (Dankovich et al., 2016). However, these methods have disadvantages of their own, such as high maintenance costs, producing secondary pollutants and difficulty in operations as well as forming harmful carcinogenic disinfection by-products (Cao et al., 2018; Dimapilis et al., 2018; El-Zayat, 2009).

Alternative methods such as biosorption have been developed to tackle water pollution issues due to their availability, cost-effectiveness, sustainability, eco-friendly, reusability and potential to remove and recover metals (Al-Homaidan et al., 2018; Zare et al., 2018; Javanbakht et al., 2014). Bio-sorbents materials such as rice husk, orange peel, sawdust, algae and fungi have been used for the removal of heavy metals from wastewater (Rangabhashiyam and Balasubramanian, 2019; Elsherif et al., 2017; Gola et al., 2016; Lata and Samadder, 2014; Lim et al., 2008).

Polymeric adsorbents have recently emerged as potential alternatives to traditional adsorbents due to their vast surface area, surface chemistry, adsorption of heavy metal ions, high thermal stability, pore size distribution, and regeneration potential (Mahmoodi et al., 2013; Huang et al., 2012; Virji et al., 2005; Li et al., 2002). The aromatic polyaniline (PANI) and its derivatives, poly (Ortho-phenylenediamine) (PoPDA), poly(m-phenylenediamine) (PmPDA) and poly(p-phenylenediamine) (PpPDA) have attracted great attention due to simple preparation, electrical conductivity, low cost, and environmental stability ((Lakouraj et al., 2014). Various studies have been conducted on the PANI derivatives for their removal efficiency of different metal ions as well as phosphates and were reported (Mdlalose et al., 2017; Archana and Jaya Shanthi, 2015; Chai et al., 2015; Wang and Liao, 2012; Tang et al., 2011; Huang et al., 2006).

Moreover, PANI and its derivatives have been used in conjunction with other functional materials which include agricultural waste products, natural polymers, organic and inorganic materials to enhance the surface area and morphology of the adsorbents (Zare et al., 2018). PANI/sawdust and PANI/ rice husk ash nanocomposites have been used for the removal of heavy metals and had a high affinity for them (Ghorbani, and Eisazadeh, 2013; Mansour et al., 2011; Ansari and Mosayebzadeh, 2010). Hence in this study, adsorption using poly-phenylenediamine incorporated with grapefruit peel and diatom biomass powders on the polymer matrix was used as a cost-effective, accessible, and easy-to-use adsorbent. Poly-phenylenediamine is a low toxicity diamine, while the grapefruit peels and diatom biomass are considered as nuisance, dirty and causing ecological problems. Hence, using these materials is a sustainable method because they will be transformed from being an ecological burden to a resource that can be used for the remediation of heavy metals. Moreover, this will be the first study to have used poly-phenylenediamine incorporated with grapefruit peel and diatom biomass in the polymer matrix for the remediation on water contaminated by Cr^{6+} and Cd^{2+}, PO_4^{3-} ions and pathogens.

6.3 Material and methods

6.3.1 Chemicals and reagents

In conducting the experiments for this work, the chemicals used were of analytical reagent grade. $CdN_2O_6{\cdot}4H_2O$, $K_2Cr_2O_7$, $(NH_4)_2\ S_2O_8$, CH_3COCH_3, NaCl, HCl, NaOH, KCl, p-phenylenediamine used were purchased from Rochelle and Merch chemicals, (Johannesburg, South Africa). The chemicals were used directly without further purification. Deionized water was used for stock solution preparations and in the dilutions of standards during the experiments.

6.3.2 Preparation of adsorbents

6.3.2.1 Synthesis of poly-phenylenediamine

The synthesis of poly- pPD was done by a modified method adopted from Mdlalose et al. (2017) and Pham et al. (2011). pPD (1.62 g, 0.015 mol) was briefly dissolved in HCl (50 mL, 0.1 M) and stirred for 3 h on an ice bath at a 400 rpm stirring rate. After that, the pPD polymerization was initialized by the addition of an oxidant solution of ammonium persulfate (3.42 g) in HCl (25 mL, 0.1 M) for 30 min. Thereafter, the resulting mixture was stirred for 24 h at room temperature to complete the polymerization process of the pPD monomer. The reaction was stopped by adding 15 mL acetone and the resulting sludge product was washed with de-ionized water and dried at 60 °C for 24 h in an oven.

6.3.2.2 Synthesis of biomass-polymeric adsorbent

The biomass-polymeric adsorbent was prepared by dissolving pPD (1.62 g, 0.015 mol) in HCl (50 mL, 0.1 M) in an ice bath and stirred for 3 h at 400 rpm stirring rate. After that, grapefruit peel powder (0.4 g) and dried diatom biomass (0.2 g) were added into the solution and stirred for 20 min at 600 rpm. pPD polymerization was then initiated by adding ammonium persulfate (3.42 g) in HCl (25 mL, 0.1 M) for 30 min. Thereafter, the resulting mixture was stirred for 24 h at room temperature to complete the polymerization process of the biomass-polymeric adsorbent. The reaction was stopped by adding 15 mL acetone after 24 h elapsed and the resulting residue was washed with de-ionized water and dried at 60 °C for 24 h in an oven.

6.3.3 Preparation of stock solutions

The concentration of 1000 mg/L cadmium, chromium and phosphate solutions were prepared by dissolving 2.744 g of $CdN_2O_6 \cdot 4H_2O$, 2.82 g of $K_2Cr_2O_7$ and 1.44 g of KH_2PO_4 in a 1L volumetric flask with Millipore water respectively. The working solutions were prepared by diluting the stock solutions to 50 mg/L concentration to conduct further experiments.

6.3.4 Instruments

The functional groups of the solid samples of pPD/GFP/diatom adsorbent were identified by an ALPHA Bruker FT-IR Spectrophotometer (Berlin, Germany) within the range of 400-4000 cm^{-1}. The surface morphology was determined by SEM and EDS to provide the elemental composition of the adsorbent with an (FEI Nova NanoSEM 230 with the field emission gun equipped with an Oxford Xmax SDD detector operating at an accelerating voltage of 20Kv). For the EDS detector, Oxford X-Max with INCA software was used to characterize the sorbent material. The mineralogical and phase identification was determined by XRD type PANalytical X'Pert Pro powder diffractometer for qualitative sample analysis. The filtrates of Cr^{6+} and Cd^{2+} were analysed by ICP AES) and PO_4^{3-} was analysed with Ion Chromatography. The filtrates of Cr^{6+} and Cd^{2+} were analysed by Thermo iCAP 6200 ICP AES and PO_4^{3-} was analysed by ion chromatography. Autoclave model KT-30L AC220V was used to sterilize the bacterial media.

6.3.5 Point of zero charge (pHpzc)

The pH at point-of-zero charge was determined by mixing 0.2 g of pPD/GFP/diatom adsorbent in 0.01 M KCl solutions. The pH of solutions was adjusted to desired values between 3 and 11 by adding 0.1 M HCl or 0.1 M NaOH. A volume of 25 mL of the solutions was poured into plastic bottles which were agitated on a thermostat water bath shaker at 150 rpm for 24 h at

room temperature. The equilibrium pH (pH_f) of each mixture was measured and the intersection pH-initial against ΔpH curve gives the pHpzc value.

6.3.6 Antimicrobial testing

6.3.6.1 Preparation of media agar

The medium agar 1 plate was prepared by using 0.5% 0f sodium chloride, 1% yeast, 1.5% agar and 1.6% tryptone which were mixed in 250 mL ultrapure water. A magnetic stirrer was used at 250 rpm to completely dissolve the media. The dissolved media was then autoclaved at 121˚ C for 15 min to sterilize the agar media. After the media has cooled down, 25 mL of the media was added into a sterile petri dish and left to solidify.

Three bacterial strains were used for microbial testing which includes *Klebsiella Pneumoniae*- ATCC 700603; Escherichia coli- ATCC 25922 IN; *Staphylococcus Aureus*- ATCC 259231 TM. The bacteria strains swaps were streak on the medium agar plates which were incubated at 37˚C for 24 h. 3-5 colonies of bacteria were selected from the agar plate using a loop and were inoculated in 5 mL Mueller -Hinton agar broth which was incubated for at least 2 h at 37˚ C.

6.3.6.2 Antimicrobial test

The bacterial efficacy of grapefruit peel, diatom biomass, GFP/diatom and pPD/GFP/diatom adsorbents were determined by using the standard agar-well disc diffusion method by Bauer (Bauer, 1966) disk diffusion test to observe the zone of inhibition (mm). A volume of 50 µL of the incubated suspension was inoculated on the sterile medium agar 1 which was divided into equal parts. Pipette tips (1-5 mL) were used to punch small circles at the center to suspend the adsorbent material. 0.1 g of the adsorbent was added into 1 mL ultrapure water to dissolve the adsorbent. Thereafter, 50 µL of the bacterial strains were inoculated into the sterile medium 1 agar, then 50 µL sorbent (1 mL /0.1 g) was added into the punched circles which was immediately incubated for 24 h at 37˚C. The minimum zone of inhibition was observed and measured after 24 h.

6.4 Adsorption procedure

The adsorption experiments were carried out to determine the effect of different experimental parameters such as contact time, initial metal concentration, pH and effect of temperature. Contact time was varied from 1 to 120 min. The effect of initial metal concentration and adsorption isotherms were evaluated by varying the concentration from 10 to 200 mg/L. Moreover, solution pH was evaluated by adjusting from 3 to 11 using 0.1 M NaOH and 0.1 M

HCl. All experiments were carried out by using 50 mL of Cr^{6+}, Cd^{2+} and PO_4^{3-}. After shaking time elapsed, metal ion samples were filtered and analyzed by ICP AES. spectrometer and Ion Chromatography for the phosphate ions. The adsorption capacity of pPD/GFP/diatom adsorbent to Cr^{6+}, Cd^{2+} and PO_4^{3-} was calculated by equations (1) and (2).

$$q = (C_0 - C_e) \times \frac{V}{w} \quad (1)$$

$$\% \text{ Removal } = \frac{(C_0 - C_e)}{C_0} \times 100 \quad (2)$$

where Co is the initial metal ions concentration (mg/L); Ce is the metal ions concentration at equilibrium (mg/L); V is the volume of solution (L) and w mass of the adsorbent (g).

6.5 Results and discussions

6.5.1 FTIR results

The visible peaks were obtained around the regions of 3223, 2095, 1562, 1491, 1411, 1275, 1026, 816 cm^{-1}. It was observed that the presence of hydroxyl group (-OH) around 3223 cm^{-1} is attributed to the stretching vibration of the N–H group (Pham et al., 2011). The peaks at 2095 cm^{-1} are attributed to C-H groups which displayed aliphatic vibrations of lignin polysaccharides due to the presence of grapefruit peels (Nguyen et al., 2013). Furthermore, peaks at the region of 1562 cm^{-1} may be attributed to C=N vibrations of phenazine ring or stretching vibrations of quinoid rings in the polymer matrix. It could also be attributed to C=O vibrations of peptide linkages (Archana and Jaya, 2014; Baghayeri et al., 2013). The peaks at around 1491 cm^{-1} and 1411 cm^{-1} may be attributed to C–N–C which is associated with the stretching vibrations of benzenoid and quinoid imine (Baghayeri et al., 2013). Around the regions of 1275 cm^{-1}, the peaks may be attributed to -C-O which are associated with non-ionic carboxylic groups as discussed previously. Moreover, the peaks at 1026 cm^{-1} may be attributed to the C-O group due to C-OH associated with alcoholic groups and carboxylic acids. Lastly, the peaks at around 816 cm^{-1} may be due to C-H bending vibrations of benzene bases in the phenazine skeletons (Hao et al, 2009).

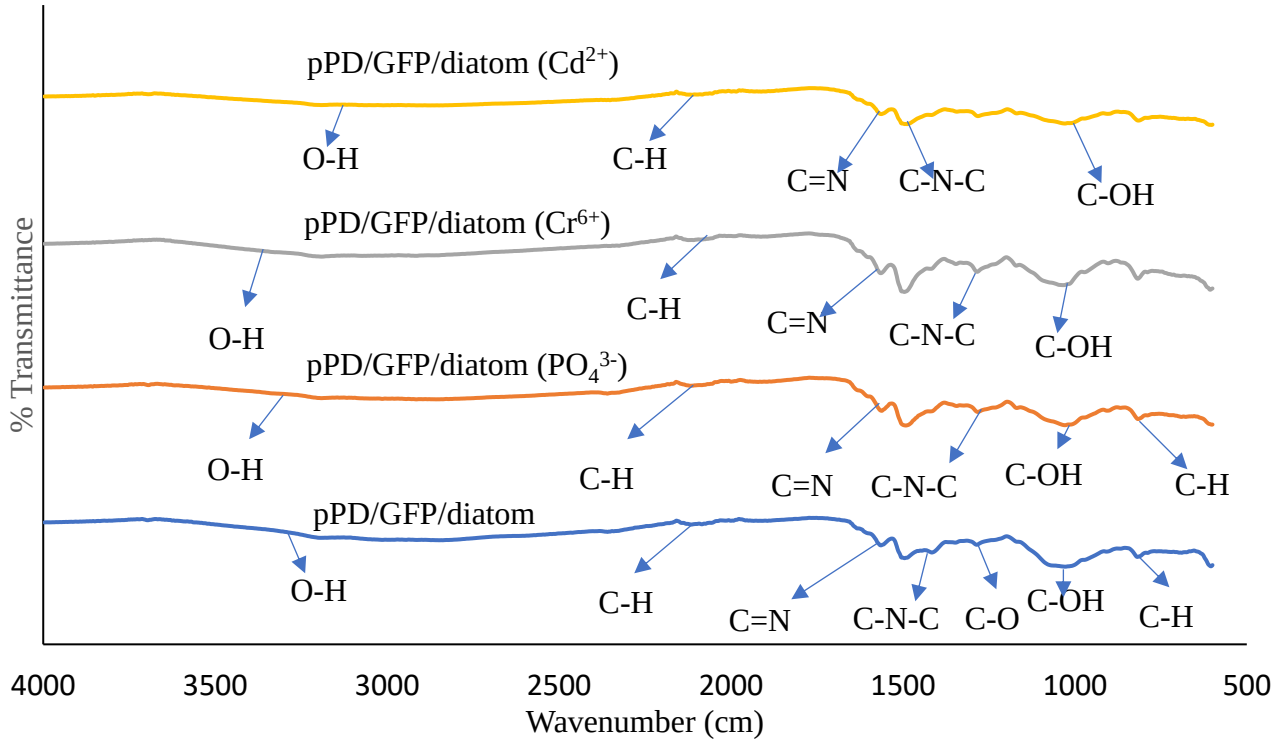

Fig.38. FTIR spectra for pPD/GFP/diatom adsorbent and after the treatment of Cr^{6+}, Cd^{2+} and PO_4^{3-} ions.

6.5.2 XRD results

The mineral phase of the pPD/GFP/diatom adsorbent was revealed by the X-ray diffraction spectrum. The pattern of the adsorbent ranged between 5-80 theta which can be observed from Fig. 39. Furthermore, the X-ray diffraction spectrum indicated that the adsorbent material consists of a crystalline structure. This is due to the presence of Mascagnite, $(NH4)_2SO_4$ and Hydrazine Sulfate, $N_2H_6SO_4$ as the identified mineral phases which were dominating. The presence of these mineral phases is due to the usage of ammonium persulphate as an oxidant in the synthesis of pPD/GFP/diatom adsorbent. Furthermore, a large fraction of biomass was also present. This was due to the presence of grapefruit peel powder and diatom biomass.

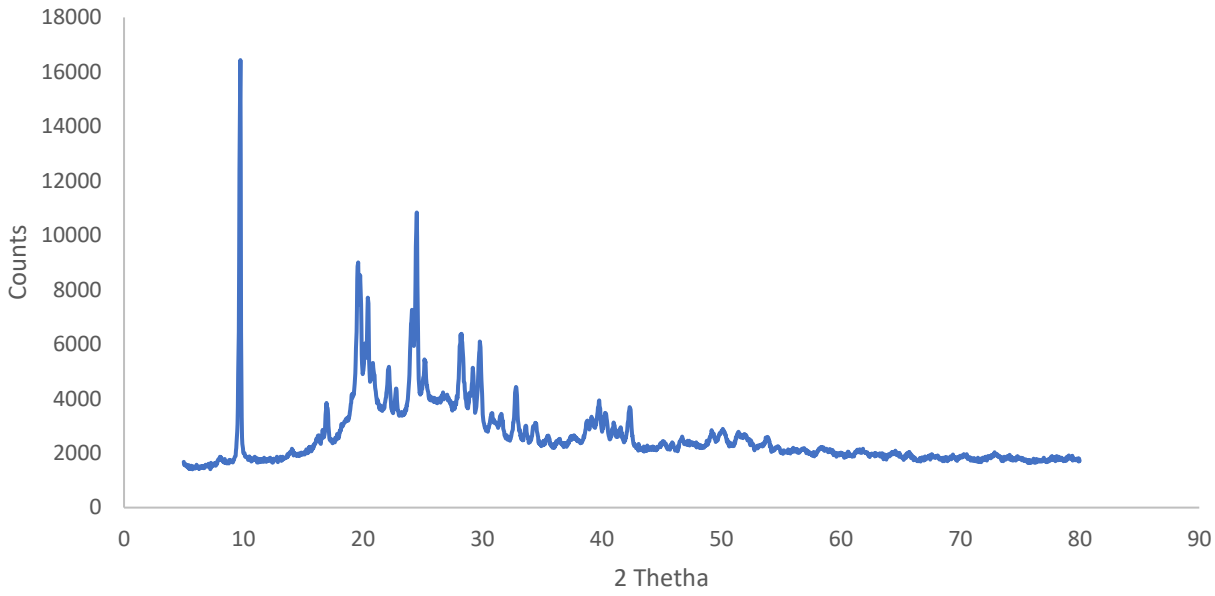

Fig. 39. XRD spectra for pPD/GFP/diatom adsorbent

6.5.3 SEM-EDS

Figure 40 shows the surface morphologies of the raw pPD/GFP/diatom adsorbent and after the treatment of Cr^{6+} and Cd^{2+} metal ions as well as PO_4^{3-} ions. From the raw adsorbent (a), the surface has a spherical or pebble-like shape with the appearance of pores. The EDS for the raw diatom biomass (Fig. 40(a)) revealed some of the elements that are present on the surface of the adsorbent which includes Mg, Fe, Al, Si with N, Ca, K, C and O as well. This indicated that the biomass-polymeric adsorbent was also composed of aluminosilicate material as validated by the EDS spectra which has already been alluded to earlier. Moreover, it was reported that the existence of N and S atoms in the main chain structure of the conductive polymers such as poly-phenylenediamine is responsible for the adsorption of the pollutants (Zare et al., 2018). Hence, after the treatment of Cr^{6+}, Cd^{2+} and PO_4^{3-} ions (Fig. 40(b-d)), the morphology seemed conglomerated due to the attachment of the pollutant ions to the pores of the pPD/GFP/diatom adsorbent after agitation with time which was assured by their presence on the EDS spectra.

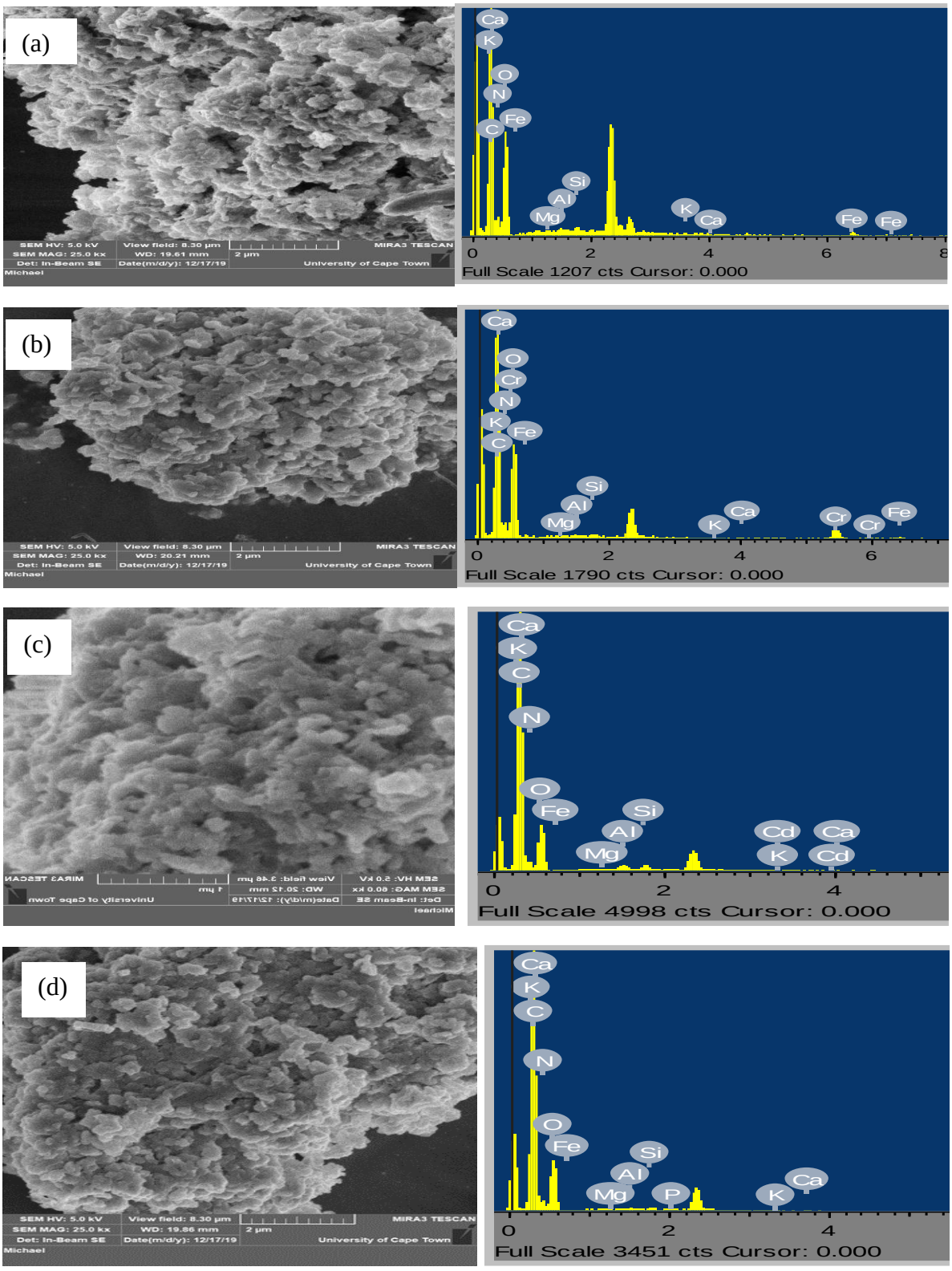

Fig. 40. SEM images of pPD/GFP/diatom adsorbent (a); after Cr (b); Cd (c) and PO_4^{3-}(d) treatments with their respective EDS.

6.6 Batch experimental results

6.6.1 Effect of pH and pHpzc.

The data revealed in Fig. 41 (a), shows the sorption capacity of Cr^{6+} increasing with an increase in pH with the highest percentage removal obtained at pH 9 to be 99. 71%. After pH 9, the percentage removal and adsorption capacity decreased from 91 to 87%. The decrease in sorption was due to the alkaline region which is associated with hydroxyl groups competing through ion exchange. However, at low pH, protonation to surface hydroxyl groups of pPD/GFP/diatom adsorbent occurs, thereby imparting positive charges to the surface, hence the low adsorption capacity and percentage removal of Cr^{6+} occurred. This is similar to what was obtained by Naga Babu et al. (2017). Su et al. (2013) also confirmed that low solution pH in the acidic region is beneficial for the protonation of the adsorbent surface. Furthermore, Unceta et al. (2010) also revealed that chemical species of Cr (VI) range from chromate (CrO_4^{2-}) and dichromate ($Cr_2O_7^{2-}$) between the pH of 6.5–14 through hydrogen chromate ($HCrO_4^-$). Fig. 41(b), shows sorption capacity for Cd^{2+} to be increasing with an increase in pH with optimum pH of 11 at a 99.27 % removal rate. Although from pH 9 there is slow uptake of Cd^{2+} by the pPD/GFP/diatom adsorbent due to the state of equilibrium being reached. This could be as a result of electrostatic attraction between Cd^{2+} ions and the surface charge of the adsorbent since the surface is negatively charged at higher pH values. However, Fig. 41 (c) shows that the removal efficiency increasing with an increase in pH, with a rapid increment at low pH, where fluctuations were observed. The optimum pH was obtained at pH 9 at 55%. After pH 9, the adsorption capacity and percentage removal decrease to 50% because at higher pH, the alkaline region is associated with hydroxyl groups which change the surface of the adsorbent to be negatively charged, thus resulting in a repulsive interaction between the pPD/GFP/diatom adsorbent and PO_4^{3-}. Similar results were reported by Lu et al. (2013) and Su et al. (2013).

Furthermore, the pHpzc was used in this study to determine the surface charge of the pPD/GFP/diatom adsorbent to determine the chemical processes that are responsible for the removal of Cr^{6+}, Cd^{2+} and PO_4^{3-} ions (Fig. 41(d)). The pHpzc is defined as the point where the net surface of the material has a zero charge. pHpzc also helps to identify the surface charge of an adsorbent. For example, the surface is negatively charged when the pH is above pHpzc and positively charged when the pH is below pHpzc. In this case, the pHpzc was found around pH 3.

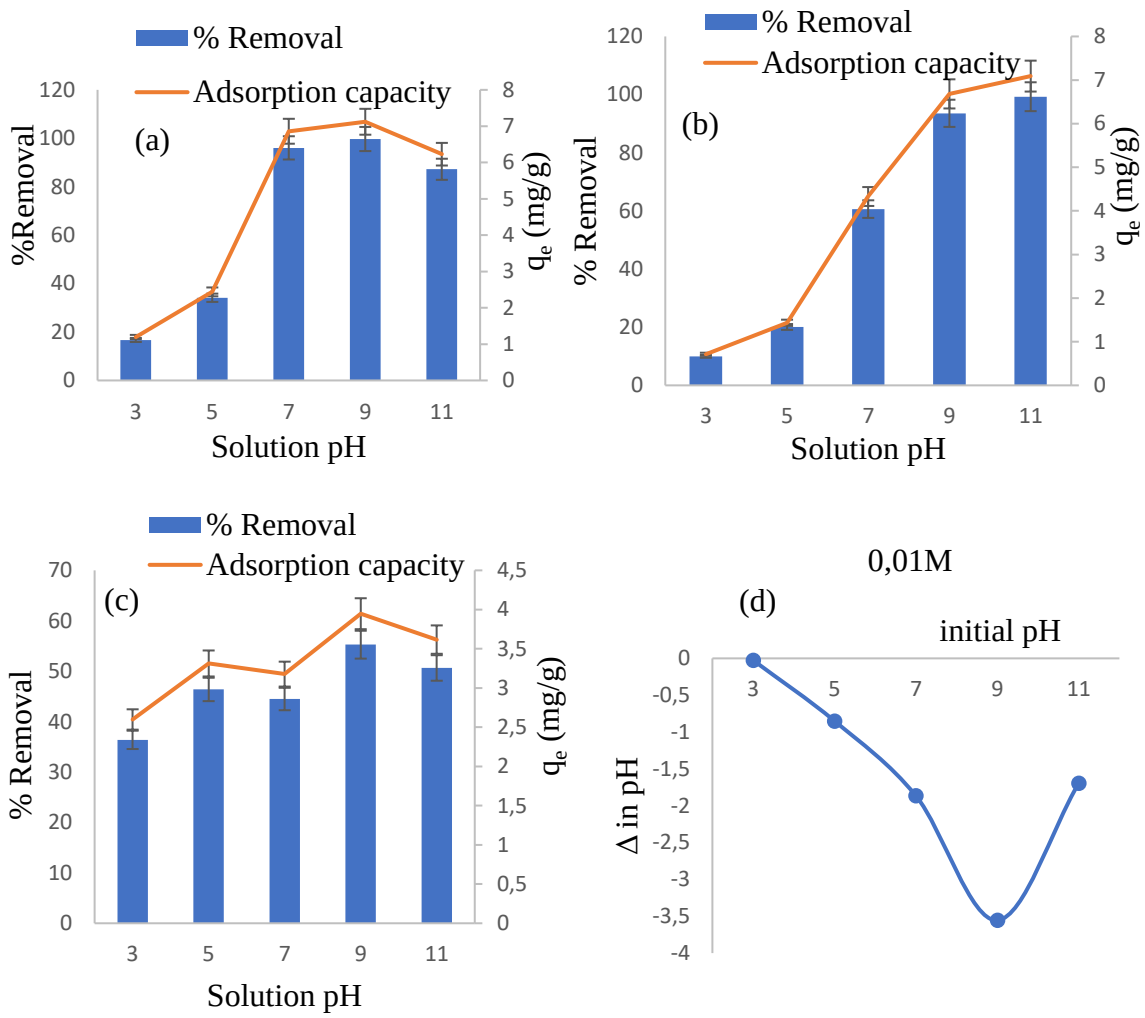

Fig. 41. Effect of pH for Cr $^{6+}$ (a), Cd^{2+} (b) and PO_4^{3-} (c) and pHpzc (d).

6.6.2 Effect of contact time and kinetics modeling

The effect of contact time for Cd^{2+}, Cr^{6+} and PO_4^{3-} ions were evaluated between the ranges of 1-120 min to evaluate the uptake efficiency of these ions by pPD/GFP/ diatom adsorbent. Fig. 42 shows the percentage removal and the adsorption capacity to be increasing with time, although some fluctuations can be observed. This is an indication of an increase in the accessibility and vacant active binding sites at the surface of the pPD/GFP/diatom adsorbent and the inherent functional groups thereof (Naga Babu et al., 2017). From the results obtained, the highest Cr^{6+} percentage removal and the adsorption capacity were obtained at around 90 min. For Cd^{2+}, the highest percentage removal and the adsorption capacity were obtained at 30 min, which revealed that the adsorbent material has a high affinity for Cd^{2+} metal ions with a removal efficiency of > 80%. This was higher than all percentage removals of Cr^{6+} and PO_4^{3-} ions. Furthermore, the highest percentage removal and adsorption capacity of PO_4^{3-} were

obtained at 120 min, although the reduction in the driving force of the pPD/GFP/ diatom adsorbent had already occurred as early as 30 min.

The overall results showed that at the beginning of time, the reaction was rapid since there are a lot of active sites available for the adsorption process to occur up to observable time (30 min) where the adsorbent becomes saturated, and all sites become occupied leading to the low driving force of the adsorption process which results in a state of equilibrium to reach.

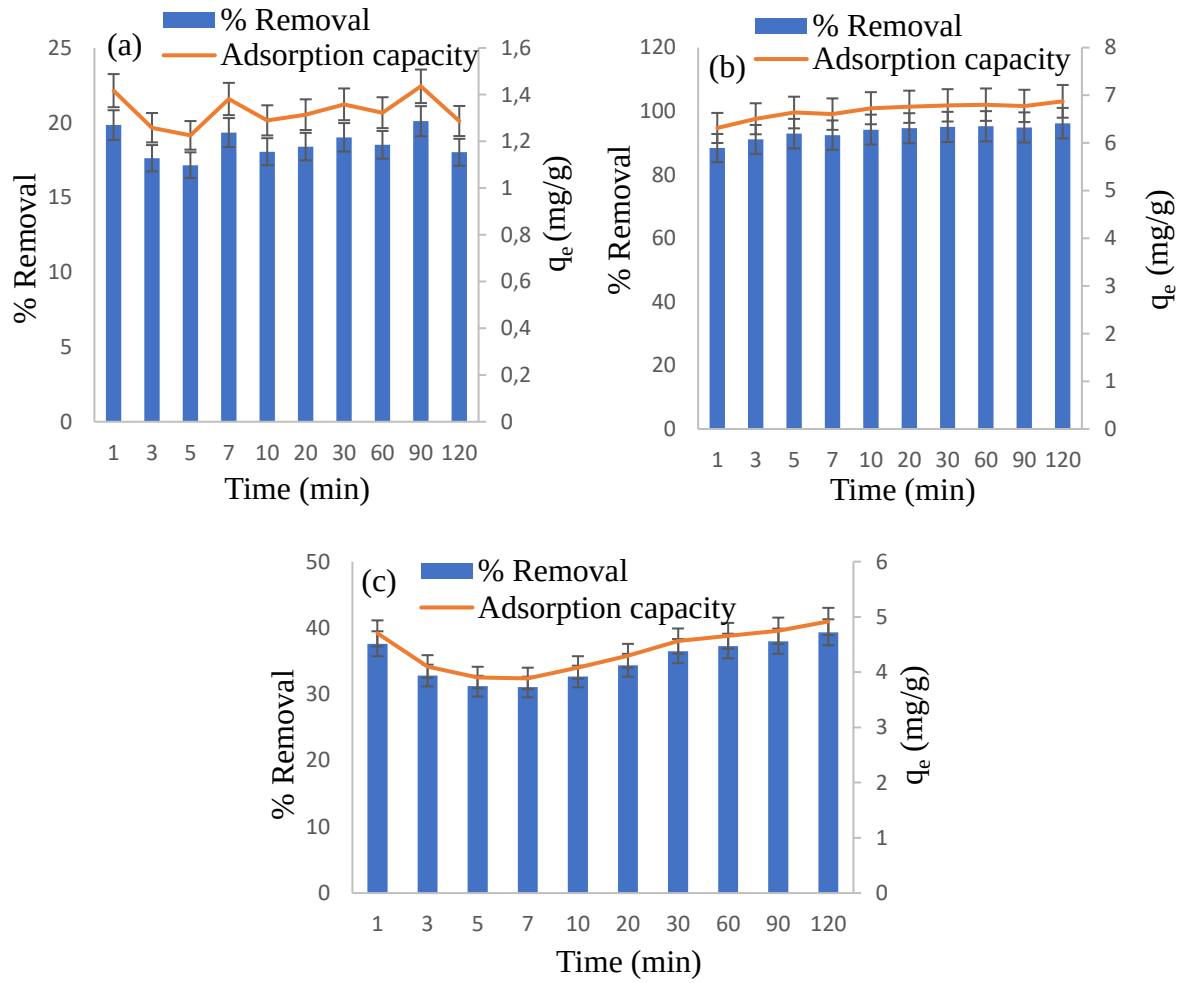

Fig. 42. Effect of contact time for Cr^{6+}, Cd^{2+} and PO_4^{3-} ions against the percentage removal and adsorption capacity. (Experimental conditions: dosage, 0.2 g; volume, 50 mL; neutral pH; initial concentration, 50 mg/L and shaking speed, 250 rpm).

The kinetic modeling was determined using the non-linearized pseudo-first-order, pseudo-second-order and linearized intra-particle diffusion. The models are expressed in equations (3) to (5) respectively.

$$q_t = q_e(1 - e^{-kit}) \quad (3)$$

$$q_t = \frac{qe^2 k_2 t}{1+k_2 q_e t} \quad (4)$$

$$q_t = k_t t^{0.5} + ci \quad (5)$$

where q_e and q_t (mg/g) are the amounts of adsorption that occurred at time t (min) for pseudo-first-order, k_1 is the pseudo-first-order adsorption rate constant min^{-1} at equilibrium, while k_2 (g/mg/min) is the equilibrium rate constant of pseudo-second-order adsorption. For the intra-particle diffusion kinetics, q_t is the amount adsorbed (mg/g) regarding time (t) (min), and k_t is the intra-particle diffusion rate constant in (mg/g/min) C_i is a constant related to the thickness of the boundary layer (mg/g).

The results for the pseudo-first-order and pseudo-second-order kinetic models are displayed in Table 12. The results for pseudo-first-order kinetics indicated the coefficient of determination (R^2) for Cr^{6+}, Cd^{2+}, and PO_4^{3-} ions were all > 0.99. The root mean square errors (RSME) results were 0.092; 0.108; 0.263 while the reduced chi-square (RCS) values were 0.007; 0.002; 0.017 for Cr^{6+}, Cd^{2+}, and PO_4^{3-} respectively. However, the coefficient of determination for pseudo-second-order kinetics for Cr^{6+}, Cd^{2+} and PO_4^{3-} were 0.532; 0.940 and 0.742 while the RSME results were 0.089; 0.060; 0.244 and the reduced chi-square results were 0.006; 0.001 and 0.015 respectively. Based on the R^2 values only, the rate-limiting step for the adsorption process seemed to be pseudo-first-order kinetics. This means that the adsorption occurred via physisorption. However, when including the other evaluation parameters such as the RSME and RCS values, results indicated that pseudo-second-order kinetics was the rate-limiting step for the adsorption process for this study. This means that the adsorption process occurred via chemisorption processes. It can then be concluded that the adsorption process occurred through both mechanisms with pseudo-second-order being more favorable.

Furthermore, the linearized kinetic models which include the intra-particle diffusion are discussed below. The intra-particle diffusion rate usually undergoes three processes: firstly, the external film diffusion. Secondly, the intra-particle interaction and thirdly, the intra-particle diffusion slowing down due to extremely low adsorbate concentration in the solutions (Gorzin and Bahri Rasht Abadi 2018; Ho et al., 2000).

Table 13 shows the results of the intra-particle diffusion. From the table, it was observed that the R^2 values for Cr^{6+}, Cd^{2+} and PO_4^{3-} were 0.2303, 0.6405 and 0.5161 while the thickness of the boundary layer results was 1.0824; 6.4887 and 4.0007. Furthermore, the diffusion rate constants values were 0.0131; 0.039 and 0.0788. this indicated that the results were not only

governed by pseudo-first-order and pseudo-second-order kinetics only, but other mechanisms are also responsible for the adsorption processes by the pPD/GFP/diatom adsorbent towards Cr^{6+}, Cd^{2+} and PO_4^{3-} ions.

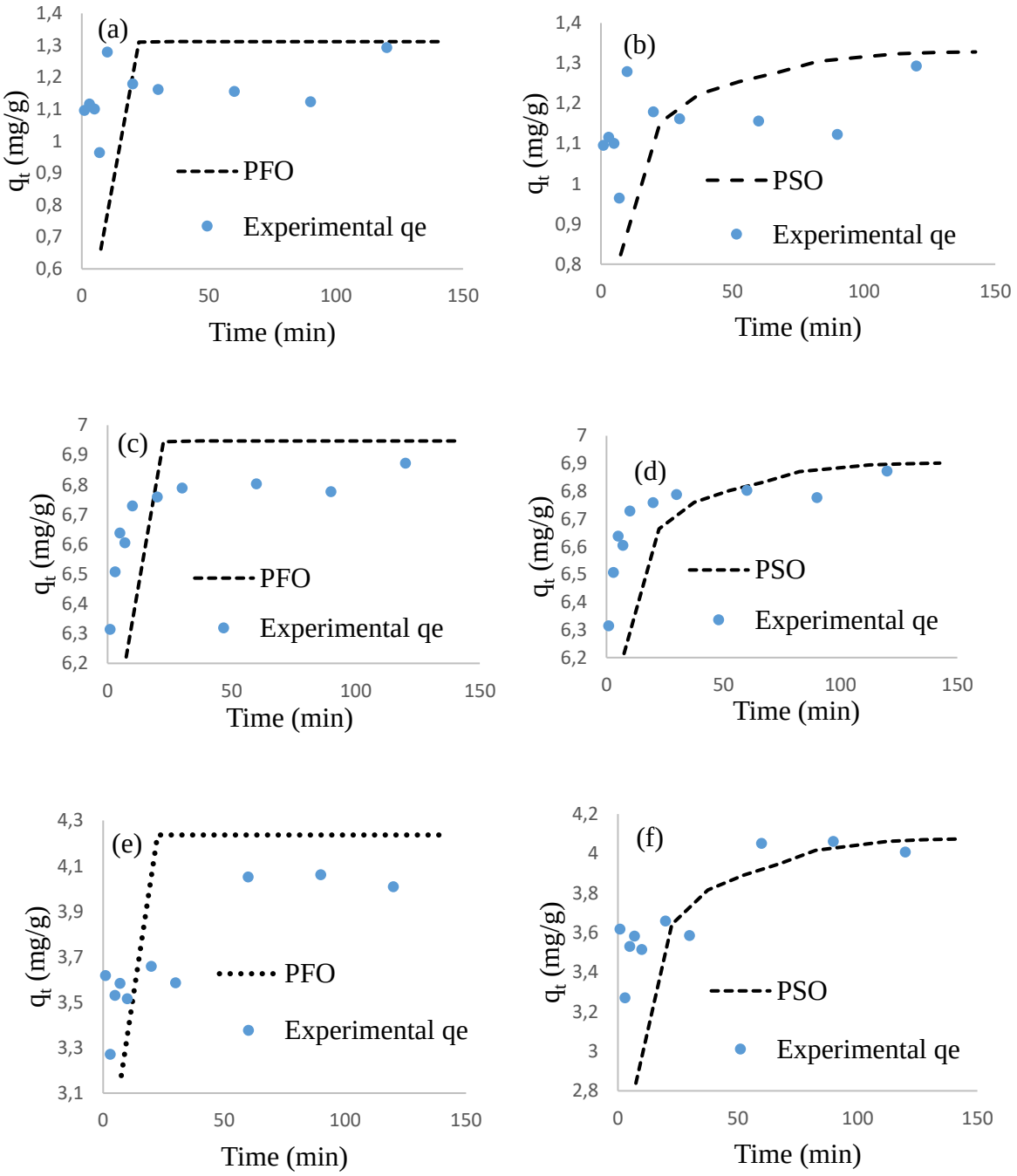

Fig. 43. Non-linear plots for pseudo-first and pseudo-second order adsorption kinetics for Cr^{6+} (a;b), Cd^{2+} (c;d) and PO_4^{3-} (e;f) in aqueous solutions.

Table 12: Non-linear kinetic models for Cr^{6+}, Cd^{2+} and PO_4^{3-}

Non- linear	Parameters	Cr^{6+}	Cd^{2+}	PO_4^{3-}
PFO	k_1	3.010	2.801	3.840
	q_t	1.152	6.720	3.695
	R^2	0.999	0.999	0.998
	RCS	0.007	0.002	0.017
	RSME	0.092	0.108	0.263
PSO	k_2	8.966	1.776	2.541
	q_t	1.167	6.781	3.757
	R^2	0.532	0.940	0.742
	RCS	0.006	0.001	0.015
	RSME	0.089	0.060	0.244

Table 13: Linear kinetics parameters for Cr^{6+}, Cd^{2+} and PO_4^{3-} ions in aqueous solutions

Intra-particle diffusion	Parameter	Cr^{6+}	Cd^{2+}	PO_4^{3-}
	K_{id}	0.01	0.04	0.08
	C	1.08	6.49	4.00
	R^2	0.23	0.64	0.52

6.6.3 Effect of initial concentration and adsorption isotherms

The effect of initial concentration for Cr^{6+}, Cd^{2+} metals (a-b) and PO_4^{3-} (c) ions in solutions was evaluated at various concentrations (10-200 mg/L) and various temperatures. Fig. 44 showed that the higher the concentration, the higher the adsorption capacity and the lower the percentage removal becomes as the temperature increased for the metal ions. Similar results were obtained by Naga Babu et al. (2017). The increase in adsorption capacity could be due to the active sites of the pPD/GFP/diatom adsorbent surrounded with more Cr^{6+} and Cd^{2+} ions in the solution which enhances the adsorption process as a result of the driving force of the concentration gradient. The decrease in removal efficiency could be due to the reduction in the mass gradient between the pPD/GFP/diatom adsorbent and Cr^{6+} and Cd^{2+} interphase as a result of saturation of adsorbent active sites.

However, the percentage removal and adsorption capacity decrease with an increase in concentration only at room temperature. Although the highest percentage removal and adsorption capacity can also be observed at 298 K temperature. This could mean that room temperature yields better removal efficiency and adsorption capacity for PO_4^{3-} ions. Furthermore, the percentage removal and adsorption capacity increased as concentration and temperature increased. This also indicated that temperature played a role in the adsorption processes.

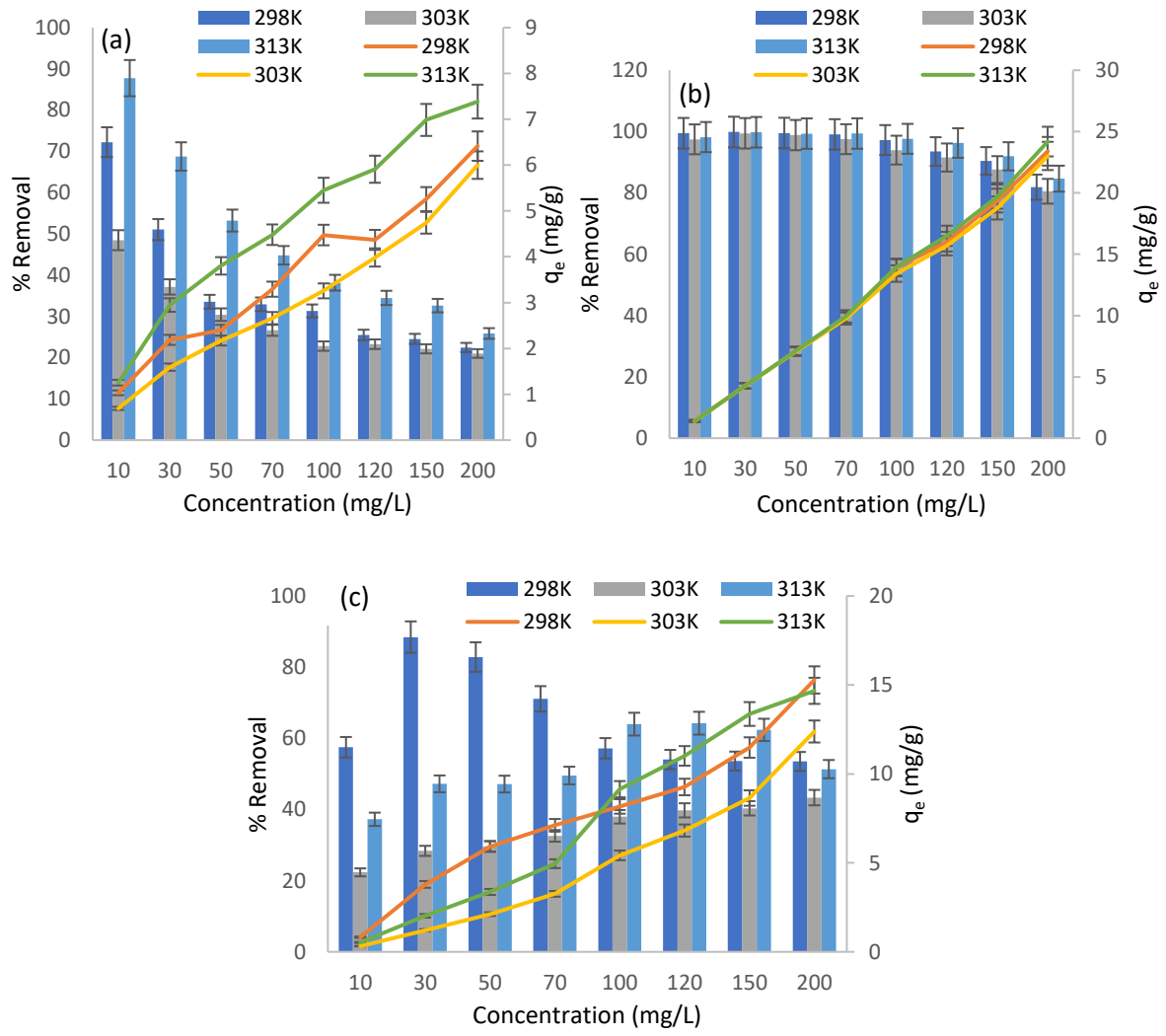

Fig. 44. Effect of initial concentration for Cr^{6+}(a); Cd^{2+}(b) and PO_4^{3-} (c). (Experimental conditions: Time, 24 h; dosage, 0.35 g; neutral pH; volume, 50 mL; shaking speed, 250 rpm).

The adsorption isotherms for Cr^{6+}, Cd^{2+} and PO_4^{3-} were modelled using Freundlich and Langmuir. The non-linear Langmuir equation is given Equation (6).

$$q_e = \frac{q_m K_L C_e}{1+K_L C_e} \quad (6)$$

where q_e is the adsorption capacity (mg/g), q_m (mg/g) is the maximum adsorption capacity, C_e (mg/L) is the equilibrium concentration, k_L is the Langmuir biosorption equilibrium constant (L/mg). A plot of C_e/q_e against C_e gives the Langmuir parameters.

Langmuir isotherm can further be determined through a dimensionless separation factor, which is R_L and it is given in equation (7).

$$R_L = \frac{1}{1 + k_L C_i} \quad (7)$$

where C_i (mg/L) is the initial ion concentration, K_L is Langmuir isotherm constant and R_L provides an indication of whether the adsorption is unfavourable ($R_L > 1$), favourable ($0 < R_L < 1$), irreversible ($R_L = 0$) or linear ($R_L = 1$).

Freundlich isotherm model on the other hand was used to determine whether adsorption occurred on a heterogeneous surface to create a multi-layered surface (Freundlich,1907). The non-linear equation of Freundlich isotherm is expressed on equation (8).

$$q_e K_f C e^{\frac{1}{n}} \quad (8)$$

where K_f and 1/n are empirical constants that show the biosorption capacity and the adsorption intensity respectively. When $0 < 1/n < 1$, the adsorption is favourable; when $1/n > 1$, the adsorption is unfavourable and when $1/n = 1$, the adsorption is irreversible.

The R^2 values for Cr^{6+}, Cd^{2+} and PO_4^{3-} were reasonable on both Langmuir and Freundlich isotherm models. However, the R^2 values for all the adsorbates were higher on Freundlich than Langmuir, which indicated that the adsorption process occurred on a heterogeneous multi-layered surface. This was further supported by the Freundlich n values which were greater than zero and less than 1 for all the adsorbates across all temperatures which means favourability of the adsorption process. Furthermore, the maximum adsorption capacities obtained for Cr^{6+} were 8.94, 12.68 and 8.20 (mg/g); Cd^{2+} were 20.09, 21.25 and 21.90 (mg/g) while PO_4^{3-} were 7.53, 15.89 and 33.45 (mg/g) which were increasing with temperature (298K-313K). This showed that temperature played a role in increasing the adsorption capacity of the pPD/GFP/diatom adsorbent towards Cr^{6+}, Cd^{2+} and PO_4^{3-} ions. Additionally, the adsorption capacities were higher for Cd^{2+} and PO_4^{3-} ions than those obtained from Cr^{6+} metal ions. This

showed that the pPD/GFP/diatom adsorbent has a high affinity for Cd^{2+} and PO_4^{3-} ions which were also influenced by an increase in temperature.

Dubinin Radushkevich's (D-R) isotherm model was also for the adsorption of the pollutant ions in this study. In this model, when E is less than 8 kJ/mol, adsorption is said to have occurred via physisorption and when if E is between 8 and 16 kJ/mol via chemisorption. The linear D-R model can be expressed as:

$$lnq_e = lnq_o - \beta e^2 \quad (9)$$

where qe (mg/g) is the amount of ions adsorbed per unit weight of adsorbent, qo being the maximum adsorption capacity, β is the coefficient constant, E (KJ/mol) is the mean sorption energy, Ɛ is the Polanyi potential. The mean sorption energy can be expressed by equation (10).

$$E = \sqrt{\frac{1}{2\beta}} \quad (10)$$

where R is the gas constant (J/mol K) and T is the temperature (K).

In Table 14, the data indicated that the Q_{max} values for Cr^{6+} and PO_4^{3-} adsorbates increased with an increase in temperature through the highest values were obtained in PO_4^{3-} then Cr^{6+}. This indicated that temperature played a significant role in enhancing the adsorption capacity of the adsorbent towards Cr^{6+} and PO_4^{3-} ions. The Q_{max} values for Cd^{2+} however, were decreasing with an increase in temperature. This means temperature shows no influence on the adsorption capacity of pPD/GFP/ diatom adsorbent towards Cd^{2+}, which could be due to difficulty in ion-exchange mechanisms as alluded to earlier. The R^2 values for Cd^{2+} and PO_4^{3-} were increasing with an increase in temperature while decreasing with an increase in temperature for Cr^{6+}. However, PO_4^{3-} has a better coefficient of determination values than the metal ions. This shows high attraction towards the phosphate ions by the pPD/GFP/ diatom adsorbent during the adsorption process. Furthermore, the D-R mean adsorption energy was less than 8 kJ/mol for all the adsorbates which means the reaction involved was physical.

This showed that the adsorption mechanisms responsible for the reaction by pPD/GFP/diatom adsorbent was governed by both physisorption and chemisorption processes and the reaction was favorable.

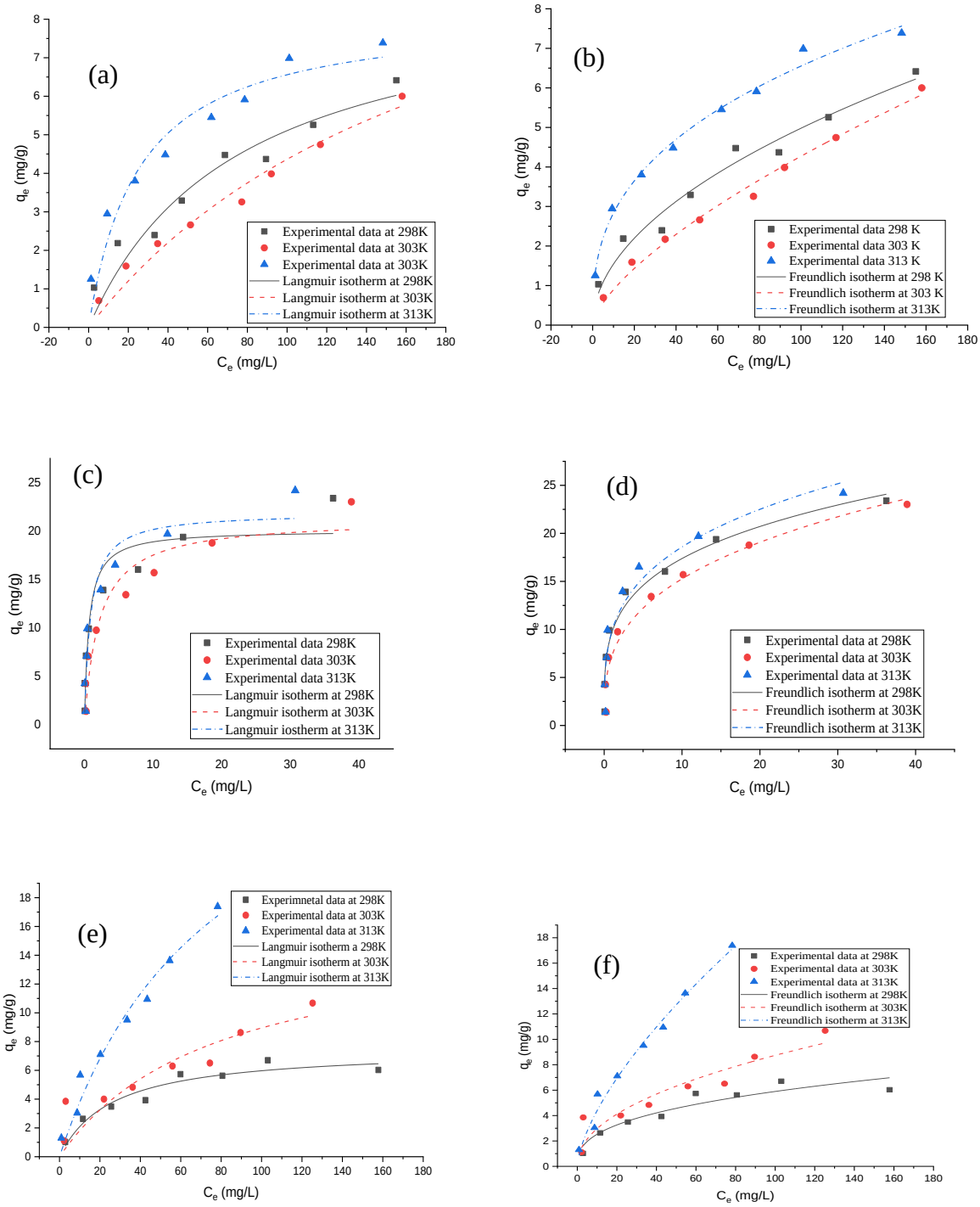

Fig. 45. Graphs showing Langmuir and Freundlich adsorption isotherms for Cr^{6+} (a; b), Cd^{2+} (c; d) and PO_4^{3-} (e; f) ions.

Table 14: The non-linear isotherm parameters for Langmuir, Freundlich and DR models

	Cr^{6+}			Cd^{2+}			PO_4^{3-}		
Temperature (K)	298	303	313	298	303	313	298	303	313
Langmuir									
Q_m (mg/g)	8.94	12.68	8.20	20.09	21.25	21.90	7.53	15.89	33.45
K_L (L/mg)	0.01	0.01	0.04	1.56	0.47	1.15	0.04	0.01	0.01
R^2	0.93	0.97	0.93	0.91	0.92	0.91	0.94	0.78	0.97
Adj R^2	0.91	0.97	0.92	0.89	0.90	0.90	0.93	0.74	0.97
R_L	0.61	0.29	0.33	0.01	0.04	0.02	0.34	0.61	0.61
RCS	0.27	0.11	0.35	6.31	5.28	6.21	0.28	2.31	1.00
Freundlich									
KF ((mg/g)/(mg/L)n)	0.48	0.19	1.23	9.70	7.28	9.85	1.08	1.01	0.95
N	0.51	0.68	0.36	0.25	0.32	0.28	0.37	0.47	0.66
R^2	0.97	0.99	0.99	0.96	0.96	0.92	0.90	0.88	0.98
Adj R^2	0.97	0.99	0.99	0.96	0.96	0.91	0.88	0.86	0.98
RCS	0.11	0.04	0.05	2.40	2.28	5.49	0.45	1.26	0.54
Dubinin-Radushkevvich									
βD (mol^2/kJ^2)	2.00E-06	8.00E-06	6.00E-07	3.00E-08	8.00E-08	4.00E-08	3.00E-06	2.00E-06	5.00E-07
q_{max}(mg/g)	3.86	3.33	5.10	15.72	14.58	14.41	4.79	6.69	8.56
E (kJ/mol)	0.5	0.25	0.91	4.08	2.5	3.54	0.41	0.5	1
R^2	0.64	0.68	0.74	0.79	0.68	0.51	0.79	0.76	062

6.6.4 Thermodynamics

The thermodynamics parameters for the sorption of Cr^{6+}, Cd^{2+} and PO_4^{3-} ions were determined at various temperatures ranging from 298 to 313 K (Table 15). The data showed the degree of randomness, type of reaction and the rate of spontaneity during the adsorption process by the pPD/GFP/diatom adsorbent which were determined by various thermodynamic parameters such as the enthalpy change, Gibbs free energy change and the entropy change. The following equations were used to determine the thermodynamics parameters:

$$\mathrm{InK_D} = \frac{\Delta \mathrm{H}^\circ}{\mathrm{R}} + \frac{\Delta \mathrm{S}^\circ}{\mathrm{R}} \quad (11)$$

where, ΔH° (KJ/mol) and ΔS° (J/mol K) are the enthalpy and entropy change respectively during the biosorption process, which was calculated from the intercept and slope of the linear plot.

$$\Delta G^\circ = \Delta H^\circ - T\Delta S^\circ \quad (12)$$

where ΔG is the free Gibbs energy change, R and T represent the ideal gas constant (8.314 J mol^{-1} K^{-1}) and absolute temperature (K)

$$K_D = \frac{C_s}{C_e} \quad (13)$$

where K_D is the equilibrium constant at a constant temperature, C_e (mg/L) and C_s (mg/L) are equilibrium concentrations of sorbate and the amount of sorbate adsorbed, respectively.

Table 15 illustrates the results obtained for the thermodynamic parameters for Cr^{6+}, Cd^{2+} and PO_4^{3-}. From the data, the reaction which occurred during sorption of the adsorbates by the composite was endothermic for Cr^{6+} and PO_4^{3-}. However, for Cd^{2+}, it was an exothermic reaction. The results were validated by a positive ΔH° for Cr^{6+} and PO_4^{3-} and a negative ΔH° for Cd^{2+}. The Gibbs free energy change (ΔG°) results were negative values which increased with temperature. This indicated that the reactions which occurred were spontaneous and feasible.

Furthermore, the positive ΔS° indicated that there was an increase in randomness for Cr^{6+} and Cd^{2+} adsorbates during the reaction process which supports the ion-exchange adsorption mechanisms at their respective adsorption pH values. However, PO_4^{3-} ΔS° was negative, which indicated a decrease in randomness by the pPD/GFP/diatom adsorbent. Furthermore, ΔH° values for Cd^{2+} were less than 40 KJ/mol, which indicated that the adsorption by pPD/GFP/diatom adsorbent was physical while for Cr $^{6+}$ and PO 4 3- ΔH° values were greater

than 40KJ/mol which indicated that adsorption by pPD/GFP/diatom adsorbent involved chemical processes. This was also supported by the adsorption modeling kinetics.

Table 15: Illustrates the thermodynamic parameters for Cr^{6+}, Cd^{2+} and PO_4^{3-}

	Cr^{6+}	Cd^{2+}	PO_4^{3-}
ΔH◦ (KJ/mol)	72.061	-4.197	50.086
ΔS◦ (J/mol K)	324.653	115.822	-68.910
	ΔG◦ (kJ/mol)		
298 K	-96.675	-34.519	-0.317
303 K	-98.298	-35.098	-0.322
313 K	-101.544	-36.257	-0.332

6.6.5 Antimicrobial evaluation

The antimicrobial activity of pPD/GFP/diatom composite, grapefruit peel powder and diatom biomass adsorbents were evaluated in this study to test their potency towards antimicrobial activities through what is known as minimum zone of inhibition. Fig. 46 shows the susceptibility of these materials towards *Escherichia coli*, *Klebsiella pneumoniae* and *Staphylococcus aureus* with the minimum zone of inhibitions. The obtained minimum zone of inhibitions obtained was 8 mm and 7 mm for *Escherichia coli* by diatom biomass, grapefruit/diatom and pPD/GFP/diatom adsorbents respectively. For *K. pneumoniae*, the minimum zone of inhibitions obtained was 7 mm and 9 mm by grapefruit peel powder and pPD/GFP/diatom adsorbents while 0 mm zone of inhibitions were obtained for Staphylococcus aureus by all the adsorbents.

The obvious zone of inhibitions for *Escherichia coli* and Klebsiella pneumoniae could be due to the presence of Mg and Fe on the surface of the diatoms as well as the functional groups such as the hydroxyl groups which are known to have antimicrobial properties that help in cell disruption of the microbes by inactivating the cell properties as well as disrupting their DNA, even leading to their death (Lee et al., 2011; Cho et al., 2006). Moreover, the ammonium persulfate which is a chemical oxidant from the synthesis of pPD contains some antimicrobial properties as well which oxidize the lipid membrane of the bacteria, therefore bursting it, allowing the adsorbent to diffuse and kill the bacteria (Kucekova, 2014; Gizdavic-Nikolaidis et al., 2013; Shi et al., 2006). The presence of chlorine also, during the synthesis of pPD played a role in killing and reducing microbial pathogens because of its disinfection properties.

Furthermore, the presence of the phenazine groups as indicated by FTIR plays a role in antimicrobial properties. They are known to possess biological properties such as antimicrobial, anticancer and antimalaria (Jiang et al., 2018). However, there was no zone of inhibitions observed for Staphylococcus aureus by all the adsorbents. This could mean that the adsorbents have antimicrobial potency for gram-negative bacterial species than gram-positive. Additionally, it could be as a result of multidrug resistance (MDR) and extremely drug resistance (XDR) which exhibit resistance to nearly all antibiotics available hence even with such functional groups present on the surface of the adsorbent which is known to break down the cell activities of bacteria are failing to perform such functions (Hersh et al., 2012; Magiorakos et al., 2012).

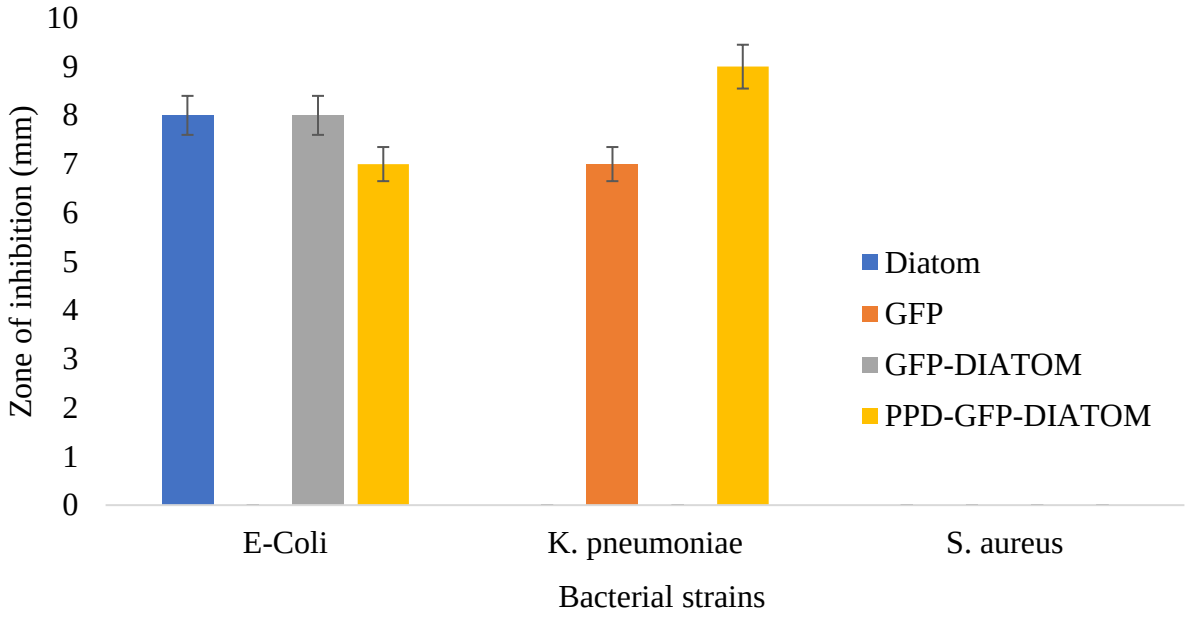

Fig. 46. Antimicrobial susceptibility of pPD/GFP/ diatom, grapefruit peel powder and diatom biomass on different strains of bacteria.

6.6.6 Comparative studies

The comparison studies on the sorption of Cr^{6+}, Cd^{2+} and PO_4^{3-} ions by grapefruit peel, diatom biomass, GFP/diatom and pPD/GFP/diatom adsorbents were compared with various bio-sorbents materials as illustrated in Table 16. The adsorption capacities were compared with those from the study to see their efficiency in remediating contaminated water.

Table 16: Comparison studies on the sorption capacity of Cr^{6+}, Cd^{2+} and PO_4^{3-} by various sorbent materials.

Pollutants	Sorbents	Sorbent type	Adsorption capacity (mg/g)	Reference
Cr^{6+}	PANI/SiO_2 composite	-	63.41	Karthik and Meenakshi,2014
	Grapefruit peels	Plant	90.09	This study
	Diatom biomass	Algae	5.66	This study
	GFP/diatom	Plant and Algae	1.41	This study
	pPD/GFP/diatom	Biomass-polymeric	12.68	This study
Cd^{2+}	Ulva lactuca	Algae	29.1	Ghoneim et al 2014
	Aloe vera waste	Plant	104.2	Noli et al., 2019
	Grapefruit peel	Plant	47.14	This study
	Diatom biomass	Algae	5.27	This study
	GFP/diatom	Plant and Algae	1.34	This study
	pPD/GFP/diatom	Biomass-polymeric	21.90	This study
PO_4^{3-}	Silica-sulfate	-	51.63	Jutidamrongphan et al., 2012
	Grapefruit peel	Plant		This study
	Diatom biomass	Algae	19.13	This study
	GFP/diatom	Plant and Algae	33.45	This study
	pPD/GFP/diatom	Biomass-polymeric	33.45	This study

6.7 Conclusion

A success incorporation of grapefruit peel powder and diatom biomass into pPD matrix was achieved through chemical polymerization process to produce pPD/GFP/diatom adsorbent, which successfully removed Cr^{6+}, Cd^{2+} and PO_4^{3-} in water. This was also revealed by the morphological data which confirmed that there was an interaction of metal ions and nutrients by various functional groups in the pPD/GPF/diatom adsorbent. The sorption capacity of the pPD/GFP/diatom adsorbent depends on the optimization parameters such as contact time, pH, and initial concentration of Cr^{6+}, Cd^{2+} and PO_4^{3-}. The sorption kinetics revealed both pseudo-first-order and pseudo-first were the rate-limiting steps that governed the adsorption process indicating that physisorption and chemisorption took place during sorption processes. The adsorption equilibrium data were best described by Freundlich isotherm, indicating that adsorption occurred on a heterogeneous multi-layered surface. The thermodynamics data revealed that the reaction was endothermic for Cr^{6+} and PO_4^{3-}. However, for Cd^{2+}, it was an

exothermic reaction. Furthermore, the thermodynamic data reveals that the reaction processes were feasible and spontaneous across all temperatures for the adsorbates and there was an increase in randomness for Cr^{6+} and Cd^{2+} metal ions while a decrease in randomness for PO_4^{3-} was obtained by the pPD/GPF/diatom adsorbent in solutions. Furthermore, the majority of the adsorbents have antimicrobial potency towards *Escherichia coli and Klebsiella pneumoniae* due to their inherent functional properties. However, they do not indicate any potency for *staphylococcus aureus.*

References

Akpor, O. B. and Muchie, B., 2011. Environmental and public health implications of wastewater quality. *African Journal of Biotechnology*, *10*(13), pp. 2379-2387.

Albadarin, A.B., Collins, M.N., Naushad, M., Shirazian, S., Walker, G. and Mangwandi, C., 2017. Activated lignin-chitosan extruded blends for efficient adsorption of methylene blue. *Chemical Engineering Journal*, *307*, pp.264-272.

Ansari, R. and Mosayebzadeh, Z., 2010. Removal of basic dye methylene blue from aqueous solutions using sawdust and sawdust coated with polypyrrole. *Journal of the Iranian Chemical Society*, *7*(2), pp.339-350.

Archana, S. and Jaya Shanthi, R., 2014. Synthesis and characterization of poly (p-phenylenediamine) in the presence of sodium dodecyl sulfate. *Research Journal of Chemical Sciences.*

Archana, S. and Jaya Shanthi, R., 2015. Removal of Cr (VI) from tannery effluent using synthesized polyphenylenediamine nanocomposites. *International Journal of ChemTech Research*, *8*(5), pp.85-89.

Asadollahzadeh, M., Raoufi, N., Rezakazemi, M. and Shirazian, S., 2018. Simulation of nonporous polymeric membranes using CFD for bioethanol purification. *Macromol Theory Simul*, *27*(3).

Bauer, A.W., 1966. Antimicrobial susceptibility testing by a standardized single disk method. *Am Journal of Clinical Pathology*, *45*, pp.493-496.

Cao, D.Q., Song, X., Fang, X.M., Yang, W.Y., Hao, X.D., Iritani, E. and Katagiri, N., 2018. Membrane filtration-based recovery of extracellular polymer substances from excess sludge and analysis of their heavy metal ion adsorption properties. *Chemical Engineering Journal*, *354*, pp.866-874.

Chai, L., Wang, T., Zhang, L., Wang, H., Yang, W., Dai, S., Meng, Y. and Li, X., 2015. A Cu–m-phenylenediamine complex induced route to fabricate poly (m-phenylenediamine)/reduced graphene oxide hydrogel and its adsorption application. *Carbon*, *81*, pp.748-757.

Cho, M., Kim, J.H. and Yoon, J., 2006. Investigating synergism during sequential inactivation of Bacillus subtilis spores with several disinfectants. *Water Research*, *40*(15), pp.2911-2920.

Dankovich, T.A., Levine, J.S., Potgieter, N., Dillingham, R. and Smith, J.A., 2016. Inactivation of bacteria from contaminated streams in Limpopo, South Africa by silver-or copper-nanoparticle paper filters. *Environmental Science: Water Research & Technology*, *2*(1), pp.85-96.

Dimapilis, E.A.S., Hsu, C.S., Mendoza, R.M.O. and Lu, M.C., 2018. Zinc oxide nanoparticles for water disinfection. *Sustainable Environment Research*, *28*(2), pp.47-56.

Elsherif, K.M., Ewlad-Ahmed, A.M. and Treban, A., 2017. Removal of Fe (III), Cu (II), And Co (II) from aqueous solutions by orange peels powder: Equilibrium study. *Journal of Biochemistry and Molecular Biology Research*, *2*(6), pp.46-51.

El Zayat, M., 2009. Removal of heavy metals by using activated carbon produced from cotton stalks.

Ghoneim, M.M., El-Desoky, H.S., El-Moselhy, K.M., Amer, A., Abou El-Naga, E.H., Mohamedein, L.I. and Al-Prol, A.E., 2014. Removal of cadmium from aqueous solution using marine green algae, Ulva lactuca. *The Egyptian Journal of Aquatic Research*, *40*(3), pp.235-242.

Ghorbani, M. and Eisazadeh, H., 2013. Removal of COD, color, anions and heavy metals from cotton textile wastewater by using polyaniline and polypyrrole nanocomposites coated on rice husk ash. *Composites Part B: Engineering*, *45*(1), pp.1-7.

Gizdavic-Nikolaidis, M.R., Bennett, J.R., Swift, S., Easteal, A.J. and Ambrose, M., 2011. Broad spectrum antimicrobial activity of functionalized polyanilines. *Acta biomaterialia*, *7*(12), pp.4204-4209.

Gola, D., Dey, P., Bhattacharya, A., Mishra, A., Malik, A., Namburath, M. and Ahammad, S.Z., 2016. Multiple heavy metal removal using an entomopathogenic fungi Beauveria bassiana. *Bioresource Technology*, *218*, pp.388-396.

Gorzin, F. and Bahri Rasht Abadi, M.M., 2018. Adsorption of Cr (VI) from aqueous solution by adsorbent prepared from paper mill sludge: Kinetics and thermodynamics studies. *Adsorption Science & Technology*, *36*(1-2), pp.149-169.

Hao, Q., Sun, B., Yang, X., Lu, L. and Wang, X., 2009. Synthesis and characterization of poly (o-phenylenediamine) hollow multi-angular microrods by interfacial method. *Materials Letters*, *63*(2), pp.334-336

Hersh, A.L., Newland, J.G., Beekmann, S.E., Polgreen, P.M. and Gilbert, D.N., 2012. Unmet medical need in infectious diseases. *Clinical Infectious Diseases*, *54*(11), pp.1677-1678.

Ho, Y.S., Ng, J.C.Y. and McKay, G., 2000. Kinetics of pollutant sorption by biosorbents. *Separation and purification methods*, *29*(2), pp.189-232.

Huang, M.R., Lu, H.J. and Li, X.G., 2012. Synthesis and strong heavy-metal ion sorption of copolymer microparticles from phenylenediamine and its sulfonate. *Journal of Materials Chemistry*, *22*(34), pp.17685-17699.

Huang, M.R., Peng, Q.Y. and Li, X.G., 2006. Rapid and effective adsorption of lead ions on fine poly (phenylenediamine) microparticles. *Chemistry–A European Journal*, *12*(16), pp.4341-4350.

Järup, L., Berglund, M., Elinder, C.G., Nordberg, G. and Vanter, M., 1998. Health effects of cadmium exposure–a review of the literature and a risk estimate. *Scandinavian Journal of Work, Environment & Health*, pp.1-51.

Jiang, J., Guiza Beltran, D., Schacht, A., Wright, S., Zhang, L. and Du, L., 2018. Functional and structural analysis of phenazine O-methyltransferase LaPhzM from Lysobacter antibioticus OH13 and one-pot enzymatic synthesis of the antibiotic Myxin. *ACS Chemical Biology*, *13*(4), pp.1003-1012.

Jutidamrongphan, W., Park, K.Y., Dockko, S., Choi, J.W. and Lee, S.H., 2012. High removal of phosphate from wastewater using silica sulfate. *Environmental chemistry letters*, *10*(1), pp.21-28.

Karthik, R. and Meenakshi, S., 2014. Removal of hexavalent chromium ions using polyaniline/silica gel composite. *Journal of Water Process Engineering*, *1*, pp.37-45.

Kucekova, Z., Humpolicek, P., Kasparkova, V., Perecko, T., Lehocký, M., Hauerlandova, I., Saha, P. and Stejskal, J., 2014. Colloidal polyaniline dispersions: antibacterial activity, cytotoxicity and neutrophil oxidative burst. *Colloids and Surfaces B: Biointerfaces*, *116*, pp.411-417.

Lakouraj, M.M., Zare, E.N. and Moghadam, P.N., 2014. Synthesis of novel conductive poly (p-phenylenediamine)/Fe_3O_4 nanocomposite via emulsion polymerization and investigation of antioxidant activity. *Advances in Polymer Technology*, *33*(1).

Lata, S. and Samadder, S.R., 2014. Removal of heavy metals using rice husk: a review. *International Journal of Environmental Research and Development*, *4*(2), pp.165-170.

Lee, W.H., Wahman, D.G., Bishop, P.L. and Pressman, J.G., 2011. Free chlorine and monochloramine application to nitrifying biofilm: comparison of biofilm penetration, activity, and viability. *Environmental Science & Technology*, *45*(4), pp.1412-1419.

Li, X.G., Huang, M.R., Duan, W. and Yang, Y.L., 2002. Novel multifunctional polymers from aromatic diamines by oxidative polymerizations. *Chemical Reviews*, *102*(9), pp.2925-3030.

Lim, J.H., Kang, H.M., Kim, L.H. and Ko, S.O., 2008. Removal of heavy metals by sawdust adsorption: equilibrium and kinetic studies. *Environmental Engineering Research*, *13*(2), pp.79-84.

Lǔ, J., Liu, H., Liu, R., Zhao, X., Sun, L. and Qu, J., 2013. Adsorptive removal of phosphate by a nanostructured Fe–Al–Mn trimetal oxide adsorbent. *Powder Technology*, *233*, pp.146-154.

Magiorakos, A.P., Srinivasan, A., Carey, R.T., Carmeli, Y., Falagas, M.T., Giske, C.T., Harbarth, S., Hindler, J.T., Kahlmeter, G., Olsson-Liljequist, B. and Paterson, D.T., 2012. Multidrug-resistant, extensively drug-resistant and pandrug-resistant bacteria: an international expert proposal for interim standard definitions for acquired resistance. *Clinical Microbiology and Infection*, *18*(3), pp.268-281.

Mahmoodi, N.M., Najafi, F. and Neshat, A., 2013. Poly (amidoamine-co-acrylic acid) copolymer: Synthesis, characterization and dye removal ability. *Industrial Crops and Products*, *42*, pp.119-125.

Mansour, M.S., Ossman, M.E. and Farag, H.A., 2011. Removal of Cd (II) ion from wastewater by adsorption onto polyaniline coated on sawdust. *Desalination*, *272*(1-3), pp.301-305.

Mdlalose, L., Balogun, M., Setshedi, K., Tukulula, M., Chimuka, L. and Chetty, A., 2017. Synthesis, characterization and optimization of poly (p-phenylenediamine)-based organoclay composite for Cr (VI) remediation. *Applied Clay Science*, *139*, pp.72-80.

Min, Y.L., Wang, T., Zhang, Y.G. and Chen, Y.C., 2011. The synthesis of poly (p-phenylenediamine) microstructures without oxidant and their effective adsorption of lead ions. *Journal of Materials Chemistry*, *21*(18), pp.6683-6689.

Naga Babu, A., Krishna Mohan, G.V., Kalpana, K. and Ravindhranath, K., 2017. Removal of lead from water using calcium alginate beads doped with hydrazine sulphate-activated red mud as adsorbent. *Journal of Analytical Methods in Chemistry*, *2017*, pp 13.

Naidoo, S. and Olaniran, A., 2013. Treated wastewater effluent as a source of microbial pollution of surface water resources. *International Journal of Environmental Research and Public Health*, *11*(1), pp.249-270.

Nebel, B.J. and Wright, R.T., 1993. *Environmental Science: The Way The World Works*. Prentice Hall Professional.

Nguyen, H.D., Mai, T.T.T., Nguyen, N.B., Dang, T.D., Le, M.L.P. and Dang, T.T., 2013. A novel method for preparing microfibrillated cellulose from bamboo fibers. *Advances in Natural Sciences: Nanoscience and Nanotechnology*, *4*(1), p.015016.

Noli, F., Kapashi, E. and Kapnisti, M., 2019. Biosorption of uranium and cadmium using sorbents based on Aloe vera wastes. *Journal of Environmental Chemical Engineering*, *7*(2), p.102985.

Pham, Q.L., Haldorai, Y., VAN HOA, N.G.U.Y.E.N., Tuma, D. and Shim, J.J., 2011. Facile synthesis of poly (p-phenylenediamine)/MWCNT nanocomposites and characterization for investigation of structural effects of carbon nanotubes. *Bulletin of Materials Science*, *34*(1), pp.37-43.

Rangabhashiyam, S. and Balasubramanian, P., 2019. Characteristics, performances, equilibrium and kinetic modelling aspects of heavy metal removal using algae. *Bioresource Technology Reports*, *5*, pp.261-279.

Schoeters, G., Hond, E.D., Zuurbier, M., Naginiene, R., Van den Hazel, P., Stilianakis, N., Ronchetti, R. and Koppe, J.G., 2006. Cadmium and children: exposure and health effects. *Acta Paediatrica*, *95*, pp.50-54.

Shi, N., Guo, X., Jing, H., Gong, J., Sun, C. and Yang, K., 2006. Antibacterial effect of the conducting polyaniline. *Journal of Materials Science and Technology*, *22*(3), pp.289-290.

Sonone, S.S., Jadhav, S., Sankhla, M.S. and Kumar, R., 2020. Water Contamination by Heavy Metals and their Toxic Effect on Aquaculture and Human Health through Food Chain. *Letters in Applied NanoBioScience*, *10*(2), pp.2148-2166.

Su, Y., Cui, H., Li, Q., Gao, S. and Shang, J.K., 2013. Strong adsorption of phosphate by amorphous zirconium oxide nanoparticles. *Water Research*, *47*(14), pp.5018-5026.

Sud, D., Mahajan, G. and Kaur, M.P., 2008. Agricultural waste material as potential adsorbent for sequestering heavy metal ions from aqueous solutions-A review. *Bioresource Technology*, *99*(14), pp.6017-6027.

Tang, R., Li, Q., Ding, L., Cui, H. and Zhai, J., 2012. Reactive sorption of mercury (II) on to poly (m-phenylenediamine) microparticles. *Environmental Technology*, *33*(3), pp.341-348.

Unceta, N., Séby, F., Malherbe, J. and Donard, O.F.X., 2010. Chromium speciation in solid matrices and regulation: a review. *Analytical and Bioanalytical Chemistry*, *397*(3), pp.1097-1111.

Virji, S., Kaner, R.B. and Weiller, B.H., 2005. Hydrazine detection by polyaniline using fluorinated alcohol additives. *Chemistry of Materials*, *17*(5), pp.1256-1260.

Wang, Z. and Liao, F., 2012. Synthesis of poly(ortho-phenylenediamine) fluffy microspheres and application for the removal of Cr (VI). Journal of Nanomaterial, pp. 1–7.

World Health Organization, WHO/UNICEF Joint Water Supply and Sanitation Monitoring Programme, 2015. Progress on sanitation and drinking water: 2015 update and MDG assessment. World Health Organization.

Zare, E.N., Lakouraj, M.M. and Ramezani, A., 2016. Efficient sorption of Pb (II) from an aqueous solution using a poly (aniline-co-3-aminobenzoic acid)-based magnetic core-shell nanocomposite. *New Journal of Chemistry*, *40*(3), pp.2521-2529.

Zare, E.N., Motahari, A. and Sillanpää, M., 2018. Nanoadsorbents based on conducting polymer nanocomposites with main focus on polyaniline and its derivatives for removal of heavy metal ions/dyes: a review. *Environmental Research*, *162*, pp.173-195.

CHAPTER 7

7.1 General conclusions

The study reported grapefruit peel powder (GFP), diatom biomass, grapefruit peel/ diatom (GFP/diatom) and poly-phenylenediamine (pPD/GFP/diatom) as different adsorbents which were used for the removal of Cr^{6+}, Cd^{2+} and PO_4^{3-} ions as well as pathogens from water. The synthesis of pPD/GFP/diatom adsorbent was successful through chemical polymerization. The morphology of the adsorbent was done by FTIR, XRD and SEM-EDS which revealed various functional groups, mineral phases as well as the shape and elements present on the surface of the adsorbent which played a role in the removal of Cr^{6+}, Cd^{2+} and PO_4^{3-} ions. The batch sorption studies on the uptakes of Cr^{6+}, Cd^{2+} and PO_4^{3-} from aqueous solutions by the various adsorbents were investigated as a function of pH, contact time, adsorbent dosage and initial concentration. The adsorption kinetics by grapefruit peel powder, diatom biomass, grapefruit peel/ diatom and pPD/GFP/diatom on Cr^{6+}, Cd^{2+} and PO_4^{3-} ions revealed that physisorption and chemisorption mechanisms were responsible for the adsorption processes as well as intra-particle diffusions. The data revealed that the adsorption isotherm modeling was described by both Freundlich and Langmuir on the sorption of Cr^{6+}, Cd^{2+} and PO_4^{3-} ions depending on the adsorbent. The thermodynamic data revealed that the adsorption process was spontaneous and feasible in all the adsorbents across all temperatures. The antimicrobial activities of *Escherichia coli*, *Staphylococcus aureus* and *Klebsiella pneumoniae* by the adsorbents showed that grapefruit peel powder, diatom biomass, grapefruit peel/ diatom and pPD/GFP/diatom had antimicrobial potency. The adsorbents possess the ability to treat and remediate wastewater for the possible long-term treatment of wastewater for the well-being of people and the cleanliness of their surrounding environment.

7.2 Recommendations

As the study is being concluded, some areas still need more clarity and addressing to improve the work and add more knowledge to the scientific research community. Therefore, recommendations were brought forth to highlight specific areas which still need exploring:

- Further experiments should be done on the stability of the synthesized pPD/GFP/diatom adsorbent into the filtrates.
- Detailed studies should be done on the functional entities and mechanisms within the synthesized pPD/GFP/diatom towards the antimicrobial properties.

- Recovery and re-use of the metal ions and phosphate ions for industrial purposes should be carried out.
- More studies (column experiments) should be done to test the suitability of pPD/GFP/diatom adsorbent for household use.
- Field application studies should also be explored
- Regeneration studies should be done to check the economic viability of the synthesized pPD/GFP/diatom adsorbent towards the metal ions and phosphate ions